SOLUBILITY OF TRIGLYCERIDES IN SUPERCRITICAL CARBON DIOXIDE

A Thesis

submitted in fulfilment of the requirements for the Degree

of

Doctor of Philosophy in Chemical and Process Engineering

to the

University of Canterbury

by

David L. Pearce.

University of Canterbury

1990

voor Milja

zonder jouw liefde, steun en geduld,

zou niets hiervan mogelijk geweest zijn

Acknowledgments

I would like to thank the following people for their invaluable assistance:

I have been very fortunate to have Dr. Pat Jordan as my main supervisor. It was at his instigation that this project started, and he has been responsible for keeping me going with a steady stream of new ideas when I had run out. I hope that some of your scientific reasoning and engineering commonsense has rubbed off on me.

My associate supervisor Professor Emeritus Arthur Williamson has been always willing to give me advice on thermodynamic matters, especially in the latter stages of this work.

It has been an education to work with two supervisors who were always available when needed, and so willingly gave of their time and advice

This work was funded by a postgraduate scholarship from the Energy Research and Development Committee. This assistance allowed me to keep body and soul together and also provided an invaluable opportunity to attend two overseas conferences. The equipment was funded by a grant from the University Grants Committee.

The Industrial Processing Division of the DSIR provided financial assistance for the purchase of chemicals and travel within New Zealand. In addition to this, the staff of IPD were most helpful when I was in the process of designing and constructing my equipment. They also kindly provided me with a copy of their bibliography.

The construction of the experimental equipment would not have been possible without the willing assistance of the Mechanical and Electrical Technicians of the Department. Thank you all. I would especially like to thank David Brown, for always being on hand to offer practical hints during the design and construction of the apparatus.

I would like to thank all the staff and visitors of the Chemical Engineering Department for giving me assistance as I needed it. In particular, Prof. F.P. Stein (Lehigh University) and Dr. P.J. McElroy helped me with thermodynamics and Miss. L.K. Maynard who assisted during the printing of this work.

I would like to thank my postgraduate colleagues for all their friendship and freely given advice and assistance over the past few years. It has been a pleasure knowing you and I wish you all well in the future.

I must express my gratitude to the following people for their assistance during this work: Dr. J.S. Smaill (Mechanical Engineering Dept.), during the design of the high pressure cell; Tony Wells, of the Chemical Engineering Department, University of New South Wales, for kindly providing a copy of his bibliography in the early stages of this work; Process Developments Limited for the loan of the dry test meter; the staff of the NZ Dairy Research Institute for their generous technical assistance; and the NZ Dairy Board for financial assistance received during the preliminary part of this study.

My family and in-laws deserve special mention for their support and encouragement as the work progressed. My parents in particular, have never shied away from having a Ph.D. student for a son.

Finally, I would like to thank my wife, Milja. It is difficult to know if this would have been completed in time if you were not there, always helping and motivating me when things were not going well.

Table of Contents

Table of Figures

Abstract

The solubilities of four saturated, mono-acid triglycerides: Trilaurin, Trimyristin, Tripalmitin and Tristearin have been determined in supercritical Carbon Dioxide, at 35, 40, 47 and 55°C and at CO_2 densities of 0.57, 0.66, 0.73, 0.78, 0.84 and 0.89 $g.cm^{-3}$. These solubilities were reproducible to within 10% and agreed well with those of a previous worker, in the mid-to-high density range.

The experimental data were correlated using several theoretical and empirical methods. Of the empirical methods, regression of the triglyceride solubility data against a linear function of temperature and density was found to give the least mean square deviation. When a suitable functional form was used for the binary interaction parameter, the Carnahan Starling modification to the van der Waals equation of state was the most satisfactory theoretical correlation tested.

A new experimental apparatus to determine solubilities in supercritical fluids was designed and constructed. The design featured the particular advantage that a microsampling technique using direct coupling to an HPLC apparatus was used to take samples of the high pressure saturated CO_2 stream. This obviated problems due to depressurisation of the outlet stream.

Carbon dioxide was chosen to be the solvent for its low critical properties, low toxicity and ready availability. The triglycerides were selected as solutes for their relevance to the Dairy and Food Industries.

During the course of this work literature references to solubility data since 1982 were compiled.

1

Introduction

1.1 Introduction

The first evidence of the solvating power of supercritical fluids came over 110 years ago. Hannay and Hogarth (1879) observed the dissolution of Potassic Iodide (and subsequently I_2, KBr, $CoCl_2$ and $CaCl_2$) in supercritical Ethanol, as part of a study into the continuity of liquids and gases. They made an Iodide/Ethanol solution and heated it. "No precipitation of the solid could be seen, even at a temperature of 350°C". They also made general observations about the variation of solid solubility with pressure at fixed temperature and the variation with temperature at fixed pressure. Other early work included an extension to high pressure geological processes with the influence of water on rock formation (Niggli, 1912) and in the power industry with the problem of silica deposits on steam turbine blades (Kennedy, 1950). Early patent applications included those of Messmore (1943) with a process for the de-asphalting of oils, and Katz and Kurata (1940) who filed a patent application to use supercritical gas mixtures to separate liquid hydrocarbon mixtures. Zhuze (1959) looked at using compressed hydrocarbon gases for extracting lanolin from wool and also extracting crude oils and residues. Booth and Bidwell (1949) have further reviewed the early work. More recently, supercritical fluids have been investigated in a wide range of processes including diffusion (Debenedetti, 1984), precipitation polymerisation (Kumar, 1986), waste removal (Helling, 1986), as a reaction medium (Johnston and Kim, 1985), in biochemical reactions (Willson, 1987) and in the production of powders and films (Matson *et al*, 1989).

In industry, supercritical extraction processes are used for the decaffeination of coffee (Zosel, 1978), hop extraction (Laws *et al*, 1980), waste product clean-up (Modell, 1982). Zosel (1978) is credited with stimulating recent industrial interest in the area of supercritical fluid extraction (SFE) (Paulaitis *et al*, 1983).

Several general review articles have been written about SFE by Paulaitis *et al* (1983), Williams (1981) and Ely and Baker (1983). Krukonis (1988) provides an excellent outline of the development of the process in Europe and The USA. McHugh and Krukonis (1986)

have recently written an introductory text on SFE. This includes a review of the 'review' literature on supercritical fluid technology, process examples and a comprehensive list of patents.

The term 'supercritical' refers to the fact that a solvent is at a temperature above its vapour-liquid critical temperature. For practical reasons, however, the supercritical region of interest is considered to be bounded by $P_r \geq 1.0$ and $0.9 \leq T_r \leq 1.2$ (Paulaitis *et al*, 1983). The subscript 'r' denotes a reduced property i.e. the ratio of a property to its critical property (for example, $P_r = \frac{P}{P_c}$).

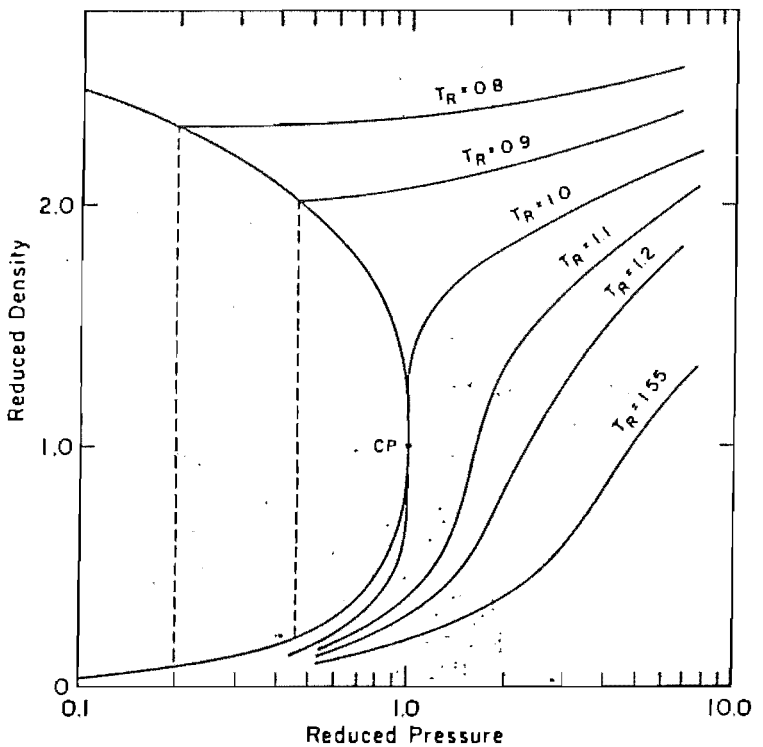

Figure 1.1 Phase Diagram for a Substance

Figure 1.1 (Paulaitis *et al*, 1983) shows a reduced pressure, reduced density diagram for a substance. In the region around the critical point, the solvent becomes highly compressible. This is illustrated by the change in slopes of the isotherms - from nearly horizontal at high and low densities, to nearly vertical close to the critical density. In the vicinity of the critical point the solvent density is sensitive to small changes in temperature and pressure. The solvent density can in fact be continuously varied by changing the temperature and pressure.

The solvent power of a supercritical solvent is directly related to fluid density (Paulaitis *et al*, 1983). This suggests that a solute will be most soluble at high solvent densities and least soluble at low solvent densities. Figure 1.1 shows that at a reduced temperature between 1.0

and 1.1, high densities are attainable with lower pressures than at reduced temperatures greater than 1.55 for example. The solvent power of a supercritical fluid can be further increased by the addition of small amounts (typically 3-5 weight %) of a co-solvent (entrainer) (McHugh and Krukonis, 1986). The presence of an entrainer modifies other properties of the fluid (for example polarity) and can change supercritical fluid selectivity. One can see that extraction conditions can be chosen to maximize the solubility of a solute and separation conditions selected to minimize solute solubility.

The variation in density is not the only interesting phenomenon that appears near the critical point. The diffusion coefficient approaches zero as the critical point is neared and the specific heat of a pure substance becomes infinite at the critical point. Also, thermal conductivity and viscosity show anomalous behaviour in the critical region (Paulaitis *et al*, 1983).

Table 1.1 (Paulaitis *et al*, 1983) shows an order of magnitude comparison of the transport properties of liquids, supercritical fluids and gases. One can see from this table that SCF's have liquid-like densities, and viscosities and diffusivities that are intermediate between the corresponding properties for liquids and gases.

Table 1.1 Transport Properties of Liquids, Gases and SCF.

Phase	Density $kg.m^{-3}$	Viscosity Nsm^{-2}	Diffusivity cm^2s^{-1}
Liquids	10^3	10^{-3}	10^{-5}
Gases	1	10^{-5}	10^{-1}
SCF‡	700	10^{-4}	10^{-4}

‡ for CO_2 at 20 MPa, 310 K.

The choice of supercritical fluid (SCF) can be complex. It is based on availability, critical temperature and pressure, absolute solubility of the möeity in the solvent, solvent toxicity and solvent selectivity.

Table 1.2 (Williams, 1981) lists some commonly examined supercritical solvents, with their critical properties.

Table 1.2 Critical Properties of Common Supercritical Solvents.

Substance	Critical Temperature (K)	Critical Pressure (MPa)	Critical Density ($g\ cm^{-3}$)
Methane	191	4.60	0.162
Ethylene	282	5.03	0.218
Carbon Dioxide	304	7.38	0.468
Ethane	305	4.88	0.203
Propane	370	4.24	0.217
Ammonia	406	11.3	0.235
Benzene	562	4.89	0.302
Water	647	22.0	0.322

1.2 Applications of SFE in New Zealand

1.2.1 Background.

Pearce and Jordan (1988) have outlined the prospects for the application of SFE in New Zealand. The conclusions were that SFE was most likely to be used in the area of "light industry", which include the food and pharmaceutical industries. It was suggested that commercial implementation is most likely to come from either a primary producer interested in producing small volumes of high value products, or small volume production of speciality chemicals from biological sources. The Dairy Industry, with a large variety of products, showed the greatest potential for the introduction of a new technology.

1.2.2 Solute Choice

At a meeting between the University of Canterbury (represented by Dr. P.J. Jordan), the New Zealand Dairy Research Institute (NZDRI) and the New Zealand Dairy Board (NZDB), several general areas of interest were defined:

1. Extraction of Whey Protein Concentrate (WPC) to remove off-flavour and lipid impurities.
2. Extraction of flavour components from Anhydrous Milkfat (AMF) for subsequent recombination.

3. Production of a cheese flavour concentrate by SFE.
4. Recovery of alcohol and other compounds from whey fermentation.
5. Fat fractionation.

For these areas of interest, several common objectives could be defined;

1. Determine solubility of the solute (flavour component/fat) and residual matrix in the supercritical fluid.
2. Investigate solute solubility in a variety in solvents.
3. Obtain extraction rate data.
4. Examine the effect of any co-solvent (entrainer) on the solubility.
5. Look at the functionality of the residue.
6. Examine the possibility of using a two stage extraction process.
7. Look at the design of a continuous plant.

These objectives showed that the need, as far as the industry was concerned, was for reliable solubility data and solubility prediction methods, leading to the design of a continuous extraction plant. Some work had already been done in the area of flavour extraction (Calame and Steiner, 1982) and in the area of oil solubility (Friedrich and Pryde, 1984). Seed oils (such as palm and soya oils) had been examined, but there were no data for pure triglyceride solubilities. It was considered that the most benefit would come from the examination of the solubility of pure triglycerides. It was hoped that such data would lead to predictions of solubilities of triglyceride mixtures and eventually to the understanding and prediction of the solubility process in a complex triglyceride mixture such as palm oil or butter.

1.2.2.2 Triglycerides.

Triglycerides play a vital role in human and animal life. They are a major form of energy storage and are metabolised by the body to produce the essential fatty acids required for growth. Humans obtain the necessary dietary triglycerides principally from butter, margarine and cooking oils. Triglycerides are complex three-chain molecules. They are formed on the esterification of fatty acids with the glycerol molecule. In natural systems, the number of carbon atoms in a fatty acid chain is usually an even number and can vary from two carbon atoms to over twenty carbon atoms. Fatty acids chains can be either saturated or unsaturated. Owing to the complexity of these molecules, a nomenclature has been devised to classify the many molecule species into groups, depending on the kind of fatty acids that they contain.

mono-acid triglycerides containing only one type of fatty acid,
di-acid triglycerides containing two types of fatty acid and,
tri-acid triglycerides containing three fatty acids.

An example of the possible complexity of triglyceride mixtures is found in Litchfield (1972, page 9) "Triglyceride mixtures from animal sources are usually more complex (than those

from plant sources) and may contain 10 to 40 different acids, which could form a possible 1 000 to 64 000 different triglycerides. Butterfat, one of the most complex natural fats, is known to contain at least 142 different fatty acids which could generate a staggering 2 863 288 possible triglyceride species"! Figure 1.2 illustrates the diversity of the principal triglycerides found in milkfat (Norris, 1977).

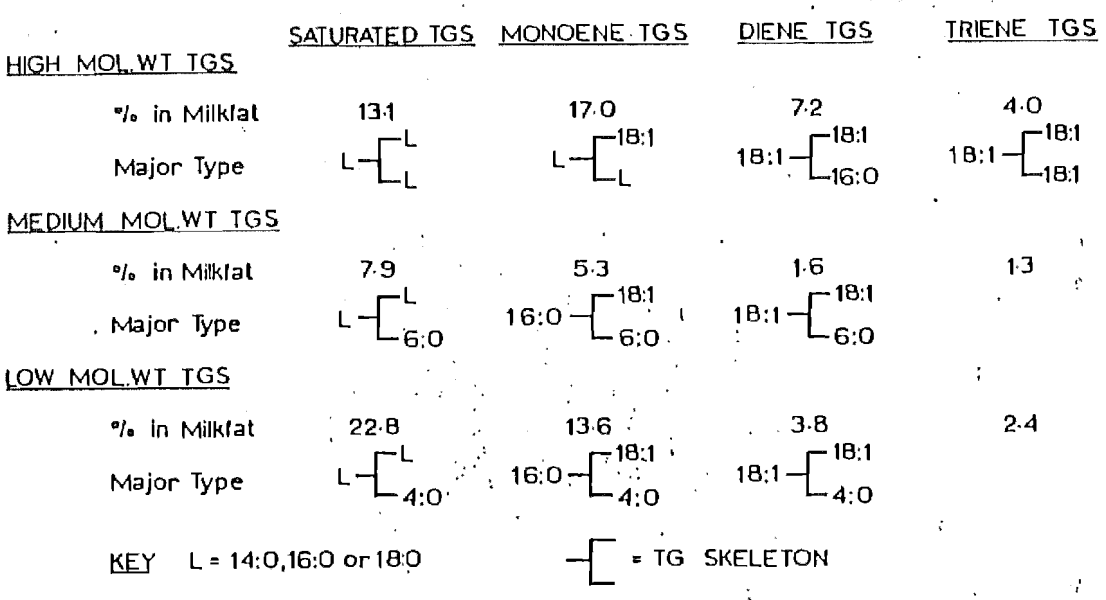

Figure 1.2 Principal Triglycerides Found in Butterfat.

For the purposes of solubility determination, many of these triglycerides were unobtainable in the necessary quantities and purity required for extraction studies, or were prohibitively expensive. Therefore it was decided to investigate pure, saturated, mono-acid triglycerides. These would range from the 3*C-12 trilaurin, to 3*C-18 tristearin (where C-x indicates the length of the fatty acid group attached to the glycerol backbone). This series ranges from a solid that melts at 45°C to a very high melting solid.

1.2.3 Solvent Choice

As shown in table 1.2, there is a large variety of possible supercritical solvents. Discussions with staff at the NZDRI suggested that from a commercial point of view, any solvent that would detrimentally alter the product flavour and functionality, or possibly leave a residue in a product was to be avoided. Carbon Dioxide became the obvious choice. The factors that were taken into account were;

1. Availability - CO_2 is readily available in high purity and at low cost.

2. Toxicity - CO_2 is non toxic and hence poses no threat to the laboratory environment if either discharged or there is a seal failure.
3. Critical Temperature - For dairy products, the maximum desirable processing temperature is considered to be 55°C to 60°C. Above these temperatures, any proteins present will begin to be denatured. CO_2, with a critical temperature of 31°C enabled use of reduced temperatures of up to 1.1 without likely damage to the material being processed.
4. Sensitivity - even at elevated temperature and pressure CO_2 has no effect on the flavour of most food products.

1.3 Objectives of this Work

The aims and objectives of this work were to;

1. Review the SFE literature and compile a comprehensive bibliography of SFE papers applicable to the food industries.
2. Design, build and commission an extraction apparatus.
3. Generate new solubility data for the chosen solutes.
4. Compare the performance of the theories in predicting experimental solubilities.

1.4 Organisation of Thesis

This thesis is divided into seven chapters and several appendices.

Chapter 1. A brief introduction to supercritical fluid extraction is presented. The reasons for the choice of solute and solvent are outlined. The aims and objectives of the project are stated.

Chapter 2. Chapter 2 is divided into two parts. The first part presents a review of the experimental data gathered during the course of this work. The results of this review are discussed. Part two presents a review of the commonly used solubility prediction methods.

Chapter 3. The literature pertaining to apparatus for the determination of solubility data is reviewed and discussed. The design of the apparatus is presented and the experimental method is detailed.

Chapter 4. In this chapter, the experiences gained in the construction and testing of the equipment are discussed. A comparison between the results from this work and those from the literature is made to verify the system. The limitations of the equipment and possible solutions to these limitations are outlined.

Chapter 5. The results from the experimental programme are presented in graphical and tabular form. Comments are made regarding these solubilities.

Chapter 6. In this chapter a comparison between the experimental solubilities and those obtained from the other theories is made. The prediction and correlation methods are compared and their applicability is commented upon.

Chapter 7. Conclusions from the current work are presented. Some recommendations for further work are suggested.

There are several appendices. These contain the workshop drawings, an equipment list, the raw solubility measurements and HPLC calibration data. The collected bibliography is available on microfiche and a copy may be obtained from Dr. P.J. Jordan.

2

Literature Review

2.1 Introduction

This chapter has been divided into two sections. In the first section, a review of collected solubility data is presented; in the second section prediction and correlation methods are reviewed. These sections are labelled 2a and 2b respectively. For convenience, the references for data compiled in the tables presented in Section 2a are included at the end of that section. They are listed in alphabetical order and numbered. The papers referred to in section 2b are listed in the references chapter.

2a.1 Introduction to Data Review.

Paulaitis *et al* (1983) have reviewed the solubility literature until 1982. The solutes they survey are divided into solids and liquids. For the solids the most common solvent used is CO_2. Other solvents included the light hydrocarbons, ethane and ethylene. The solids range from simple hydrocarbons (Naphthalene) to complex natural products (Coal Tar). Only a few studies presented results for solid mixtures. The authors noted that the object of many of the studies was data other than solubility measurements (for example second virial coefficients). Many of the studies involving liquid solutes were concerned with obtaining information about intermolecular interactions (using Argon, Nitrogen and Hydrogen as solvents).

Randall (1982) reviewed solubility data for solid and liquid solvents in dense gases. The results presented are in many cases the same as those papers used in the review of Paulaitis and co-workers. The range of compounds is the same. Unlike Paulaitis *et al* (1983), Randall has reviewed data for mixed solvents. Randall identified CO_2, Ethylene and n-Pentane as the most commonly used solvents

The review presented below was initiated by a need to obtain papers detailing solubilities of triglycerides, fats, oils and food and related products in supercritical solvents. Information

on experimental supercritical fluid extraction system design was also sought. This review is not exhaustive and the data are not critically evaluated. This review covers papers published from 1982 hence most papers reviewed by Randall (1982) and Paulaitis et *al* (1983) have not been included.

To start the review, an on-line search of Chemical Abstracts (CA), Food Science and Technology Abstracts (FSTA), Agricola and Compendix databases was performed (with keywords used);

CA (solubility or extraction) and (milk()fat or oil or lipid or glyceride or protein) and supercritical and (solvent of CO_2 or fluid or gas). 77 refs.

FSTA (solubility or extraction) and (milk()fat or oil or lipid or glyceride or protein or mono- or di- or tri-glyceride) and supercritical and (solvent of CO_2 or fluid or gas). 59 refs.

Compendix (solubility or extraction) and (milk()fat or oil or lipid or glyceride or protein or mono- or di- or tri-glyceride) and supercritical and (solvent of CO_2 or fluid or gas). 20 refs.

Agricola (solubility or extraction) and (milk()fat or oil or lipid or glyceride or protein or mono- or di- or tri-glyceride) and supercritical and (solvent of CO_2 or fluid or gas). 14 refs.

From these collected references, certain journals were targeted for the bulk of the data collection. This early search produced many general articles, review papers and some data for the extraction of seed oils and pharmaceutical compounds. Subsequent searching of Chemical Abstracts and various journals looked at experimental methods and prediction (or correlation) methods. We were also fortunate to have access to the collected references of the Industrial Processing Division of the New Zealand Department of Scientific and Industrial Research (IPD) and the supercritical group at the Department of Chemical Engineering and Industrial Chemistry, University of New South Wales.

The data presented below have been divided by extraction solvent. Starting with pure components, the solutes are listed alphabetically. The "mixtures" listed in tables 2.1 and 2.2 are artificial e.g. 50% naphthalene and 50% phenanthrene. Palm oil is treated as a pure compound although it is a complex lipid mixture. Mixtures are listed separately again by solvent and alphabetically by solute (for mixtures, the solute that appears first alphabetically is listed first). In the case of solvent mixtures, the additive is called an entrainer and listed in the "comments" section of the table. In all cases the conditions are presented in the units given in the papers.

No attempt has been made to search the patent literature. McHugh and Krukonis (1986) have compiled a list of over 200 patents, presented in an appendix in their book.

Table 2.1 Solubility Data for Pure Compounds

Solute	Conditions	Comments	Ref
Carbon Dioxide			
Acetone	-50 - 50°C 17-63 Bar		45
	313,333 K 20-150 Bar	Phase Equilibria, See also Mixtures	81
Acridine	35°C 90-350 Bar	Entrainers: Acetone, Methanol.	30
	35-70°C 60-360 Bar		89
Acrylonitrile	25°C 900-1200 psi		69
Alkaloids	40°C 80-200 Bar		91
Almonds	60°C 100-400 Bar		17
2-Aminobenzoic Acid	35°C 90-350 Bar	Entrainers: Methanol, Acetone.	30
2-Aminofluorene	35-70°C 60-360 Bar		89
5-Aminoindole	308 K 8-18 MPa		80
Anethole	40°C 40-150 Bar		93
Anhydrous Milk Fat	50-70°C 100-350 Bar	Fractionation	1
Animal Tissue	40°C 90-350 Bar		97
Anthracene	313 K 100-200 Bar		62
	35°C 120-350 Bar	Entrainer: Methanol. See also Mixtures	28
	20-95°C 69-1156 Bar		107
	308,318 K 103-273.1 Atm	See also Mixtures	57
	30-70°C 90.6-414.5 Bar		52
Behenyl Behenate	40-60°C 100-250 Atm		21
1,4-Benzenediol	25°C, 32°C 2500 psi		24

Benzoic Acid	45.1°C 101 Bar	Graphical (Recorded Over Time)	8
	25°C, 32°C 2500 psi		24
	35°C 120-350 Bar	Entrainer: Methanol. See also Mixtures	28
	318-338 K 120-280 Bar		60
	35.1-70.1°C 101-363 Bar		89
	55°C 200 202 Bar	Entrainers: Benzene, Acetone, Cyclohexane, Methylene Chloride.	88
	35°C 120-350 Bar	Entrainers: Acetone, n-Octane, Methanol.	30
Biphenyl	35.8-57.5°C 104.6-484.0 Bar		72.
	55.2°C 503-530 atm		82
n-Butanol	52, 72°C 5000-10000 psi		35
(Z)-Butenedioic Acid	25°C, 32°C 2500 psi		24
Butterfat	80°C 200 Bar	15 Hours contact	54
	40-250°C 100-400 Bar	Patent	5
Cafestol	40-80°C 80-250 Atm		21
Canola Seed	40°C 30, 35 MPa		15
	55°C 36 MPa	Rate data	64
Carvone	40°C 40-150 Bar		93
Carbazole	313 K 100-200 Bar		62
Caryophyllene	40°C 40-150 Bar		93
Castor	40°C 90-300 Bar	Entrainers: Hexane, Benzene, IPA, Methanol, Water, Chloroform.	97
Castor Oil	52-72°C 5000-20000 psi		35
Cedar Wood	45°C 300 Atm		44
Chewing Gum	45°C 300 Atm		44
p-Chlorphenol	36°C 79-236.7 atm	102	

Cholesterol	35-60°C 100-350 Bar	Entrainers: Methanol, Ethanol, Acetone	104
	40-80°C 80-250Atm		21
Cinnamon	300 atm	No temperature information	44
Copra	40-60°C 300-900 Bar,		9
Corn Oil	50-90°C 8000-12000 psi		66
Cotton Seeds and Oil	40°C 350 Bar	Seeds.	96
	50°C 8000 psi		91
	50-80°C 8000-15000 psi	Flaked Seed	68
Crude Oils	40°C 100-200Atm,	Graphs from a conference presentation	39
1,10-Decandiol	318-328 K 13-31 MPa	See also Mixtures	20
	318-328 K 133-308 Bar	See also Mixtures	84
Decanoic Acid	25°C, 32°C 2500 psi		24
DDT	40,80°C 100 Atm	Entrainers: Methanol, Toluene	31
	40°C 210-350 Bar	From Soil	7
Dibenzothiophene	309-338 K 76-276 Bar	See also Mixtures	76
2,4-Dichlorophenol	36°C 79.9-236.7 Bar		102
Dihydroxybenzenes	328 K 310 Bar		59
2,6-Dihydroxybenzoic Acid	25°C, 32°C 2500 psi		24
2,3-Dimethylnaphthalene	308-328 K 80-280 Bar		60
2,6-Dimethylnaphthalene	308-328 K 80-280 Bar		60
2,2-Dimethylpropanoic Acid	25°C, 32°C 2500 psi		24
2,6-Dinitrophenol	25°C, 32°C 2500 psi		24
2,6-Dinitrotoluene	25°C, 32°C 2500 psi		24
Di(o-xylyl)ethane	25°C, 32°C 2500 psi		24
Dyes	40°C 80-200 Bar		91
Efrotomycin	40°C 5000 psi	Entrainers: Acetone, Methanol, Acetic Acid, t-Butylamine	63

Emmental Cheese	14-50°C 200-400 Bar		18
EPA	50°C 150 Bar	From Codfish Oil	33
Ergosterol	40°C 80-200 Bar		94
	35°C 250,277 Bar		104
Erosterol	35-60°C 100-350 Bar		104
Estradiol	40°C 80-200 Bar		94
Ethanol	360-400 K 80 Bar		11
	313,333 K 20-150 Bar	Phase Equilibria, See also Mixtures	81
Ethinylestradiol	40°C 80-200 Bar		94
Ethyldodecanoate	25°C, 32°C 2500 psi		24
Ethylene Glycol	52,72°C 5000-10000 psi		35
Eugenol	40°C 40-150 Bar		93
Fatty Acids.	323 K 8-25 MPa	Lauric, Myristic, Palmitic	2
	313-353 K 5-20 MPa.	Oleic Acid	85
	35-60°C 20-30 MPa	Stearic, Palmitic, Myristic, Oleic.	12
	318-338 K 140-575 Bar,	Palmitic	58
	40-60°C 65-200 Bar	Stearate, Myristate, Oleate, Linoleate, Laurate.	105
	40-60°C 80-250Atm	Stearic, Oleic, Behenic	21
Fluorene	313 K 100-200 Bar		62
	30-70°C 7-48.35 MPa		52
2-Fluorophenol	25°C, 32°C 2500 psi		24
Ginger Oil	0-10°C 8-80atm	Liquid CO2	79
Glycerol	52,72°C 5000-10000 psi		35
Hexachloroethane	308-328 K 80-280 Bar		60
1-Hexadecanol	318-338 K 141-415 Bar		58

Hexamethylbenzene	35°C 100-350 Bar	Entrainers: Acetone, Methanol.	30
	35°C 100-350 Bar	Pure and Entrainers: n-Pentane, n-Octane, n-Unadecane.	29
	30-70°C 6.9-48.3 Bar		52
Hops	0-10°C 8-80atm	Liquid CO2	79
	40°C max	Liquid. No Pressure data	103
o,m&p-Hydroxybenzoic Acid	373 K 200-400 Bar		59
5-Hydroxyindole	308 K 8-18 MPa		80
Imipenem	40°C 5000 psi		63
Indole-3-aldehyde	308 K 8-18 MPa		80
Indole-3-Carboxylic Acid	308 K 8-18 MPa		80
IPE	-50 - 50°C 17-63 Bar	Liquid CO2	45
Jojoba Oil and Beans	20-80°C 150-2600 Bar		95
	40°C 200 Bar,		97
	40°C 350 Bar		96
	52,72°C 5000-10000 psi		35
Juniper Berry	0-10°C 8-80atm	Liquid CO2	79
Krill	80°C 250 Bar		106
Lemon Oil	303 313 K 4-9 MPa		23
	50-80°C 100,200 Bar		75
	40-80°C 150-2600 Bar		95
	40°C 300 Bar		17
Lilac	34°C 90 Bar		17
Limolene	40°C 80 Bar		8
	40°C 40-150 Bar		93
Lupin	25-80°C 100-500 Bar		98
	40°C 350 Bar	Crushed	96
2-Methyl-3-hexanol	25°C, 32°C 2500 psi		24

1-Methylnaphthalene	308 K 3.7-7.8 MPa	Chromatographic determination	3
Methyl-nitrobenzoate Isomers	308 K 80-280 Bar	See also Mixtures	19
o-Methoxyphenol	25°C, 32°C 2500 psi		24
Methoxy-1-tetralone Isomers	308 K 80-280 Bar	See also Mixtures	19
5-Methoxyindole	308 K 7-19 MPa		86
Mevinolin	40°C 5000 psi	Entrainers:Acetone, Methanol, Acetic Acid, t-Butylamine	63
Monocrotaline	308-328 K 18-27 MPa	Entrainer: Ethanol	87
Naphthalene	35-64.9°C 81-290 Atm		72
	313 K 100-200 Bar		62
	35°C 120-243 Bar		29
	308-328 K 91-170 atm	Graphical	99
	309,328 K 76-277 Bar	See also Mixtures.	76
	308 K 3.2-6.5 MPa	Chromatographic	3
	308 K 90-220 Bar		6
	328 K 125-253 Bar		60
	40°C 3350 psi		63
	318,328 K 83-276 Bar	See also Mixtures	19
2-Naphthol	45.1°C 362 Bar	Graphical (Recorded over time)	8
	35-70°C 60-360 Bar		89
	35°C 120-350 Bar	Entrainer: Methanol. See also Mixtures	28
	35°C 90-350 Bar	Entrainers: Methanol.	30
α&β-Naphthol	308-328 K 91-170 atm	See also Mixtures	99
1,4-Naphtholquinone	35-70°C 60-360 Bar		89
2-Nitroacetophenone	25°C, 32°C 2500 psi		24
2-Nitrobenzahdehyde	25°C, 32°C 2500 psi		24
o&p-Nitrophenol	25°C, 32°C 2500 psi		24

Octadecane	310-320 K 110-220 Bar	(+ 24 deravitives) See note 1	90
Orange Peel	45°C 300 Atm		44
Oxindole	308 K 8-18 MPa		80
Palm Oil	50-80°C 100,200 Bar		75
	75°C 80-400 Bar	Entrainer: Ethanol	14
Palmityl Behenate	40 50 60°C 100-250Atm		21
PCB's	40°C 210-350 Bar	From Soil	7
Peanut Oil	25°C 530 Bar	From Peanut Flakes	40
	50°C 8000 psi		91
Pepper	60°C 100-400 Bar		17
Phenanthrene	313 K 100-200 Bar	(See also Mixtures)	62
	30°C 80-220 Bar		6
	35°C 100-350 Bar	Entrainers: n-Pentane, n-Octane, n-Unadecane.	29
	318-338 K 120-280 Bar		60
	30-70°C 8.1-41.5 MPa		52
	55°C 111-305 Bar	Entrainers: Benzene, Acetone, Cyclohexane, Methylene Chloride.	88
Phenol	36,60°C 80-250 atm		102
Phthalic Anhydride	35°C 90-350 Bar	Entrainers: Acetone.	30
Poly(ethylene-co-propylene)	to 150°C 2.76-31.0 MPa	Phase Behaviour	70
Propylene Chlorohydrin	25°C 900-1200 psi		69
Pyrene	35-70°C 8.7-48.3 MPa		52
Pyrethrym	20-40°C 80-150 Bar		16
Pyrrole	25°C, 32°C 2500 psi		24
Pyrrolidine	25°C, 32°C 2500 psi		24
Radix Valerianae	313 K 96 Bar		101

Rape Oil and Seeds	25-75°C 70-200 Bar	Seeds. Rate Data	55
	313.5-373.15 K 10-85 MPa	Oil	56
	323-373 K 10-85 MPa	Oil.	47
	30-40°C 100-250 Bar	Oil	16
	60°C 350,750 Bar	Entrainer: Propane	32
Rosemary	45°C 300 Atm		44
Sigmasterol	35-60°C 100-350 Bar	Entrainers: Acetone, Ethanol, Methanol	104
Sitosterol	40°C 80-200 Bar		94
Skatole	308 K 7-19 MPa		86
Solasodin	40°C 80-200 Bar		94
Soy Oil flakes and seeds	52,72°C 5000-10000 psi	Oil	35
	0°C 5000 psi	Oil, compared to hexane	36
	25-80,°C 100-600 Bar	Oil, Graphical	74
	50°C 8000 psi	Oil	67
	40-80°C 100-500 Bar	Oil, Graphical	98
	40-80°C 100-2500 Bar	Oil Graphical	95
	50°C 200 Bar	Oil Defatting	34
	50°C 150 Bar	Oil Deodourisation	34
	50,60°C 2000-10000 psi,	Beans	37
	40°C 350 Bar	Flakes. Compared to Hexane	96
	40°C 200 Bar	Beans	97
	50°C 8000 psi	Beans, Flakes	91
Spruce Needles	45°C 300 Atm		44
Sunflower Seeds	25-80°C 100-400 Bar		73
	40°C 80-200 Bar		91
Tall Oil	47°C 250 Bar		43
Terpenes	25-80°C 150-2600 Bar		95

2,6,10,14-Tetramethylpentadecane	25°C, 32°C 2500 psi		24
Thyme	80 atm	No temperature information	44
α-Tocopherol	40-80°C 100-250Atm		21
Toxaphene	40°C 210-350 Bar	From Soil	7
Triethylene Glygol	52,72°C 5000-10000 psi		35
Triclycerides	313-333 K 9.8-27 MPa	Olein, Stearin. Entrainer: Methylacetate, Ethanol, Ether, Acetone, Ethyl Acetate	47
	25-75°C to 200 Bar	Glycerol trioleate	55
	323 K 9.5-30 MPa	Laurin, Myristin, Palmitin (see also Mixtures)	2
	313,333 K 9.8-27 MPa	Stearin	48
	313 K 19.6 MPa	Olein, Entrainers: Ethanol, Ether, Acetone, Ethyl Acetate, Ethylene Dichloride	48
	35-60°C 20-30 MPa	Olein, Stearin. (see also Mixtures)	12
	40-80°C 80-250 Atm	Butyrin, Palmitin, Stearin, Olein, Linolein	21
	35-55°C 8.3-36.9 MPa	Laurin, Myristin, Palmitin, Stearin	83
2,4,4-Trimethyl-1-pentanol	25°C, 32°C 2500 psi		24
Trout Lipids	40-50°C 13.8-34.5 MPa	Entrainer: Ethanol	42
Triphenylmethane	30-50°C 6.9-41.4 MPa		52
Valeranone	40°C 40-150 Bar		93
Vanillin	42-56°C 80-220 Bar		6
Water	50-80°C 100-250Atm		21
Wax	40-100°C 150-500 Bar	Montan Crude	10
Wheat Germ	12-40°C 200 Atm	Graphical	100
Wine	20°C 60-65Atm		53
n-Butane			
Ethanol	360-400 K 80 Bar		11

Ethane			
Acridine	35-70°C 60-360 Bar		89
2-Aminofluorene	35-70°C 60-360 Bar		89
5-Aminoindole	308 K 8-18 MPa		80
Anthracene	30-70°C 10.4-48.3 MPa		52
Benzoic Acid	55°C 100-300 Bar	Entrainers: Benzene, Cyclohexane, Acetone, Methylenechloride	88
	35-70°C 60-360 Bar		89
Biphenyl	35-70°C 60-360 Bar		89
n-Dotriacontane	308-318 K 6.5-20 MPa		78
5-Hydroxyindole	308 K 8-18 MPa		80
Indole-3-aldehyde	308 K 8-18 MPa		80
Indole-3-carboxylic Acid	308 K 8-18 MPa		80
5-Methoxyindole	308 K to 20 MPa		86
Naphthalene	20-45°C 4.2-27.7 MPa		52
	35.1-55.0°C 51-364 Bar		89
2-Naphthol	35-70°C 60-360 Bar		89
1,4-Naphthoquinone	35-70°C 60-360 Bar		89
Oleic Acid	313-353 K 5-20 MPa		85
Oxindole	308 K 8-18 MPa		80
Phenanthrene	30-60°C 6.9-41.4 MPa		52
	35-70°C 60-360 Bar		89
	55°C 100-300 Bar	Entrainres: Benzene, Cyclohexane, Acetone, Methylenechloride	88
Skatole	308 K to 20 MPa		86
n-Triacontane	308-318 K 6.5-20 MPa		78
Triphenylmethane	30-50°C 6.9-38.3 MPa		52

Ethylene			
5-Aminoindole	308 K 8-18 MPa		80
Anthracene	50-85°C 10.4-48.3 MPa		51
Benzoic Acid	318-338 K 120-280 Bar		60
2,3-Dimethylnaphthalene	308-328 K 80-280 Bar		60
2,6-Dimethylnaphthalene	308-328 K 80-280 Bar		60
Fluorene	25-70°C 6.9-48.3 MPa		52
Hexamethylbenzene	25-70°C 6.3-48.3 MPa		52
Hydroxyindole	308 K 8-18 MPa		80
Indole-3-aldehyde	308 K 8-18 MPa		80
Indole-3-carboxylic Acid	308 K 8-18 MPa		80
Methoxyindole	308 K to 20 MPa		86
Naphthalene	25-50°C 5.6-17.3 MPa		51
Oxindole	308 K 8-18 MPa		80
Oleic Acid	20-126°C 100-300 Bar		14
Palm Oil	75°C 80-400 Bar	Entrainer: Ethanol	14
Phenanthrene	318-338 K 80-280 Bar		60
	25-70°C 5.6-27.7 MPa		51
Pyrene	45,75°C 8.4-48.3 MPa		52
Skatole	308 K to 20 MPa		86
Methane			
Acetone	-50 - 50°C 17-63 Bar		45
Coal Tar	to 200°C to 150 Bar		77
Hexadecane	to 200°C to 150 Bar		77
IPE	-50 - 50°C 17-63 Bar		45

Nitrogen			
Acetone	-50 - 50°C 17-63 Bar		45
IPE	-50 - 50°C 17-63 Bar		45
Palm Oil	75°C 80-400 Bar	Entrainer: Ethanol	14
Nitrous Oxide			
Crude Opium	40°C 80-200 Bar		91
Palm Oil	75°C 80-400 Bar	Entrainer: Ethanol	14
Propane			
Ethanol	360-400 K 80 Bar		11
n-Octadecane	390, 420 K up to 60 Bar	See also Mixtures	27
Phenanthrene	390, 420 K up to 60 Bar	See also Mixtures	27
Trifluorochloromethane			
Acridine	35-70°C 60-360 Bar		89
2-Aminofluorene	35-70°C 60-360 Bar		89
Benzoic Acid	35-70°C 60-360 Bar		89
Naphthalene	35-70°C 60-360 Bar		89
2-Naphthol	35-70°C 60-360 Bar		89
1,4-Naphthoquinone	35-70°C 60-360 Bar		89
Oleic Acid	-125 - -50°C 50-330 Bar		14
Palm Oil	75°C 80-400 Bar	Entrainer: Ethanol	14
Phenanthrene	35-70°C 60-360 Bar		89
Trifluoromethane			
Acridine	35-70°C 60-360 Bar		89
2-Aminofluorene	35-70°C 60-360 Bar		89
5-Aminoindole	308 K 8-18 MPa		80
Anthracene	35-70°C 60-360 Bar		89

Benzoic Acid	35-70°C 60-360 Bar		89
5-Hydroxyindole	308 K 8-18 MPa		80
Indole	308 K to 20 MPa		86
Indole-3-aldehyde	308 K 8-18 MPa		80
Indole-3-Carboxylic Acid	308 K 8-18 MPa		80
5-Methoxyindole	308 K to 20 MPa		86
Naphthalene	35-70°C 60-360 Bar		89
2-Naphthol	35-70°C 60-360 Bar		89
1,4-Naphthoquinone	35-70°C 60-360 Bar		89
Oxindole	308 K 8-18 MPa		80
Phenanthrene	35-70°C 60-360 Bar		89
Skatole	308 K to 20 MPa		86
Water			
Car Tyre	653 K 23 MPa		38
Coal	650 K 22 MPa		25
Glucose	650 K 22 MPa		25
Xenon			
Naphthalene	35,45°C 105-268 Bar		71

Note 1. Schmitt and Reid examined 25 model compounds, Octadecane through to Tetracosane with related monofunctional groups. The derivatives included sulphides, amines, phosphines, ketones and others.

Table 2.2 Solubilities of Mixtures

Solute 1	Solute 2	Conditions	Ref
Ammonia			
Biphenyl	Dodecane	53.7, 97.7°C 104.8, 188.1 atm	26
CO_2			
Acetone	Water	313,333 K 20-150 Bar	81
Anthracene	2-Naphthol	35°C 100-300 Bar	28
	2-Aminobenzoic Acid	35°C 100-300 Bar	28
	Carbazole	313 K 100-200 Bar	62
	Fluorene	313 K 100-200 Bar	62
	Phenanthrene	308, 318 K 103-239 Bar	57
		313 K 100-200 Bar	62
Benzoic Acid	1,10-Decanediol	308,318 K 163-300 Bar	20
		308,318 K 163-300 Bar	84
	Hexamethylbenzene	35°C 100-300 Bar	28
	Naphthalene	308, 318 K 120-280 Bar	61
	Phenanthrene	308 K 120-280 Bar	61
Biphenyl	Dodecane	53.7, 97.7°C 104.8, 188.1 atm	26
	Naphthalene	308, 318 K 6-28 MPa	41
Carbazole	Phenanthrene	313 K 100-200 Bar	62
Dibenzothiophene	Naphthalene	309 K 75-275 Bar	76
2,3-Dimethylnaphthalene	2,6-Dimethylnaphthalene	35,50°C 115-124 Bar	50
		308, 318 K 120-280 Bar	61
	Naphthalene	308 K 120-280 Bar	61
	Phenanthrene	308, 318 K 120-280 Bar	61
2,6-Dimethylnaphthalene	Phenanthrene	308 K 120-280 Bar	61

Docosahexaenoic Acid	Eicosapentaenoic Acid	60°C 140, 150 Bar	65
Hexadecane	Hexadecanol	70°C 200 Bar	13
	Octadecane	70°C 200 Bar	13
Hexadecanol	Octadecane	70°C 120, 200 Bar	13
Fatty Acids	Linoleic,Linolenic,Oleic	305, 313 K 9.3, 10.8 MPa	49
	Linoleic,Stearic, Linolenic,Oleic.	313K 8.8-10.8MPa	46
	Palmitic, Arachidic, Behenic, Stearic, Linoleic, Oleic, Linolenic	313-333K 9.8-27 MPa	47
5-Methoxy-1-tetralone	7-Methoxy-1-tetralone	308 K 110 Bar	19
6-Methoxy-1-tetralone	7-Methoxy-1-tetralone	308 K 110 Bar	19
Methyl-m-Nitrobenzotae	Methyl-o-Nitrobenzotae	308 K 110 Bar	19
Methyl-o-Nitrobenzotae	Methyl-p-Nitrobenzotae	308 K 110 Bar	19
Naphthalene	Phenanthrene	308 K 120-280 Bar	61
		308, 318 K 6-28 MPa	41
	Phenol	308, 318 K 6-28 MPa	41
α-Naphthol	β-Naphthol	308-328K 91-170 atm	99
Oleic Acid	α-Tocopherol	60°C 160 Atm	4
	Water	60°C 115 Atm	4
	α-Tocopherol/Water	60°C 115 Atm	4
Palmitic Acid	Stearic Acid	40°C 20MPa	12
Trilaurin	Trimyristin	313 K 8-30 MPa	2
	Tripalmitin	313 K 8-30 MPa	2
	Trimyristin/Tripalmitin	313 K 8-30 MPa	2
Trimyristin	Tripalmitin	313 K 8-30 MPa	2
Triolein	Tristearin	40°C 20MPa	12
	Tristearin	313 K 19.6 MPa	47

Ethane			
Hexadecanol	Octadecane	70°C 120 Bar	13
Biphenyl	Dodecane	53.7, 97.7°C 104.8, 188.1 atm	26
Ethylene			
2,3-Dimethylnaphthalene	2,6-Dimethylnaphthalene	308 K 120-280 Bar	61
N_2O			
Hexadecanol	Octadecane	70°C 120 Bar	13
Octadecane	Salicylic Acid Phenyl Ester	70°C 120 Bar	13
Propane			
n-Octane	Phenanthrene	388, 419 K 42.7, 54 Bar	27

2a.2 Comments.

Since the reviews of Randall (1982) and Paulaitis *et al* (1983) were published, many workers have published solubility data for compounds as diverse as chewing gum and DDT. Much of this data appears to have been generated with a view to future commercial development. This is especially true of the food type solutes (e.g. cinnamon and ginger) and solutes of interest to the pharmaceutical industry (e.g. steroids). In many cases, naphthalene and phenanthrene have been examined as a means of system verification.

There have been several studies of the effect of functional groups on solute solubility (Dandage, 24, Kurnik and Reid, 61, Schmitt and Reid, 90). These have included studies of several similar compounds (commonly derivatives of a parent molecule) in one solvent. The effect of a variety of diverse solvents on a selection of solutes has also been examined (Schmitt and Reid, 89). These two types of studies help in understanding the intermolecular interactions and in defining what happens in the solubility process. Several studies have examined the effect of entrainers (Larsen and King, 63, Schmitt and Reid 88). These have involved changing both the type and amount of entrainer studied. This knowledge can assist in choosing the most appropriate solvent for a particular extraction. The effect of a second solute on the solubility of a first has also been examined. With the mixtures the most commonly used solvent was CO_2.

While CO_2 is still the dominant solvent, other solvents are being investigated. This trend is prompted both by a desire to investigate solvents with different characteristics and because many solutes have an absolute solubility in CO_2 that is too low for commercial exploitation.

2a.3 Previous Work on Triglycerides.

At the time of this search, the only published values found for pure triglycerides were those of Chrastil (21), King *et al* (55) and Ikushima *et al* (48). The compounds examined were Tristearin, Trilinolein, Triolein, Tripalmitin and Tributyrin. These solubilities were obtained at one or two temperatures, commonly 40 and 60°C and over a pressure range of 9 to 30 MPa. Only Chrastil examined solutes other than Tristearin and Triolein. There is a lack of data for medium chain triglycerides, Trilaurin, Trimyristin and Tripalmitin. No studies have compared the effect of chain length on solubility for more than two solutes, or for more that three temperatures.

During the course of this work, Bamberger *et al* (2) and Brunetti *et al* (12) published data for pure triglycerides. Bamberger obtained data for Trilaurin, Trimyristin and Tripalmitin at 40°C and over a pressure range of 9 to 30 MPa.

The experimental data obtained during the course of the following work has been compared to that of Chrastil, Ikushima, Bamberger and Brunetti. Comparison of their results with this work is discussed in §4.5.2.

2a.4 References.

1. Arul, J., Boudreau, A., Makhlouf, J., Tardif, R. and Sahasrabudhe, M.R., 1987, Fractionation of Anhydrous Milk Fat by supercritical carbon dioxide., *J. Food Sci.*, **52** (5), 1231-1236.

2. Bamberger, T., Erickson, J.C., Cooney, C.L. and Kumar, S.K., 1988, Measurement and model prediction of solubilities of pure fatty acids, pure triglycerides and mixtures of triglycerides in supercritical carbon dioxide, *J. Chem. Eng. Data,* **33**(3), 327-333.

3. Barker, I.K., Bartle, K.D. and Clifford, A.A., 1988, Measurement of solubilities in fluids at supercritical temperatures and lower pressures using chromatographic retention.*Chem. Eng. Comm.,* **68**, 177-184.

4. Bertucco, A., Guarise, G.B., Dahir, M. and Navazio, G., 1988, Refining Fatty Acids with Supercritical CO_2. *Proc. Int. Symp. Supercrit. Fluids, Nice France.,*791-798.

5. Biernoth, G., Merk, W., 1985, Fractionation of Butterfat Using a Liquefied Gas or a Gas in the Supercritical State., *U.S. Patent,* **4,504,503**, March 12.

6. Billoni, N., Jose, J. and Merlin, J.C., 1988, Solubility of Heavy Components in Supercritical CO_2 Using direct coupled SFE-HPL Chromatography.*Proc. Int. Symp. Supercrit. Fluids, Nice France.,*373-380.

7. Brady, B.O., Chien-Peng C. Kao, Dooley, K.M., Knopf, F.C. and Gambrell, R.P., 1987, Supercritical Extraction of Toxic Organics from Soils., *Ind. Eng. Chem. Res.,* **26**, 261-268.

8. Brandani, V., del Re, G., di Giacomo, G. and Ferri, E., 1989, Solubility of Solids and Liquids in Supercritical Fluids, *Proc. Int. Symp. Supercrit. Fluids, Nice France.,*93-98.

9. Brannolte, H.D., Mangold, H.K. and Stahl, E., 1983, Effects of Pressure and Temperature of Supercritical Carbon Dioxide on the Extraction of Triacylglycerols from Plant Tissue., *Chem. Phys. Lipids*, **33**, 297-299.

10. Braun, G. and Schmidt, H., 1984, High Pressure Extraction of Crude Montan Wax., *Ber. Bunsenges. Phys. Chem.*, **88**, 891-894.

11. Brignole, E.A. Andersen, P.M. and Fredenslund, Aa., 1987, Supercritical Fluid Extraction of Alcohols from Water., *Ind. Eng. Chem. Res.*, **26**, 254-261.

12. Brunetti, L., Daghetta, A., Fedeli, E., Kikic, I. and Zanderighi, L., 1989, Deacidification of Olive Oils by Supercritical Carbon Dioxide, *JAOCS*, **66**(2), 209-217.

13. Brunner, G., 1983, Selectivity of Supercritical Compounds and Entrainers with Respect to Model Substances, *Fluid Phase Equilibria*, **10**, 289-298.

14. Brunner, G. and Peter, S., 1982, On the Solubility of Glycerides and Fatty Acids in Compressed Gases in the Presence of an Entrainer., *Sep. Sci. & Tech.*, **17** (1), 199-214.

15. Bulley, N.R., Fattori, M., Meisen, A. and Moyls, L., 1984, Supercritical Fluid Extraction of Vegetable Seed Oils., *JAOCS*, **61** (8), 1362-1365.

16. Bunzenberger, G., Lack, L. and Marr, R., 1983, CO_2 Extraktion., *Chem. Ing. Tech.*, **55**, 320-321.

17. Calame J.P. and Steiner R., 19 June 1982, CO_2 Extraction in the Flavour and Perfumery Industry.*Chem. & Ind.*,399-402.

18. Castera, A., Morin, O. and Coustille, J.L., 1988, Supercritical CO_2 Extraction of the Free Fatty Acids and other Volatile Components from a food Product for their analysis by coupling DCI/GC/MS.*Proc. Int. Symp. Supercrit. Fluids, Nice France.*,727-734

19. Chang, H. and Morrell, D.G., 1985, Solubilities of Methoxy-1-tetralone and methyl nitrobenzoate isomers and their mixtures in supercritical carbon dioxide, *J. Chem. Eng. Data*, **30**, 74-78.

20. Chimowitz, E.H. and Pennisi, K.J., 1986, Process Synthesis Concepts for Supercritical Gas Extraction in the Crossover Region., *AIChE J.*, **32** (10), 1665-1676.

21. Chrastil, J., 1982, Solubility of Solids and Liquids in Supercritical Gases., *J. Phys. Chem.*, **86**, 3016-3021.

22. Christianson, D.D., Friedrich, J.P., List, G.R., Warner, K., Bagley, E.B., Stringfellow, A.C. and Inglett, G.E., 1984, Supercritical Fluid Extraction of Dry-Milled Corn Germ with Carbon Dioxide, *J. Food Sci.*, **49**, 229-232.

23. Coppella, S.J. and Barton, P., 1985, Supercritical Carbon Dioxide Extraction of Lemon Oil., *Am. Chem. Soc. Div. Fuel Chem.*, **30** (3), 195.

24. Dandge, D.K., Heller, J.P. and Wilson K.V., 1985, Structure Solubility Correlations: Organic Compounds and Dense Carbon Dioxide Binary Systems., *Ind. Eng. Chem. Prod. Res. Dev.*, **24** (1), 162-166.

25. Deshpande, G.V., Holder, G.D., Bishop, A.A., Gopal, J. and Wender, I., 1984, Extraction of Coal Using Supercritical Water., *Fuel*, **63**, 956-960.

26. Dhalewadikar, S.V., Seckner, A.J., McHugh, M.A. and Guckes, T.L., 1987, Separation of Dodecane-Biphenyl Mixtures using Supercritical Ethylene, Carbon Dioxide and Ammonia., *Ind. Eng. Chem. Res.*, **26**, 976-982.

27. Dimitrelis, D. and Prausnitz, J.M., 1989, Solubilities of n-Octadecane, Phenanthrene and n-Octadecane/Phenanthrene Mixtures in Supercritical Propane at 390 and 420 K and Pressures to 60 bar., *J. Chem. Eng. Data,* **34**(3), 286-291.

28. Dobbs, J.M. and Johnston, K.P., 1987, Selectivities in pure and mixed supercritical fluid solvents., *Ind. Eng. Chem. Res.*, **26**, 1476-1482.

29. Dobbs, J.M., Wong, J.M. and Johnston, K.P., 1986, Nonpolar Co-Solvents for Solubility Enhancement in Supercritical Fluid Carbon Dioxide., *J. Chem. Eng. Data,* **30** (3), 303-308.

30. Dobbs, J.M., Wong, J.M., Lahiere, R.J. and Johnston, K.P., 1987, Modification of Supercritical Fluid Phase Behaviour Using Polar Cosolvents., *Ind. Eng. Chem. Res.*, **26**, 56-65.

31. Dooley, K.M., Kao, C-P., Gambrell, R.P. and Knopf, F.C., 1987, The use of entrainers in the supercritical extraction of soils contaminated with hazardous organics., *Ind. Eng. Chem. Res.*, **26** (10), 2058-2062.

32. Eggers, R., Sievers, U. and Stein, W., 1985, High Pressure Extraction of Oil Seed.*JAOCS*,**62**(8),1222-1230.

33. Eisenbach, W.O., 1984, Supercritical Fluid Extraction: A Film Demonstration., *Ber. Bunsenges. Phys. Chem.*, **88**, 882-887.

34. Eisenbach, W.O., 1988, Extraction and Fractionation of Natural Products. *Proc. Int. Symp. Supercrit. Fluids, Nice France.*,719-725.

35. Eissler, R.L. and Friedrich, J.P., 1988, Estimation of supercritical fluid-liquid solubility parameter differences for vegetable oils and other liquids from data taken with a stirred autoclave., *JAOCS*, **65**(5), 764-767.

36. Friedrich, J.P. and List, G.R., 1982, Characterisation of Soybean Oil Extracted by Supercritical Carbon Dioxide and Hexane., *J. Agric. Food Chem.*, **30**, 192-193.

37. Friedrich, J.P. and Pryde, E.H., 1984, Supercritical CO_2 Extraction of Lipid Bearing Materials and Characterisation of the Products., *JAOCS*, **61** (2), 223-228.

38. Funazukuri, T., Takanashi, T. and Wakao, N., 1987, Supercritical extraction of used automotive tire with water., *J. Chem. Eng. Japan*, **20** (1), 23-27.

39. Funk, E.W., 1985, Figures from presentation to the ACS meeting Chicago, Sept.

40. Goodrum, J.W. and Kilgo, M.B., 1988, Modeling of liquid CO_2 extraction of Peanut Oil in a fixed bed.*Trans. of the ASAE.*, **31**(3), 926-929.

41. Gopal, J.S., Holder, G.D. and Kosal, E., 1985, Solubility of solid and liquid mixtures in supercritical carbon dioxide., *Ind. Eng. Chem. Proc. Des. Dev.*, **24** (3), 697-701.

42. Hardarottir, I. and Kinsella, J.E., 1988, Extraction of Lipid and Cholesterol from Fish muscle with supercritical fluids., *J. Food Sci.*, **53**(6), 1656-1658.

43. Harvala, T., Alkio, M. and Komppa, V., 1987, Extraction of tall oil with supercritical carbon dioxide., *Chem. Eng. Res. Des*, **65**, 386-389.

44. Hawthorne, S.B., Krieger, M.S. and Miller, D.J., 1988, Analysis of flavour and fragrance compounds using supercritical fluid extraction coupled with gas chromatography., *Anal. Chem.*, **60** (5), 472-477.

45. Hicks Jr., P.J. and Prausnitz, J.M., 1981, Solubility of Acetone and Isopropyl Ether in Compressed Nitrogen, Methane and Carbon Dioxide., *J. Chem. Eng. Data*, **26**, 74-80.

46. Ikushima, Y., Arai, M., Hatakeda, K., Ito, S., Saito, N. and Goto, T., 1988a, Selective extraction of a mixture of Stearic, Oleic, Linoleic and Linolenic acid methyl Esters with supercritical carbon dioxide using a gas-flow method.*J. Chem. Eng. Japan*, **21**(4), 439-441.

47. Ikushima, Y., Hatakeda, K., Ito, S., Saito, N., Asano, T. and Goto, T., 1988b, A supercritical Carbon Dioxide extraction from mixtures of triglycerides and higher fatty acid methyl esters using a gas-effusion type system., *Ind. Eng. Chem. Res.*, **27** (5), 818-823.

48. Ikushima, Y., Saito, N., Hatakeda, K., Iot, S., Asano, T. and Goto, T., 1985, Effects of Entrainers on the Extraction of Triglycerides with Supercritical Carbon Dioxide., *Chem. Lett.*, 1789-1792.

49. Ikushima, Y., Saito, N. and Goto, T., 1989, Selective Extraction of Oleic, Linoleic and Linolenic Methyl Esters fom their Mixture with Supercritical Carbon Dioxide-Entrainer Systems and a Correlation of the Extraction Efficiency with a Solubility Parameter., *Ind. Eng. Chem. Res.*, **28**(9), 1364.

50. Johnston, K.P., Barry, S.E., Read, N.K. and Holcomb, T.R., 1987, Separation of isomers using retrograde crystallisation from supercritical fluids. *Ind. Eng. Chem. Res.*, **26**(11), 2372-2377.

51. Johnston, K.P. and Eckert, C.A., 1981, An Analytical Carnahan-Starling-van der Waals Model for Solubility of Hydrocarbon Solids in Supercritical Fluids., *AIChE J.*, **27** (9), 773-779.

52. Johnston, K.P., Ziger, D.H. and Eckert, C.A., 1982, Solubilities of Hydrocarbon Solids in Supercritical Fluids. The Augmented van der Waals Treatment., *Ind. Eng. Chem. Fundam.*, **21**, 191-197.

53. Jolly, D.R.P., 1981, Wine Flavour Extraction with Liquid Carbon Dioxide., *Process Biochem.*, 36-40.

54. von Kaufmann, W., Biernoth, G., Frede, E., Merk, W., Precht, D. and Timmen, H., 1982, Fraktionierung von Butterfett durch Extriktion mit Überkritischem CO_2., *Milchwissenschaft*, **37**, 92-96.

55. King, M.B., Bott, T.R., Barr, M.J. and Mahmud, R.S., 1987, Equilibrium and Rate Data for the Extraction of Lipids using Compressed Carbon Dioxide., *Sep. Sci. & Tech.*, **22** (2&3), 1103-1120.

56. Klein, T. and Schulz, S., 1989, Measurement and Model Prediction of Vapour-Liquid Equilibria of Mixtures of Rapeseed Oil and Supercritical Carbon Dioxide, *Ind, Eng. Chem. Res.*, **28**(7), 1073-1081.

57. Kosal, E. and Holder, G.D., 1987, Solubility of Anthracene and Phenanthrene Mixtures in Supercritical Carbon Dioxide., *J. Chem. Eng. Data,* **32**, 148-150.

58. Kramer, A. and Thodos, G., 1988, Solubility of 1-Hexadecanol and Palmitic Acid in supercritical carbon dioxide., *J. Chem. Eng. Data,* **33**(3), 230-234.

59. Krukonis, V.J. and Kurnik. R.T., 1985, Solubility of solid aromatic isomers in carbon dioxide., *J. Chem. Eng. Data*, **30**, 247-249.

60. Kurnik, R.T., Holla, S.J. and Reid, R.C., 1981, Solubility of Solids in Supercritical CO_2 and Ethylene., *J. Chem. Eng. Data*, **26** (1), 47-51.

61. Kurnik, R.T. and Reid, R.C., 1982, Solubility of Solid Mixtures in Supercritical Fluids., *Fluid Phase Equilibria*, **8**, 93-105.

62. Kwiatkowski. J., Lisicki, Z., Majewski, W., 1984, An Exerimental Method for Measuring Solubilities of Solids in Supercritical Fluids., *Ber. Bunsenges. Phys. Chem.*, **88**, 865-869.

63. Larson, K.A. and King, M.L., 1986, Evaluation of Supercritical Fluid Extraction in the Pharmaceutical Industry., Biotech. Prog. 2 (2), 73.

64. Lee, A.K.K., Bulley, N.R., Fattori, M. and Meisen, A., 1986, Modelling of Supercritical Carbon Dioxide Extraction of Canola Oilseed in Fixed Beds., *JAOCS*, **63** (7), 921-925.

65. Liong, K.K., Chaplin, R.P., Foster, N.R., Regtop, H. and Wells, R. 1988, Supercritical Fluid Extraction of Essential Fatty Acids from Marine Sources. *CHEMECA '88* 788-792.

66. List, G.R. and Friedrich, J.P., 1985, Processing Characteristics and Oxidative Stability of Soybean Oil Extracted with Supercritical CO_2 at 50oC and 8,000 psi., *JAOCS*, **62** (1), 82-84.

67. List, G.R., Friedrich, J.P. and Christianson, D.D., 1984a, Properties and Processing of Corn Oils Obtained by Extraction with Supercritical Carbon Dioxide., *JAOCS*, **61** (12), 1849-1851.

68. List, G.R., Friedrich, J.P. and Pominski, J., 1984b, Characterization and Processing of Cottonseed Oil Obtained by Extraction with Supercritical Carbon Dioxide., *JAOCS*, **61** (12), 1847-1849.

69. McGovern, W.E. and Rice, P.N., 1988, Critical Fluid Extraction treatment of oranic wastewater*Pollution Eng.*, **20**(9), 122-126.

70. McHugh, M.A. and Guckes, T.A., 1985, Separating polymer solutions the supercritical fluids., *Macromol.*, **18** (4), 674-680.

71. McHugh, M.A., Watkins, J.J., Doyle, B.T. and Krukonis, V.J., 1988, High pressure Naphthalene-Xenon phase behavior., *Ind. Eng. Chem. Res.*, **27**, (6), 1025-1033.76.

72. McHugh, M. and Paulaitis, M.E., 1980, Solid solubilities of nathphalene and biphenyl in supercritical Carbon dioxide., *J. Chem. Eng. Data*, **25** (4), 326-329.

73. Mangold, H.K., 1984, Extraction and Fractionation of Lipids with Supercritical Carbon Dioxide and Other Inorganic Solvents., Fats for the Future Conference, Auckland N.Z., 44-55.

74. Mangold, H.K., 1983, Liquefied Gases and Supercritical Fluids in Oilseed Extraction., *JAOCS*, **60** (2), 226-228.

75. Mathias, P.M., Copeman, T.W. and Prausnitz, J.M., 1986, Phase Equilibria for Supercritical Extraction of Lemon Flavours and Palm Oils with Carbon Dioxide., *Fluid Phase Equilibria*, **29**, 545-554.

76. Mitra, S., Chen, J.W. and Viswanath, D.S., 1988, Solubility and Partial molar volumes of heavy aromatic hydrocarbons in supercritical CO_2., *J. Chem. Eng. Data*, **33**, 35-37.

77. Monge, A. and Prausnitz, J.M., 1983, An Experimental Method for Measuring Solubilities of Heavy Fossil-Fuel Fractions in Compressed Gases to 100 Bar and 300°C., in "*Chemical Engineering at Supercritical Fluid Conditions*", Paulatis, M.E., et al Eds, Ann Arbor Science, 159-172.

78. Moradinia, I. and Teja, A.S., 1985, Solubilities of Solid n-Alkanes in Supercritical Ethane., *Am. Chem. Soc. Div. Fuel Chem.*, **30** (3), 40.

79. Moyler, D.A., 1984, Carbon Dioxide Extracted Ingredients for Fragrances., *Perfumer and Flavourist*, **9**, 109-114.

80. Nakatani, T., Ohgaki, K. and Katayama, T., 1989, Solubilities of Indole Derivatives in Supercritical Fluids, *J. Supercrit. Fluids*, **2**(1), 9.

81. Panagiotopoulos, A.Z. and Reid, R.C., 1986, High-Pressure Phase Equilibria in Ternary Fluid Mixtures with a Supercritical Component., *Am. Chem. Soc. Div. Fuel. Chem.*, **30** (3), 571-582.

82. Paulatis, M.E., McHugh, M.A. and Chai, C.P., 1983, Solid Solubilities in Supercritical Fluids at Elevated Pressures., in "*Chemical Engineering at Supercritical Fluid Conditions*", Paulatis, M.E., et al Eds, Ann Arbor Science, 139-158.

83. Pearce, D.L., 1990, Solubilities of Triglycerides in Supercritical Carbon Dioxide. Ph.D. Thesis, University of Canterbury, Christchurch, New Zealand.

84. Pennisi, K.J. and Chimowitz, E.H., 1986, Solubilities of Solid 1,10-Decanediol and a Solid Mixture of 1,10-Decanediol and Benzoic Acid in Supercritical Carbon Dioxide., *J. Chem. Eng. Data,* **31** (3), 285-288.

85. Peter, S., Seekamp, M. and Bayer, A., 1988, Dissolution of Oleic Acid in Dense Gases, *Proc. Int. Symp. Supercrit. Fluids, Nice France.*,99-106.

86. Sako, S., Shibata, K., Ohgaki, K. and Katayama, T., 1989, Solubilities of Indole, Skatole and 5-Methoxyindole in Supercritical Fluids, *J. Supercrit. Fluids,* 2(1), 3.

87. Schaeffer, S.T., Zalkow, L.H. and Teja, A.S., 1989, Modelling of the Supercritical Fluid Extraction of Monocrotalene from *Crotalaria Spectabilis*, *J. Supercrit. Fluids,* 2(1), 15.

88. Schmitt, W.J. and Reid, R.C., 1986a, The Use of Entrainers in Modifying the Solubility of Phenanthrene and Benzoic Acid in Supercritical Carbon Dioxide and Ethane., *Fluid Phase Equilibria*, **32**, 77-99.

89. Schmitt, W.J. and Reid, R.C., 1986b, Solubility of monofunctional Organic solids in chemically diverse supercritical fluids., *J. Chem. Eng. Data,* **31** (2), 204.

90. Schmitt, W.J. and Reid, R.C., 1988, The solubility of paraffinic hydrocarbons and their derivatives in supercritical carbon dioxide., *Chem. Eng. Comm.*, **64**, 155-176.

91. Snyder, J.M., Friedrich, J.P. and Christianson, D.D., 1983, Effect of Moisture and Particle Size on the Extractability of Oil from Seeds with Supercritical CO_2., *JAOCS*, **61** (12), 1851-1856.

92. Stahl, E., 1980, Extraction of Natural Products with the Means of Supercritical Gases., *Rev. Latinoamer Quim.*, **11**, 1-7.

93. Stahl, E. and Gerard, D., 1985, Solubility Behaviour and Fractionation of Essential Oils in Dense Carbon Dioxide., *Perfumer and Flavorist*, **10**, 29-37.

94. Stahl, E. and Glatz, A., 1984, Extraction of Natural Substances with Supercritical Gases,10. Communication: Qualitative and Quantitative Determination of Solubilities of Steroids in Supercritical Carbon Dioxide., *Fette-Seifen-Anstrichmittel*, **86** (9).

95. Stahl, E. and Quirin, K.W., 1984, Extraction of Natural Substances with Dense Gases., *Pharm. Res.*, **5**, 189-194.

96. Stahl, E., Quirin, K.W. and Blagrove, R.J., 1984, Extraction of Seed Oils with Supercritical Carbon Dioxide: Effect on Residual Proteins., *J. Agric. Food Chem.*, **32**, 938-940.

97. Stahl, E.,Quirin, K.W. and Mangold, H.K., 1982a, Extraction and Fractionation of Complex Lipid Mixtures with Dense CO_2 on a Micro Scale, *Chem. Phys. Lipids*, **31** (4), 319-324.

98. Stahl, E.,Quirin, K.W. and Totani, N., 1982b, Extraction et Fractionnement de Lipides et d'Autres Produits Naturels à l'Aide de Gaz Supercritiques et Liquéfiés., *Revue Française des Corps Gras*, 29, 259-263.

99. Tan, Chung-Sung. and Weng, Jin-Yih., 1987, Solubility measurements of Naphthol isomers in supercritical CO_2 by a recycle technique., *Fluid Phase Equilibria*, **34** (1), 37-47.

100. Taniguchi, M., Tsuji, T., Shibata, M. and Kobayashi, T., 1985, Extraction of Oils from Wheat Germ with Supercritical Carbon Dioxide., *Agric. Biol. Chem.*, **49** (8), 2367-2372.

101. Unger, K.K. and Roumeliotis, P., 1983, On-line High Pressure Extraction-HPLC. 1. Equipment Design and Operation Variables, *J. Chromatogr.*, 519.

102. Van Leer, R.A. and Paulaitis, M.E., 1980, Solubilities of Phenol and Chlorinated Phenols in Supercritical Carbon Dioxide., *J. Chem. Eng. Data*, **25** (3), 257-259.

103. Vollbrecht R., 1982, Extraction of Hops with Supercritical CO_2, *Chem. & Ind.*, 19 June, 397-399.

104. Wong, J.M. and Johnston, K.P., 1986, Solubilization of Biomolecules in Carbon Dioxide Based Supercritical Fluids., *Biotech. Prog.*, 2 (1) .

105. Wu, A.H., Stammer, A. and Prausnitz, J.M., 1988, Extraction of Fatty-Acid Methyl Esters with Supercritical Carbon Dioxide.*Proc. Int. Symp. Supercrit. Fluids, Nice France.*, 107-114.

106. Yamaguchi, K., Murakami, M., Nakano, H., Konosu, S., Kokura, T., Yamamoto, H., Kosaka, M. and Hata, K.1986, Supercritical Carbon Dioxide Extraction of Oils from Antarctic Krill*J. Agric. Food Chem.*, **34**, 904-907.

107. Zerda, T.W., Wiegand, B. and Jonas, J., 1986, FTIR Measurements of Solubilities of Anthracene in Supercritical CO_2.*J. Chem. Eng. Data*, **31**(3), 274-277.

2b Introduction to Solubility Prediction Methods.

Several approaches have been used for predicting and/or correlating the solubility of a solute in a supercritical fluid. These include;

Ideal solution theory.

Various methods for activity coefficient estimation.

The use of an equation of state (EOS) to estimate directly the fugacity of the solute.

Lattice theories and

Empirical correlations.

Although these treatments are not the only ones that have been used for solubility prediction, they represent the most common methods and in some cases the most approachable.

Recently, two excellent reviews examining methods for modelling SCF extraction processes have been published. Johnston *et al* (1989) listed the methods that have been used in the past fourteen years for examining solid/fluid and liquid/fluid equilibria. They considered cubic equations of state, perturbed hard-sphere EOS, lattice models, solution theory and Monte Carlo simulations. The effect of co-solvents (entrainers) on the modelling process was also examined. Johnston *et al* concluded that no single theory can treat all cases and that the choice of theory depends on the application. For the correlation of solubilities at isothermal conditions, the use of the enhancement factor with density at constant temperature was recommended. If the prediction of solubilities was required, the use of a hard-sphere perturbation model was suggested. It was noted that a weakness in many of the models examined was the reliance on the ideal gas state as a reference state. The lack of vapour pressure data (especially for non-volatile solutes) was noted. This can make the ideal reference state approximate at best, thus introducing errors into the model predictions. Care in model use in the near critical region ($\rho_r \leq 1.3$) was stressed.

In their review, Brennecke and Eckert (1989) briefly examined the experimental solubilities given in the literature before examining the prediction methods. They discussed the ability of the methods to predict derivative properties (excess enthalpy of mixing and solute partial molar volume) as well as solubilities. Like Johnson *et al* (1989) they examined the cubic, virial and perturbation forms of equations of state, lattice-gas treatments, an empirical method and the influence of mixing rules on the models. They observed that to successfully model solubilities and derivative properties, it is necessary to take into account the complex intermolecular interactions between the solvent and solute in the vicinity of the critical point.

They conclude that both the cubic EOS and perturbation models are good for data correlation, but are weak for solubility prediction or modelling the derivative properties.

It is noted by Brennecke and Eckert (1989) that there are two generic approaches to solubility prediction; one where the supercritical fluid is assumed to be a compressed gas and a second which assumes that the supercritical fluid is an expanded liquid. They assert that a compressed gas type EOS is easier to use because of the greater ease of obtaining the necessary parameters (vapour pressures). None of the methods is recommended for prediction as all require parameters which must be obtained by fitting measured solubility data. An accurate, truly predictive equation seems to be a long way away.

2b.1 Ideal Solubility Models.

The equations for the solubility of a solid in a liquid at a given temperature and pressure, can be found by equating the chemical potential of the solute in the solid phase to the chemical potential of the solute in the solution. The derivation of this method is well documented (Williamson, 1967). The result obtained is (assuming the enthalpy of fusion is temperature independent);

$$R\ln x_2 = -\Delta_f H\left(\frac{1}{T} - \frac{1}{T_m}\right) \qquad (2.1)$$

where $\Delta_f H$ = the enthalpy of fusion of the solid,
T = temperature,
T_m = the melting point of the solid,
x_2 = the mole fraction of the solid in solution and
R = the universal gas constant

This simple model implies that as the heat of fusion of the solid decreases, the solid should more readily dissolve. This model suggests that a plot of $\ln x_2$ against $\frac{1}{T}$ would produce a straight line of slope $\frac{-\Delta_f H}{R}$.

For a highly non-ideal system where one of the components is in a supercritical state, it is necessary to modify some of the assumptions used in the derivation of equation 2.1. In general the enthalpy of fusion of the solid will not be independent of temperature and there will be deviations from ideality in the form of solute-solvent interactions. Equation 2.1 can then be written in the form (Prausnitz *et al*, 1986);

$$R\ln\gamma_2 x_2 = -\Delta_f H\left(\frac{1}{T} - \frac{1}{T_m}\right) + \Delta C_p \ln\left(\frac{T}{T_m}\right) + \Delta C_p\left(\frac{T_m}{T} - 1\right) \qquad (2.2)$$

where γ_2 = the activity coefficient of the solid in the liquid phase,

ΔC_p = the difference between the solid and liquid heat capacities.

The activity coefficient is used to represent the solution non-idealities. It is necessary to find a suitable expression for the activity coefficient, γ_2, that takes into account these deviations and in particular the effects of the variation of the solvent density with temperature and pressure.

2b.1.2 Liquid Solution Theory Modifications to Ideal Solubilities

Prausnitz *et al* (1986) outline the development of solution theory using Raoult's law ideal solution as a starting point. The approaches presented include those of van Laar and Scatchard and Hildebrand. The reader is referred to Chapters 6&7 in Prausnitz et *al* for the derivations of the relations which are presented and discussed here.

Van Laar's theory is based on the assumptions that there is no volume change on mixing and that the resulting solution is athermal (no entropy change on mixing). An excess property is defined as the difference between a real property and ideal property (Prausnitz *et al,* 1986);

$$X^E = X^R - X^I \tag{2.3}$$

where X is some general property.

Van Laar's assumptions lead to the expression equating the excess molar Gibbs Free Energy to the molar internal energy of the system;

$$g^E = u^E \tag{2.4}$$

where g^E = the molar Gibbs free energy of the compound,

and u^E = the molar internal energy.

Van Laar's other important assumptions were that the pure fluid properties can be described by the van der Waals (1873) equation and the van der Waals mixing rules applied to any mixture of these components. This theory leads to the following equations for activity coefficients;

$$\ln(\gamma_1) = \frac{A'}{\left[1+\frac{B'}{A'}\frac{x_1}{x_2}\right]^2} \tag{2.5}$$

$$\ln(\gamma_2) = \frac{B'}{\left[1+\frac{A'}{B'}\frac{x_2}{x_1}\right]^2} \tag{2.6}$$

$$A' \equiv \frac{b_1}{RT}\left(\frac{\sqrt{a_1}}{b_1} - \frac{\sqrt{a_2}}{b_2}\right)^2 \qquad (2.7)$$

$$B' \equiv \frac{b_2}{RT}\left(\frac{\sqrt{a_1}}{b_1} - \frac{\sqrt{a_2}}{b_2}\right)^2 \qquad (2.8)$$

where a_n and b_n are the van der Waals coefficients for the pure components (see §2b.2)

The lack of agreement between this theory and experimental results is attributed by Prausnitz *et al* (1986) to the use of the van der Waals equation and its mixing rules to describe the fluid behaviour. A' and B' are dependent on the critical properties of the components (through the van der Waals coefficients) and the system temperature, but not the system pressure and hence not the density of the solvent. It is not surprising that there is no pressure dependence, as the theory was developed for liquid mixtures at atmospheric pressure. It is not expected that this model will give a good description of the CO_2 properties at high pressures and hence the prediction of mixture properties will not be good. Therefore it is not expected that this method for determining activity coefficients would be useful and it was not considered further.

In the Scatchard-Hildebrand theory (Hildebrand and Scott, 1962) which derives from the van Laar treatment, a parameter c is defined;

$$c \equiv \frac{\Delta_v u}{v^L} \qquad (2.9)$$

where $\Delta_v u$ = is the energy of complete vaporisation and
v^L = the molar volume of the liquid.

This parameter was derived from an expression for the internal energy of the binary fluid (relative to the ideal gas at the same temperature and pressure) that assumed the excess volume of the system was zero and the energy was a quadratic function of the volume fraction. The other assumption was that the entropy of mixing vanishes at constant temperature and pressure. This results in an expression similar to equation 2.4 equating g^E and u^E. Using equation 2.4 to equate the energies, the above assumptions and defining the solubility parameter,

$$\delta = \sqrt{c} = \left[\frac{\Delta u^E}{v^L}\right]^{\frac{1}{2}} \qquad (2.10)$$

one arrives at the expression for the activity coefficients;

$$RT\ln(\gamma_1) = v_1\Phi_2^2[\delta_1 - \delta_2]^2 \qquad (2.11)$$

$$RT\ln(\gamma_2) = v_2\Phi_1^2[\delta_2 - \delta_1]^2 \qquad (2.12)$$

where Φ_a = the volume fraction of component a and,

v_a = the molar volume of component a.

Hildebrand and Scott correlated the solubility of Iodine with solubility parameter for several solvents. It was found that the solubility parameter theory best matched the observed solubility behaviour when the solvent was spherical and did not possess a significant dipole.

For dilute solutions, such as those found in supercritical extraction, the volume fraction, Φ_1, of the solvent can be assumed to be one. In order to estimate the parameter δ, some simplifying assumptions have to be made. Allada (1984), in following the procedure of Hildebrand and Scott (1962), replaced the u^E term with the approximation $\Delta_V H$ - RT and redefined δ_2 as;

$$\delta_2 = \left(\frac{\Delta_V H - RT}{v^L} \right)^{\frac{1}{2}} \tag{2.13}$$

For the solvent, the solubility parameter can be approximated by departure functions (Allada, 1984) and 2.10 is rewritten;

$$\delta_1 = \left(\frac{(E^* - E)}{RT_c} \frac{P_r}{T_r} \frac{1}{Z} P_c \right)^{\frac{1}{2}} \tag{2.14}$$

where E^* = the internal energy of the fluid isothermally expanded to 'zero' pressure,

E = the internal energy of the fluid at the desired temperature and pressure,

T_c = the critical temperature,

P_c = the critical pressure,

Z = the compressibility factor,

T_r = the reduced temperature $\frac{T}{T_c}$,

P_r = the reduced pressure $\frac{P}{P_c}$,

To evaluate the energy departure function, $\left(\frac{\Delta E}{T_c} \right)$, (where ΔE is defined as $(E^* - E)$) for the fluid at the system temperature and pressure, one needs to use a suitable equation of state for Z . The value for the enthalpy departure can then be determined and hence the energy departure can be evaluated from (Prausnitz *et al*, 1986)

$$\frac{\Delta E}{T_c} = \frac{\Delta H}{T_c} - (1-Z)\, RT_r \tag{2.15}$$

where ΔH = the enthalpy departure function H^*-H (similar to ΔE above).

Daubert (1985) has published FORTRAN code that uses the method of Lee and Kessler (1975) to evaluate Z and departure functions. This code was used in the estimation of the CO_2 solubility parameter. Equation 2.13 was used to estimate the solubility parameter of each triglyceride.

2b.1.3 Compressed Gas Modification to Ideal Solubilities

Johnston and Eckert (1981) define an enhancement factor, E, to describe the non-idealities in the fluid phase as;

$$E = \frac{P\, y_2}{P_2^{sat}} \qquad (2.16)$$

where P = the system pressure,
y_2 = the solubility of component 2 in the fluid and
P_2^{sat} = the saturated vapour pressure of the solute.

This factor is the ratio of the measured solubility to the ideal solubility and is a gas phase activity coefficient. Johnston and Eckert (1981) also suggest that plotting log enhancement factor against solvent density will yield a straight line, and further, that the enhancement factor will be a function of temperature. The determination of enhancement factors depends on evaluating the solute vapour pressure. Equation 2.16 is used in conjunction with the standard relations for the solubility of a solute (Prausnitz *et al*, 1986) to determine the fugacity of the solute in the fluid phase, and hence define the system non-idealities.

2b.2 Thermodynamic Modelling with Cubic Equations of State.

Van der Waals' (1873) has modified the ideal gas equation of state to the familiar form of;

$$P = \frac{RT}{v\text{-}b} - \frac{a}{v^2} \qquad (2.17)$$

where v = the molar volume of the fluid,
a = a constant that accounts for attractive forces of the molecules,
b = a constant that accounts for the molecular volumes, or repulsive forces.

Equation 2.17 can be rewritten in the general form (Carnahan and Starling, 1972);

$$P = P_R + P_A \qquad (2.18)$$

where P_R represents the repulsive effects and
P_A represents the attractive effects.

There have been many attempts to modify the van der Waals Equation (vdW). Two of the best known of these are the Redlich & Kwong Equation (1949) (RK);

$$P = \frac{RT}{v-b} - \frac{a}{v(v-b).\sqrt{T}} \qquad (2.19)$$

and the Peng & Robinson Equation (1976), (PR);

$$P = \frac{RT}{v-b} - \frac{a(T)}{v(v+b) + b(v-b)} \qquad (2.20)$$

These and other similar EOS cubic in volume, have retained the basic vdW structure of a repulsive and an attractive term but differ in the manner in which the attractive term has been evaluated. The advantage of a cubic equation in the form of 2.18 is that the intermolecular repulsive and attractive forces can be independently accounted for.

Haselow *et al* (1986) have reviewed the predictive power of nine equations of state. Eight of these equations are cubic in volume, the ninth is a complex function of volume. The equations were evaluated for their ability to predict solubility of an involatile solute in a supercritical solvent. Of 31 systems examined, no critical parameters (T_c, P_c and ω) are available for 17 and so these parameters had to be estimated before the calculations could be performed. Reid *et al* (1987) present group contribution methods for estimating T_c and P_c. While these methods give reasonable estimates, reliable experimental data are preferred.

The solvents examined by Haselow *et al* (1986) included CO_2 and Ethylene. Solutes examined included Naphthalene, Phenanthrene, Phenol and Benzoic Acid. For each of the equations tested, mixing rules described in the original papers were used to evaluate the constants (for example, a & b in equation 2.20 above). An objective function, W, defined as;

$$W = \sum_{i=1}^{n} \left\{ \ln \left(\frac{y_{i\,exp}}{y_{i\,cal}} \right) \right\}^2, \qquad (2.21)$$

where $y_{i\,exp}$ represents the experimental data and

$y_{i\,cal}$ represents the estimated data,

was minimised for each fitting parameter. The deviations of the predicted values from the experimental values were reported. Haselow *et al* (1986) concluded that the RK equation provided the best fit, with an average deviation of 17 % where the critical parameters were available, and an average deviation of 34 % where estimates of the critical parameters were used.

By examining the molecular dynamic simulations for hard sphere interactions, Carnahan and Starling (1972) modified the van der Waals' equation (2.17) to;

$$P = \frac{RT(1+\zeta+\zeta^2-\zeta^3)}{v\,(1-\zeta)^3} - \frac{a}{v^2} \qquad \text{CSvdW.} \quad (2.22)$$

where $\zeta = \frac{bp}{4}$

A similar modification was made to the the Redlich Kwong EOS yielding

$$P = \frac{RT(1+\zeta+\zeta^2-\zeta^3)}{v\,(1-\zeta)^3} - \frac{a}{\sqrt{T}\,v\,(v+b)} \qquad \text{CSRK.} \quad (2.23)$$

Carnahan and Starling concluded that the replacement of the approximate van der Waals hard sphere repulsion term with one more closely describing 'real' hard sphere interactions, halved the average deviations in the case of the original vdW equation and reduced the deviation by a factor of five for the RK equation.

Johnson and Eckert (1981) used the CSvdW equation to model hydrocarbon solubility in supercritical fluids. Using equations 2.22 and 2.23 and a relation for the fugacity coefficient of the solute (ϕ_2) in the CSvdW equation,

$$\ln(\phi_2 Z) = \frac{3\zeta^3-9\zeta^2+8\zeta}{(1-\zeta)^3} - \frac{2(y_1 a_{12} + y_2 a_{22})}{RTv} \qquad (2.24)$$

they estimated solubilities for Naphthalene/Ethylene, Phenanthrene/Ethylene and Anthracene/Ethylene systems. The calculated results are compared with experimental results by using a deviation function;

$$\frac{\text{standard deviation}}{\text{mean}} = \frac{\left[\sum_{i=1}^{n} \{y_{i\,exp} - y_{i\,cal}\}^2\right]^{\frac{1}{2}}}{(n-1)^{.5}.y_{i\,exp}} \qquad (2.25)$$

where n = the number of data points compared,
and the other symbols are defined above.

Using this function, the average deviation between the experimental solubilities and the calculated results for Phenanthrene/Ethylene at 45°C, for example, is 0.104 if the CSvdW equation is used, 0.141 for the Redlich Kwong equation and 0.074 for the CSRK equation. This illustrates that the CSvdW equation provides a better description of the experimental solubility than the Redlich Kwong equation, but not as good as the CSRK equation. For most of the systems studied by Johnston and Eckert (1981), this trend is apparent. They also

observe that the CSvdW equation closely models the observed behaviour, except in the region of low solvent density.

Johnson *et al* (1982) further modify the CSvdW theory to account for the enhanced attractive forces in the region of the critical point ($\rho \leq 1.5\rho_c$). They use a model based on the molecular dynamics of a square-well fluid to give a much better approximation to the observed behaviour.

It was decided to use the CSvdW equation of state as a representative cubic EOS. This decision was taken because the CSvdW equation provides a better model of the experimental solubilities than equation 2.17. With the CSvdW equation of state, values are available for the b parameter (Johnston and Eckert, 1981) and hence only one parameter needs to be fitted to the experimental results. In addition during this work, the majority of experimental measurements were to be taken at solvent densities greater than $1.5\rho_c$ and there the inclusion of the perturbation term of Johnston (1982) could not be justified.

2b.3 Lattice Models of Solubility.

In lattice models, a 3-dimensional pseudo-lattice structure is postulated for the fluid. It is assumed that the molecules occupy cells defined by the lattice, or sites defined by the lattice points and that movement of the molecules is restricted to vibration about equilibrium positions. In assuming this structure, the lattice cells are assumed to have some co-ordination number, z, describing the number of nearest neighbours to any one cell. The equations that describe these theories have been described elsewhere (Guggenheim, 1952, Barker, 1963) and only a brief outline will be given here.

Consider a mixture of two types of molecules, A and B. The model assumes that for each A molecule on the lattice, there will be both A-A and B-A interactions. It is assumed that the only significant interactions are from nearest neighbours. For each of these interactions, there is an associated potential energy. The potential energy contributions are then considered for all the molecules on the lattice - giving an expression for the free energy of the system. From this equation, the other thermodynamic properties can be derived and the model compared to the observed behaviour.

The theories for simple fluids can be extended to mixtures of molecules of different sizes, such as solutions of long chain polymers in solvents. In these modifications, the general polymer (r-mer) is considered to be a chain of r segments each of which occupies a site on the lattice. The free energy of the mixture is calculated in the same manner as for the simple liquids and the properties determined.

Kumar *et al* (1987) have used this polymer approach of Guggenheim (1952) and Flory (1970) to derive a similar EOS for polymer/monomer solutions. In this derivation, each lattice site is assumed to be occupied by a segment of an r-mer or assumed to be empty (occupied by a hole). It is assumed that there are N_0 holes and N_1 molecules. An equation for the Helmholtz free energy of the system (A) is defined;

$$A = -k_B T \ln \Omega \tag{2.26}$$

where k_B = Boltzmann's constant and
Ω = a canonical partition function.

Kumar *et al* (1987) choose to divide the partition function into two parts;

$$\Omega = \Omega_c \, \Omega_{ke} \tag{2.27}$$

where Ω_c accounts for the positioning of the molecules in the system and
Ω_{ke} accounts for the kinetic energy contributions to the partition function.

By avoiding taking temperature derivatives in the derivation, Ω_c is used interchangeably with Ω. Using the equations of Guggenheim (1952), Kumar *et al* (1987) derive a configurational canonical partition function Ω_c;

$$\Omega_c \cong \lambda(T)^{N_1} \frac{(N_0 + r_1 N_1)!}{N_0! N_1!} \left[\frac{(N_0 + q_1 N_1)!}{(N_0 + r_1 N_1)!}\right]^{\frac{z}{2}} * \exp\left[\frac{\beta}{2} z N_1 q_1 \varepsilon_{11} \frac{N_1 q_1}{(N_0 + q_1 N_1)}\right] \tag{2.28}.$$

Equation 2.28 is substituted into 2.26 and the relation (Prausnitz *et al*, 1986)

$$P = -\left(\frac{\partial A}{\partial V}\right)_T \tag{2.29}$$

is used giving the equation of state.

$$\frac{\tilde{P}}{\tilde{T}} = \ln\left[\frac{\nabla}{\nabla + 1}\right] + \frac{z}{2} \ln\left[\frac{\nabla + (q_1/r_1) - 1}{\nabla}\right] - \frac{\vartheta^2}{\tilde{T}} \tag{2.30}$$

where (~) denotes a reduced variable (defined in the paper)
z = the lattice co-ordination number (set to 10),
q_1 = the effective chain length for the molecule,
r_1 = the number of lattice sites that each molecule occupies,
ϑ = the effective surface area fraction of the molecules in the lattice,
v = the molar volume of the compound,

N = a number of molecular species and

$\lambda(T)$ = a temperature-dependent function that accounts for molecular conformations.

Because lattice theories take into account the different sizes of the molecules, it is expected that this approach would provide a better description of the observed behaviour than the cubic equations of state.

At the time of writing this thesis, an approach had been made to Dr. Kumar for a copy of the computer code required for the implementation of his equation. To date, it has not been possible to obtain a copy of this code, and therefore this method is not discussed in Chapter 6.

2b.4 Empirical Correlations.

The aim of the empirical correlation approach is to develop general relations which gives a good description of the observed behaviour for a wide variety of substances. This approach is well known in the field of Chemical Engineering, with Reid *et al* (1987) publishing a book of design and empirical correlations.

Gurdial *et al* (1989) have qualitatively reviewed three data correlation methods for supercritical solutions;

Log enhancement factor versus density (Johnson and Eckert, 1981).

Log solubility versus log density (Chrastil, 1982, Johnston and Kumar, 1988) and

Log enhancement factor versus a complex function of solubility parameter (Ziger and Eckert, 1982).

The ability of these relations to correlate solid solubility in supercritical solvents was evaluated by Gurdial *et al* (1989) for 11 solutes with a range of functional groups and dipole moments in CO_2. The conclusions from Gurdial's work are that of the relations, the first two were suitable for non-polar solutes, but as the solute polarity increased, the first correlation yielded straight line relations that were not parallel and the second correlation produced departures from linearity. Although the relation of Ziger and Eckert was shown to be sensitive to variation of thermal properties of the solutes, it proved better at correlating the data over a large range of solute functional groups and polarities.

3

Experimental

3.1 Introduction

One of the aims of this project was to design and build a flexible laboratory scale supercritical fluid extraction system. As supercritical fluid extraction technology was new to this Department, the author felt that it was necessary to review the extraction methods presented in the literature. Our final system design was based on this review.

3.2 Literature Review

There are two main configurations of experimental apparatus listed in the literature. The "once through" or "continuous" method (Johnston and Eckert, 1981) and the "recycle" or "equilibrium" techniques (Diepen and Scheffer ,1948). McHugh and Krukonis (1986) use the terms "dynamic" and "static" to describe the two different approaches. The terms "dynamic" and "static" refer to the means of passing the solvent through the system. This convention will also be used in this review. The difference in the two procedures is that unlike the static methods, the dynamic methods uses a single pass of solvent through the extraction cell.

3.2.1 Dynamic Methods

With this method (as with the static methods), the solvent is passed through a (packed) bed of solute. The flow of solvent is chosen so that the solvent is saturated with solute on leaving the extraction cell. Most apparatus is of the general configuration; cylinder-compressor-surge tank/pressure control-heating system-extraction cell(s)-sampling devices (as shown in Figure 3.1).

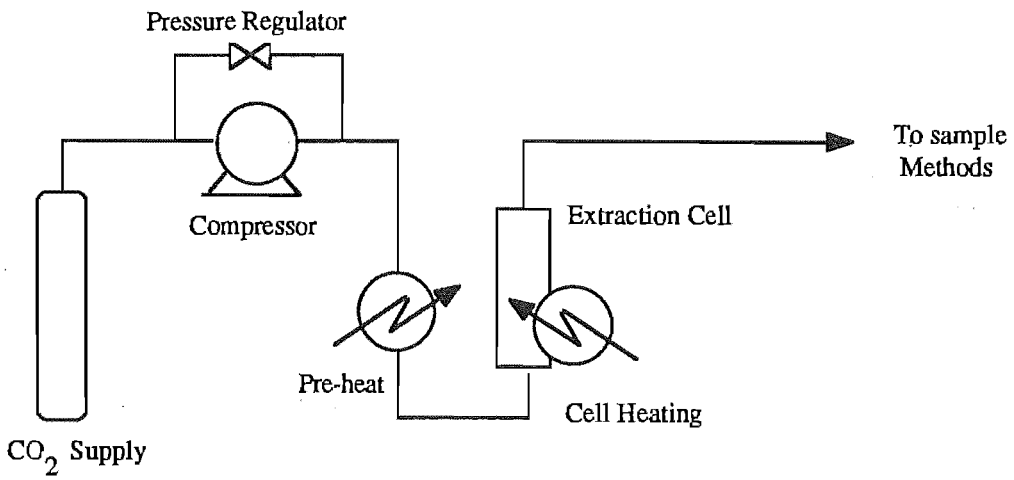

Figure 3.1 General Configuration for Dynamic Methods.

The solvent supply to the compressor is either liquid or gas. A liquid solvent is often preferred as higher mass flows through the system are possible. This is most desirable during the pressurisation of the system. The compressor output is typically controlled by either a surge tank (Johnston and Eckert, 1981, Kurnik *et al*, 1981) and/or a pressure regulator (Arul *et al*, 1987, Chimowitz and Pennisi, 1986). These devices give the operator the flexibility of choosing both the operating pressure and output flowrate independently. Dobbs *et al* (1986) claim that a constant flow of solvent, with pressure control to within 1% (commonly ±0.1 - 0.2 MPa) is obtainable using the surge tank and the regulator together.

From the compressor, the high pressure solvent passes through a length of heated tubing. The purpose of this is to bring the solvent to a temperature within 1K of the desired operating temperature. A constant temperature bath (Chang and Morrell, 1985) or a length of heating tape wound around the tube (Dobbs *et al*, 1986) can be used.

The preheated solvent then passes into the extraction cell. The pressure cell can be maintained at the desired operating temperature by using a constant temperature bath, or a suitable length of heating tape. A single pressure vessel can be used (King *et al*, 1987), or two cells in series may be preferred (Hicks and Prausnitz, 1981). The criterion for determining whether one or two vessels are required for a given extraction, seems to be the desired solvent flowrate through the system. Pennisi and Chimowitz (1986) suggest that for solvent flow rates in the range of 0.014 - 0.054 standard cubic meters per hour per square centimetre cross sectional area of extraction cell, the solute solubility will be independent of the flowrate. This suggests that in this flow regime the fluid is saturated with the solute as it leaves the vessel. Bamberger *et al* (1988) observe that for solvent flows in the range of 10.8 - 18.8 $mg.s^{-1}$ per square centimetre cross sectional area of extraction cell, the solubility is

independent of flow. For flows higher than these, a second pressure cell is required to ensure saturation.

The method of packing the sample cell with the solute is important. The use of some inert packing (e.g. glass beads or glass wool) is considered essential in ensuring that the solute is well distributed in the cell, while also helping to prevent solid samples from compacting under pressure. This packing also helps stop the solvent from creating channels in the solute and eluting from the cell unsaturated (see also §3.3.7.1). The use of beads also helps to keep the cell volume to a minimum - an important consideration for expensive samples. Krukonis and Kurnik (1985) and Chang and Morrel (1985) pack the vessel with alternate layers of solid and glass wool (see figure 3.2). Chimowitz and Pennisi (1986) prefer a mixture of equal parts of solute and glass beads, while Dobbs *et al* (1986) use a mixture of 100 mesh sand and solute. All the workers use glass wool or some other porous material to hold the sample in the extraction cell. This helps to distribute the solvent stream through the bed and prevents any solute from being entrained in the outlet fluid stream.

In the majority of the configurations, the fluid stream appears to pass upwards through the extraction vessel. This works well for dense solid samples, however if liquid samples are to be extracted, there could be problems with the density differences between the solvent and the solute (see also §4.6).

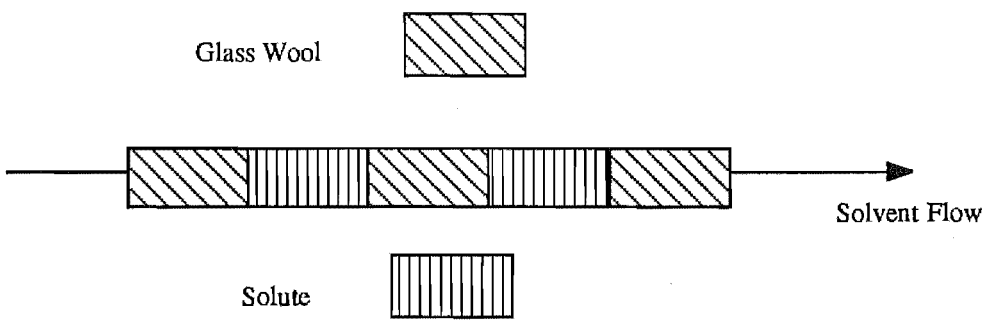

Figure 3.2 Glass Wool Packing Method

3.2.2 Static Methods

The static methods fall into two distinct groups. There are methods where the solvent is pumped around the system (recycle methods, King *et al*, 1987, Tan and Weng, 1987) and techniques where the solvent and solute are mixed by a stirrer for long enough for equilibrium to be attained (Chrastil, 1982, Coppella and Barton, 1985, Diepen and Schaffer, 1948).

3.2.2.1 Recycle Method

With solvent recycle, the cell is charged with a mass of solute and then pressurised with the solvent to the desired pressure and heated to the required temperature. The solvent inlet is then closed and the solvent is circulated around the apparatus until equilibrium is attained. Circulation is achieved by either the compressor in-line (King *et al,* 1987) or a separate metering pump in the system (Tan and Weng, 1987), as shown in figures 3.3 and 3.4. The use of a separate metering pump is advantageous for two reasons. Firstly, the compressor will not become contaminated with the solute as the saturated solution passes around the system or when the system is depressurised. Secondly, the compressor must operate as both a compressor and a circulation pump. When the device is used for the former, the recycle line will then be closed. It is then necessary to pressurise the system to a pressure greater than the desired operating pressure to allow for the pressure drop when the recycle line is introduced to the system.

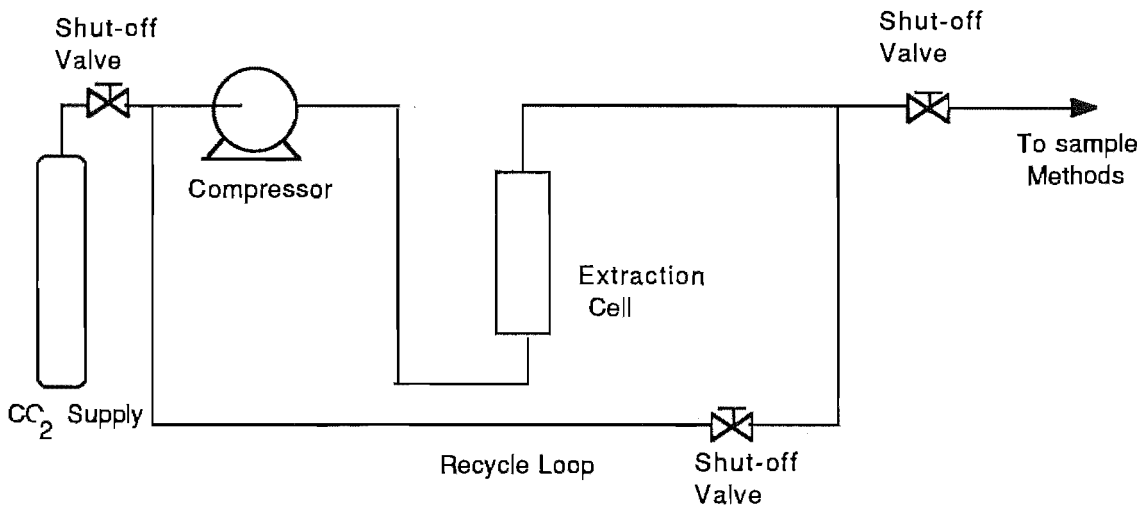

Figure 3.3. Recycle With the Compressor.

Figure 3.4 shows a configuration for fluid circulation using a recycle pump. When such a pump is used, the compression can take place as before, except now there is no need to shut off the recycle line. An HPLC pump would be ideal for this type of operation. They can operate at pressures of 40 MPa and deliver very low solvent flowrates (to 0.01 $ml.min^{-1}$). Once the system is at equilibrium, a sample of the fluid phase is taken and analysed.

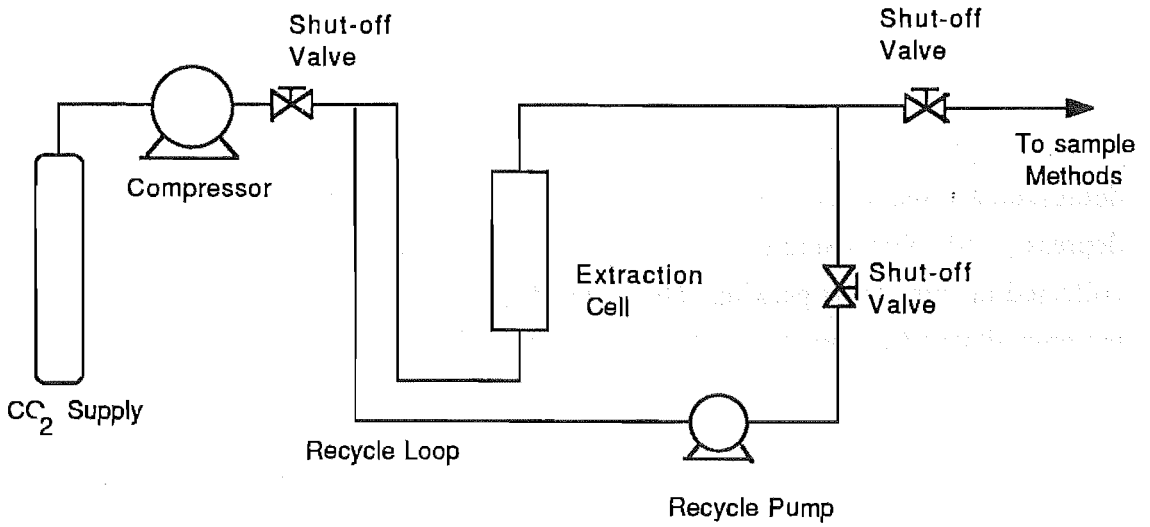

Figure 3.4. Recycle With Internal Pump.

When using either a separate pump or a compressor for circulating the solvent, the pressure fluctuations experienced in a closed system can cause problems. Tan and Weng (1987) identifies this problem but do not give any indication as to the magnitude of the observed fluctuations or any solution to the problem. King *et al* (1987) do not mention this as a problem.

3.2.2.2 Equilibrium Method

The equilibrium method is illustrated by Chrastil (1982). Here a sample cell is charged with some mass of solute and then the cell is raised to the desired pressure by the introduction of the solvent. The system is isolated and then the solvent and solute are allowed to come to equilibrium. Chrastil achieves this by using a magnetic stirring device. Once the solution is at equilibrium, a sample is collected for analysis.

3.2.3 Sample Methods and Analysis Techniques

Sampling is frequently performed by either using U-tubes for sampling or using a 6-port valve to take the samples (microsampling).

3.2.3.1 U-Tube Sampling

The use of U-tubes in cold traps is the easiest method of collecting a sample (Johnston and Eckert, 1981, Kurnik and Reid, 1982). The saturated supercritical fluid expands through a heated valve and is then passed through one or more U-tubes. An ice/brine mixture in the cold trap is suggested by Pennisi and Chimowitz (1986). In many cases, to ensure the

complete collection of the solute, two traps are used. The micrometering valve is also used to control the flow of the fluid through the apparatus. It is necessary to ensure this valve is heated to prevent the outgoing solvent stream from freezing. As the outlet stream depressurises, the solute previously dissolved in the solvent stream will precipitate. The depressurised solvent/solute suspension passes to the cold trap system where the solute is collected in some inert packing. The solute-free solvent then passes out to some form of metering device (a rotameter and/or a dry test meter) and finally to atmosphere. This system is illustrated in figure 3.5. Knowing the mass of the solute collected and the amount of gas collected, the solubility of the solute is determined.

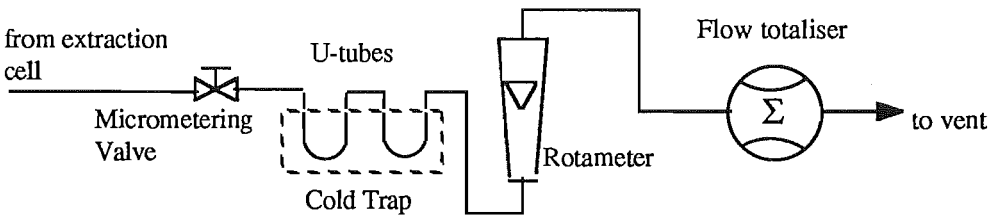

Figure 3.5 Cold Trap Sampling.

3.2.3.2 Microsampling

Microsampling has been in use for over ten years since McHugh and Paulaitis (1980) suggested the use of a 6-port valve to take a small sample of the saturated fluid. 6-Port valves are standard devices used widely for HPLC sample injection. These valves can have loops of known volume attached. The internal configuration of the valves allows the saturated fluid stream to flow through, or by-pass, the loop. This technique was further developed by Wong and Johnston (1986) and by Dobbs and co-workers (1986, 1987). After contacting the solute, the supercritical fluid passes through the sample loop of the valve on its way out of the system (figure 3.6).

Once the system is at steady state, the micrometering valve is switched and the loop isolated from the saturated fluid stream. The loop contents are then removed for analysis.

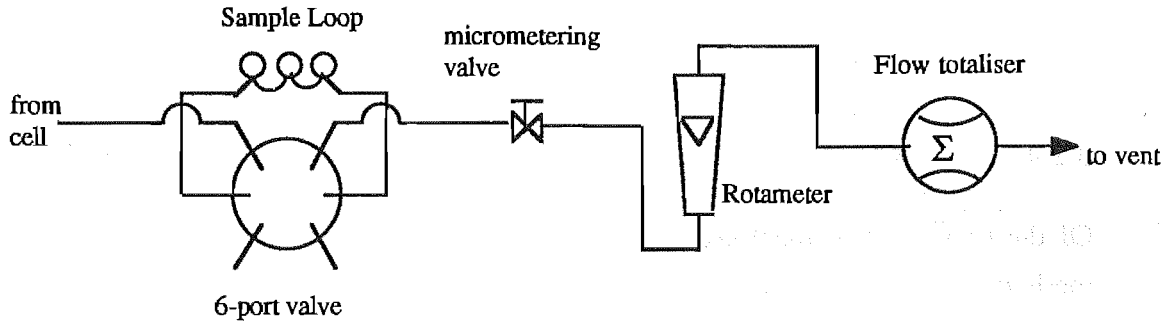

Figure 3.6 Microsampling.

3.2.3.3 Thin Layer Chromatography Sampling

Stahl *et al* (1980) have developed a solubility method that uses a micro-sampling technique based on thin layer chromatography (TLC). A mass of sample (commonly solid) is placed in a metal block. The block is then heated, vaporising the sample. At the same time, the carrier gas (solvent) is passed slowly over the solute. The saturated solvent/solute-vapour mixture is depressurised onto a prepared TLC plate. The spotted plate is then developed using conventional TLC methods. This technique requires more expertise than the static or dynamic methods and will not be further discussed. Furthermore, this technique is of most use as a qualitative screening method. This analysis method was not considered to be useful for this project.

3.2.3.4 Analysis Techniques

The most common method of analysis is the gravimetric technique. This method can be used with both the U-tube and microsampling techniques. Here the collected sample is accurately weighed and then by measuring the amount of gas used during the run, the solubility can be quickly determined. In the case of mixtures of solutes in the sample to be analysed, the most widely used methods are Gas Chromatography (GC), Gas Chromatography/Mass Spectroscopy (GC/MS), High Pressure Liquid Chromatography (HPLC) and Nuclear Magnetic Resonance (NMR). Accuracy for these techniques is usually ±4%. The methods listed above claim reproducibility in the region of ±5% (Johnston and Eckert, 1981). Hicks and Prausnitz (1981) claim ±1%.

3.2.4 Discussion

3.2.4.1 Extraction Method

Of the two types of methods, dynamic and static, most workers prefer to use dynamic methods.

McHugh and Krukonis (1986) give the following comparison between dynamic and static methods (the static method that they refer to has a view cell).

DYNAMIC:

Advantages	Disadvantages
Off the shelf equipment available	Solid can clog the metering valve
Easy sampling	Solute entrainment at high flowrates
Quick and accurate	Can have undetected phase changes
Data for fractionation	Density changes possible
	Care needed with multicomponent samples
	Cannot detect mutual solubilities

STATIC:

Advantages	Disadvantages
Visual phase equilibrium determination	No stripping data
Phase transitions visible	Expensive, have to custom build equipment
Easily handle heavy liquids and polymers	Window failure possible
Solid and liquid solubility determination possible without sampling	
Use a minimum amount of solute	
Sample multicomponent phases.	

The main advantage of the dynamic method appears to be solubility data are generated much more quickly than by static methods and with no loss of accuracy. There are several manufacturers of supercritical screening apparatus or dynamic equipment, for example Nova Swiss (Effrekiton, Switzerland) and Superpressure Inc.(Jessup Maryland, U.S.A.).

If it is not possible to use a dynamic technique to generate solubility results, then equilibrium methods would be preferred. This method should produce a simpler experimental technique than the dynamic methods since all that is required is to charge the vessel with the solid and the solvent and provided for intimate contact between the solute and solvent. It is of course necessary to have some form of solvent circulation, an autoclave with some form of magnetically driven stirrer would be ideal (and expensive). The equilibrium methods seem to be too time consuming for the measurement of single component solubilities. Chrastil (1982) suggests a wait of the region of 1-3 hours for the system to come to equilibrium.

When multicomponent solvent mixtures are being used, a sight glass will be important where there is doubt as to whether the solvent mixture forms a single phase (Schmitt and Reid, 1986). It is desirable to have a single phase. With a multiple phase solvent an enhanced solubility due to a change in the nature of the solvent will not be observed, but rather an average solubility resulting from the combined effects of the individual solvent properties would be apparent.

3.2.4.2 Sampling

With the introduction of microsampling, the speed of solubility determination has increased markedly. Dobbs *et al* (1986) list the following advantages of microsampling:

1. It is a good method of dealing directly with multicomponent samples.
2. Thermally labile materials are easily handled because the sampling occurs before the heated valves.
3. Sample volume is independent of the solvent flow.
4. There is a decrease in the run time.
5. There are no problems for the sampling method associated with the plugging of the micrometering valve.
6. Small samples can be taken.
7. Glass traps are unnecessary.

The author agrees with the points that Dobbs *et al* (1986) has raised, but thinks that several points need expanding upon.

Firstly, the method of dealing with multicomponent mixtures (ternary or higher) will necessarily be different to the method for examining the binary systems. With a binary SCF + solute system, the solute solubility will be a constant value for each fixed temperature & pressure. For a ternary or higher mixture (solvent, a,b,...) y_a (and y_b, ...) the apparent solubility of each component will be influenced by the degree of extraction and the presence of other components the solute mixture.

Secondly, the clogging of the micrometering valve becomes less of a problem with the 6-port valve sampling than when dealing with the cold traps and a gravimetric system. When a 6-port valve is used for sampling, the sample is taken before the pressure is decreased. This means that using one of these valves reduces the effect of micrometering valve blockage/clearing problems. It should be noted that a rush of solvent and solute through the system, caused by such a blockage/clearing cycle will mean that the system has to come to steady state again before another sample can be taken.

Dobbs *et al* (1986) omit mention of another advantage of using the 6-port valve - the ability to choose the size of the sample loop used. This allows for the use of a small sample loop for the very soluble solutes and a larger loop for the less soluble solutes. This removes the need to run the equipment for long periods of time to collect enough sample for accurate mass loss determination.

McHugh and Paulaitis (1980) and Dobbs *et al* (1986) operate their multi-port valves in the following manner. The valve is filled with the sample and then switched to a closed line. This line is slowly depressurised and the solvent is collected over water (care is needed to ensure that the water is saturated with the solvent prior to depressurisation). The precipitated solid is then dissolved in a suitable solvent for further analysis.

Neither McHugh and Paulaitis (1980) nor Dobbs *et al* (1986) mention one of the most important advantages that microsampling offers the experimenter - the potential of having an on-line sampling technique. One way this is possible would be to sweep the sample directly to the HPLC as illustrated by Billoni *et al* (1988) and Pearce and Jordan (1989). By using two 6-port valves (see figure 3.8), an HPLC system can be incorporated and the contents of the sample loop taken directly onto the column for analysis. In this manner, the depressurisation stage outlined by McHugh and Paulaitis is avoided.

In this method the sample valves are switched and the HPLC solvent is passed directly through the sample loop sweeping the supercritical solvent and precipitated solute along towards the HPLC column. As the valves are switched the pressures of the sample and HPLC system will change. Billoni *et al* (1988) use methanol as the HPLC mobile phase which is claimed to dissolve the CO_2. They use U.V. detection. CO_2 is transparent to U.V. light and so there will not be a CO_2 peak. Using this method, one can sample the outgoing solvent stream quickly, the time taken for the solute peak to elute from the HPLC column is the limiting step. Care needs to be taken to ensure that the HPLC mobile phase and column combination will retard the solute (see §4.3.2). If the solute is not retarded, the solute peak might be swamped by the supercritical solvent peak, or by the disturbances that the depressurisation of the solvent in the sample loop may cause to the detector. If the pressure disturbances are unacceptable, then the sample loop must be depressurised prior to mobile

phase introduction. Perhaps the biggest advantage of coupling the 6-port valve sampling directly to the HPLC, is that there is almost no possibility of solute loss during the sampling procedure.

Other advantages of this technique include the small (10-100µl, depending on the loop size), constant sample sizes and a speedy means of measuring solubilities at a constant temperature. When used in conjunction with a recirculation system, the sample loop needs to be flushed with the supercritical solvent after each sample is taken. This removes any HPLC mobile phase contamination of the SFE system.

One final piece of information needs to be obtained, the mass of supercritical solvent in the sample loop. To determine this, the loop volume and solvent density must be known. It is also necessary to have calibrated the detection system for the solute to be investigated.

The on-line sampling method can also be used to monitor the approach of the SFE system to steady state. If the system is not at steady state when a sample is taken, successive samples will show this. It is also a good means of seeing how the system behaves under multicomponent extraction (stripping) conditions.

Unger and Roumeliotis (1983) use microsampling with a two stage depressurisation. To try to avoid the problems of solute loss, they depressurise their sample through two HPLC columns. The HPLC mobile phase is then switched through these columns and onto an analytical column. In their system they rely upon a rotameter to monitor CO_2 loss/use. The arrangement of their 6-port valves is of some concern. In the case of a switching failure (having the valves switched in the wrong order), the supercritical fluid could be sent directly to the HPLC system. A method which avoids this problem is outlined in §3.3.1.

Subsequent to the design and construction of the equipment, the author was made aware of a paper by Larsen and King (1986). They used a direct coupling to HPLC without the depressurisation of Unger and Roumeliotis (1983). The compounds that they investigated were detectable with U.V. and U.V. detectors are not flow sensitive. Unfortunately, to analyse triglycerides with U.V., the mobile phase cannot contain a solvent that absorbs U.V. light above 210 nm, this precludes the use of acetone in a mobile phase mixture. Acetone absorbs UV light at frequencies up to 330 nm. If no acetone is used then a short chain triglyceride will take about 30 minutes to elute from the system, too long for one sample. Thus the flow sensitive Refractive Index (R.I.) detection method was used and the solvent tuned to retain the solute on the column long enough to avoid the CO_2 peak (see §4.3.2)

3.2.5 Conclusions

Based upon the literature review, for the single solute systems, the dynamic methods would be preferred. These techniques are faster than the static or recycle techniques and no less accurate. In some (dilute) cases they are probably more reliable (McHugh and Paulaitis, 1980).

The preferred sampling method is the microsampling technique of McHugh and Paulaitis (1980). This method is non-intrusive and when coupled to an HPLC or other analysis device, gives the operator a powerful on-line analytical tool.

It should be possible to construct a system that incorporates the advantages of both the dynamic and the recycle methods (see figures 3.3 & 3.4) The operator then has the choice of techniques within the same apparatus.

3.3 Supercritical Fluid Solubility Apparatus

3.3.1 Design Considerations

One of the stated aims of this project was to design, build and commission a new supercritical fluid extraction apparatus in the Chemical & Process Engineering Department. It was therefore necessary to design and build the most flexible system possible, within the constraints of the budget. Based on the review above (§3.2), it was decided to design and build a system that could be used equally well in either a dynamic or in a static (recirculation) mode.

Other design considerations were:

Independent pressure and flow control,
Independent control of the temperature of both the compressor head and the main water bath,
Choice of solvent flow direction through the cell, either top-to-bottom, or vice versa,
Access to the internal plumbing for any future modifications,
On-line sampling technique,
Maximum design pressure of 680 bar (10 000 psi),
Quick changes in bath temperature and
Ability to use a variety of extraction vessel sizes

The final system configuration is shown below in Fig. 3.7. The dotted lines indicate the boundaries of the two water baths.

The design objectives were met by the inclusion of the recycle line, taken from between the sampling and metering points and returning to the system on the inlet side of the compressor. This gave the option of two experimental techniques: a dynamic technique and a recirculation technique. With the recirculation configuration, the outlet line is blocked off and the solvent is recycled around the system. When operating in this mode, it was envisaged that the compressor would be used as the recirculation device, although a separate recycle pump would be preferred.

The addition of a pressure regulator across the compressor gave the required independent control of system pressure and solvent flowrate. At temperatures above 50°C and pressures above 250 bar, flow values of 0.014 - 0.054 standard cubic meters per hour per square centimetre cross sectional area of extraction cell (see §3.2.1 above) were found only to be attainable when no regulator was present.

The direction of flow of solvent through the apparatus can be controlled by operating valves 2,7,4 and 5 (figure 3.7). Closing valves 2 and 5 (only) forces the solvent to flow from bottom-to-top and closing valves 7 and 4 (only) makes the solvent to flow from top-to-bottom. The system was operated in the bottom-to-top mode for solid sample processing.

It was decided to use the microsampling technique of McHugh (§3.2.1.2 above). A 6-port valve was placed in the system between the outlet of the cell and the micrometering valve as shown in fig. 3.7. This 6-port valve was connected to a second similar valve which was linked to the departmental Waters HPLC equipment. This 6-port valve combination is more fully illustrated in fig. 3.8. The line volume between the two 6-port valves does not have to be exactly known but to prevent too much sample diffusion prior to the HPLC column, this volume should be minimised. Tubing with an inside diameter of 1mm was used for these lines.

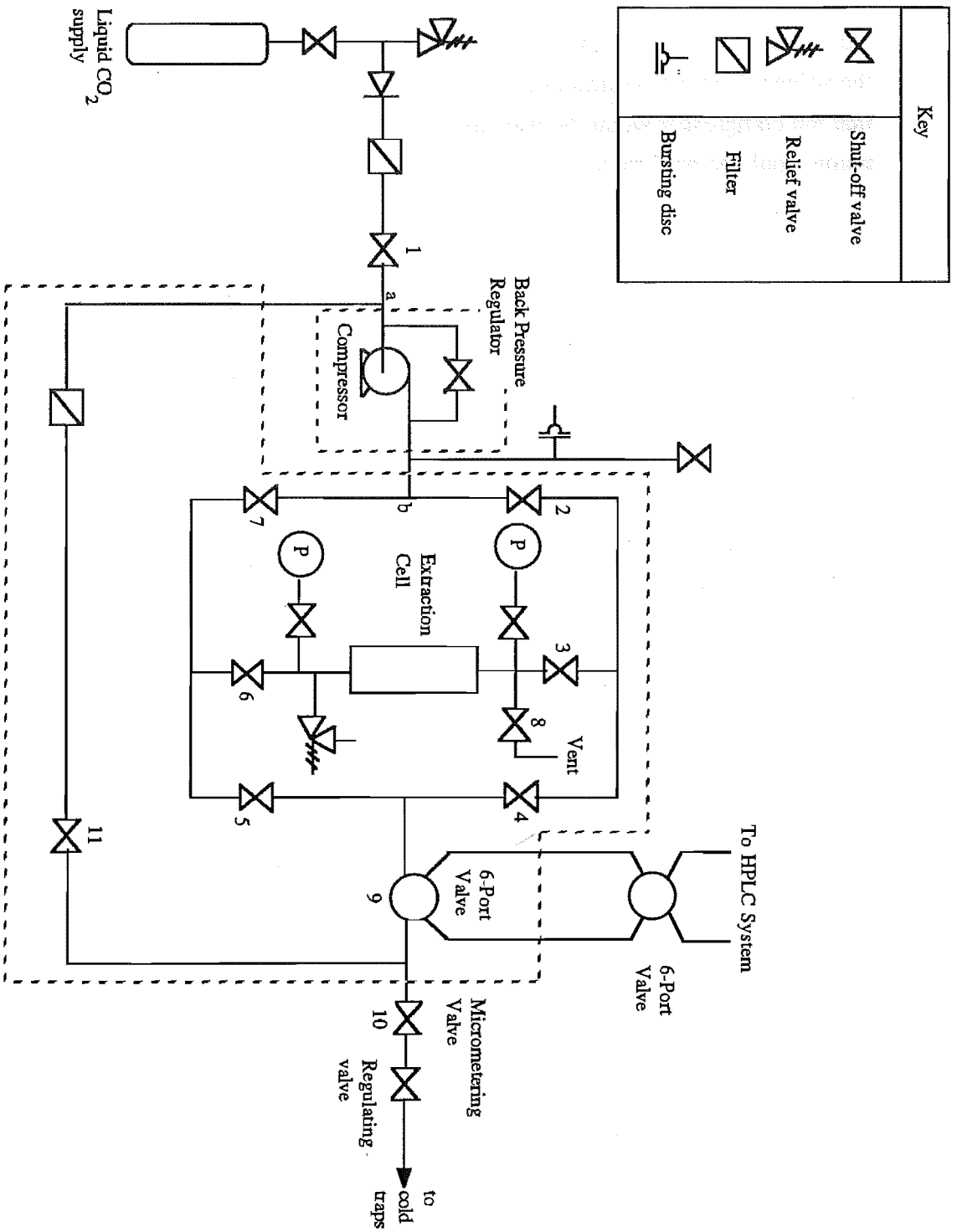

Figure 3.7 System Line Diagram

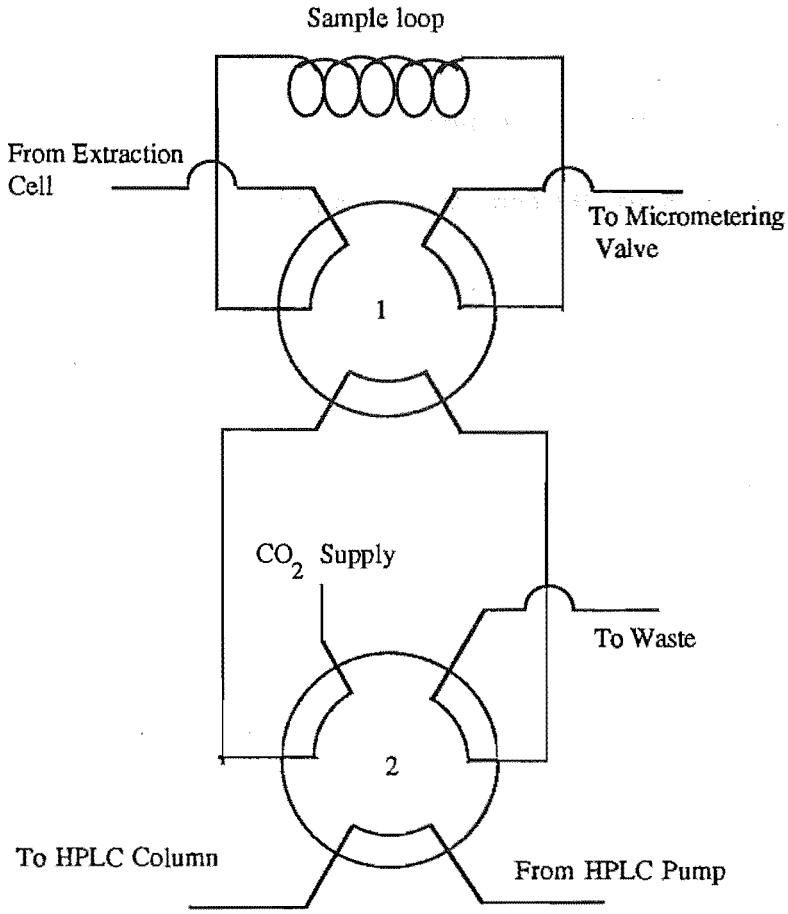

Figure 3.8. Six-port valve configuration.

The reasons for adopting this sampling technique are outlined above (§3.2.4) and can be summarised:

Only small samples are required,
Sample size is reproducible,
Direct passage from the cell to HPLC,
Speed.

If sending the samples directly to the HPLC is not desired, the samples can be collected for future analysis using the procedure of Dobbs *et al* (1986) and McHugh and Paulaitis (1980). The problems associated with this choice of method and their solutions are detailed elsewhere (§4.4).

The maximum design pressure was 680 bar (10 000 psi). The survey of solubility data (Chapter 2a) suggested that the majority of measurements had been made at pressures lower than 70 MPa. Therefore the 70 MPa pressure limit seemed realistic and should encompass the likely range of pressures investigated in this (and future) SCF solubility work. For the initial work, a cell with a pressure limit of 400 bar was constructed.

It was decided to house the compressor head and the main unit in separate baths. These baths were linked by a recirculation pump. Water was drawn from the bottom of the main tank and sent either to the compressor bath or back to the main bath. The compressor bath can be isolated and operated at a separate temperature. Each bath has a separate drain.

Steam and cold water services were plumbed into the main water bath. This gives one the ability to 'quickly' change the main bath temperature by either direct steam injection or cold water addition. Figure 3.9 below, shows the position of services in the system. Design drawings of the main bath, compressor bath and the main support frame are given in Appendix 1.

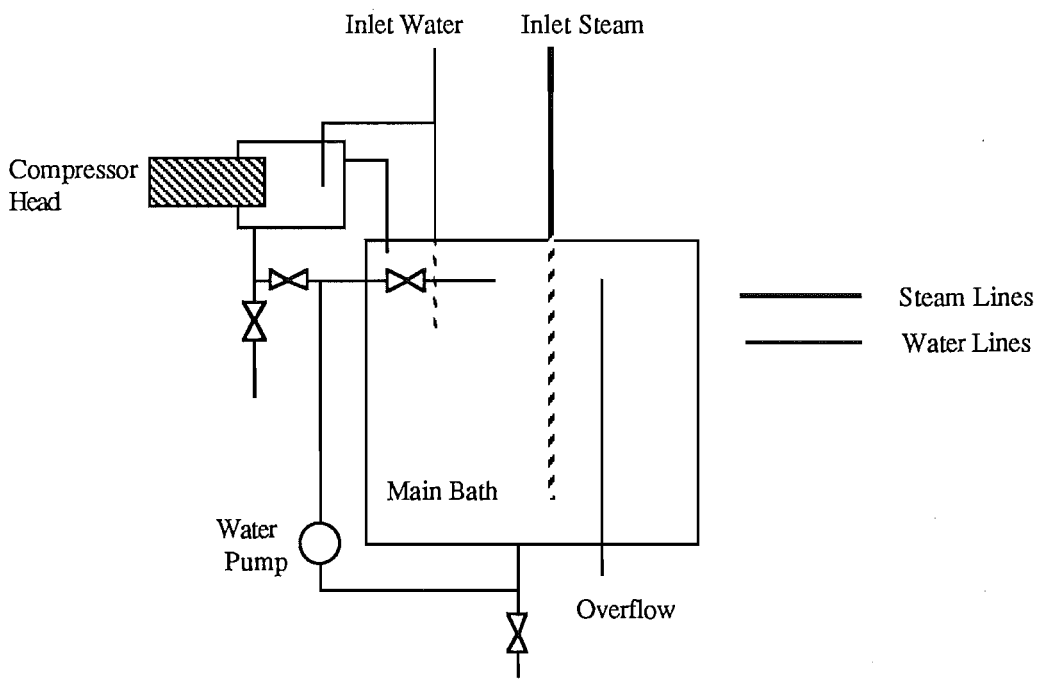

Figure 3.9. System Services.

3.3.2 Valve and Fitting Selection

It was decided to use 1/8" valves, fittings and tubing throughout the system. This size was chosen to keep the non-cell volume small. The system pressure limit was set at 10,000 psig (68 MPa). For these reasons and based on the experience of the IPD, Autoclave Engineers' Inc. (Erie, Pennsylvania, U.S.A.) valves and fittings were used for the high pressure regions of the system. The valves and fittings used in the construction of this apparatus are listed in Appendix 1.

3.3.3 Compressor Selection

The compressor chosen was a Newport Scientific Inc. (Jessup, Maryland, U.S.A.) model 46-13411-2 motor driven, single ended, diaphragm compressor. It is capable of generating pressures of up to 10,000 psig, (68 MPa), with a maximum compression ratio of 14:1. The compressor displaces 0.26 $in^3.stroke^{-1}$ at atmospheric pressure.

3.3.4 Water Bath and Valve Cage Design

In order to ensure that leaking valves were easily fixed, faulty parts easily replaced, future modifications and cleaning could be easily performed and for easy system operation, it was decided to to mount the system valves on a cage made of 40 x 40 x 3 mm 316 Stainless Steel angle with inside dimensions 470 x 570 x 350 mm (a drawing is found in Appendix 1). The cage was supported by two cross pieces made of 50 x 50 x 6 mm mild steel. These two cross pieces rested on the top of the main bath and allowed the cage to be immersed in the heating fluid. The valves were fixed to the cage by means of pieces of 316 SS, which were welded to the cage in the case of the angle pattern valves, and bolted directly to the cage in the case of the straight pattern valves. The low pressure (400 Bar) cell was held in place by a bracket that was bolted onto side of the cage.

The mild steel cross pieces had holes drilled to allow for lifting cables (attached to a block and tackle) to be fixed when the cage was lifted out of the tank. The problem of making and breaking line connections when the valve cage was removed from the bath was overcome by placing two tees on the side of the main bath. At these points (labelled a & b in fig 3.7), the lines to the main unit could be broken when necessary. This eliminated the need to provide extra points for breaking the lines (E.g., elbows). The other connections that needed to be broken when the cage was removed were the connections to the tank-mounted 6-port valve.

The cage that held the "Pyrotenax" heating coil in place was made from four brass strips (with suitable grooves) in the corners. These pieces were held in place by two pieces of 316 stainless steel rods (see Appendix 1 for drawings). The cage was 650 x 550 x 500mm. This cage fitted outside the valve frame.

The main water bath measured 750 x 660 x 660. It was supported by a frame made from 50 x 50 mild steel RHS. This frame (see Appendix 1) raised the top of the bath 1.113 m and elevated the compressor 1.106 m from the floor. The compressor head was enclosed in a bath that measured 300 x 300 x 270. The water circulation system consisted of a magnetically driven pump (see §3.3.5) and lengths of 1" copper pipe. Both of the baths had 1.5" overflow lines.

The flow between the two baths could be switched in the following ways:

1. from the base of the main water bath to the base of the compressor bath. The water impinged upon the compressor head and overflowed through a pipe into the main bath,
2. from the base of the main water bath to the top of the main bath. The compressor bath was isolated.

The main bath was insulated with 50 mm expanded polystyrene sheets on the sides and the base. The top remained open. The compressor bath was insulated with two layers of 3 mm thick Armstrong insulating tape. The copper circulation pipes were insulated with Armstrong-Nylex "Armaflex" insulating tube (20 mm ID x 10 mm thick for the main lines and 28 mm ID X 13 mm thick for the overflow lines). To provide a uniform temperature throughput the main water bath, a stirrer (§3.3.5) was mounted onto the side of the valve cage. This stirrer gave excellent circulation.

Plate 1 shows a view of the valve cage out of the main water bath and plate 2 shows a plan view of the whole system (with the cage in position in the main water bath)

3.3.5 Electronics

The main water bath was heated with 2 x 41 m coils of National Electric "Pyrotenax" HCHHIL2000 heating cable (at 0.65 kW). The main water bath temperature was controlled to within ± 0.1 K by an on-off controller manufactured by the Departmental Electronics Workshop. The controller monitored the temperature of main water bath and adjusted the load to the heating coils as required. The base load was applied to the other coil with a variable voltage transformer.
The heating coils were protected from a low water level (i.e. not exposed to the air while on) with a Stuart Type F1 (MK III) mercury float switch.

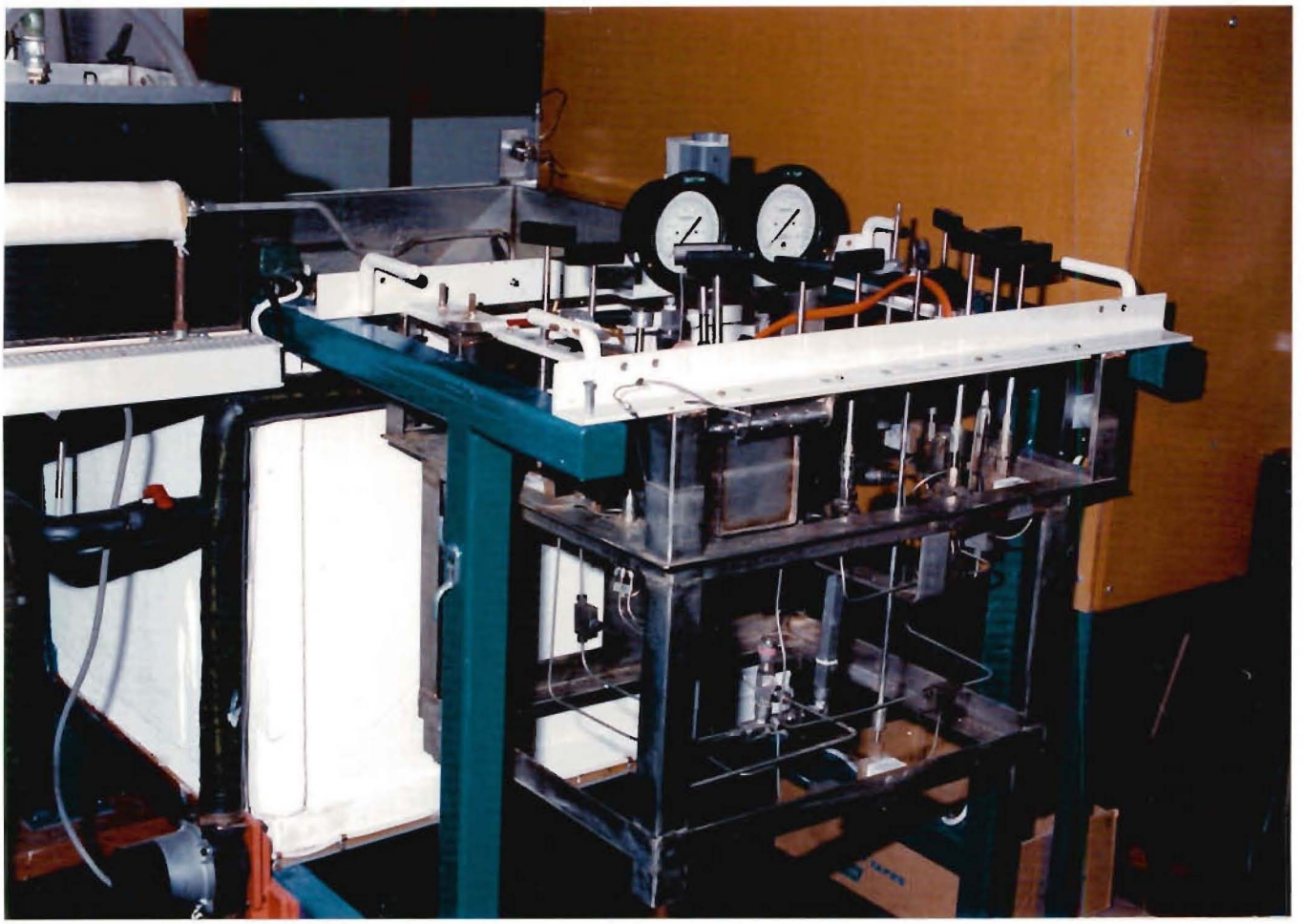

Plate 1 Detail of the Valve cage

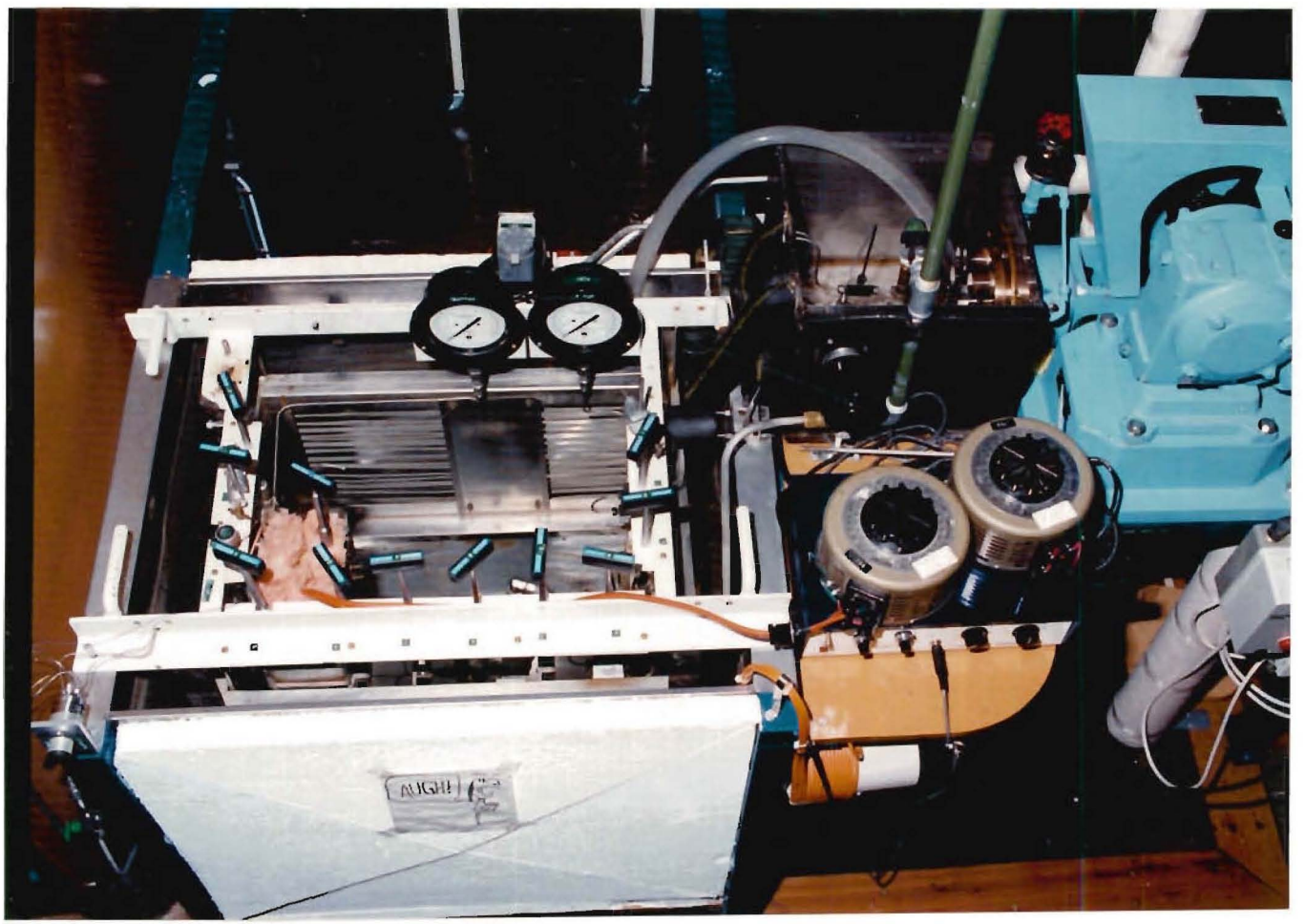

Plate 2 Plan of the Finished System

The bath was stirred with an ASEA Class F motor (0.25 kW, 1380 rpm) onto which a marine impeller was attached.
The bath was protected from overtemperature with a Honeywell L6189 controller.
The whole system could be electrically switched off and isolated by using a Cutler-Hammer type T178 emergency stop switch, with a T1 type base.
The micrometering valve was heated with 1 m of Isopad "Unitrace IUR-30" (30 W/M @240V) heating tape.
The water was circulated between the two baths by a Levco (Auckland, New Zealand) "Comet 2" magnetically driven pump.

3.3.6 Pressure Vessel Selection and Design

3.3.6.1 Introduction

In a high pressure extraction system, the pressure cell is an important component. For an apparatus such as that described above, the pressure vessel will occupy typically 80% of the system volume. For this work, two pressure vessels were used. A 400 bar (40 MPa) cell and a 700 bar (70 MPa) cell. The 400 bar vessel was used for the majority of the work.

3.3.6.2 400 Bar Cell

The 400 Bar cell was a 6" length of 0.5" nominal ID hex nipple tubing (Cajon SS-8-HLN-6.00). This length of tubing was connected to two Swagelok quick-connects, (SS-QF4 and SS-QF8). The advantage of using this sort of connection system was that it was easy to open and close the cell a large number of times, without having to worry about the resealing of Swagelok fittings. This would be especially necessary during the commissioning stage. If necessary, the O-rings could be replaced. The cell also had a Swagelok relief valve fitted (§3.3.8).

3.3.6.3 700 Bar Cell Design

To complement the operation of the 400 bar cell, a 700 bar cell with an internal volume of 300 cm^3 was designed and constructed. Design calculations are shown in Appendix 2. The construction material chosen was Avesta 2205 - a duplex, ferritic, austenitic Stainless Steel. The design limit of the material was the 0.2% proof stress 360 $N.mm^{-2}$ at 100°C. The cell had an internal diameter of 46 mm and the walls were 27.8 mm thick. The vessel used a threaded closure and sealed onto an O-ring.

3.3.7 Sample Holders

Most workers (§3.2.1) choose to contact their solid samples in some packed-bed formation. All use glass beads (or wool)/solute mixtures and all have glass wool or some other filtering device at the outlet of the cell. It was decided to make a sample holder that could be filled with solute and then be easily added to or removed from the pressure vessel with a minimum of trouble. The reason for using a sample holder rather than packing the solute directly into the cell was that the cell could remain in situ for long periods of time and only needed to be removed for periodic cleaning.

3.3.7.1 Solid Sample Holders

A solid sample holder was designed for the 400 bar cell. It was a thin walled tube with threaded ends. These ends had holders fitted which in turn had 7μm frits welded into them. The frit holders screwed into the sample holder itself (Figs 3.10 and 3.11). The frits helped give a good distribution of the solvent in the cell, while also helping to prevent any entrainment of the solid in the outlet solvent stream. Both holders had O-ring grooves cut into them and O-rings fitted, to seal against the sides of the cell and prevent the possibility of the solvent by-passing the solute.

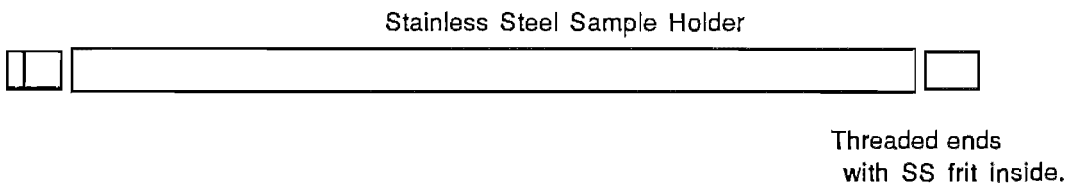

Figure 3.10. Solid Holder for the Small Cell.

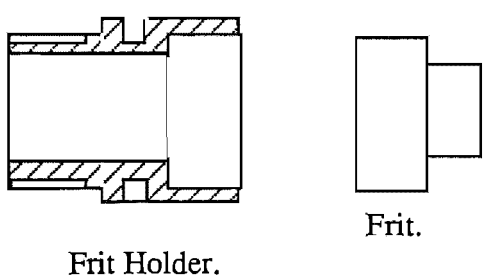

Figure 3.11. Detail of the Frit and Holder.

Each frit had a thread tapped into the open end. These threads mated with the thread of a tool made up to aid in the placement and subsequent removal of the holder from the cell. The cell was loaded with the holder by opening the top and lowering the holder into place. The

vertical orientation of the pressure vessel within the water bath made it impractical for it to be completely removed during loading and unloading of the sample holder. The tool, therefore, assisted in this process.

3.3.8 Safety Features

The use of high operating pressures involved in SFE means that certain safety features are essential. The system was protected from over pressure from the compressor by the installation of the bursting disc unit (Appendix 1), fitted with Inconel prebulged discs (rated at 8600 psig) on the outlet line from the compressor. There is no valve between the compressor outlet and the bursting disc. The 400 bar pressure cell was protected with a Swagelok 4R3A series relief valve (fitted with a 4000-5000 psig spring) in the case of the 400 bar cell and a directly inserted bursting disc (as above) in the case of the 700 bar cell. The ball check valve (Appendix 1) was mounted between the compressor and the CO_2 cylinder. The electronic protection of the system is outlined above (§3.3.5)

3.4 The HPLC System

The samples were analysed by a modular HPLC system. This consisted of a:

Waters 510 HPLC Pump,
Waters 501 HPLC Pump,
Waters Automated Gradient Flow Controller,
Waters 745B Data Module,
Waters R401 Differential Refractive Index Detector,
Brownlee RP18 Column

The HPLC system was configured as shown in figure 3.12.

For all solutes examined, the mobile phase flow was set at 1.0 $ml.min^{-1}$, giving a column back-pressure of approximately 350 psig. The RI detector attenuation was set at 64 x for Trilaurin, 32 x for Trimyristin and 16 x for Tripalmitin and Tristearin. During the course of the experiments, the HPLC analyses were performed isocratically. The mobile phase was pre-mixed and filtered prior to use.

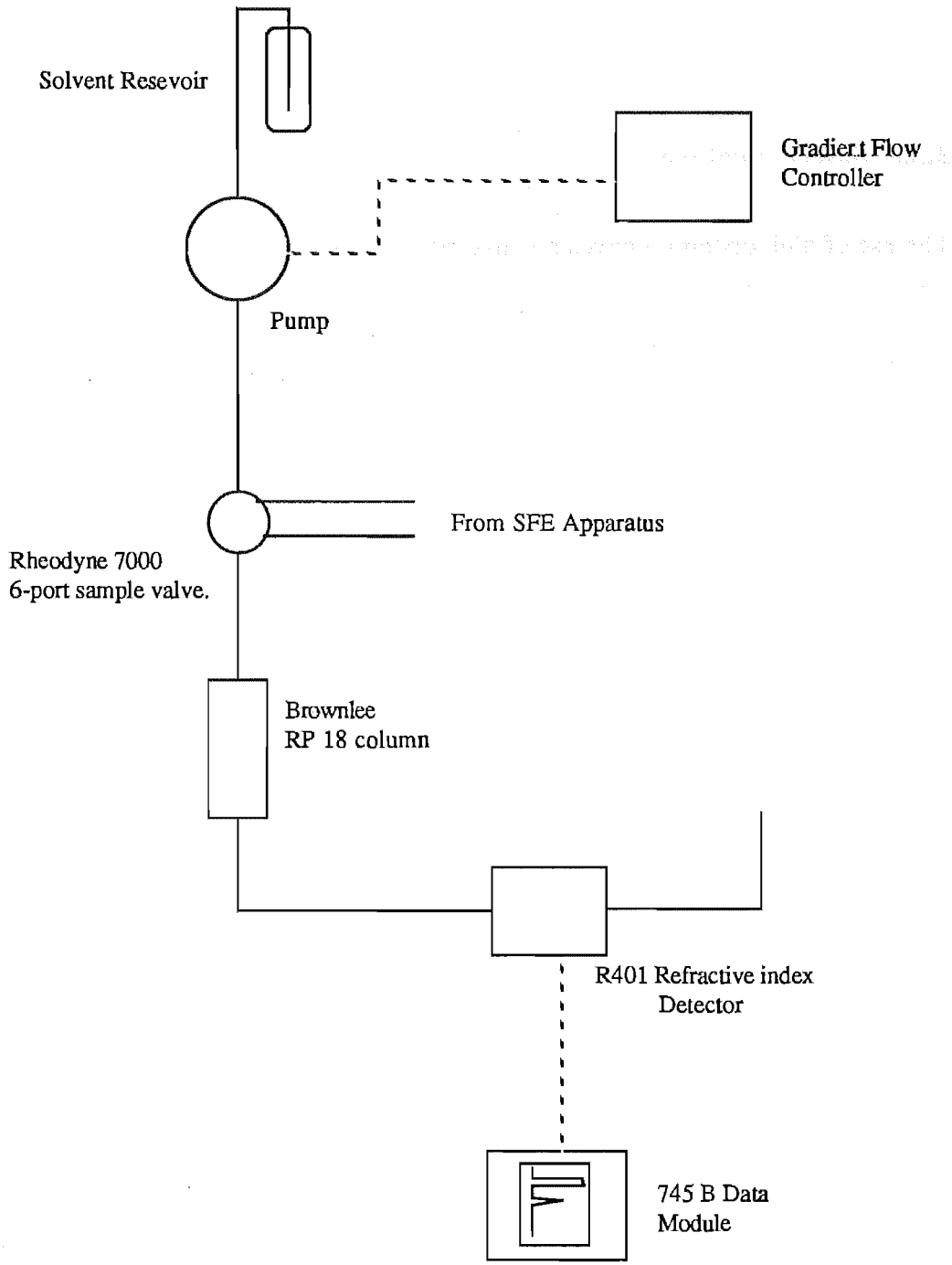

Figure 3.12. HPLC Configuration.

3.5 Experimental Method

3.5.1 Introduction

This section details the experimental plan and the final operating procedure used for measuring solubilities. For convenience, the procedure is broken up into several sections. This procedure never varied, although the solute extracted, the HPLC mobile phase and the HPLC detector parameters did vary from solute to solute. While all these extractions were preformed, the recycle loop was removed from the system (to prevent accidental recycle, compressor contamination and system cross contamination).

3.5.2 Experimental Plan

Each triglyceride would be examined at 40°C over a pre-determined density range and then at 35, 47 and 55 °C. In this way it was hoped that solubility and density could be correlated over a range of temperatures and that the solubility at these common conditions could be correlated with solute molecular mass.

Temperatures were measured with a mercury-in-glass thermometer. The range of this instrument was -10 to 110 °C, and it was graduated in 0.1°C. Pressures were measured with two 3D 25504-39B11-ISOD pressure gauges. The range of these was 0 to 100 MPa with 0.5 MPa divisions.

The mercury-in-glass thermometer was calibrated prior to use against a platinum resistance thermometer which had had its resistance measured and compared with standard thermometers held by the DSIR Physics and Engineering Laboratories. The mercury-in-glass thermometer was compared at 0°C and 60.6°C. It was found that the mercury-in-glass thermometer read 0.2°C and 60.8°C respectively. For experimental measurements, this constant deviation was allowed for. The thermometer was immersed in the main water bath, adjacent to the pressure cell, for all readings

The two pressure gauges used were calibrated by the DSIR Southern Industrial Development Division. They used a Bundenberg dead weight tester. The gauges were tested with applied pressures of 2000, 8000 and 12000 psig, and readings of 2018, 7918 and 11934 psig were recorded. The maximum deviation of the gauges was 1 %. The pressure gauge linked to the inlet of the pressure vessel was used for all pressure readings.

3.5.3 Loading the Cell

The cell was loaded with alternating layers of glass beads and solute. The first and last layers were beads. The layers were added with the aid of a clean glass funnel. The 'bottom' of the sample holder was closed. Periodically, during the packing procedure, the cell was tapped on the bench to assist in reducing solute voidage. When the last bead layer was added, the holder was closed. At this point any damaged O-rings were replaced. A thin film of a silicon lubricant (Arandee Chemicals Silicone Paste A4) was smeared onto the O-rings to stop any binding between the rubber and the cell wall. The holder was then pushed into the cell until the top of the holder was positioned just below the the rim of the hexagonal tube.

3.5.4 Getting to Temperature and Pressure

When the sample holder was in position, the pressure vessel was closed and the CO_2 slowly introduced. Care was taken to ensure that valves #2 and #7 (see figure 3.7) were open during the solvent introduction. In general, valves #2-#7 were kept open until the run had properly started. This prevented any sudden pressure drop across the cell and the holder. If these valves were not open, the applied pressure could try to force the sample holder out of the pressure vessel, damaging both in the process. If the CO_2 was introduced and, for example, valve 2 was closed, the holder could be forced downwards to the bottom of the pressure vessel allowing CO_2 by-passing to occur during extraction. Care had to be taken to introduce the CO_2 slowly, otherwise the displacement of the sample holder could be rapid! When the system was at bottle pressure, the water baths were filled from the high pressure water supply. It was normal practice to isolate and fill the compressor bath prior to CO_2 introduction to the system. In this way, the compressor head could be cooled down to below ambient temperature when the compression started. When the bath was cool/cold, there was a lower chance of CO_2 evaporation in the head during compression and more importantly, the system could be filled with liquid CO_2. The use of the liquid was estimated to decrease the time taken to get to pressure from about 30 minutes to about 5 minutes.

After checking for leaks, the compressor was started and the system taken to the operating pressure. Typically, it took 2-3 minutes to raise the pressure from 5 MPa to over 7.5 MPa. Once the pressure was above this point, compression proceeded quickly. If the water in the bath was at 15-18°C, the pressure could increase by up to 5 MPa per stroke. The system was compressed to above the operating pressure and the pressure corrected by altering the setting of the back-pressure regulator. Once the operating pressure was set, the electrical systems were turned on (the micrometering valve heating tape, the water circulation pump, the stirrer motor and the heating coils) and live steam was introduced to the bath to accelerate heating.

The approach to temperature was monitored with the mercury-in-glass thermometer described above. Once the desired operating temperature was reached, the steam was shut off, the controller set-point adjusted, the base heat load adjusted and the system allowed about 15 minutes to reach thermal equilibrium. Water bath temperature drift was monitored by a semiconductor probe, linked to a narrow range thermometer. The thermometer output ($10mV°C^{-1}$) was plotted on a chart recorder, with a range of 10mV (or 1°C) full scale. Using this method, the temperature deviation was seen to be better than ±0.01K.

When the system was at pressure and during the heating of the bath, the compressor head bath was re-introduced into the water circulation system. In this way, the compressor head was bought up to the operating temperature along with the rest of the system. It was found that pressure fluctuations due to compression were kept to a minimum (commonly ±0.1 MPa) this way.

3.5.5 Operation

While the system was being heated and while thermal equilibrium was being reached, the HPLC system was turned on and mobile phase flushed through the HPLC system. This allowed the HPLC column to come to steady state and the baseline to stabilize. The Gapmeter was fixed to the side of the valve cage and connected to a clean cold trap. The trap had been previously cleaned with chloroform and filled with glass wool to trap the entrained solute. This trap was immersed in a vacuum flask containing an ice/water mixture. The temperature of the heated valve was monitored with a thermocouple linked to a digital voltmeter to ±1°C. The heating load was continually adjusted to keep the micrometering valve temperature in a region of 80-90°C.

Once the system was at temperature, pressure and thermal equilibrium, the compressor was re-started. The micrometering valve was almost fully closed and then the system outlet valve was slowly opened. There was usually a pressure surge through the Gapmeter at this point. The micrometering valve was then opened and the desired flow (0.3 - 0.5 $l.min^{-1}$) was established. The valves 2 & 5 were then shut, forcing the solvent to flow up through the solute. The system was then allowed to run in this manner for about 10-15 minutes, to allow a steady state to be reached.

Periodic adjustments to the flow and occasionally pressure (by the back-pressure regulator) were required. The CO_2 flow tended to drop off as the dissolved solute precipitated in the hot micrometering valve. Samples were taken (§3.5.6) as required. When three or four successive HPLC readings (peak areas) agreed to within 10%, the pressure of the system was increased. This pressure increase was also accompanied by a CO_2 flow increase. The flow was then adjusted back to the desired value. Again about 15 minutes was allowed for

the system to come to steady state before further samples were taken. Using the thermometer probe and chart recorder, the temperature control could be monitored. It was not usually necessary to adjust the temperature when the system was running at 35, 40 or 47°C. When operating at 55°C, with the addition of live steam, this monitoring became essential. With care, the temperature variations could be kept to better than ±0.1 K

3.5.6 Sampling

In order to avoid the problem of depressurisation on sampling, two 6-port valves were used to take samples of the high pressure supercritical fluid stream (figure 3.8). The sampling procedure was as follows (the valves (figure 3.8) are labelled 1 and 2 for convenience). Valve #1, is mounted on the valve cage and immersed in the water (valve #10 in figure 3.7). Valve #2 is mounted above the water bath);

With the HPLC turned on and at steady state, 6-port valve #2 was switched to by-pass the mobile phase from the sampling area. The sample loop was flushed with CO_2, to remove any traces of HPLC mobile phase. At this point, the HPLC integrator was started. Next, the 6-port valve #1 (containing the sample loop) was switched into the supercritical fluid outlet stream as shown in figure 3.8. When the extraction system was at steady state, the 6-port valve #2 was switched, allowing the mobile phase to flow between the two valves. The 6-port valve #1 was then quickly turned. This allows the HPLC mobile phase to flow through the sample loop and sweep any solute to the HPLC column. The valves were left in this configuration until the CO_2 peak had passed through the column. When the CO_2 peak had passed, 6-port valve #2 was switched and the sample loop purged of mobile phase. The process could then be repeated.

3.5.7 Depressurisation

When a sample programme had been completed the system was depressurised. During depressurisation there was some precipitation of the dissolved solute. The precipitation occurred in the outlet valves and in the lines. The procedure was to firstly to stop the compressor, remove the water from the water baths and then open valves #2 and #5 (to avoid passing too much CO_2 through the remaining solute). Next the micrometering valve was opened allowing the CO_2 to escape. If a quick depressurisation was required, the vent valve (#8) could also be opened. The water level was allowed to drop to below the top of the pressure vessel. Once the system was at ambient pressure, the vessel was opened and the sample holder removed. It was noted that the O-rings absorbed a large, but indeterminate amount of the solvent. This forced the O-rings to swell as the dissolved CO_2 expanded and this can prevent the removal of the sample holder from the pressure vessel.

4

Testing of Equipment and Experimental Method

4.1 Introduction

In this chapter, the sources of materials are listed and the development of the HPLC sampling technique is presented. Problems encountered during the generation of the experimental data and their solutions are presented. Experimental results for Trimyristin are compared to previously published values. Experience with a soluble liquid triglyceride, Tributyrin, is outlined. Finally, the limitations of the method are discussed and improvements are suggested.

4.2 Sources of Materials

The triglycerides used in the course of this work were obtained from the Sigma Chemical Co. (St Louis, Missouri, U.S.A.). They were all "Sigma" grade (approx. 99% pure) and were used without further purification. The product codes are;

Trilaurin	T 4891
Trimyristin	T 5141
Tripalmitin	T 5888
Tristearin	T 5016

The liquid CO_2 was obtained from New Zealand Industrial Gases (Christchurch, New Zealand) and was "Food Grade" (99.9%).

The HPLC chemicals were obtained from BDH (Poole, England). The grade used was HiPerSolv and product codes are;

Acetone	10003
Acetonitrile	15285
Chloroform	15283

The solvents were filtered with 0.2 μm pore size filters (Millipore Corp. Bedford Massachusetts, U.S.A.) type GVWP 047-00.

The HPLC column used was a Brownlee RP-18 5μ particle size 100 x 4.6 mm type 0711-0015 (Applied Biosystems Inc. San José, California, U.S.A.).

4.3 The HPLC System

4.3.1 Introduction

The decision to analyse the triglycerides by HPLC rather than GC was taken because HPLC systems are designed to analyse large, involatile molecules and operate at high pressures (up to 40 MPa).

4.3.2 Mobile Phase Selection

The choice of mobile phase for HPLC analysis of single solute, is generally determined by the desired retention time of the solute on the column. The type of column also influences the retention time of the solute. A polar (or reversed phase) column will have a greater affinity for polar molecules that a nonpolar (or normal phase) column. It is the combination of the column type and the mobile phase polarity that determines the solute's retention time. In general, the addition of a more polar component to a particular mobile phase, will increase the observed retention time for a nonpolar solute on a nonpolar column.

It was decided to use naphthalene as a test solute to verify the working of the system. This decision was taken because of the amount of naphthalene solubility data found during the literature review. Preliminary work with naphthalene showed that it was essential to retain the solute on the column until the detector no longer registered the mobile phase disturbance and a steady baseline was evident. Unfortunately, the Refractive Index (RI) detector is flow sensitive and when a SCF sample was switched into the mobile phase, the high pressure CO_2/solute mixture expanded. The expanded volume varied depending on the CO_2 density. This sudden expansion of CO_2 resulted in a mobile phase flow surge through the detector, leaving a slug of CO_2 in the system. It is thought this expansion of supercritical solvent caused solute precipitation near the 6-port valve and the sample loop. Most of the solute was then carried onto the column by the mobile phase. The sudden increase in the mobile phase flow, followed by a CO_2 slug, caused flow changes in the detector. Figure 4.1 shows a typical disturbance caused by the expansion of 10μl of high pressure CO_2 into the HPLC system. One can see that the disturbance to the detector is considerable. When the CO_2 was

switched into the mobile phase, there was a temporary decrease in the HPLC system pressure drop, from about 350 psi to around 100 psi.

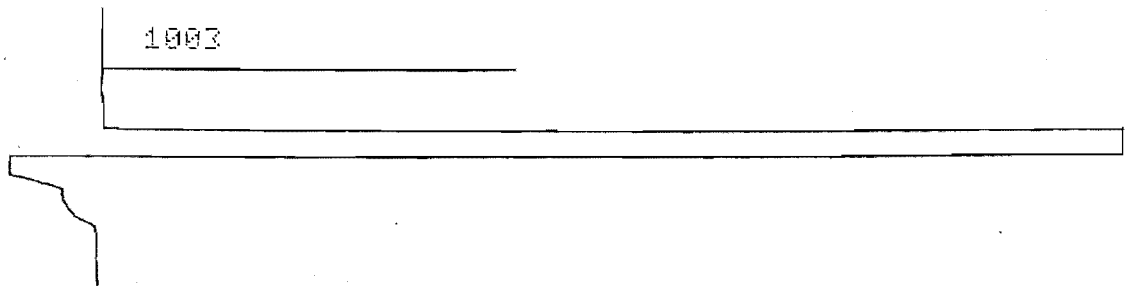

Figure 4.1 Effect of High Pressure CO_2 on Refractive Index Detector

The retention time for a given solute was dependent on the mobile phase polarity. For triglyceride molecules with a polar column, the more polar the mobile phase, the longer the triglyceride was retained on the column. The longer the triglyceride chain length, the longer the retention time on the column for a given mobile phase composition.

Lie Ken Jie (1980) suggests using a mobile phase with the composition of Acetonitrile:Acetone (2:1) for separating saturated triglycerides of carbon number 26, 30, 32, 34, 36 and 42. For this work, triglycerides of carbon number 36, 42, 48 and 54, were used. For the first triglyceride investigated, Trimyristin (carbon number 42), the mobile phase composition suggested by Lie Ken Jie was used. It was found that at this mobile phase concentration the retention time of the triglyceride sample was too low and the solute peak was obscured by the CO_2 disturbance. The amount of acetonitrile in the mobile phase was decreased until a satisfactory retention time (8 minutes) was observed. This corresponded to a mobile phase ratio of acetone:acetonitrile of 3:1. The table 4.1 gives the final mobile phase concentrations and retention times used during this experimental programme.

To ensure the mobile phase concentrations were reproducible, the volume ratio (based on 500 ml) of the mobile phase was converted to a mass ratio. The individual components of the mobile phase were weighed out and mixed during filtering.

Table 4.1 Mobile Phase Concentrations and Solute Retention Times

Solute	Mobile Phase Ratio Acetone:Acetonitrile (v:v)	Retention Time (Minutes)	Detector Attenuation
Trilaurin	64:36	5	64
Trimyristin	75:25	8	32
Tripalmitin	83:17	7	16
Tristearin	85:15	11	16

Other factors influencing the retention time are the size of the detector disturbance and the sensitivity of the detector. For Tripalmitin and Tristearin the 10 µl loop did not deliver sufficient solute for the HPLC to give reliable readings. It was decided to replace the 10 µl loop with a 20 µl loop for Tripalmitin and with a 100 µl loop for the Tristearin. Although the increased loop size would deliver two and five times more solute to the HPLC, the solubility for Tripalmitin was expected to be approximately an order of magnitude less than that of Trimyristin at similar conditions. The RI detector attenuation was decreased from 32 to 16 for both Tripalmitin and Tristearin to compensate for the expected decrease in solubility. This increase in detector sensitivity combined with the bigger disturbance from the increased sample loop size, resulted in longer recovery times for the HPLC system to produce a stable baseline. It was not possible to maintain a steady baseline at a RI attenuation of 8.

Difficulty with the analysis was the major reason for not continuing the attempt to verify the SFE system with naphthalene as the solute. It proved difficult to find a mobile phase composition that was polar enough to retain the naphthalene on the column until the CO_2 disturbance had passed. Mobile phase compositions of acetone (100%) and methanol:water (50:50 and 70:30) were tried. The mixture of 70:30 methanol:water did give a long enough retention time, however these investigations, the column backpressure was seen to rise quickly from about 300 psi to about 2000 psi. The column was backflushed with Acetone and then with Chloroform to try and remove any contamination. The pressure drop decreased to 1400 psi. The 70:30 methanol:water was used further and the column pressure again rose to over 2000 psi. Further backflushing failed to reduce the backpressure and the column was replaced. Several possible reasons for the column failure were considered;

1. reduction in the voidage in the column from the pressure shocks during sampling,
2. swelling of the column particles, resulting in voidage reduction,
3. collection of foreign material on the column,
4. deposition of the solute in the column,

5. removal of the C18 groups from the column particles and their deposition further on the column.

Subsequent experience with Tristearin calibrations suggested that possibility 4. is the most likely. With Tristearin, it was noted that during detector calibrations the most concentrated samples did not produce the expected areas. When several injection were made from the same bottle of a concentrated standard sample, the HPLC area was initially as high as expected, but decreased with successive injections. The recorded areas approximately halved with successive injections until a steady state value was reached. This steady state value was both well below that expected for the concentrated sample and below that previously observed for other less concentrated standard solutions. This problem was only noticed for the Tristearin samples. Also for Tristearin there was a noticeable increase in the column pressure drop, although not as great as previously observed for naphthalene. The Tristearin standards were prepared with chloroform as the injection solvent. The solubility of Tristearin in chloroform is much higher than in the chosen mobile phase, hence when the injected chloroform/Tristearin sample reached the column, the Tristearin was deposited and the chloroform passed through the column. Some of the Tristearin will be dissolved by the mobile phase and carried onto the detector. The amount of solute that reaches the detector will be (at most) the saturation solubility at ambient conditions. It is possible the presence of excess solute on the column may act as a nucleation site for further Tristearin precipitation, resulting in solute deposits that could lead to column blockage and increase the column backpressure. With Tristearin the column regeneration was successful, but for the naphthalene the regeneration process was unsuccessful. For this reason, it was decided not to examine naphthalene further and to move onto the investigation of the triglycerides.

4.3.3 HPLC Calibration

The RI detector sends an electrical signal to the integrator. The integrator plots the change in detector signal and evaluates the area under the peak. This area has units proportional to millivolt seconds (mVs).

The RI settings and mobile phase compositions used during experimentation were used when the HPLC system was calibrated. A 10 µl sample loop was used with the valve/loop volume determined in the manner of Bakalyar and Spruce (1983).

Standard solutions of a known mass of solute dissolved in a known mass of chloroform were prepared. Six to eight solutions were prepared for each of the solutes examined. These standards ranged in concentration from 0.03 to 3 mass percent. Care was taken to ensure that the highest concentration standard prepared gave a detector response greater than that observed for the solute during the experimentation. Ten injections of each of these standard

samples was found to give a good estimate of the mean detector response per sample. The 95% confidence limits for ten injections ranged from ±1% for the high concentration standards to ±4% for the lower concentration solutions.

Calibration curves relating the detector response (area) to the mass of solute injected to the system were prepared. For all the solutes, an unweighted linear least squares regression procedure was used to determine the equations of best fit. For Tripalmitin, this calibration curve gave negative solubilities because of the small HPLC areas recorded. To correct for this, an unweighted linear least squares regression equation which was forced through the origin of the graph was produced. This change gave positive solubilities over the whole range of areas measured. The overall effect of this change on the calibration line was for the slope of the line to decrease - resulting in slightly lower solubilities (about 6% lower) at the high solubility end and higher solubilities (about 50% higher) at low solubilities. From this test, it was apparent that the final solubility values will be very sensitive to the calibration. The final error in the each calibration was estimated to be ±4%. The calibration curves and best fit equations are presented in Appendix 3.

4.3.4 Off-Line Data Storage

The Waters 745B data module stores chromatographic data in "bins" of variable size. The longer the trace, the bigger the bin required to store the data. The data module is equipped with an RS-232 connection port for sending the data to an off-line storage device. Bins can also be sent from the storage device back to the data module for further reprocessing as necessary. The RS-232 communications take place at 2400 BAUD for sending to the storage device and 1200 BAUD for receiving the data from the external source. The data were initially stored through an Epson QX-10 computer on floppy disks. The data was then backed up to the VAX 11-730 computer and further stored on magnetic tape.

4.4 Problems Encountered During Method Development

4.4.1 Heating the Micrometering Valve

The heating of the micrometering valve was initially a problem. It was found that if the micrometering valve was immersed in the water bath, the water provided sufficient heat to prevent the CO_2 from freezing in the valve when it expanded to atmospheric pressure. When naphthalene was extracted it was soon found that the heat input from the water bath was insufficient to prevent the precipitate from clogging the micrometering valve. This blockage was usually followed by a pressure build-up and a release of pressure as the deposited solute

was quickly cleared from the valve. This block/clear cycle was unacceptable because the system was never running at steady state. It was decided to investigate the heating of the micrometering valve by either steam or electrical heating. Electrical heating was considered most suitable.

The micrometering and shut-off valves were located in an open stainless steel box above the water bath. Heating tape was wound around the valves and the inter-connecting tubing. The space around the valves was filled with a spun fibreglass insulation to minimise heat loss. The insulated box was suspended above the water bath to prevent water from entering. The heat input to the valves was controlled by a 'Variac' variable voltage transformer.

It was found that to maintain a constant flow of the solvent/solute mixture through the valves, the valve temperature had to be raised above the melting point of the solute. If the valves are at such a temperature, then any precipitated solute will melt on contact with the valve. Any liquid that is not entrained in the outgoing solvent stream is moved away by the force of the solvent flow. Wu *et al* (1988) use a micrometering valve temperature of over 150°C when extracting fatty acid methyl esters. This was the only reference found that indicated how much heat should be applied to the valves. When the valves were heated to 80-90°C in the present work, there were no further problems with blocking and a steady CO_2 flow could be maintained.

4.4.2 Sample Loop Calibration

An integral part of the experimental technique was the use of the 6-port valve and a known volume sample loop for sampling the high pressure extraction vessel effluent. The first attempt to measure the injected volume was by collecting CO_2 expanded from the valve over water. This method was found to be irreproducible because the volume collected could not be accurately determined. A second attempt was made by weighing the empty sample loop and then weighing the loop when it was full of distilled water. The density of the water was known and hence the volume of the loop could be estimated from the mass difference. This method gave a good estimate of the loop volume, but it was not possible to determine the internal volume of the 6-port valve by this method. Bakalyar and Spruce (1983) present a method for loop and valve volume determination based on the detector response to a series of injections of known volume. For example, to calibrate the 10µl loop, a solution of acetone in acetonitrile was prepared. Samples of 2, 4, 6, 8, 10, 15, 20, 50 and 100 microlitres were injected (ten injections per sample), the areas of these injections were recorded and plotted against the injected volume.

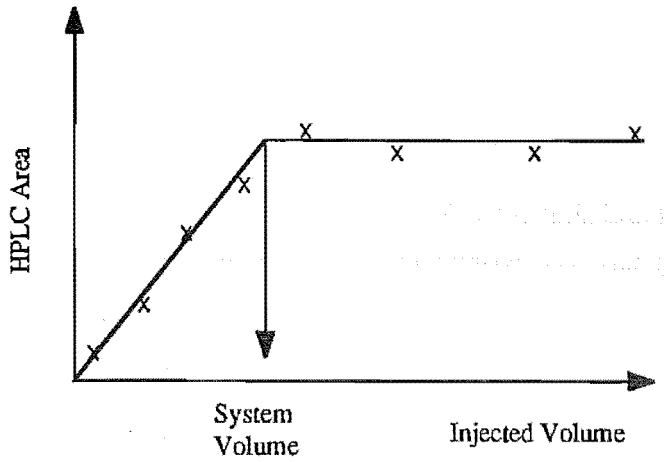

Figure 4.2 Determination of Sample Loop Volume.

Two straight lines were drawn (see fig 4.2) and the injected volume was determined from the volume coinciding with the intersection of these lines. This procedure was repeated for all the valve/loop combinations used. The final volumes used in the calculations are shown in table 4.2.

Table 4.2 Sample Loop Volumes.

Nominal Volume (µl)	Measured Volume (µl)
10	14.5
20	25.5
100	105.0

4.4.3 Solid Sample Holder

The solid sample holder caused several problems during the method development. One problem was the sealing of the holder against the sides of the pressure vessel and a second was that of the packing of the holder itself.

It was discovered that during the manufacture of the 400 bar cell, the hexagonal stock bar had been drilled from both ends. Unfortunately the piece was not correctly aligned, resulting in a bowed hole. It was possible for the sample holder to sit in the pressure vessel and the O-rings not to seal against the sides of the cell allowing CO_2 to by-pass the sample holder and give low solubilities. To remedy this the pressure vessel was reamed out and the inside

surface polished to remove any high points. The reaming did not remove the bow from the cell, but widened the hole sufficiently to allow the smooth passage of the sample holder. The O-ring groves in the holder ends were re-machined and larger O-rings fitted.

The packing of the sample holder presented a more subtle problem. Initial trials with the equal volume mixture of beads and solute gave inconsistent results. With this packing technique it is possible for the solvent to create a channel through the centre of the holder, giving the solvent the chance to by-pass the majority of the solute. When the holder was removed to be refilled and the remaining solute and beads had to be removed, it was possible to see the result of this channelling. The beads and solute had adhered to the sides of the holder and one could see through the holder. To remove this effect, the holder was re-packed with alternate layers of solute and beads. At the end of an extraction, the holder was examined. There was still evidence that some beads and solute adhered to the walls of the holder, but the effect was not as pronounced as before. The remainder of the beads fell to the bottom of the holder as the solute was extracted. The results obtained using this packing method were reproducible and the packing method was used in all further runs.

4.4.4 Contamination

One of the advantages of direct coupling to HPLC is the opportunity for trouble shooting during a series of experiments. An example of this is presented below (figure 4.3).

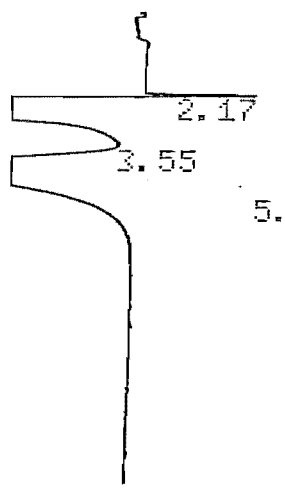

Figure 4.3 Example of System Contamination

During normal operation, only the peaks due to the CO_2 disturbance, and the small positive triglyceride peak were present. The negative peaks indicated that there was some form of contamination in the system. It was essential that the source of this contamination was identified and removed. The system was shut down and the sample holder removed. The

pressure vessel was cleaned with chloroform and placed back in the system. When the system was run again the contamination was still visible. This eliminated a solute impurity as a possible contamination source. The next step was to isolate the pressure vessel. Figure 4.4 shows the two solvent paths that were used to see if contamination was still present. The extraction vessel was by-passed by two paths to see if there was any impurity build-up in the lines during the trials.

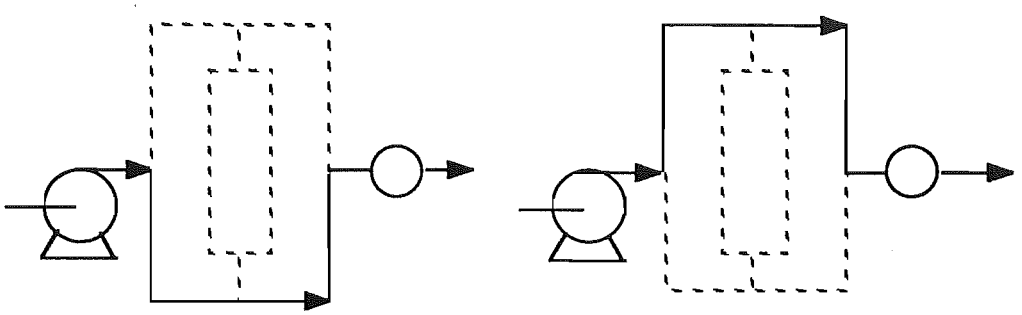

Figure 4.4 CO_2 Paths Used to Find Contamination Source

Unfortunately, the contamination was still present, pointing to several possibilities;
1. That something was being leached from the back-pressure regulator seals.
2. Grease in the 6-port valve was being transferred during the sampling process.
3. The compressor was contaminating the system, possibly through a ruptured diaphragm.

The back-pressure regulator was removed from the system and high pressure CO_2 was passed through the system, but the contamination was still visible. The second step was to replace the compressor diaphragm (Newport Scientific, 1985). At the same time, the compressor check valves were cleaned and refitted. The compressor head was flushed with chloroform to remove any residual oil from the installation process and the system re-started. This time there was no sign of contamination. The back-pressure regulator and the charged extraction vessel were re-introduced to the system and no further contamination was observed.

Close examination of the compressor diaphragm showed pitting around the outer edge. This is illustrated in plate 3. This investigation did not reveal any visible hole in the diaphragm.

Once this source of contamination had been eliminated, attention was turned to the sealing and lubricating agents used in the system. A sample of the silicone lubricant used on the O-

Plate 3 Evidence of Pitting on Compressor Diaphragm

Before

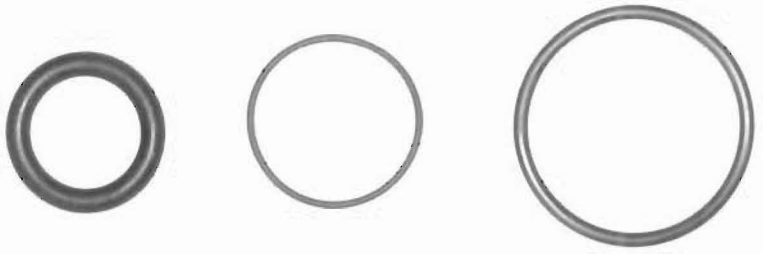

After

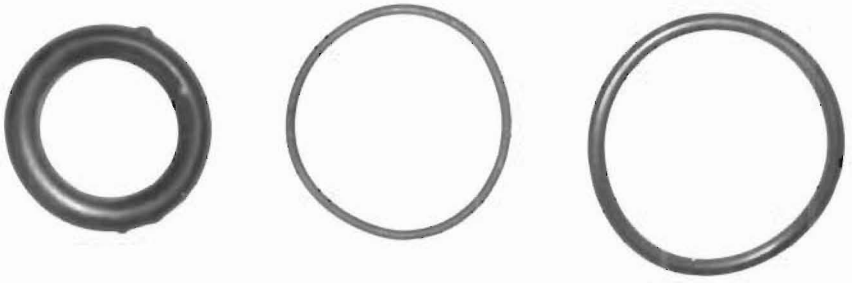

Plate 4 Effect of CO_2 on Liquid Cell O-Rings

rings (§3.5.3) was smeared onto the inside surface of the pressure vessel. Supercritical CO_2 was passed over the sample and a sample of the solvent stream sent to the HPLC. There was no sign of any contamination from this substance.

The anaerobic thread sealant SWAK used to lubricate and seal the threads of the 400 bar cell was also tested in this manner. The chromatogram for SWAK is shown in Fig 4.5.

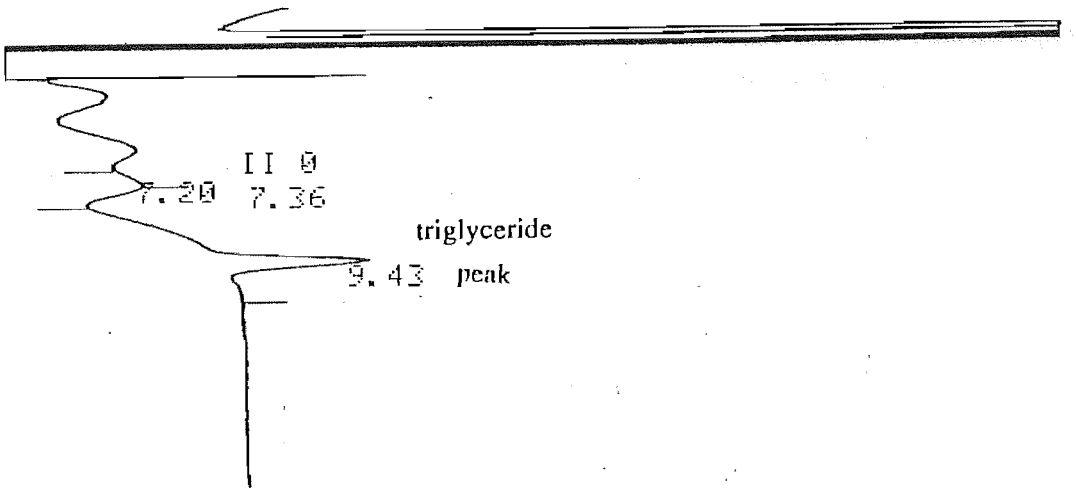

Figure 4.5 Chromatogram of SWAK (28MPa and 40°C)

The peaks of the chromatogram indicate that there could be some danger of contamination if too much of this sealant is used. The SWAK was replaced by a teflon thread tape (Ceelon Plastics Ltd. N.Z).

4.4.5 O-Rings

As mentioned in §3.5.7, the O-rings swelled up when contacted by the high pressure CO_2. This caused problems when trying remove the sample holder from the 400 bar cell. In many cases, the O-rings were destroyed during removal.

Plate 4 shows the effect of the CO_2 on the O-rings, before and after the contact. This distortion was not a problem until the system was depressurised.

4.5 Verification of Results and Experimental Error Sources

4.5.1 Verification of Reproducibility

Figures 4.6 to 4.10 show the recorded HPLC areas for Trimyristin during the verification experiments. The abscissa represents the run number and the ordinate is the HPLC area. The bars indicate average solubilities and are ascribed a ±10% error. To determine this error, the maximum and minimum areas were compared to the mean values. In most cases, the extreme values were within 10 % of the mean value. There are several points that should be noted from these plots.

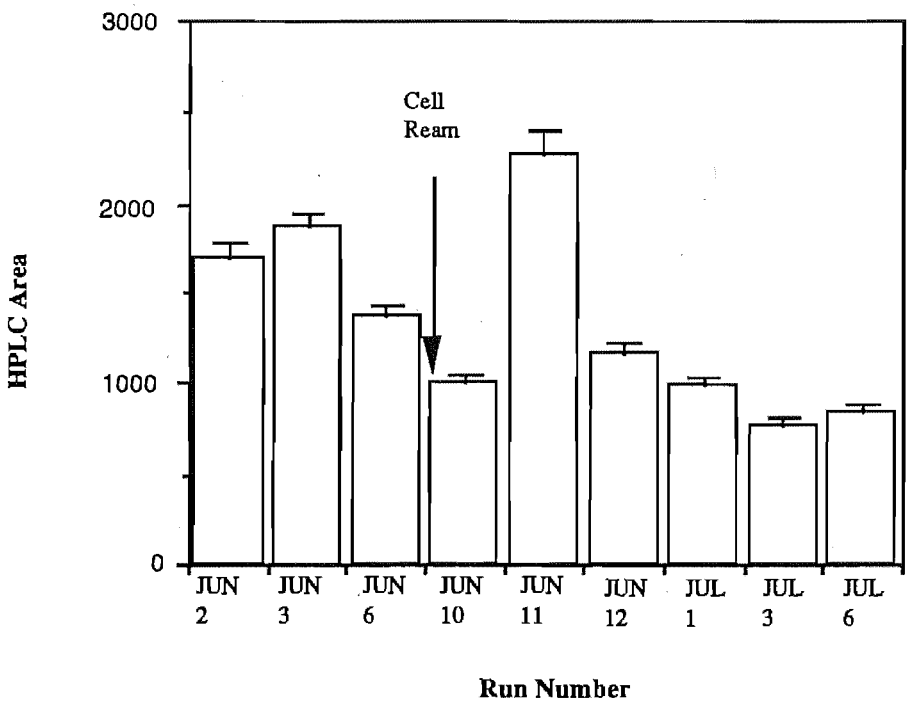

Figure 4.6 Variation in HPLC Peak Area for Solubility Measurements of Trimyristin at 40°C and 9.5 MPa

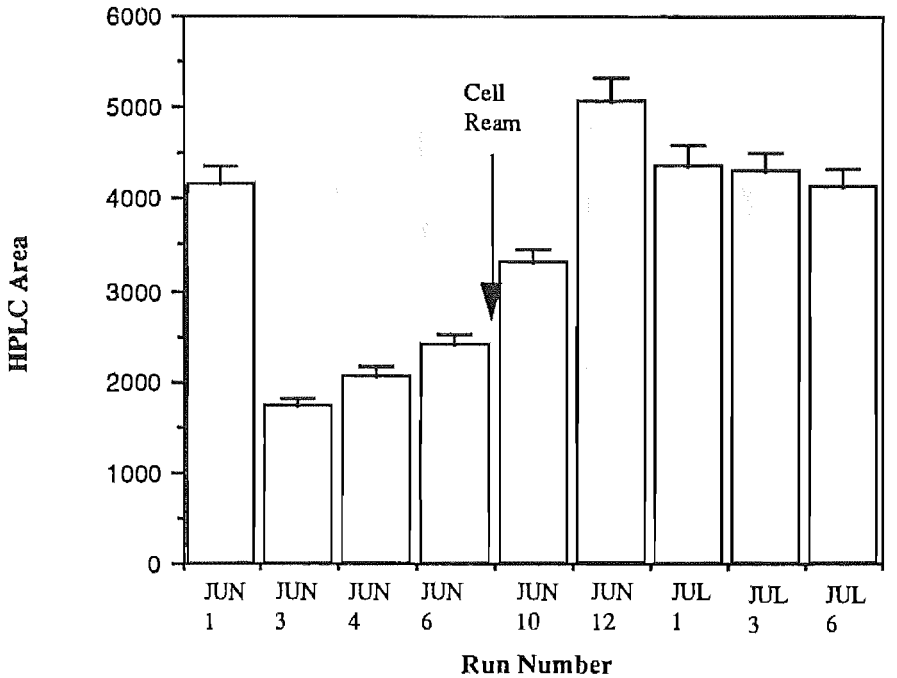

Figure 4.7 Variation in HPLC Peak Area for Solubility Measurements of Trimyristin at 40°C and 12.5 MPa

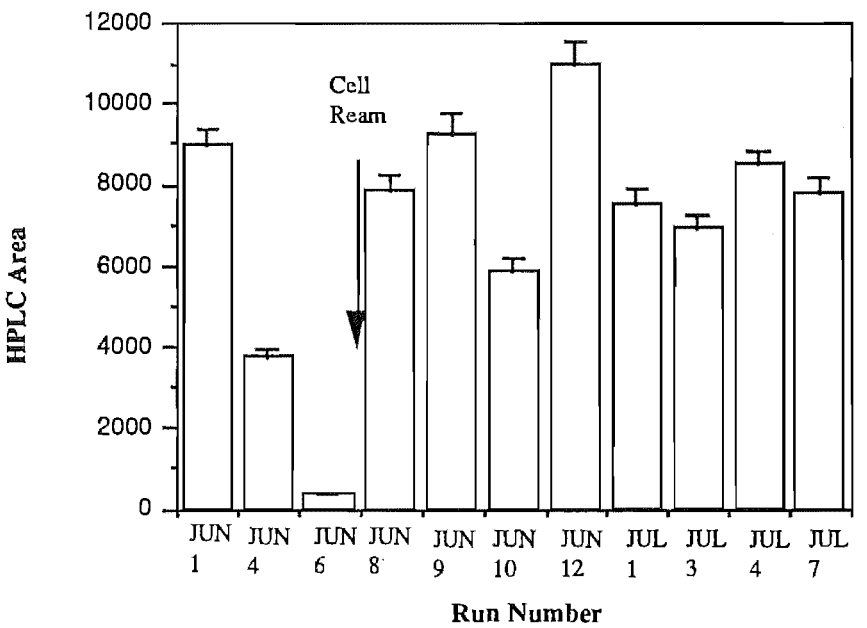

Figure 4.8 Variation in HPLC Peak Area for Solubility Measurements of Trimyristin at 40°C and 15 MPa

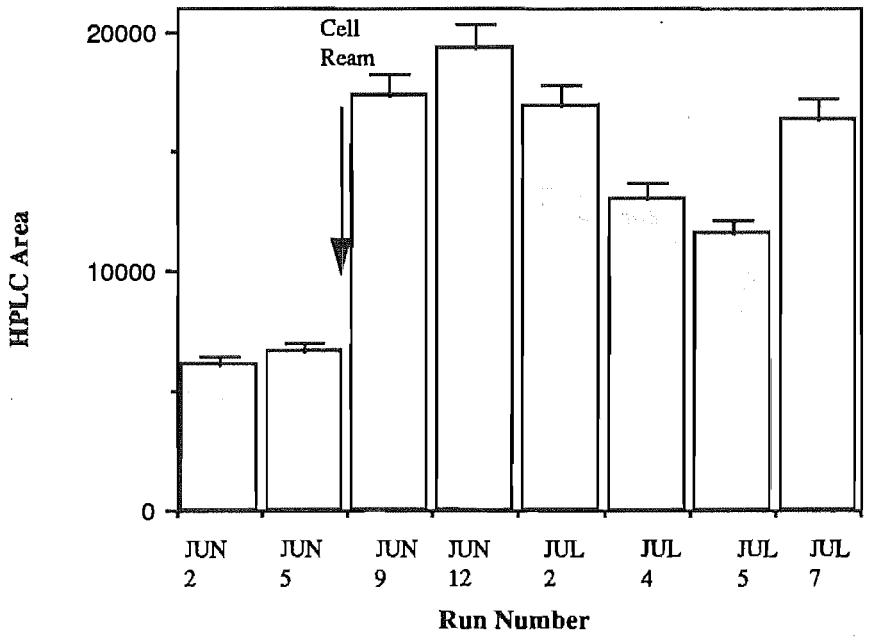

Figure 4.9 Variation in HPLC Peak Area for Solubility Measurements of Trimyristin at 40°C and 20 MPa

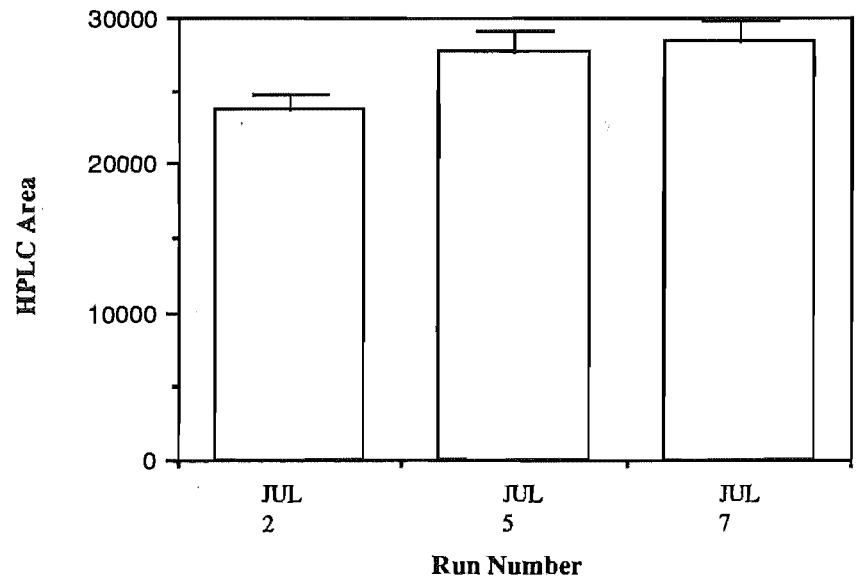

Figure 4.10 Variation in HPLC Peak Area for Solubility Measurements of Trimyristin at 40°C and 26.9 MPa

All the values obtained prior to run JUN 8 are unreliable. Between runs JUN 7 and JUN 8, the cell was reamed and polished and new o-rings were fitted to the cell. This accounts for the variation in results before this point. After this point, the holder was packed with the alternating layers of beads and solute. The results for JUN 10 are thought to be low (when

compared to the final areas) because the holder had been forced to the bottom of the pressure vessel before the run started, allowing some CO_2 to by-pass the solute. Runs JUN 11 and 12 are considered high (compared to the final areas) because of excessive sealant in the system possibly causing an entrainment effect. The data from JUL 1 onwards were used for the comparison to the results of Bamberger *et al* (1988). These figures show that the system was generating reproducible values after this run.

It should be noted that the data for 40°C and 10.5 MPa (Table A4.2) were obtained after the results were obtained for 40°C at 9.5, 12.5, 15, 20 and 26.9 MPa. The 10.5 MPa data were not obtained during the testing of the apparatus and are not presented in this section. Originally, the decision was made to attempt to duplicate the results of Bamberger whose data were taken at densities of 0.57, 0.73, 0.78, 0.84 and 0.89 $g.cm^{-3}$. When the solubility data from this work were plotted against density, it was evident that there was a gap in the data at approximately 0.66 $g.cm^{-3}$. To fill this gap, solubilities were measured at 10.5 MPa and 40°C. Measurements were also made at 12.5 MPa and 40°C to check for reproducibility. The data for 12.5 MPa agreed with the previous areas within experimental error.

The error in the experimental solubilities is estimated to be 10 percent. This error estimate came from a combination of the HPLC scatter and solute calibration. The error of the temperature reading was usually less than ±0.05 K, and at worst (308K) 0.01 %. The error in the pressure was usually less than ±0.10 MPa at high pressures (≥15 MPa) and ±0.25 MPa at low pressures. The pressure fluctuations decreased as the system temperature increased. At 35°C especially (4°C above the critical point) the fluctuations were ± 0.25 MPa - the largest observed. At the highest temperature of 55°C, the pressure variation was less than ±0.1 MPa.

Heating the compressor bath to the same temperature as the remainder of the system ensured that the solvent was at thermal equilibrium when it contacted the cell. As the compressor bath temperature increased, the incoming liquid CO_2 evaporated. This resulted in the compressor acting on a gas rather than a liquid. Hence less mass was being passed into the system per compressor stroke and the pressure pulses decreased. The installation of a surge tank to act as a CO_2 reservoir could help to further reduce the pulses to the system. These pulses (at worst) contributed ±3 % to the error of the solubility measurements.

The HPLC analysis contributed the remainder of the error in the measured solubilities. A good measure of the scatter of the results came when the RI detector was calibrated for each solute. In this process 10 injections of a standard solution were passed through the detector. Since all the injections came from the same sample and evaporation was assumed to be negligible during the course of an injection, any scatter in the areas could only come from the manner in which the integrator evaluates the signal from the detector. This is determined

from the change in relative refractive index caused by the sample flowing through the detector. The absolute error in the data remained the same for all concentrations injected, hence the error decreased as the concentration increased.

For a typical series of 10 injections (for example Trilaurin sample 5) the mean area was 11100 area units (with a standard deviation of 170 units).

A t-test for 95% confidence is $t_{.25}$

$$= \pm t_{(n-1)} \cdot \frac{\sigma_{n-1}}{\sqrt{n}}$$

$$= \pm 2.365 . \frac{170}{\sqrt{10}}$$

$$= \pm 130 \text{ area units.}$$

which is slightly lower than the standard deviation, giving an error of 1.2 %. For lower concentrations and higher detector sensitivity, this error was at worst 4%. Therefore an error of 4 % is attributed to the calibrations. This error can be added to a 4% scatter in the measured data giving an overall error of approximately 10% in the measured values. All the points for the current work have been ascribed an error of ±10% in the measured solubilities - the error bars become small when seen on a semi-log plot, slightly larger than the symbols. Each experimental solubility presented in tables 5.1 to 5.4 in Chapter 5 is an average of at least 3 samples taken at the chosen temperature and pressure. In the case of Trimyristin these data were obtained on separate days and the areas for all these points were averaged.

4.5.2 Comparison with the Results of Other Workers

Figures 4.11 to 4.13 show comparisons between data generated during this experimental programme and the data of Bamberger *et al* (1988). Examination of these graphs shows that for the systems of Trimyristin and Trilaurin in CO_2 there is good agreement between the results of this work and that of Bamberger. This agreement falls well within the experimental error for our data (Bamberger quotes an error of ±6% - or the size of the symbols on these plots) at high CO_2 densities. At low CO_2 densities these discrepancies are greater than experimental uncertainty. The plot for Tripalmitin (figure 4.13) shows a disagreement between the results of this work and those of Bamberger. It is notable that with Tripalmitin as well as for Trilaurin and Trimyristin, the differences are smallest at high density. These differences can be explained in terms of the purity of the chemicals used and the sampling and extraction techniques.

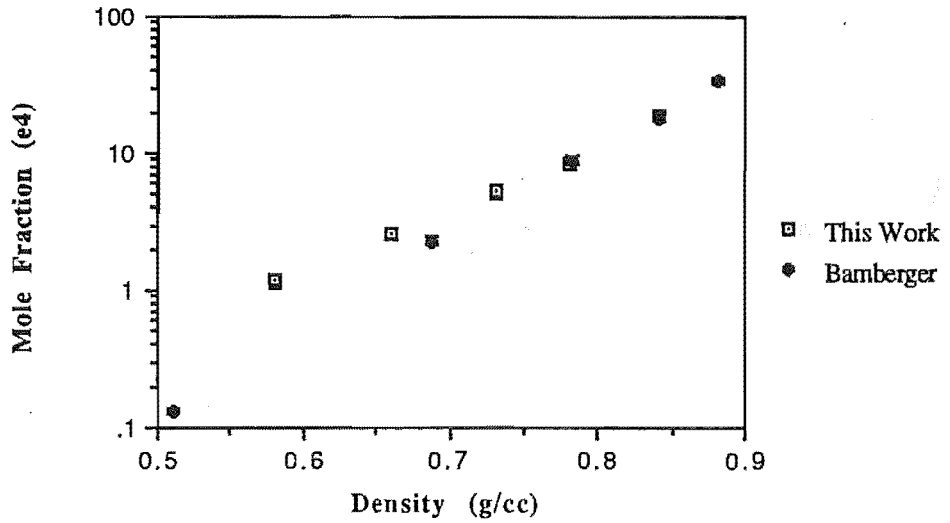

Figure 4.11 Comparison Between This Work and Bamberger *et al* (1988) for the Solubility of Trilaurin in CO_2 at 40°C

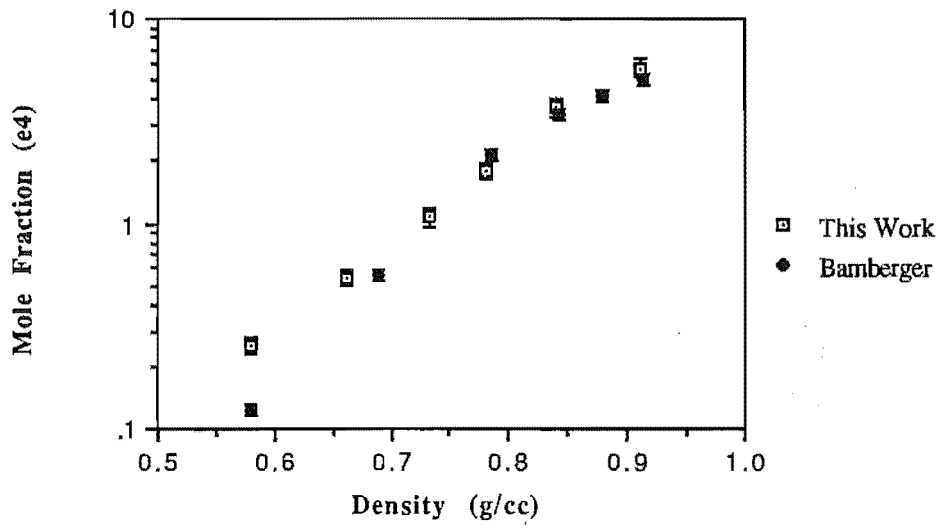

Figure 4.12 Comparison Between This Work and Bamberger *et al* (1988) for the Solubility of Trimyristin in CO_2 at 40°C

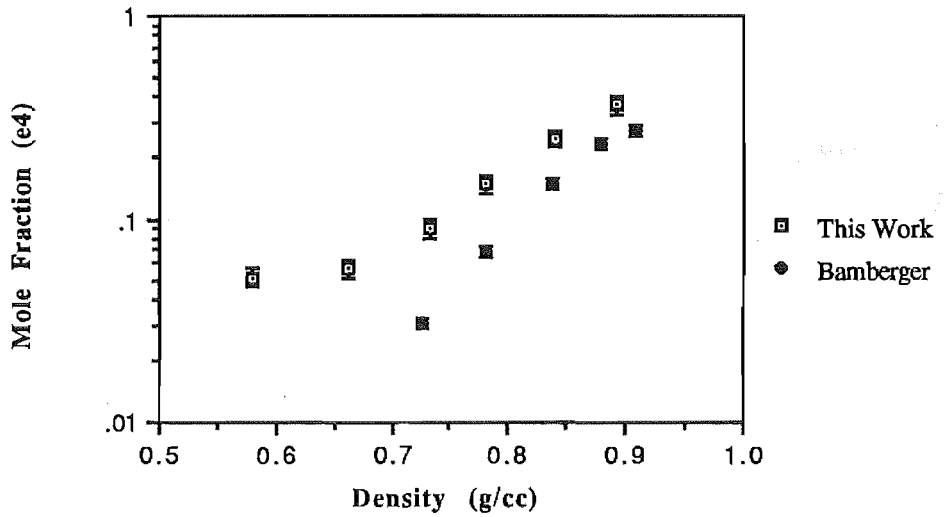

Figure 4.13 Comparison Between This Work and Bamberger *et al* (1988) for the Solubility of Tripalmitin in CO_2 at 40°C

Solute purity is one possible cause of the discrepancies between the experimental solubilities obtained from this work and the results presented by Bamberger *et al* (1988). Bamberger *et al* purified the solutes prior to extraction. Bamberger *et al* (1988) tested the solubility of Tripalmitin (at 90% and 99% purity) and compared these results to those of Chrastil (1982). They found that the solubility of the less pure solute was about an order of magnitude more soluble than the more pure one. The conclusion was the difference between their results and those of Chrastil could be explained in terms of the solute purity. For this work, the solutes were used in the 'as received' condition (approximately 99% pure). Impurities in the solutes would be expected to be detected by the HPLC system during the extraction and during the calibration stages. During the course of this work, the pressure vessel was loaded with solute and for each temperature, measurements were made at increasing densities. A charge of solute would typically last long enough for steady state readings to be obtained for at least 4 densities. Kumar and Johnston (1989) have suggested that a plot of log solubility against solvent density (or log density) would give a straight line. One would therefore expect any deviation from this exponential relation to be visible at the lowest densities - while the charge is still fresh. Nearly all the lines from this work (figures 4.11 to 4.13) are straight. This suggests that if an impurity effect is present then it is small. Bamberger *et al* have suggested that the presence of an impurity will tend to enhance the solubility.

The choice of sampling procedure could also explain the deviation between the results of this work and those of Bamberger *et al* (1988). For this work an on-line HPLC system was used, in an effort to minimise the solute loss when samples are being taken. Bamberger *et al* chose to use a gravimetric method. It is possible that using the gravimetric technique some of the solute will be lost in the sampling process. Any such loss will be most noticeable at low

solubilities where the amount of solute collected over a time period is very small. Here even the smallest mass loss could markedly alter the results.

A comparison between the experimental methods used in this work and those used by Bamberger are presented in table 4.3.

Table 4.3. Comparison of Experimental Methods

	This Work.	Bamberger
Chemicals	As received	Purified by SFE
Sample Method	On-line HPLC	Gravimetric
Mass flow CO_2	5.3-10.6 $mg.s^{-1}.cm^{-2}$	10.8-18.8 $mg.s^{-1}.cm^{-2}$
Analysis	HPLC	GLC

The other main difference between the two techniques that could contribute to any significant deviation between the two sets of experimental results is the mass flow through the systems. For this work, several CO_2 mass rates were tested and a CO_2 flow rate below 0.5 $l.min^{-1}$ (at NTP) ensured that the CO_2 was saturated upon leaving the system. A volumetric CO_2 flowrate of 0.3 $l.min^{-1}$ (at NTP) was used for all the runs. This rate is equivalent to a mass rate of 5.3-10.6 $mg.s^{-1}.cm^{-2}$, depending upon the CO_2 density.

Figure 4.14 shows a comparison between the solubility data of Tripalmitin obtained by Bamberger *et al* (1988), by Chrastil (1981) and that of this work. The order of magnitude difference between the results of Bamberger and Chrastil is evident, while the values from this work lie between the two. This difference could be explained by a combination of solute purity (for the high results of Chrastil) and sampling method (for the low results of Bamberger). Figures 4.15 and 4.16 show a comparison for Tristearin between Brunetti *et al* (1989), Ikushima *et al* (1985), Chrastil and the results of this work. As can be seen, the measured solubilities from this work are lower than all the other results. The differences between Chrastil and this work could be accounted for by the purity of the solutes chosen. This also applies to the data of Brunetti. The solutes used by Brunetti are only 65% pure. The data of Ikushima are calculated from the initial slopes of the weight % Tristearin versus CO_2 collected graph presented in his paper. This makes comparison of his data with that of other workers difficult.

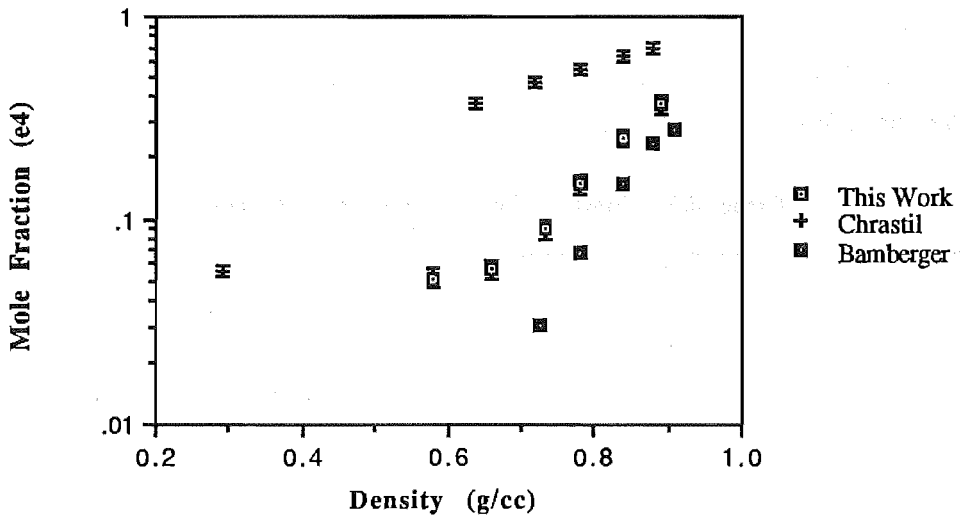

Figure 4.14 Comparison Between Three Workers for the Solubility of Tripalmitin in CO_2 at 40°C

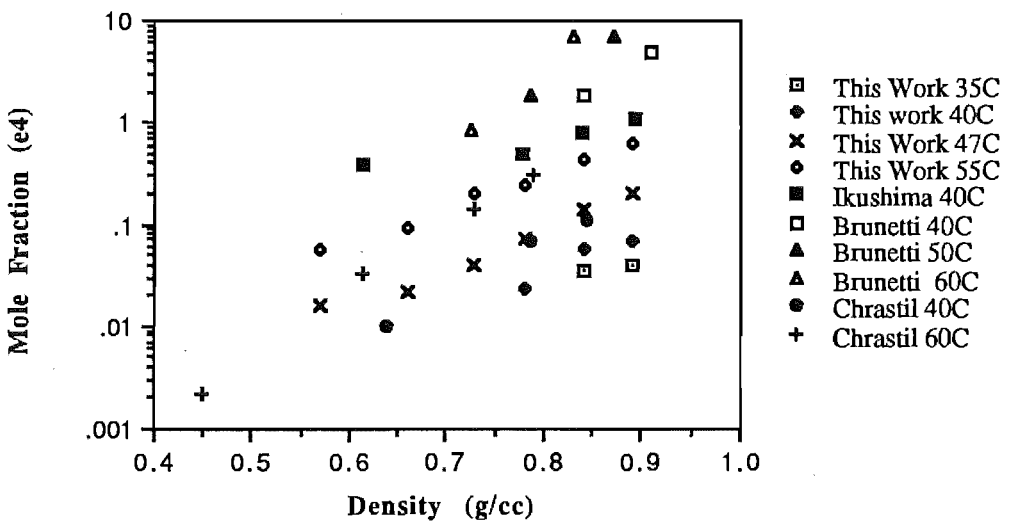

Figure 4.15 Comparison Between Workers for the Solubility of Tristearin in CO_2 at 35°C to 60°C

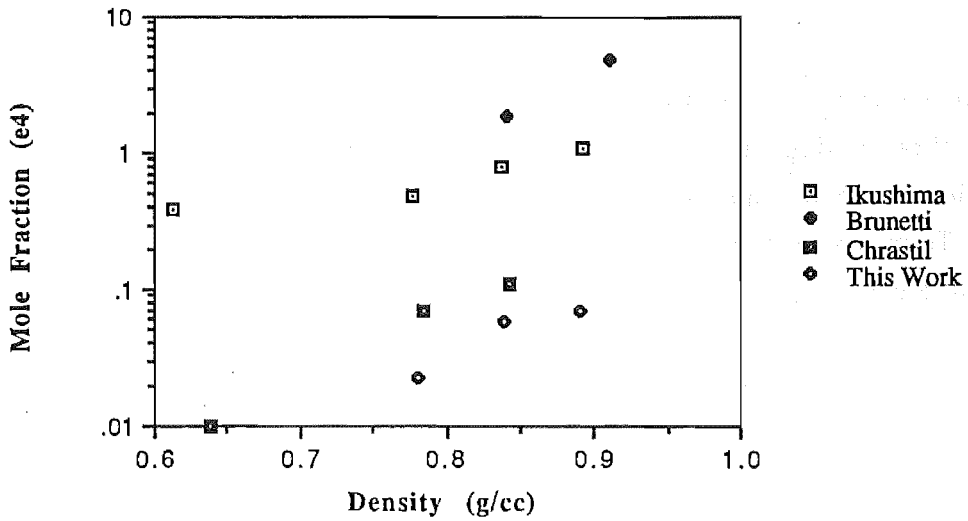

Figure 4.16 Comparison Between Workers for the Solubility of Tristearin in CO_2 at 40°C

4.5.3 Conclusions

Examination between the results obtained from this study for Trimyristin at 40°C and those presented by Bamberger *et al* (1988) shows good agreement in the mid-to-high CO_2 density range (ρ>0.7 g.cm^{-3}). Below this value, solubilities obtained in this work were 100% higher than those measured by Bamberger for Trilaurin and 50% higher than Bamgerger's Trimyristin values. For Tripalmitin, the results for this work were higher than those of Bamberger by 50% at low densities and 30% at high densities. This difference can be ascribed to the purity of the chemicals extracted and the sample methods used in the studies.

4.6 Investigations using a Liquid Solute - Tributyrin

4.6.1 Introduction

The availability of a dry gas test meter (Singer DTM-115-3) for a limited time gave the opportunity for a liquid sample holder design to be tested. The dry test meter was essential because it allowed samples to be taken gravimetrically. The holder was constructed and tested with Tributyrin (Sigma Chemical Co, #T 5142).

4.6.2 Liquid Sample Holder Design

The 400 bar cell was considered unsuitable for contacting liquids. In this cell there was no means of preventing a liquid from floating out of the top of the cell if the solvent becomes more dense than the liquid solute - the so called barotropic phenomenon (de Swaan Arons, 1989). To overcome this problem, a liquid sample holder was designed to fit into the 700 bar cell. King *et al* (1987) and Pearce and Jordan (1989) have presented ideas for such a liquid contactor. The design of Pearce and Jordan was tested. The concept behind the design was for a multipurpose holder that would work equally well for high and low density liquids and overcome the barotropic phenomenon.

During the course of a series of experiments (§3.5.5) the temperature was to remain constant and the density was to be increased from 0.57 to 0.89 $g.cm^{-3}$. The Tributyrin density was 0.85 $g.cm^{-3}$ and therefore the relative densities could change during a run. The CO_2 had to pass up through the solute when less dense than the solute and down through the liquid when the relative densities changed. A sample holder had to be designed that would send the solvent through a tortuous path. Figure 4.17 shows a schematic diagram of the sample holder. Detailed dimensioned drawings of the holder are found in Appendix 2.

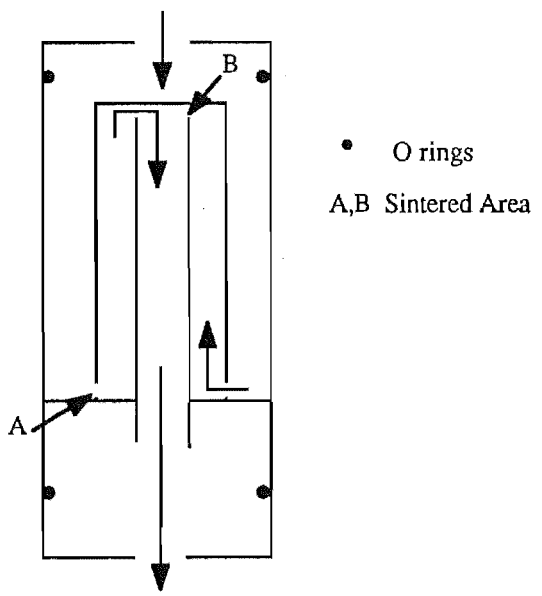

Figure 4.17 Schematic Diagram of the Liquid Sample Holder

Plate 5 Exploded View of Liquid Cell

The top and bottom of the holder had threaded ends. These threads were sealed (to prevent CO_2 by-passing) with O-rings. The bottom of the holder was fitted with an O-ring, also to prevent solvent by-passing. A spring at the top of the holder compressed this O-ring. Figure 4.18 shows the holder in position in the holder in the 700 bar pressure vessel.

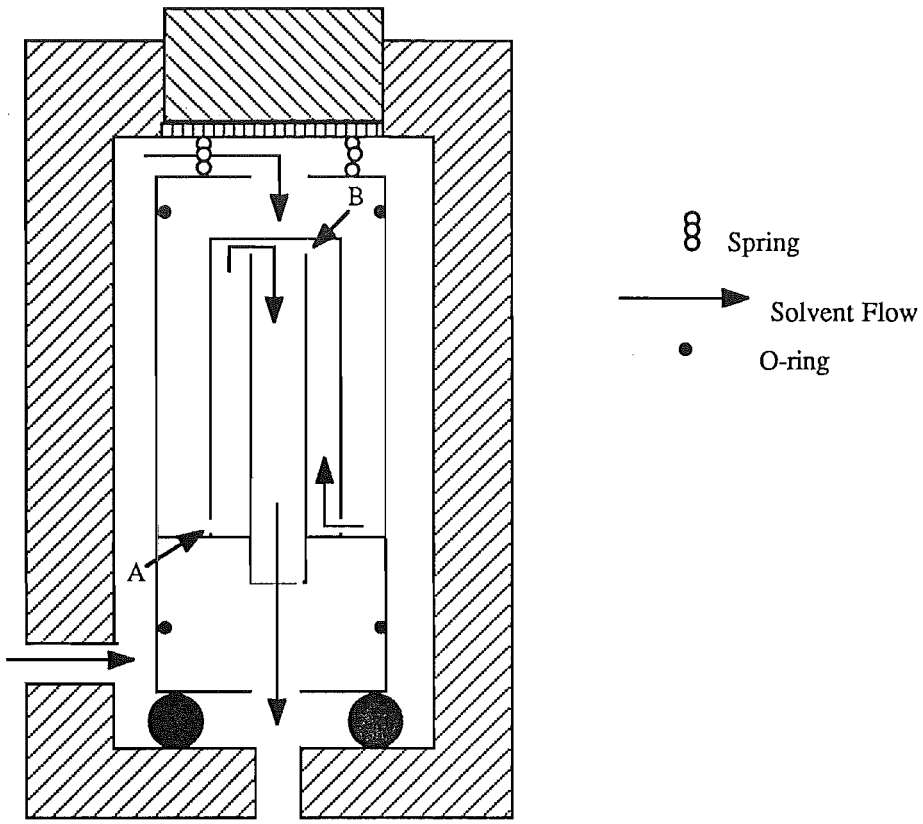

Figure 4.18. Liquid Holder in Position in the 700 Bar Cell

The points A and B of figures 4.17 and 4.18 indicate the positions where holes were drilled in the holder walls to allow the CO_2 to flow through the cell. Sintered stainless steel would have been preferred because of the large area for intimate contact between the solvent and the solute, but no suitable piece of sintered stainless steel was obtainable. It should be remembered that the solvent will be dense (0.57 - 0.89 $g.cm^{-3}$ c.f. water at 1.0 $g.cm^{-3}$) and the liquid solute will have a density in the region of 0.85 $g.cm^{-3}$. The contact will be more like that of a liquid - liquid extractor than a gas - liquid extractor. This makes a low solvent flow essential, otherwise the contact will be poor and the solvent could leave the holder unsaturated.

The holder works as follows; the liquid sample is loaded into the holder, the holder is assembled and sealed into the pressure vessel and the cell is pressurised from both ends (see §3.5.3). When the CO_2 is less dense than the liquid, the liquid occupies the region A. As the CO_2 density is increased and the relative densities change, the liquid is forced to the top of the holder and sits at point B. At the end of the extraction, the cell is be depressurised and any solute that remains in the space downstream of B is collected in a suitably placed cup. This prevents too much solute from collecting in the lines.

4.6.3 Testing With Tributyrin

4.6.3.1 Method.

The cell was filled with Tributyrin and the extraction performed. The Tributyrin was collected in one of four pre-weighed traps over ten minute time intervals. At the end of each time period the CO_2 flow was stopped, the gas meter reading was taken and the cold trap removed. The CO_2 flow was started again and further solute collected. While the new trap was being filled the old trap was weighed. The mass gain was recorded and, when combined with the collected CO_2 volume, a time averaged solubility in g solute/100 g CO_2 was determined. The liquid sample holder was used unaltered for the first few runs. The temperature used was 40°C and pressures of 9.5, 10.5 and 12.5 MPa were investigated. These results are plotted in fig 4.19.

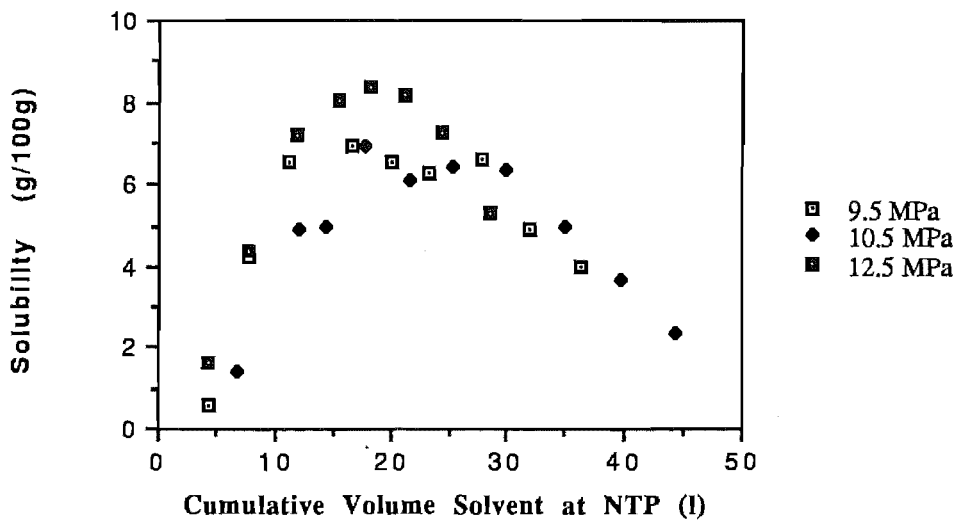

Figure 4.19 Apparent Solubility of Tributyrin in CO_2 at 9.5, 10.5, and 12.5 MPa and 40°C in the 700 Bar Cell

This figure illustrates that there is no observed variation in solubility with pressure. This is contrary to the results obtained for Trimyristin. One interesting point should be noted from this figure; there is no indication that the CO_2 was saturated at any time during the runs. It is suspected that what was happening inside the holder was that the CO_2 and Tributyrin were mixing, but that the saturated CO_2/solute mixture was being diluted in the dead space downstream from the liquid charge. The mixture leaving the cell was always at some mean composition, lower than that expected for a saturated solution. Tributyrin is very soluble in CO_2 and a 4g charge only lasted for approximately 20 minutes before sufficient Tributyrin had been removed to allow the CO_2 to by-pass the solute. This is evident from the decrease in apparent solubility with time in figure 4.19. If there was no dead volume downstream from the charge, then the solubility versus time curve could be approximated by figure 4.20.

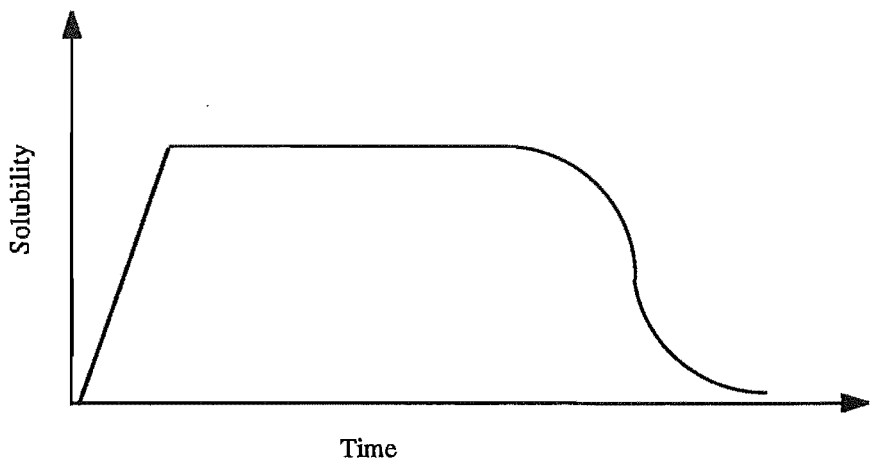

Figure 4.20 Idealised Solubility Profile for the Liquid Sample Holder

To try to minimise the downstream dead volume, this region was filled with 1mm diameter glass beads. These beads were cleaned with chloroform prior to use. The outlet from the holder and the holes at point B (figure 4.18) were covered by pieces of stainless steel gauze to prevent any beads from leaking into the system. All further extractions with Tributyrin were performed at 40°C and 9.5 MPa. The effect of decreasing this volume was to increase the apparent solubility peak by 33%, from 7 g/100g to 9 g/100g. The effect of different solvent flows and the effect of whether the beads were cleaned of excess solute, on the solubility was investigated. During the course of this work, the expected solubility plateau (fig 4.20) was not observed. This indicated that the equilibrium solubility had not yet been detected.

It was decided to modify the lower volume 400 bar cell and examine the performance of that pressure vessel when extracting liquids. It was hoped that by decreasing the cell volume, it would be possible to observe the true Tributyrin solubility. The following modifications were made; the pressure relief valve and the quickfit connector from the bottom of the cell were removed and the connection to the valve was replaced by a goose-necked piece of tubing (figure 4.21)

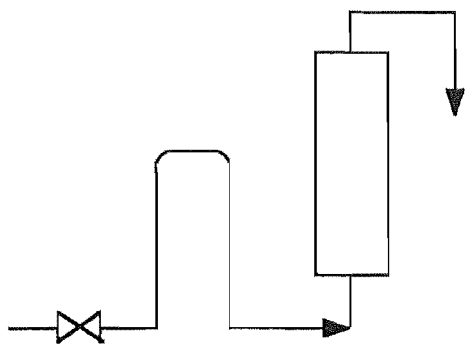

Figure 4.21 First Modification to the 400 Bar Cell

These modifications allowed the liquid sample to find its own level within the cell, without flowing to some other part of the equipment. Some of the Tributyrin was placed in the solid sample holder to see whether it could hold the liquid. It was found that the liquid leaked out around the threads and also through the sintered stainless steel frit. It was then decided to pour the liquid directly into the pressure vessel. Figure 4.22 shows the observed solubility behaviour for Tributyrin, with and without the cell packed with beads. In figure 4.23, these results are compared to those of the liquid sample holder with the beads present.

The use of the 400 bar pressure vessel resulted in a 90% increase in the observed solubility when compared to the 700 bar cell with the beads. The addition of the beads to the 400 bar cell resulted in a further 40% solubility increase. The plateau was still not observed.

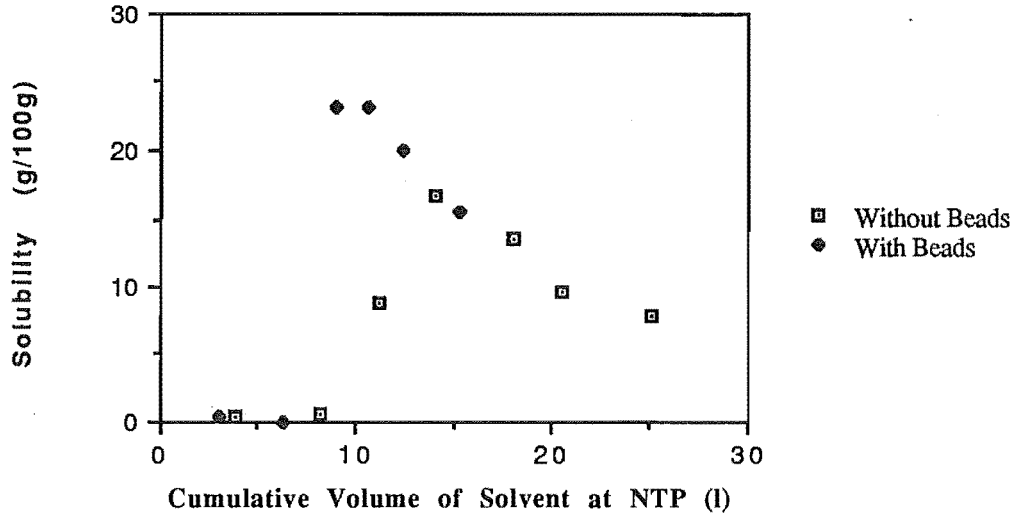

Figure 4.22 The Effect of Addition of Beads to Reduce Dead Space in the 400 Bar Cell on Apparent Tributyrin Solubility at 9.5 MPa and 40°C

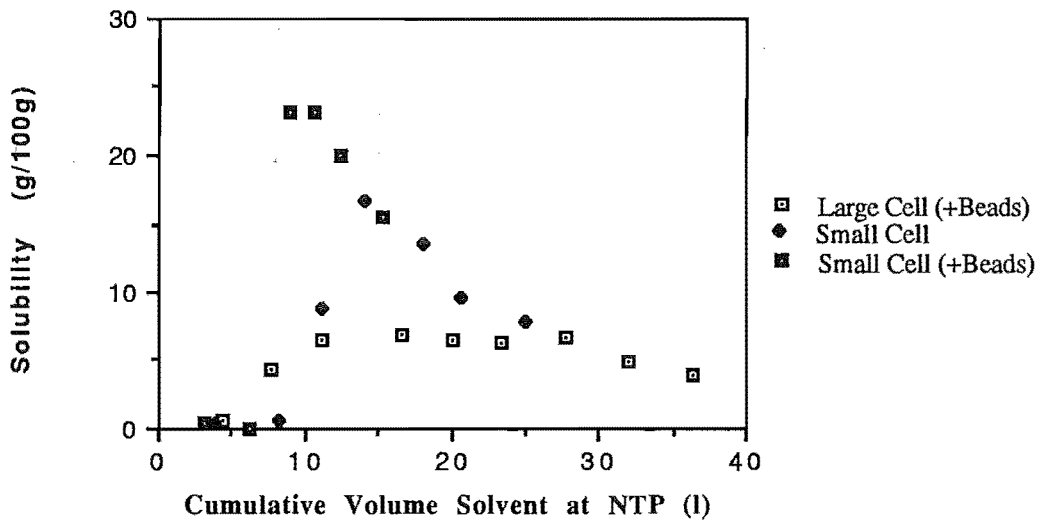

Figure 4.23 The Effect of Decreasing the Cell Volume on Apparent Tributyrin Solubility at 9.5 MPa and 40°C

It was then decided to investigate the effect of continuous solute addition on the observed solubility. With continuous addition, it was hoped that sufficient solute could be added to the extraction vessel for the CO_2 to become saturated with solute, fill the downstream space with the saturated solution and maintain this value for long enough for it to be measured. A further modification was made to the equipment. An HPLC pump was added to the system and the Tributyrin added to the CO_2 flow upstream from the extraction vessel. Figure 4.24 shows a schematic diagram of the system for continuous solute addition.

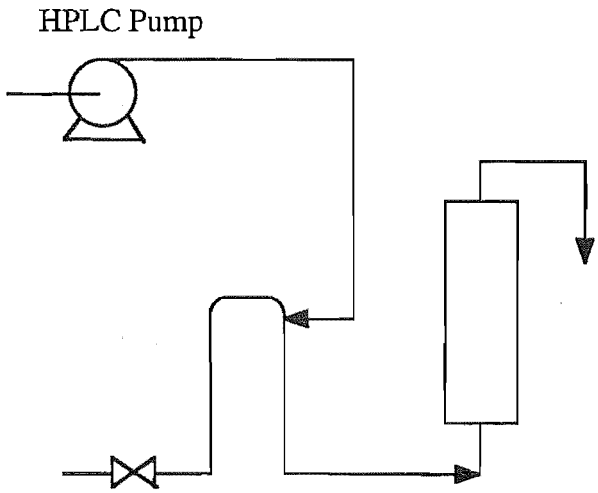

Figure 4.24 Modification of 400 Bar Cell for Direct Solute Addition

Several solute addition rates were investigated, 0.04, 0.08, 0.1 and 0.2 ml.min^{-1}. The results for addition rates of 0.1 and 0.2 ml.min^{-1} are presented in figure 4.25. The straight lines in figure 4.25 represent the steady state solubility at which an addition rate of 0.1 and 0.2 g.min^{-1} Tributyrin would exactly match the rate of extraction of Tributyrin from the cell.

Figure 4.25 shows that the observed solubility with an addition rate of 0.1 ml.min^{-1} was higher than that corresponding to the addition rate alone. This indicates that the CO_2 was not totally saturated and was removing some of the charge from the pressure vessel. Conversely for the 0.2 ml.min^{-1} addition rate, the observed solubility was lower than that for the addition rate alone, indicating that the CO_2 was saturated by the time that it leaves the cell and the excess solute is being deposited in the cell. The true solubility for Tributyrin at 9.5 MPa and 40°C is thought to lie at a value between that for the 0.1 and 0.2 ml.min^{-1} addition rates, at about 30 g/100 g CO_2. This solubility corresponds to a mole fraction of 0.042 (±10%).

Chrastil (1981) gives solubilities for Tributyrin in CO_2 at 40 and 60°C, and at pressures of 10.1 to 25.3 MPa. The value for 10.1 MPa and 40°C is 0.77 g/100g CO_2. This is over one order of magnitude lower than the value estimated from this work. One possible reason for this discrepancy is that Chrastil's solvent may not have been fully saturated with the solute, leading to low solubilities. At this point in the programme, the dry test meter had to be returned and so these investigations were discontinued.

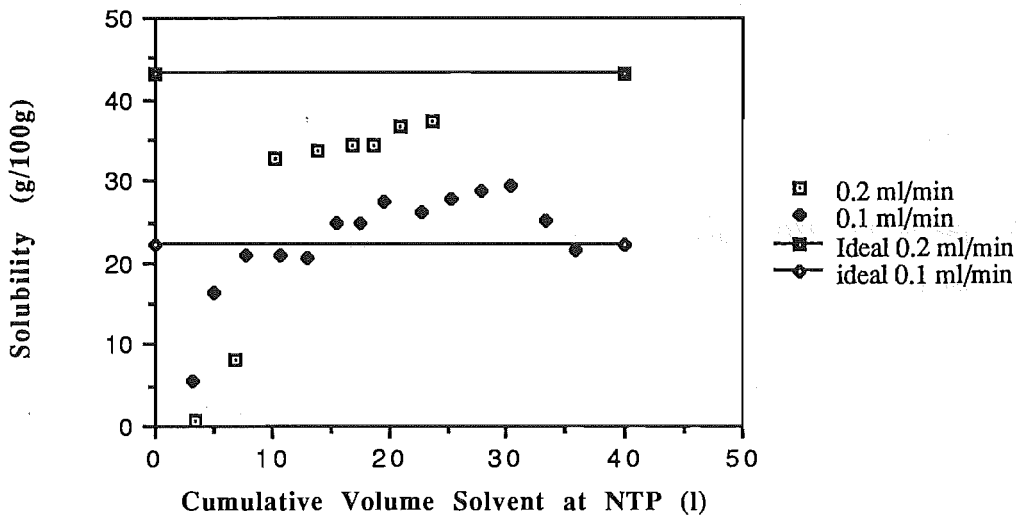

Figure 4.25 The Effect of Continuous Solute Addition on Apparent Tributyrin Solubility at 9.5 MPa and 40°C

4.6.4 Conclusions

There are several conclusions that can be drawn from this investigation. The liquid sample holder was overdesigned. The extraction system was never operated in a region where the barotropic phenomenon was likely to become a problem and so the headspace above the liquid sample and the downstream space was redundant. It is unlikely that this design would work for continuous once through extraction, unless the liquid was very insoluble and the space could be filled with saturated solution for long enough to be measured.

It is possible that the holder could generate useful data when a recycle-type experimental method was being used and the system dead volume was reduced by filling the pressure vessel with beads. Samples could then be taken by means of the 6-port valve. For a gravimetric method to be used fresh solvent would have to be introduced to the system (to maintain the system pressure during the sampling period), thus diluting the CO_2 rich phase.

The addition of the solute to the system during extraction warrants further work. This may well be the only simple means of determining the solubility of a very soluble liquid with a dynamic type apparatus.

4.7 Limitations of the Apparatus

4.7.1 Low Solubility

With the on-line HPLC method of analysis, the lower limit to the measured solubility is decreased by removing any chance of solute loss during the sampling process. In reality, any solubility limit is limited by the sampling and analysis techniques used. For the least soluble of the solutes investigated, Tristearin, it proved very difficult for the detector to give reliable results at the conditions where the solubility was expected to be the lowest. The detector sensitivity can be increased, but this means there will be an increase in the baseline noise. It is also possible to increase the size of the sample loop used (up to a maximum of 5 ml). The disadvantage of this increased sample size is the increased disturbance to flow sensitive detectors. This work showed that for the RI detector, 100µl of high pressure CO_2 produced a large disturbance and the baseline was very slow to recover.

It is possible that a change in detection method may be more sensitive in the low solubility region. High pressure windows have been used (McHugh and Krukonis, 1986) for visual observation of the extraction process. With a window a SFE system could be coupled to an Ultraviolet or Infrared spectrophotometer. A suitable wavelength could be found where the CO_2 is transparent and the solubility can be determined without having to physically take a sample.

4.7.2 High Solubility

The investigations with Tributyrin showed that problems can be encountered with very soluble liquids. Although samples of the Tributyrin were never sent to the HPLC, it is likely that HPLC would be a suitable analysis tool. The sample loop size can be decreased to 5µl and the RI detector sensitivity can be decreased. If the RI did not prove to be suitable, UV detection can be used and a wavelength with low absorbance can be chosen. If the solute was still too soluble, then a gravimetric method might prove to be superior. Some form of solute addition might have to be investigated if sufficient solute cannot be charged to enable the extraction vessel to be filled with saturated solution.

5

Results

The experimental solubilities for Trilaurin, Trimyristin, Tripalmitin and Tristearin in CO_2 measured in the course of this work are given in tables 5.1 to 5.4. They are also presented graphically in figures 5.1 to 5.8. Figures 5.1, 5.3, 5.5 and 5.7 show the experimental solubilities plotted against the solvent density at constant temperature, whereas in figures 5.2, 5.4, 5.6 and 5.8, these values are plotted against reciprocal absolute temperature at constant density. The raw solubility measurements are presented in Appendix 4. The CO_2 density was determined from the equation of Huang *et al* (1985) (Appendix 7). In all the plots presented, the density (abscissa) referred to is that of pure CO_2.

The tables present the measured solubilities at the temperature, pressure and density of each experiment. For each temperature, the solute solubility was determined at solvent densities of 0.57, 0.66, 0.73, 0.78, 0.84, and 0.89 $g.cm^{-3}$. The system pressures were adjusted to give the desired density. The temperatures were chosen to give a good coverage of the probable operating range of a commercial SFE plant. The minimum temperature of 35°C is close to the CO_2 critical temperature of 31.4°C, and the maximum temperature investigated, 55°C, is near the upper limit of thermal stability of many biological materials. The pressure range investigated (8.3 to 37.0 MPa) is limited by the critical pressure of CO_2 (7.3 MPa), and the upper pressure limit of the small pressure cell (40 MPa). The temperature range ($1.01 < T_r < 1.08$) and pressure range ($1.15 < P_r < 5.2$) include those considered useful in system design.

At very low solute concentrations there was often not enough solute in the mobile phase stream to be detected. For this reason there are only four solubility measurements for the 35°C isotherm for Tripalmitin while for Tristearin, only two solubility measurements were made at 35°C and three at 40°C.

Figures 5.1 and 5.2 show the results for Trilaurin. None of the isotherms is a true exponential fit. The 40°C isotherm shows an anomaly. The point for the lowest density has a lower measured solubility than for the same density on the 35°C isotherm. The 35°C values were re-measured, but the relative solubilities were still found to be the same. Both of these points were used in data regression and when the data were fitted by the prediction methods.

At 47 and 55°C, Trilaurin is a liquid (the melting point at ambient pressure is 46.5°C). Arnold *et al* (1963) observed that the solubility of a liquid triglyceride in aqueous ethanol is higher than that of the solid. Figures 5.1 and 5.2 show that there is no such increase that can be attributed to a phase change in the solute. No explanation has been found for this lack of solubility enhancement.

The data for Trimyristin (figures 5.3 and 5.4) do not show the same phenomenon of isotherms crossing that was evident with Trilaurin. It is interesting to note that the 55°C, and the 47°C isotherms show similar solubility values. Four of the solubilities are the same within experimental error. All the measured solubilities were included when comparisons to theories were made.

Figures 5.5 and 5.6 present the solubilities for Tripalmitin. There is one example of isotherm crossing. The solubility value for the 40°C isotherm at a density 0.57 $g.cm^{-3}$ is higher that of the 47°C isotherm at the same density. Figure 5.6 suggests that the value for the 40°C isotherm is too high. In measuring these data, the HPLC was at the limit of the sensitivity, and the peak areas measured were small with large scatter. These readings, and those for the 35°C isotherm will have errors in excess of the 10% quoted in Chapter 4. When the experimental results were compared with the theories presented in Chapter 2, the 35°C values were not used.

The number of measurements taken for Tristearin was limited by the sensitivity of the RI detector. In general, solubility values below a mole fraction of 10^{-6} could not be obtained. The data for the 47 and 55°C isotherms show the expected exponential behaviour. There are insufficient data for the 35 and 40°C isotherms for any conclusions to be drawn. When the Tristearin data were compared with the theories, only the 47 and 55°C results were used.

The solubility data has also been plotted as a function of carbon chain length at constant density and also at constant temperature. These plots are included in Appendix 5.

Figures 4.11 to 4.13 show the size of the error bars (10%) in relation to the data points. The error bars have not been included in any of the following plots as it was not felt that they would add much additional information.

Table 5.1 Solubility of Trilaurin in Supercritical Carbon Dioxide

Temperature ℃	Pressure (MPa)	CO_2 Density ($g.cm^{-3}$)	Solubility 10^4 y
35.0	8.3	0.57	1.401
	9.0	0.66	2.233
	10.5	0.73	4.178
	12.7	0.78	7.079
	17.1	0.84	14.949
40.0	9.5	0.57	1.179
	10.5	0.66	2.624
	12.5	0.73	5.221
	15.0	0.78	8.386
	20.0	0.84	18.696
47.0	10.8	0.57	2.132
	12.7	0.66	3.941
	15.3	0.73	7.241
	18.5	0.78	12.943
	24.0	0.84	28.833
55.0	13.1	0.57	3.731
	15.2	0.66	5.639
	18.5	0.73	9.154
	22.3	0.78	18.654
	28.9	0.84	38.483

Table 5.2 Solubility of Trimyristin in Supercritical Carbon Dioxide

Temperature ℃	Pressure (MPa)	CO_2 Density ($g.cm^{-3}$)	Solubility 10^4 y
35.0	8.3	0.57	0.109
	9.0	0.66	0.196
	10.5	0.73	0.429
	12.7	0.78	0.659
	17.1	0.84	1.357
	26.4	0.89	2.102
40.0	9.5	0.57	0.255
	10.5	0.66	0.539
	12.5	0.73	1.063
	15.0	0.78	1.802
	20.0	0.84	3.664
	26.8	0.89	5.716
47.0	10.8	0.57	0.397
	12.7	0.66	0.972
	15.3	0.73	2.128
	18.5	0.78	3.814
	24.0	0.84	8.568
	35.0	0.89	15.235
55.0	13.1	0.57	0.618
	15.2	0.66	1.103
	18.5	0.73	2.347
	22.3	0.78	5.247
	28.9	0.84	10.318
	37.0	0.89	18.905

Table 5.3 Solubility of Tripalmitin in Supercritical Carbon Dioxide

Temperature ℃	Pressure (MPa)	CO_2 Density ($g.cm^{-3}$)	Solubility 10^4 y
35.0	10.5	0.73	0.025
	12.7	0.78	0.046
	17.1	0.84	0.093
	26.4	0.89	0.164
40.0	9.5	0.57	0.052
	10.5	0.66	0.057
	12.5	0.73	0.089
	15.0	0.78	0.147
	20.0	0.84	0.252
	26.8	0.89	0.366
47.0	10.8	0.57	0.044
	12.7	0.66	0.152
	15.3	0.73	0.359
	18.5	0.78	0.633
	24.0	0.84	1.071
	35.0	0.89	1.736
55.0	13.1	0.57	0.231
	15.2	0.66	0.485
	18.5	0.73	1.181
	22.3	0.78	2.522
	28.9	0.84	5.234
	37.0	0.89	7.555

Table 5.4 Solubility of Tristearin in Supercritical Carbon Dioxide

Temperature ℃	Pressure (MPa)	CO_2 Density ($g.cm^{-3}$)	Solubility 10^4 y
35.0	17.1	0.84	0.034
	23.4	0.89	0.039
40.0	15.0	0.78	0.023
	20.0	0.84	0.057
	26.8	0.89	0.069
47.0	10.8	0.57	0.016
	12.7	0.66	0.022
	15.3	0.73	0.038
	18.5	0.78	0.072
	24.0	0.84	0.139
	31.5	0.89	0.195
55.0	13.1	0.57	0.057
	15.2	0.66	0.094
	18.5	0.73	0.194
	22.3	0.78	0.243
	28.9	0.84	0.438
	37.0	0.89	0.620

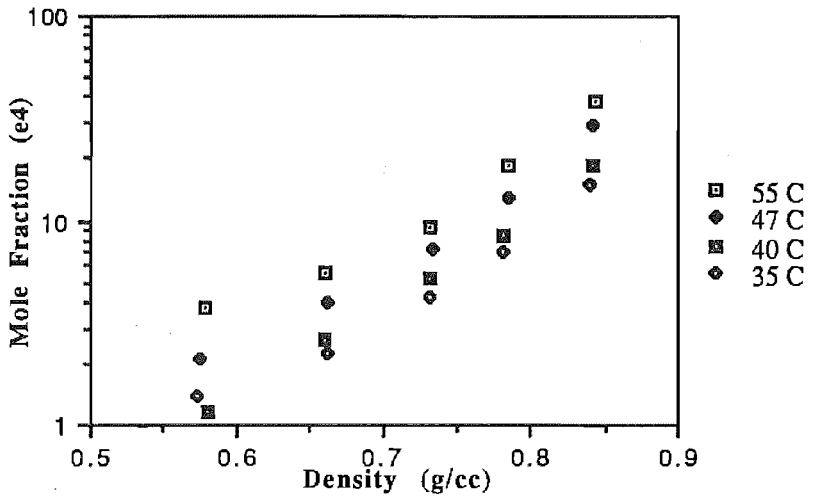

Figure 5.1 Variation of Solubility of Trilaurin in Carbon Dioxide with Density at Constant Temperature

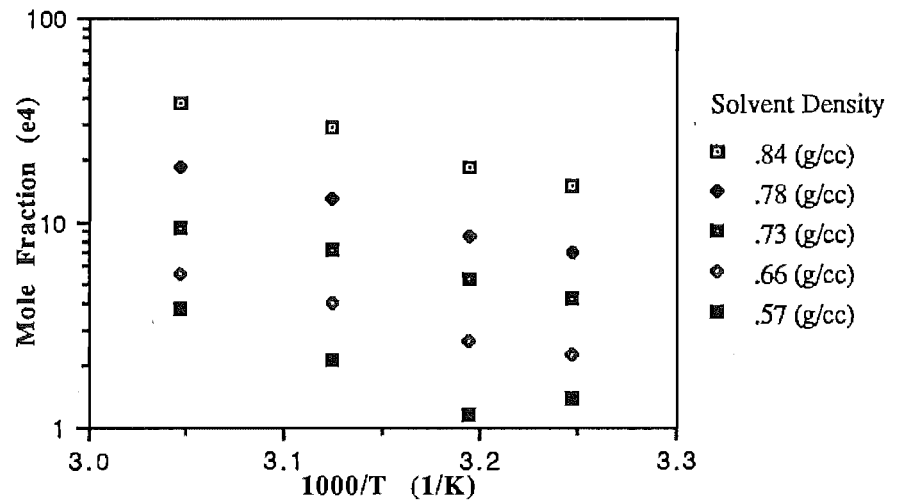

Figure 5.2 Variation of Solubility of Trilaurin in Carbon Dioxide with Reciprocal Temperature at Constant Density

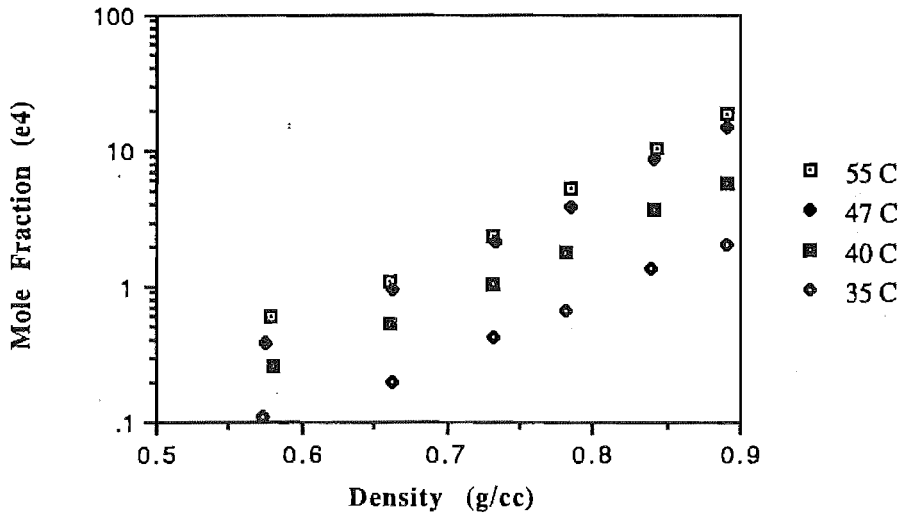

Figure 5.3 Variation of Solubility of Trimyristin in Carbon Dioxide with Density at Constant Temperature

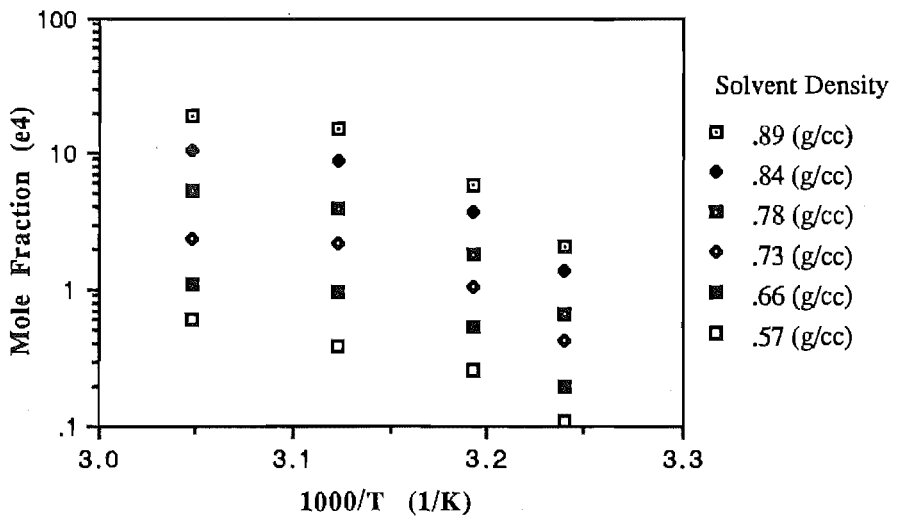

Figure 5.4 Variation of Solubility of Trimyristin in Carbon Dioxide with Reciprocal Temperature at Constant Density

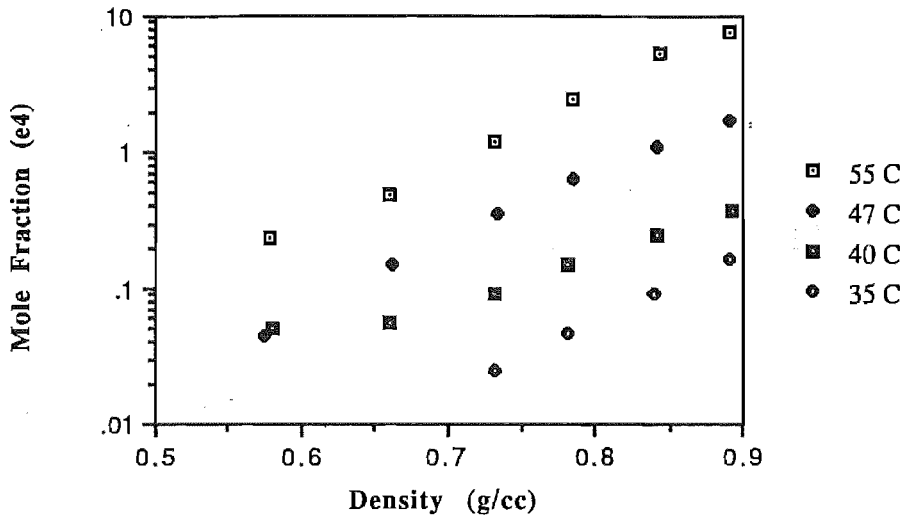

Figure 5.5 Variation of Solubility of Tripalmitin in Carbon Dioxide with Density at Constant Temperature

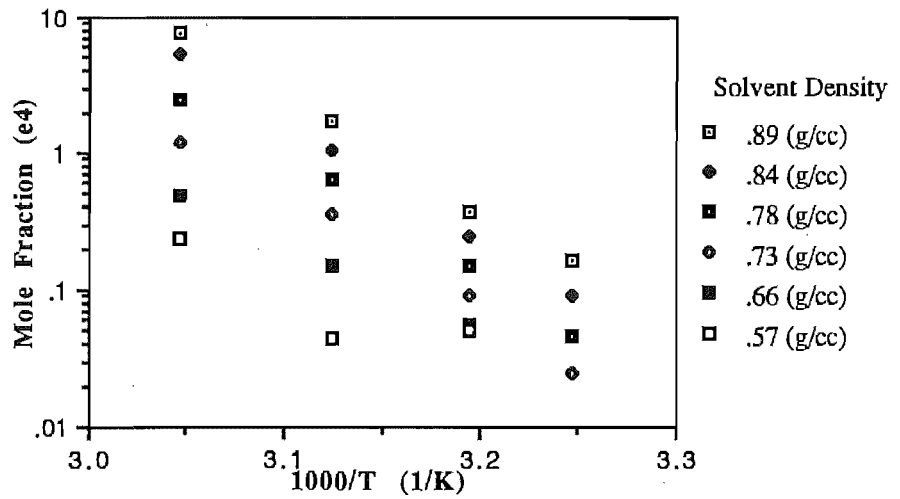

Figure 5.6 Variation of Solubility of Tripalmitin in Carbon Dioxide with Reciprocal Temperature at Constant Density

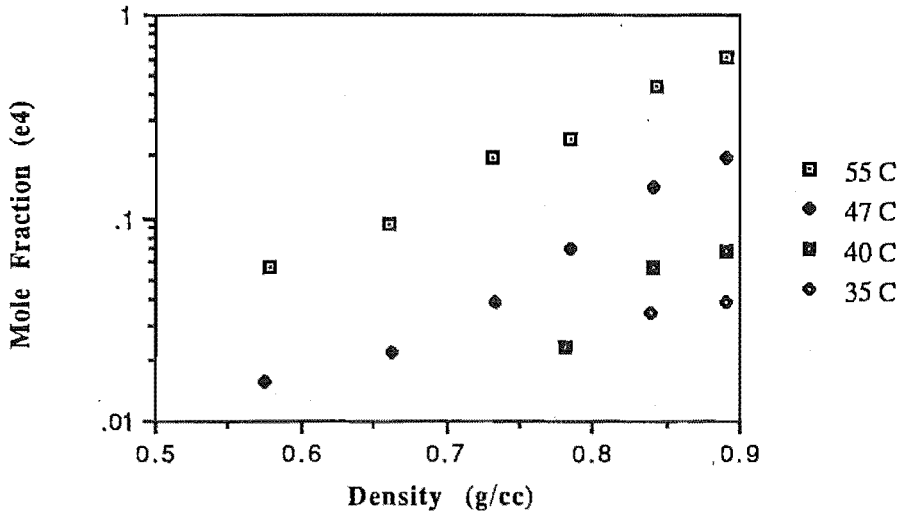

Figure 5.7 Variation of Solubility of Tristearin in Carbon Dioxide with Density at Constant Temperature

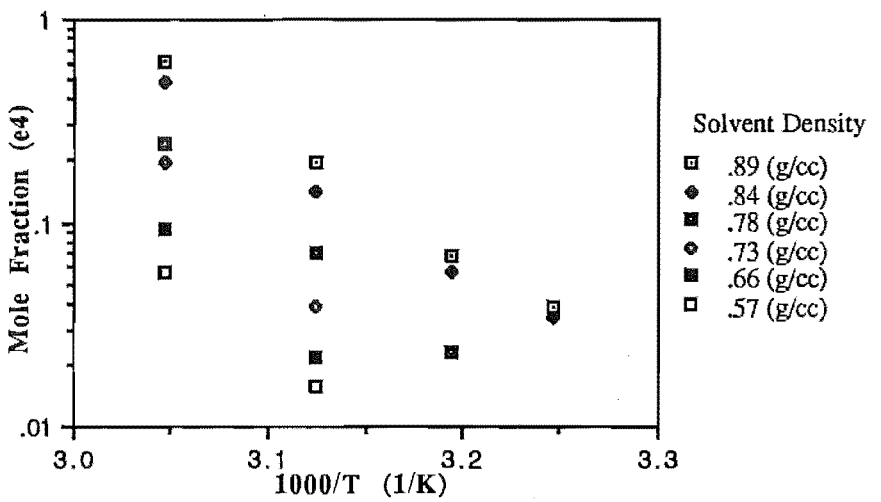

Figure 5.8 Variation of Solubility of Tristearin in Carbon Dioxide with Reciprocal Temperature at Constant Density

6

Discussion

6.1 Liquid Ideal Solubility

The equation for ideal solubility of a solid in a liquid is (2.1)

$$R\ln x_2 = -\Delta_f H\left(\frac{1}{T} - \frac{1}{T_m}\right) \qquad (6.1)$$

The derivation assumes that the intermolecular interactions are the same, there are no volume changes or entropy changes during the mixing process, the molecules are of equal size and the solvent is incompressible. It should also be noted that this approach assumes that the heat of fusion is independent of temperature and that the ideal solute solubility is independent of the solvent used.

In order to determine the ideal solubility, it is necessary to know the heats of fusion and the heat capacities of the solutes. Swern (1964) provided the references for both these properties. Charbonnet and Singleton (1947) was the source of the specific heat and fusion data for all of the triglycerides examined. Norris (1977) in his examination of the physical properties of triglycerides in milkfat, reviewed the melting point data and the heat of fusion data for, among others, Tripalmitin and Tristearin. He also independently measured these properties. His values for these properties compared well with the literature results and compared well with the data of Charbonnet and Singleton.

Table 6.1 Heat of Fusion Data.

Triglyceride	Norris ($J.g^{-1}$)	Charbonnet and Singleton ($J.g^{-1}$)
Tripalmitin	212.0	222.0
Tristearin	217.3	227.9

A value of 212.09 $J.g^{-1}$ for the heat of fusion of Tristearin was obtained from scanning calorimetry (MacGibbon, 1990). These values are all similar and so the results of Charbonnet and Singleton were used with some degree of confidence.

In their determination of specific heat data, Charbonnet and Singleton (1947) included reference to a phenomenon called 'pre-melting'. This phenomenon occurred during the heating of the solid sample and was evident from the change in slope of the heat capacity curve (when plotted against temperature). They cite dilatometric measurements which suggest a liquid-solid phase transition and not a simple solid-solid transition. The concept of 'pre-melting' is difficult to interpret. The term implies that at some temperature below the melting point, it is possible for solid and liquid to exist in equilibrium - a violation of the phase rule. It is possible for this to occur at temperatures of one or two degrees below the melting point if there are impurities present, but this phenomenon is reported at 80 degrees below the melting point! Charbonnet and Singleton do not suggest any mechanism for this phenomenon.

Charbonnet and Singleton (1947) did note that some of the data included a portion of the heat of fusion. These values were omitted when a functional form was determined for the specific heat of each triglyceride. Illingworth (1990) suggested that the commercial samples obtained from Sigma Chemicals Inc. would be completely in the β form and therefore no correction for phase transitions would be necessary in equation 2.2.

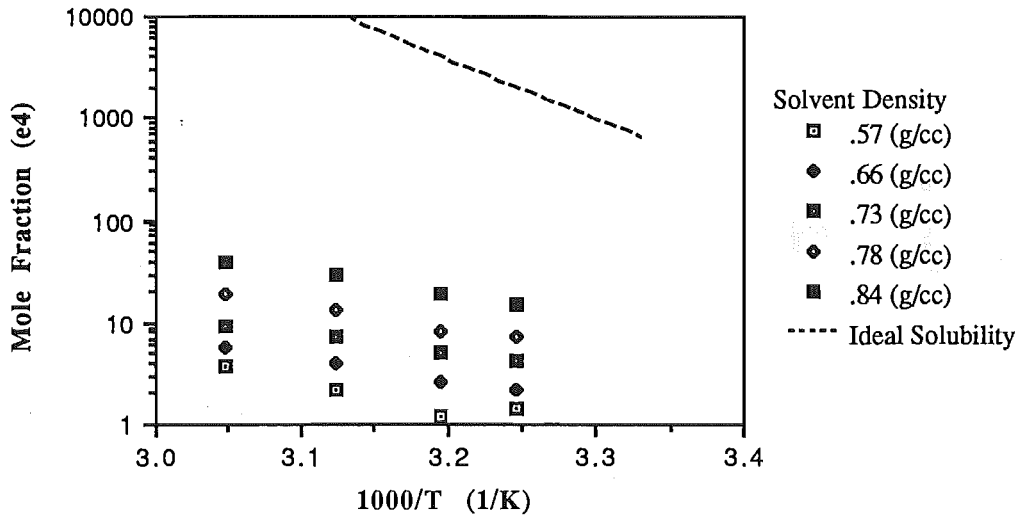

Figure 6.1 Comparison of Experimental Results with Ideal Solubility of Trilaurin

Figures 6.1 to 6.4 show comparisons between the calculated ideal solubility of each triglyceride and the experimental solubilities presented in Chapter 5. The experimental data and the theoretical curves have similar profiles, but are displaced. This indicates that the theory correctly predicts the effect of temperature on solubility, but does not take into account the effect of the solvent density (or non-idealities) on solubility. It was therefore decided to introduce a correction term, γ, into equation 6.1 to account for the non-idealities (equation 2.2). As discussed in §2b.1.2, the solubility parameter approach was used to estimate these discrepancies.

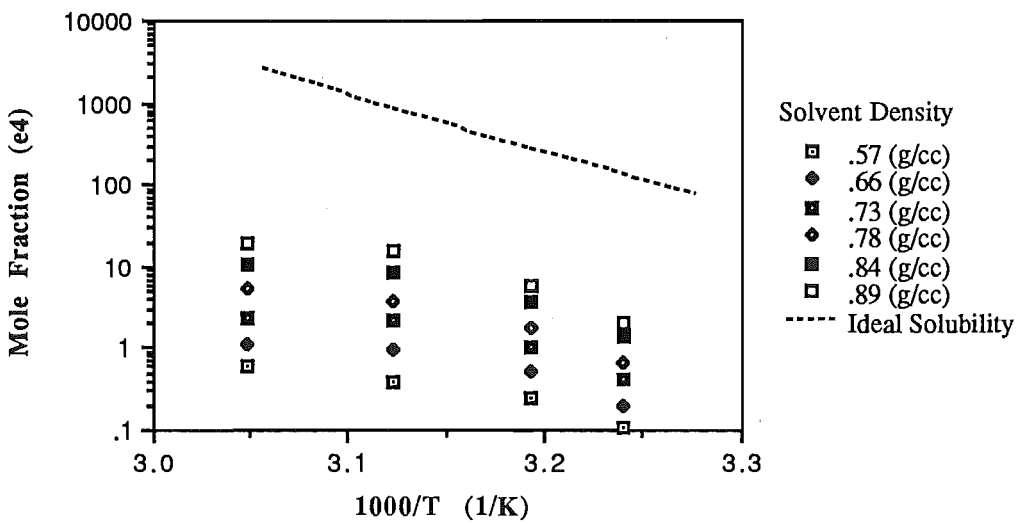

Figure 6.2 Comparison of Experimental Results with Ideal Solubility of Trimyristin

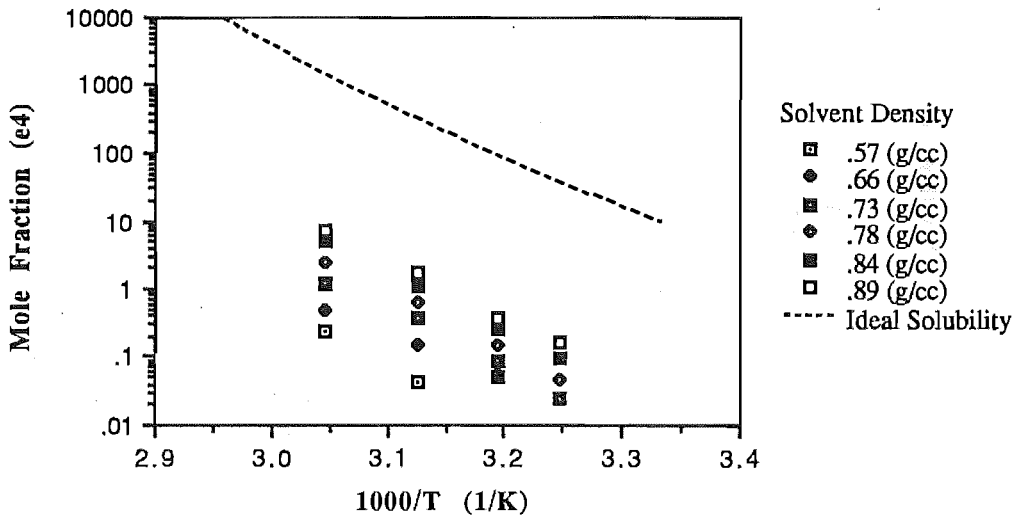

Figure 6.3 Comparison of Experimental Results with Ideal Solubility of Tripalmitin

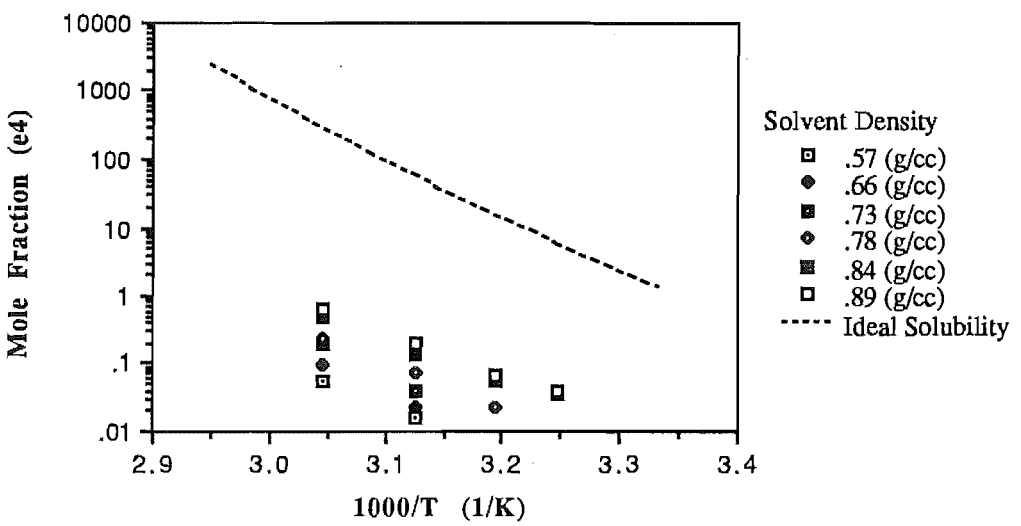

Figure 6.4 Comparison of Experimental Results with Ideal Solubility of Tristearin

6.2 Liquid Solution Theory for Activity Coefficient Determination

To evaluate the solubility parameters, δ_2, for the triglycerides, equation 2.13 was used. Solubility parameter theory assumes that the solute is a liquid and hence the molar volume used in this expression is that of a liquid. This means that when solids are examined in terms of this approach, the solids are assumed to be sub-cooled liquids. For the triglycerides, only limited molar volume data were available and liquid molar volumes (measured at high temperatures) of Swern (1964) were used uncorrected for temperature. The extra error due to this approximation was noted but not evaluated.

The other values required were the heats of vaporisation. Perry *et al* (1949) have used vapour pressure data to estimate the heat of vaporisation for a series of triglycerides. From these data, the heats of vaporisation were estimated by assuming that the Clapeyron-Clausius equation was valid over the temperature range measured. There are methods to correct the heat of vaporisation back to the boiling point (Reid *et al*, 1986), but these rely upon having the boiling points and estimates of the critical properties. Critical properties are not available for the triglycerides and therefore the heats of vaporisation of Perry were used in equation 2.13 to estimate the solubility parameter values. The values for the solubility parameters determined from these data are presented in Table 6.2.

A value for the solubility parameter of Tristearin of 18-21 $(MPa)^{0.5}$ ($\approx$ 8.8-10.3 $(cal.cm^{-3})^{0.5}$) was obtained from Barton (1983) who refers to Schmid (1973) as the source of this value. From this solubility parameter estimate, a heat of vaporisation of 106.5 $cal.g^{-1}$ was determined for Tristearin. This value is approximately 2.3 times the value of 45 $cal.g^{-1}$ given by Perry *et al* (1949). To determine whether the heats of vaporisation quoted by Perry *et al* seemed realistic (relative to the heats of fusion), values were obtained from Weast (1987) for heats of vaporisation and heats of fusion for long-chain organic compounds (n-Octacosane, n-Docosane, Lauric-, Myristic-, Palmitic- and Stearic-Acids). These values suggested that for long-chain molecules, the ratio of heat of vaporisation to heat of fusion approached two. This implied that Perry *et al* (1949) had underestimated the heats of vaporisation. The heat of vaporisation values of Perry were scaled by a factor of 2.3 and new solubility parameter values were calculated for the triglycerides. These are presented in Table 6.2.

Estimates of solubility parameters can also be obtained from solubility data of a solute in several liquid solvents. Solubilities for solutions of triglycerides in chloroform, diethyl ether and benzene have been determined by Bailey (1950).

To determine the solute solubility parameter, equation 2.2 is rewritten;

$$R\ln\gamma_2 x_2 = -\Delta_f H\left(\frac{1}{T} - \frac{1}{T_m}\right) + \Delta C_p \ln\left(\frac{T}{T_m}\right) + \Delta C_p\left(\frac{T_m}{T} - 1\right) = J \qquad (6.2)$$

$$\ln\gamma_2 = \frac{J}{R} - \ln x_2 \qquad (6.3)$$

$$\ln\gamma_2 = \frac{v_2^L (\delta_2 - \delta_1)^2 \Phi_1^2}{RT} = \frac{J}{R} - \ln x_2 \qquad (6.4)$$

where Φ = the volume fraction of the solvent

$$\text{thus } \delta_2 = \delta_1 \pm \sqrt{\frac{JT - RT\ln x_2}{\Phi_1^2 v_2^L}} \qquad (6.5)$$

if $\Phi_1^2 \approx 1$, then equation 6.5 can be written;

$$\delta_2 = \delta_1 \pm \sqrt{\frac{T(J - R\ln x_2)}{v_2^L}} \qquad (6.6)$$

The solubility parameter values for the liquid solvents were obtained from Hildebrand and Scott (1962). Solubility parameters for the triglycerides in these solvents were estimated using equation 6.6 and are given in table 6.2.

Finally, solubility parameters could also be determined from the experimental solubility data using equation 6.6. The results presented in table 6.2 are those from the highest density CO_2 and averaged for temperature.

Table 6.2 Comparison of Solubility Parameter Methods.

Triglyceride	Solubility Parameter Values† $(cal.cm^{-3})^{0.5}$			
	Perry	Barton	Bailey	Data Fit
Trilaurin	6.63	10.26	11.20	8.88
Trimyristin	6.48	10.01	11.12	9.26
Tripalmitin	6.39	9.88	11.16	9.43
Tristearin	6.18	9.50	11.15	9.55

† for convenience, the 'Perry' refers to the use of the $\Delta_v H$ data of Perry *et al* (1949) in equation 2.13, 'Barton' refers to scaling based on a value for Tristearin, 'Bailey' refers to the δ_2 value determined from fitting equation 6.6 to the data of Bailey and 'Data Fit' refers to fitting equation 6.6 to the experimental solubility data of this work.

It is apparent from table 6.2 that there is a large variation in the solubility parameters obtained for the triglycerides. This variation makes it difficult to assess the use of solubility parameters as a method of determining solute activity coefficients. To illustrate the effect of this variation, the solubility parameters estimated from the heats of vaporisation of Perry *et al* (1949), and those estimated from scaling the Tristearin solubility parameter value of Barton (1983) were used in equation 2.12 to determine the solute activity coefficients and hence solubilities. These calculations are compared to the experimental data of this work in figures 6.5 to 6.12. These graphs show that the use of the lower value of the solubility parameter means that the activity coefficient is underestimated, and the predicted solubilities are too high. These results span three orders of magnitude whereas the experimental solubilities span two orders of magnitude. When the higher value of the solubility parameter is used, the

activity coefficients are overestimated. The calculated results now span 12 orders of magnitude!

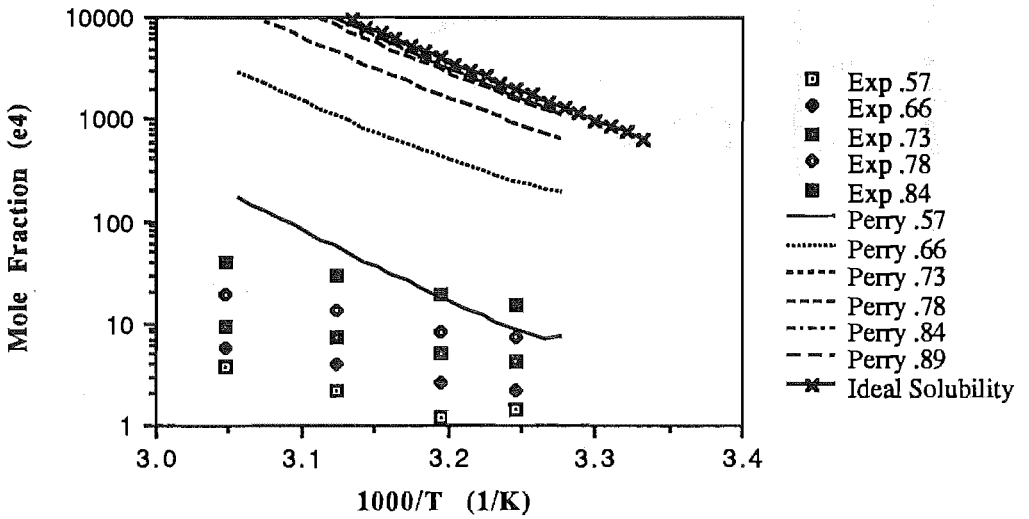

Figure 6.5 Comparison of Experimental Solubilities for Trilaurin with Predictions using Perry's Results to Obtain Solubility Parameters

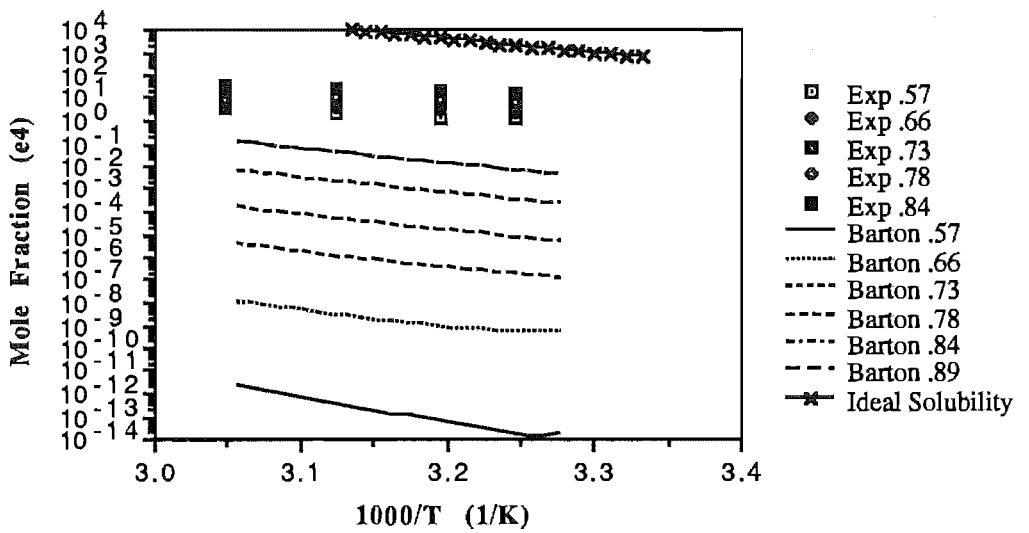

Figure 6.6 Comparison of Experimental Solubilities for Trilaurin with Predictions using Barton's Results to Obtain Solubility Parameters

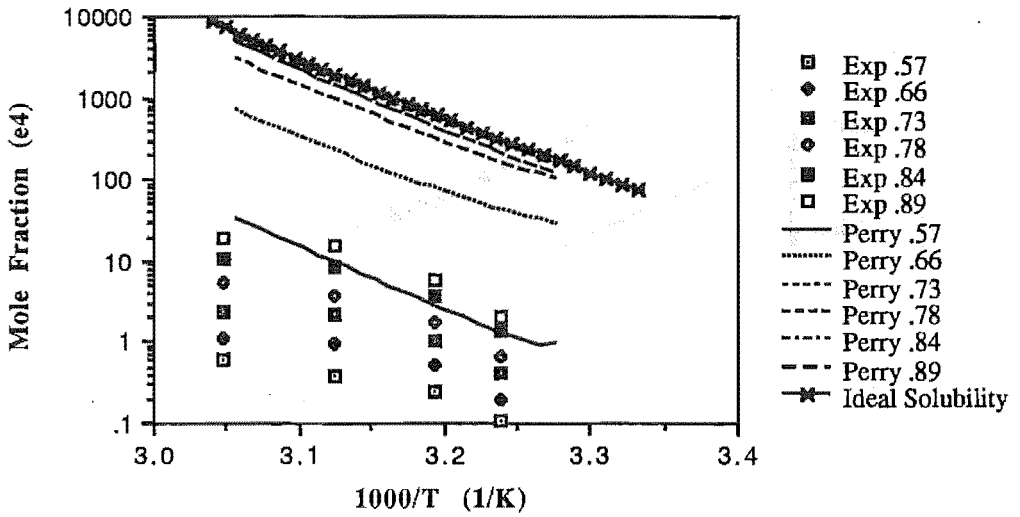

Figure 6.7 Comparison of Experimental Solubilities for Trimyristin with Predictions using Perry's Results to Obtain Solubility Parameters

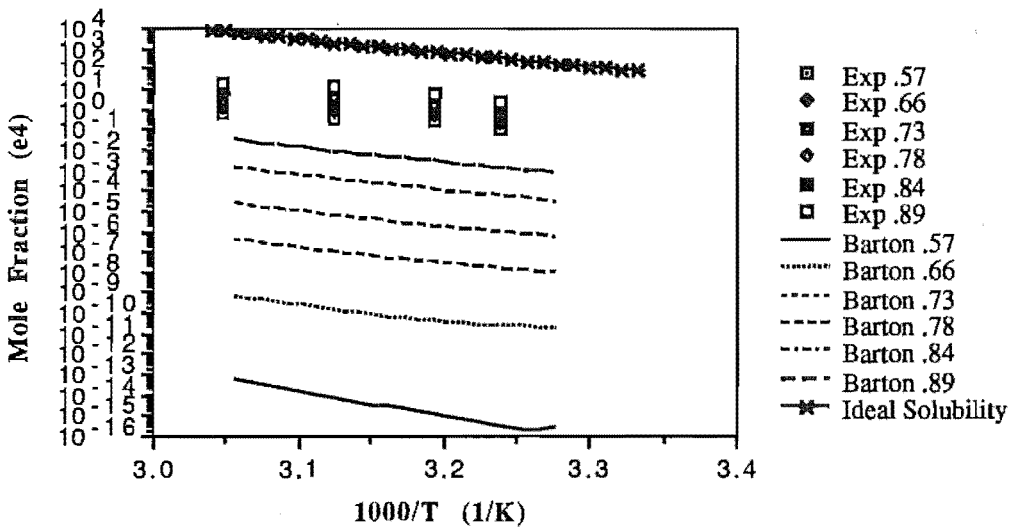

Figure 6.8 Comparison of Experimental Solubilities for Trimyristin with Predictions using Barton's Results to Obtain Solubility Parameters

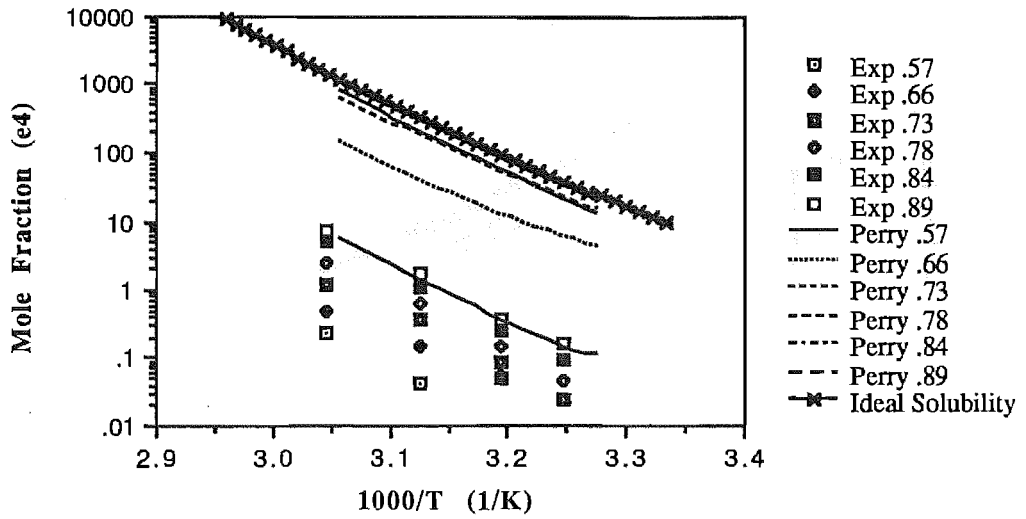

Figure 6.9 Comparison of Experimental Solubilities for Tripalmitin with Predictions using Perry's Results to Obtain Solubility Parameters

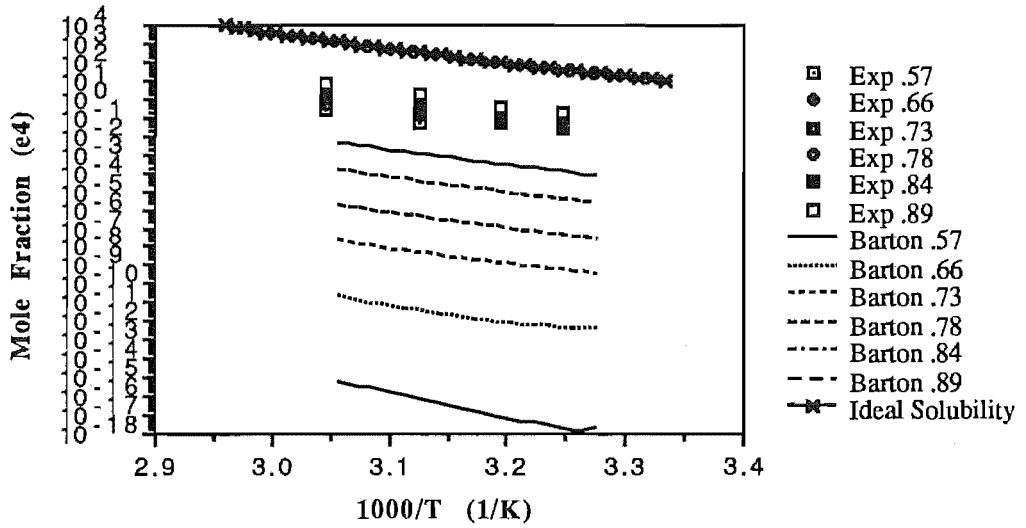

Figure 6.10 Comparison of Experimental Solubilities for Tripalmitin with Predictions using Barton's Results to Obtain Solubility Parameters

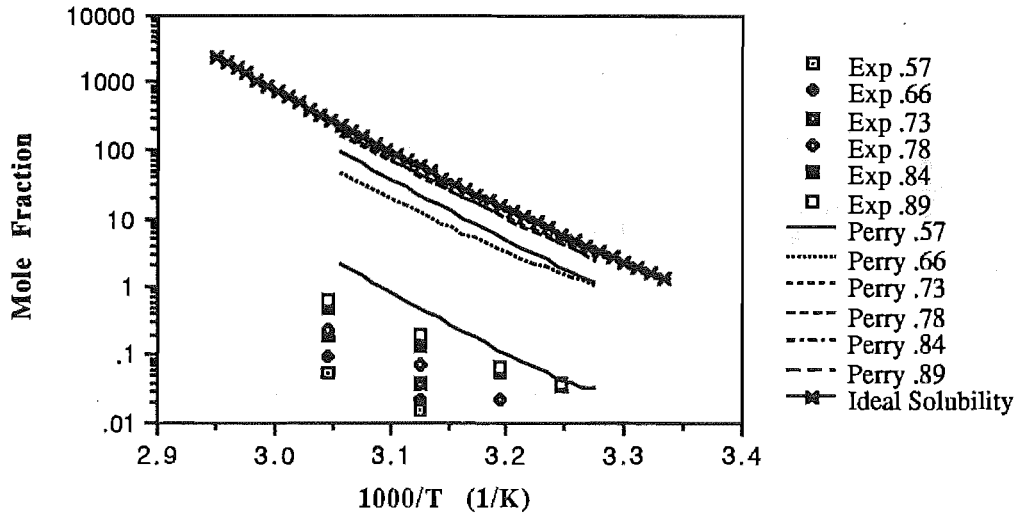

Figure 6.11 Comparison of Experimental Solubilities for Tristearin with Predictions using Perry's Results to Obtain Solubility Parameters

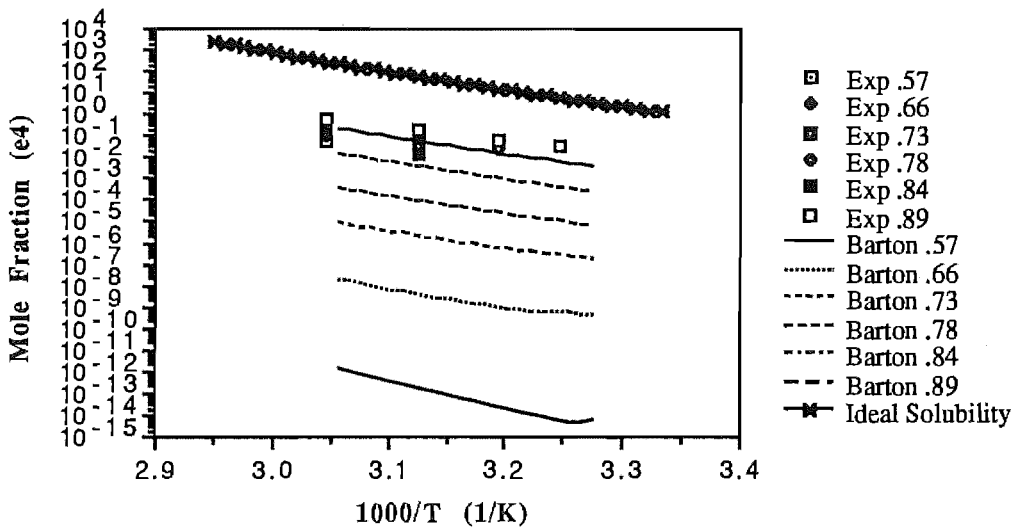

Figure 6.12 Comparison of Experimental Solubilities for Tristearin with Predictions using Barton's Results to Obtain Solubility Parameters

The large variation between the two sets of results can be accounted for by examining equation 2.12. To estimate the solute activity coefficients, the square of the difference between the solute and solvent solubility parameters is used. This squared result contributes to the logarithm of the activity coefficient. Hence a small variation in the solute solubility parameter will have a large affect on the estimate of the activity coefficients and the predicted solubility.

To estimate δ_1, the CO_2 solubility parameter, the procedure outlined by Allada (1984) (§2b.1.2) was used. This procedure allows the effect of solvent density to be taken into account when the CO_2 solubility parameter is estimated.

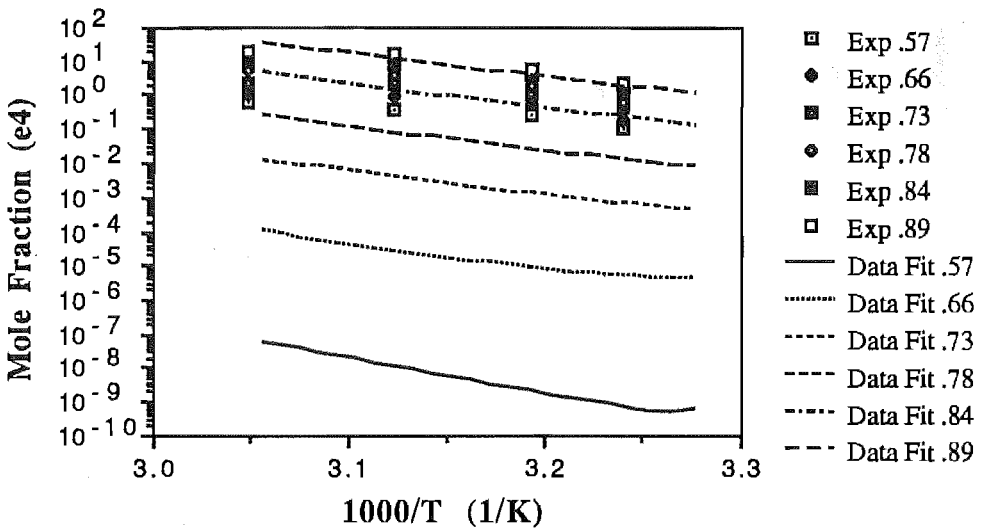

Figure 6.12a Comparison of Experimental Solubilities for Trimyristin with Predictions using a Fit to the Data to Obtain Solubility Parameters

Figure 6.12a shows the predicted solubility of Trimyristin when the value of solubility parameter determined from a fit to the experimental solubilities is used. One can see that the predicted solubility passes through the highest density experimental solubilities (as expected), but the spread of predicted solubilities is still large. It would be possible to make this method more closely fit the expreimental solubilities, but this would involve varying either δ_1 or $(\delta_2 - \delta_1)^2$ for each data set. This would give the possibility of solubility interpolation, but it is not known how beneficial this would be. For each solute, the experimental solubilities were plotted against CO_2 solubility parameter, with temperature as parameter (figs 6.13-6.16). For Trilaurin and Trimyristin the data are collapsed into a band, but for the other two solutes this behaviour is not apparent. Allada (1984) and Ikushima *et al* (1987) both suggest that the use of the solvent solubility parameter is a good method of comparing the solubility of one solute in a range of solvents. The solvents are then said to be compared at conditions of equal dissolving power. This could offer a means of predicting the solubility of a solute in a previously untested solvent, but this theory was not tested in this work.

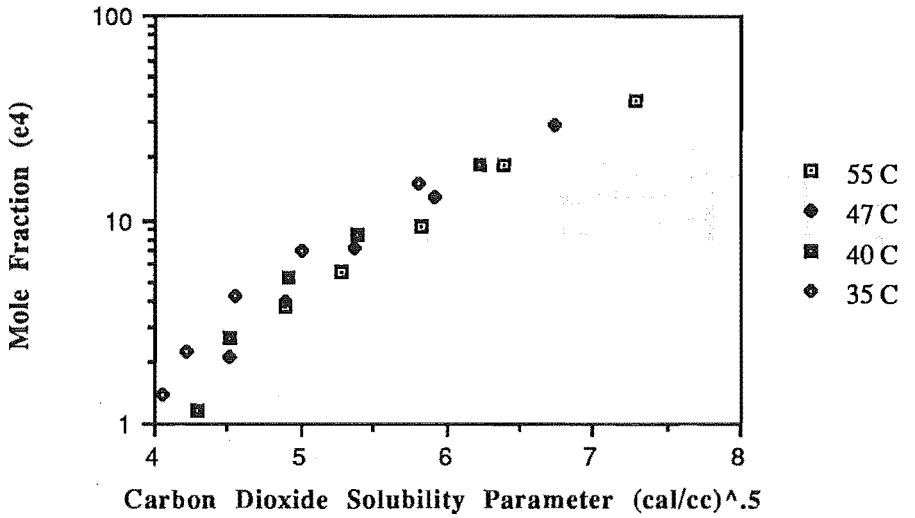

Figure 6.13 Effect of CO_2 Solubility Parameter on Experimental Solubility of Trilaurin

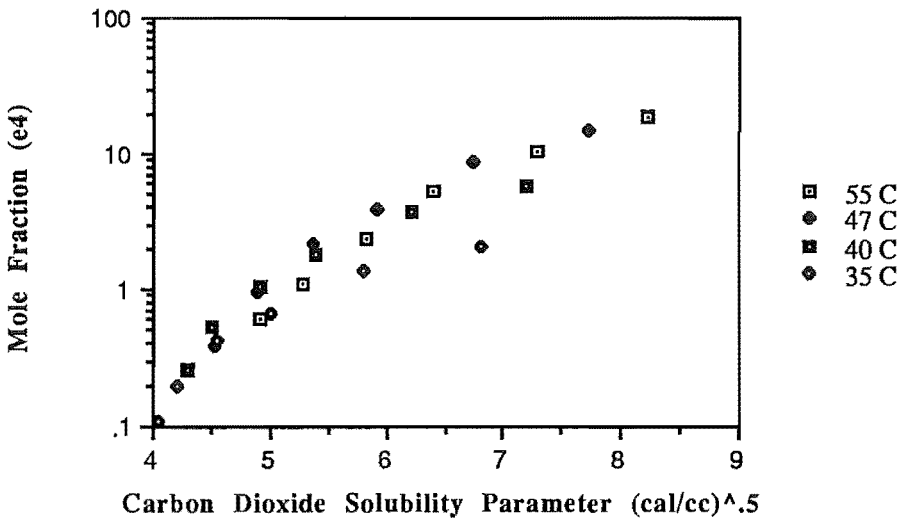

Figure 6.14 Effect of CO_2 Solubility Parameter on Experimental Solubility of Trimyristin

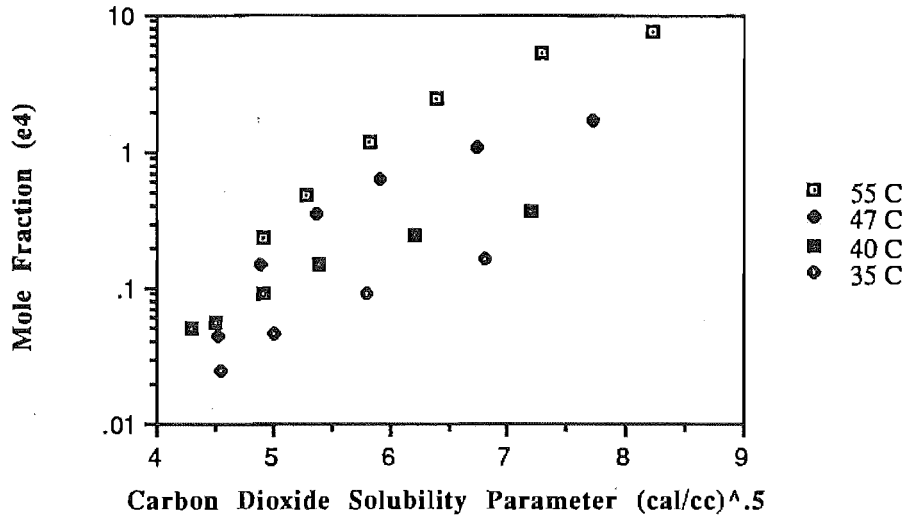

Figure 6.15 Effect of CO_2 Solubility Parameter on Experimental Solubility of Tripalmitin

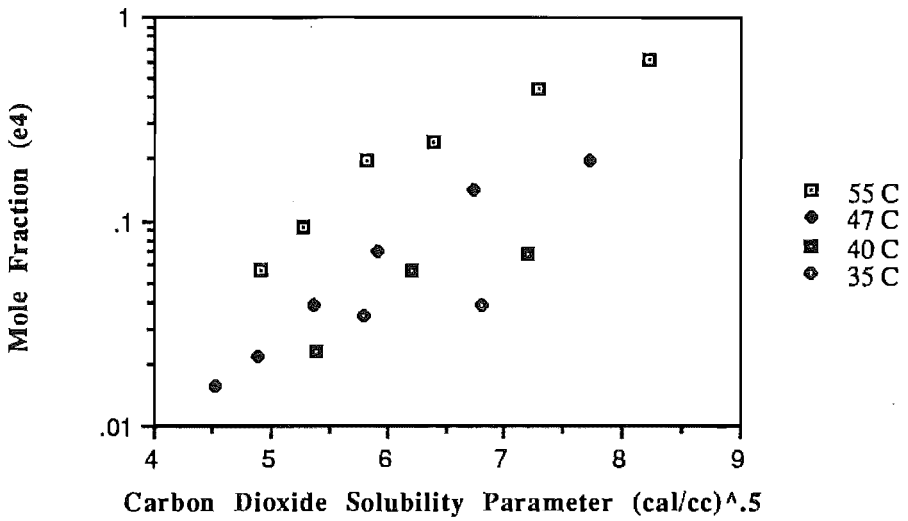

Figure 6.16 Effect of CO_2 Solubility Parameter on Experimental Solubility of Tristearin

In the solubility parameter model, it is assumed that there are no excess entropy changes or volume changes when the components mix. It would be possible to incorporate expressions for these effects into an equation (eg 6.2 or 6.4) and then use these new equations to predict the solubilities. That however is beyond the scope of this work.

Prausnitz *et al* (1986) present a method for modifying the geometric mean assumption for the dispersion forces $c_{11} = \delta_1^2 = \frac{\Delta u}{v}$ and $c_{12} = (c_{11}c_{22})^{0.5}$ to

$c_{12} = (1-l_{12})(c_{11}c_{22})^{0.5}$, where $l_{12} << 1$ and is a characteristic of the 1-2 forces. Equation 2.12 then becomes;

$$\ln\gamma_2 = \frac{v_L^2 \Phi_1^2}{RT}\left[(\delta_2 - \delta_1)^2 + 2l_{12}\delta_1\delta_2\right] \qquad (6.7)$$

No attempt was made to fit this form of equation to the experimental data - primarily because of the lack of a reliable value for solute solubility parameters.

Hildebrand and Scott (1962) have investigated the ability of this theory to model the solubility of iodine in a variety of liquid solvents. In general, the more non-ideal the system, the less likely this approach is to give a reliable estimate of the solubility. The triglyceride/CO_2 systems are highly non-ideal and therefore it is even less likely that a theory based on a simple dispersion model for the intermolecular forces (London Forces) will give a good description of these systems.

Finally, Hildebrand and Scott (1962, page 170) have commented on the variation of solubility parameters with temperature and pressure. They suggest that it is difficult and often worthless to try to apply such corrections. Such claims from the developers of the theory make one question the validity of using this approach at all. They go on to say "... The solubility parameter equations are just 'zeroth approximations' ..." implying that this method gives good qualitative description of the type of behaviour of systems while not providing accurate numerical values. This assertion is supported by the present work.

6.3 Compressed Gas Approach to Phase Equilibria

The compressed gas approach to phase equilibria, like the expanded liquid approach, involves finding a suitable means of defining the deviations from non-ideal behaviour, and then using this description to model the experimental solubilities. An enhancement factor, E, is defined as the ratio of real solubility to the ideal gas solubility (2.16);

$$E = \frac{P\, y_2}{P_2^{sat}} \qquad (6.8)$$

This is taken as a measure of the deviation of a system from the ideal behaviour. Figures 6.17 to 6.20 show how the enhancement factors for the triglyceride/CO_2 systems vary with density at constant temperature.

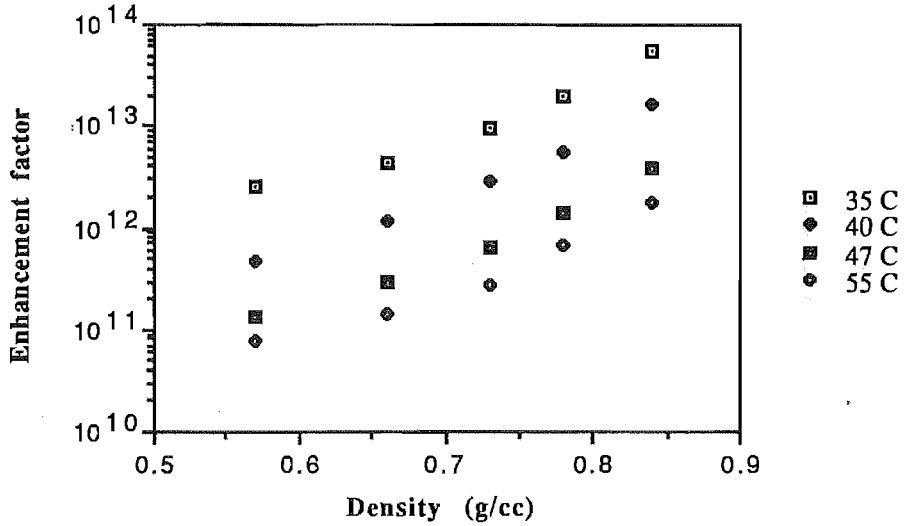

Figure 6.17 Variation of Enhancement Factor for Trilaurin from Solubility Results of this Work with Density at Constant Temperature

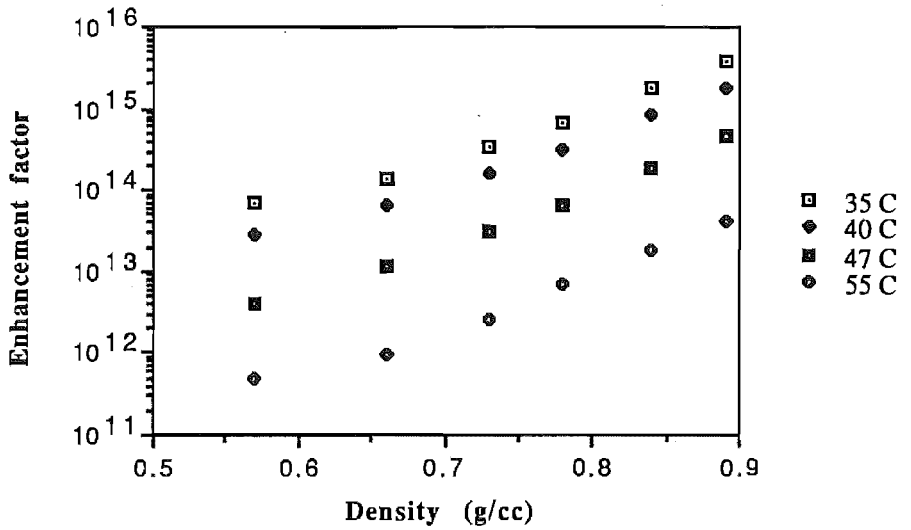

Figure 6.18 Variation of Enhancement Factor for Trimyristin from Solubility Results of this Work with Density at Constant Temperature

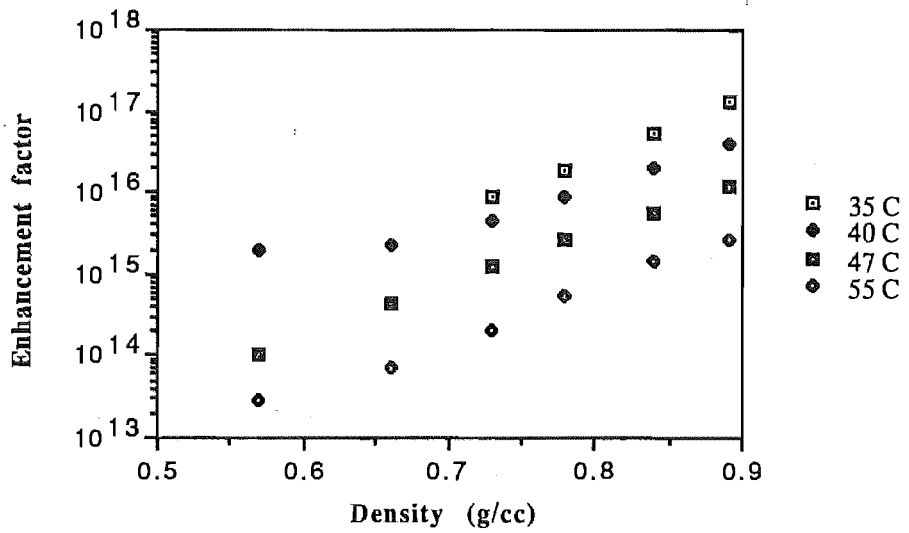

Figure 6.19 Variation of Enhancement Factor for Tripalmitin from Solubility Results of this Work with Density at Constant Temperature

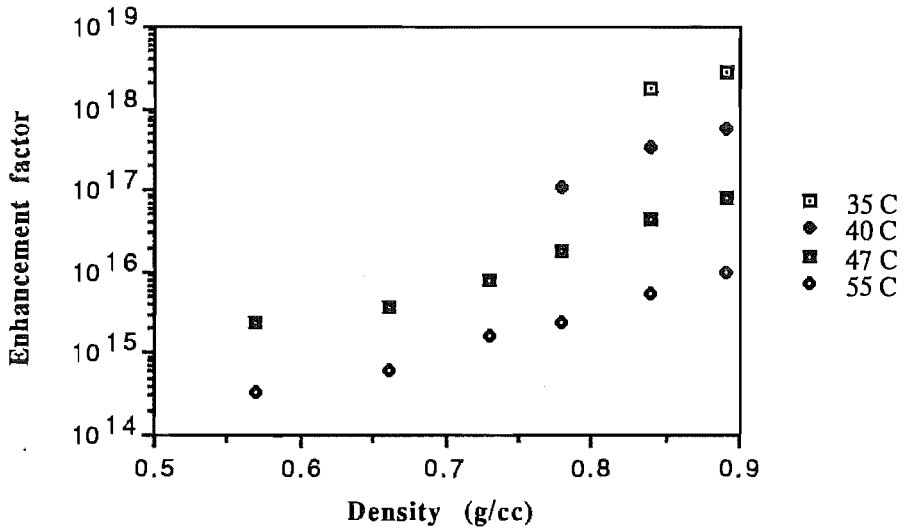

Figure 6.20 Variation of Enhancement Factor for Tristearin from Solubility Results of this Work with Density at Constant Temperature

The enhancement factor relies upon vapour pressure data to estimate the ideal solubilities. The source of these data was Perry *et al* (1949). The data of Perry *et al* were measured in the temperature range of 185 - 300°C where the triglycerides are liquids. To obtain vapour pressure data in the temperature range 35 to 55°C, the Clapeyron-Clausius relation used by Perry *et al* was extrapolated to the solid region. Perry uses an expression for the saturated liquid vapour pressure of the form;

$$\ln P^{sat} = \frac{-A}{T} + B. \qquad (6.9).$$

The coefficient A is related to the enthalpy of vaporisation, $\Delta_V H$, by

$$A = \frac{\Delta_V H}{2.3R} \qquad (6.10)$$

It was assumed that for the solid vapour pressure a similar expression could be found

$$\ln P^{sat} = \frac{-A'}{T} + B' \qquad (6.11)$$

It was further assumed that the $-A'$ term would be related to the enthalpy of sublimation, $\Delta_S H$, by;

$$A' = \frac{\Delta_S H}{2.3R}. \qquad (6.12)$$

The assumption was then made that the liquid and solid vapour pressures would be the same at the triple point. The triple point temperatures for triglycerides were not available and so the melting point was assumed to be a good approximation to the triple point. A' was found from (6.12) (it is assumed here that the heat of sublimination is equal to the sum of the heat of vaporisation and the heat of fusion), B' was found by equating (6.9) and (6.11) at the melting point. The solid vapour pressures were then determined from equation 6.11. The heat of fusion of Charbonnet and Singleton (1947) were used for these calculations. Mathias *et al* (1986) used an equation of state to estimate the vapour pressures of Tristearin and Palm Oil. The value they determine for the vapour pressure of Tristearin at 50°C is 9×10^{-16} mm Hg. The value obtained from the extrapolation of the data of Perry *et al* (1949) was 2.1×10^{-16} mm Hg. These extrapolated vapour pressures are much lower than the limit of experimental measurement ($\approx 10^{-7} - 10^{-8}$ mm Hg, Hansen, 1985). Mathias *et al* also made estimates of the critical properties of simple triglycerides (T_c ranges from 963 to 1037K for Trilaurin to Tristearin). It is not known how meaningful these data are as triglycerides decompose well below these temperatures.The vapour pressures obtained by this method are listed in table 6.3.

Owing to the approximate nature of these vapour pressure data, it was felt that this approach did not offer any advantages in solubility prediction when compared to the solubility parameter approach described above.

Table 6.3 Vapour Pressure† Data from Extrapolation.

Triglyceride	35.0°C	40.0°C	47.0°C	55.0°C
Trilaurin	3.49×10^{-12}	1.75×10^{-11}	1.32×10^{-10}	4.67×10^{-10}
Trimyristin	9.71×10^{-15}	6.37×10^{-14}	8.04×10^{-13}	1.28×10^{-11}
Tripalmitin	2.27×10^{-17}	1.93×10^{-16}	3.44×10^{-15}	7.96×10^{-14}
Tristearin	2.37×10^{-19}	2.45×10^{-18}	5.61×10^{-17}	1.71×10^{-15}

† in mm Hg

6.4 The Carnahan-Starling-van der Waals Equation of State

The Carnahan Starling van der Waals EOS is a semi-theoretical equation that requires some data fitting (through a binary interaction parameter, a_{12}) before the predicted solubility values can be generated.

From the Carnahan Starling van der Waals EOS,

$$P = \frac{RT(1+\zeta+\zeta^2-\zeta^3)}{v\,(1-\zeta)^3} - \frac{a}{v^2} \qquad (6.13)$$

the fugacity coefficient can be defined (equation 2.24),

$$\ln(\phi_2 Z) = \frac{3\zeta^3-9\zeta^2+8\zeta}{(1-\zeta)^3} - \frac{2(y_1 a_{12} + y_2 a_{22})}{RTv} \qquad (6.14)$$

and hence the solubility can be determined (Paulaitis *et al*, 1983)

$$y_2 = \frac{P_2^{sat}}{P\ \phi_2} \exp\left\{ \frac{v_2^s\ [P-P_2^{sat}]}{RT} \right\} \qquad (6.15)$$

Using equations 6.8 and 6.15, equation 6.14 is solved for a_{12}. The experimental solubilities are used in this procedure. This a_{12} value is then substituted into equation 6.14 to determine ϕ_2. This calculated value for ϕ_2 is used in equation 6.15 to determine the calculated solubility. A computer programme was written to fit a_{12} values to the experimental solubilities and then find an average a_{12} for each temperature. This average value was used in the fitting procedure. Johnston and Eckert (1981) have suggested that a_{12} will have a weak temperature dependence, but will be independent of solvent density.

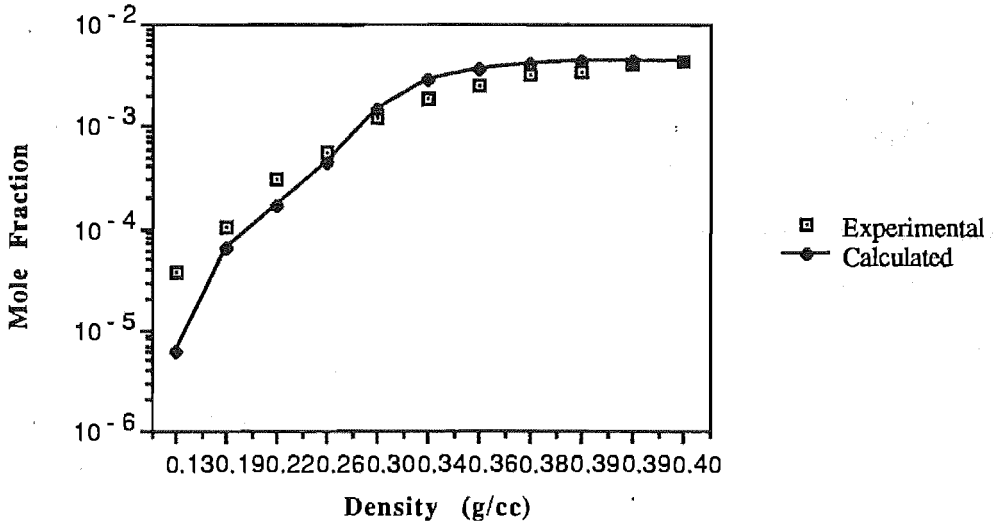

Figure 6.21 Comparison Between Experimental Solubilities of Johnston et al (1981) and Prediction (CSvdW) for Phenanthrene in Ethylene at 45°C

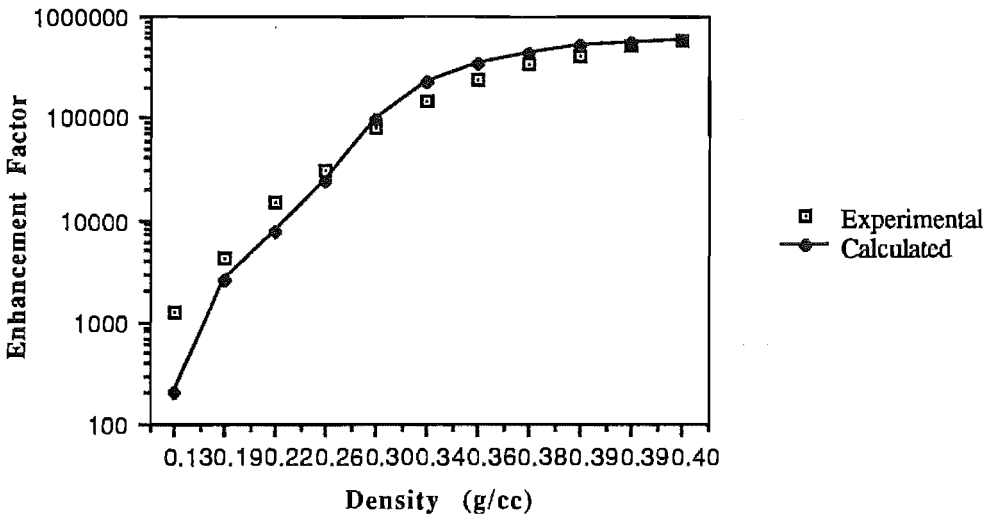

Figure 6.22 Comparison Between Experimental Enhancement Factors of Johnston et al (1981) and Prediction (CSvdW) for Phenanthrene in Ethylene at 45°C

To test the model, the values presented by Johnston and Eckert (1981) for the solubility of phenanthrene in ethylene at 45°C, were modelled (figures 6.21 and 6.22). One can see that there is a good agreement between the predictions of the equation and the experimental data for both the solubilities and the enhancement factors. It should be noted that since this fit is based on a mean value for a_{12}, the predicted locus will intercept the experimental locus at approximately the midpoint of the abscissa.

The measure of the applicability of the model fit will be the average deviation between the experimental data and the predicted data. A root mean square (RMS) error function;

$$\overline{RMS} = \sqrt{\frac{\sum(x_e - x_c)^2}{N}} \qquad (6.16)$$

where x_e = the experimental solubility,
x_c = the calculated solubility and
N = the number of data points

was defined. For the phenanthrene in ethylene data, an $\overline{RMS}$ value of 6.2×10^{-3} was obtained. This compared well with the $\overline{RMS}$ value of 2.2×10^{-3} when the log solubilities were made a linear function of density. This same model was then tested on the triglycerides solubilities from this work.

Figures 6.23 to 6.30 show the predicted solubility and enhancement factors compared to the experimental values. The interaction parameter, a_{12}, was fitted in the same manner as for the phenanthrene/ethylene system. The model underpredicts the solubility in the region of low solvent density and overpredicts the solubility at high solvent density. The same behaviour is apparent for the enhancement factors. The poor quality of the fit can be attributed to the assumptions used in the derivation of the model and also in the assumption that the fitting parameter is independent of solvent density.

In the derivation of the model, it was assumed that the behaviour of the solvent and solute could be described by a hard-sphere approximation. This will be a reasonable approximation for a small molecule like CO_2, but for a large, multiple-long chain molecule like a triglyceride, the model will be seriously in error. This also helps to explain why the model gives a good description of the phenanthrene/ethylene system. Both phenanthrene and ethylene can be described as pseudo-spherical molecules. Further, phenanthrene could be considered to be made up of a collection of ethylene units and therefore will be chemically similar (as far as the model is concerned) to ethylene. For the phenanthrene/ethylene system, the assumption that a_{12} is independent of density is a good approximation. In the case of the triglyceride/CO_2 systems, even if the CO_2 can be assumed to be a hard sphere, the triglyceride cannot, and hence the CSvdW expression will not model the observed behaviour well.

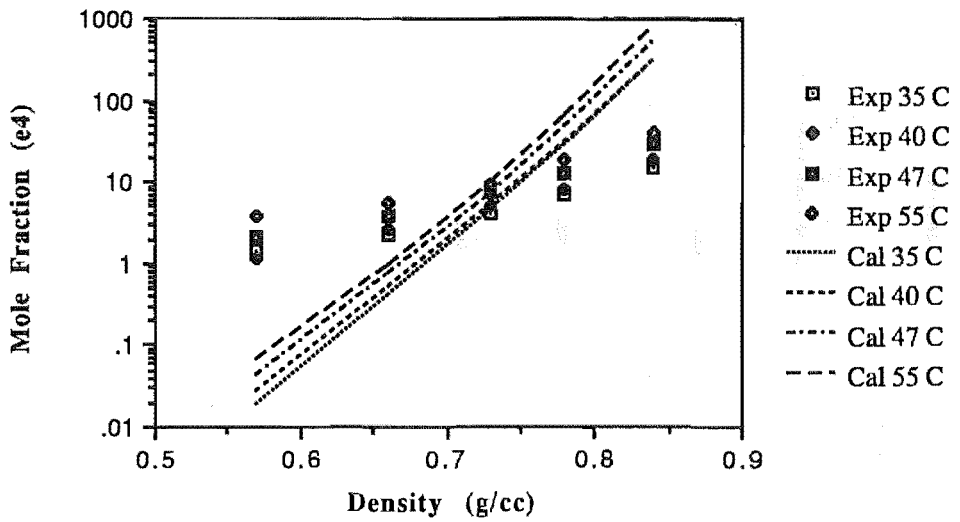

Figure 6.23 Comparison Between Experimental Solubility and Prediction (CSvdW) for Trilaurin in CO_2

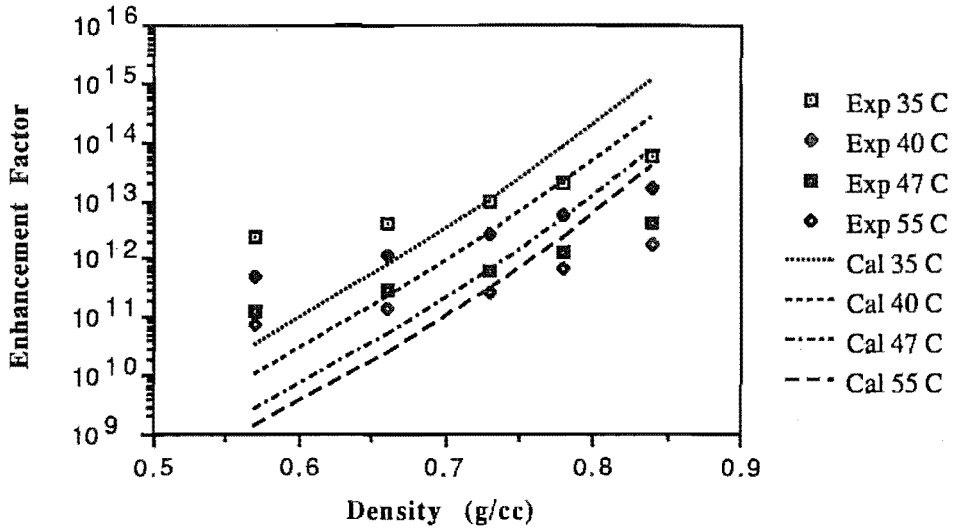

Figure 6.24 Comparison Between Experimental Enhancement Factors and Prediction (CSvdW) for Trilaurin in CO_2

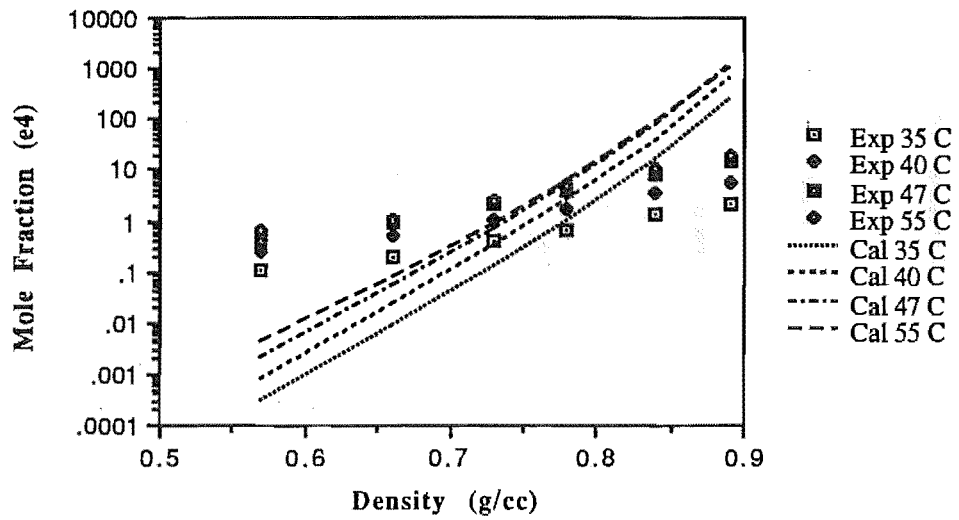

Figure 6.25 Comparison Between Experimental Solubility and Prediction (CSvdW) for Trimyristin in CO_2

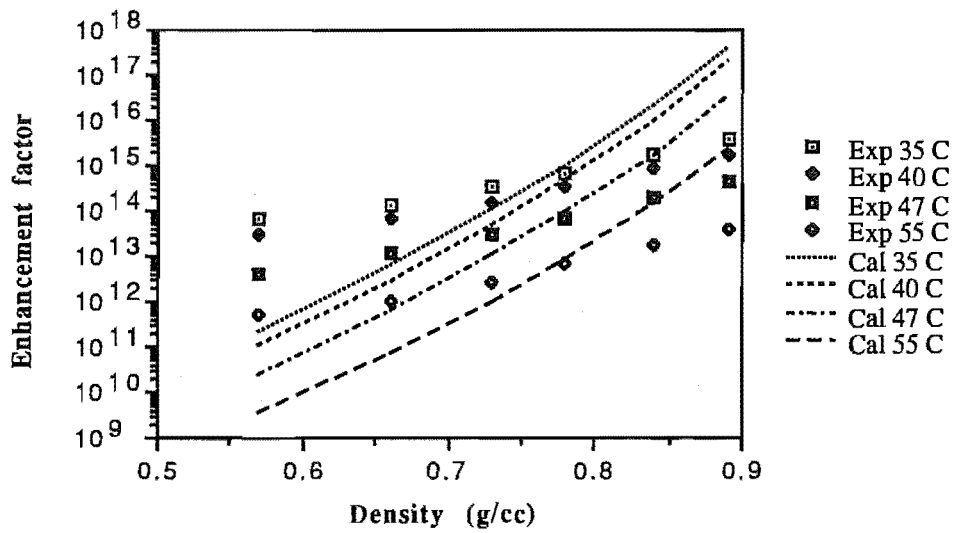

Figure 6.26 Comparison Between Experimental Enhancement Factor and Prediction (CSvdW) for Trimyristin in CO_2

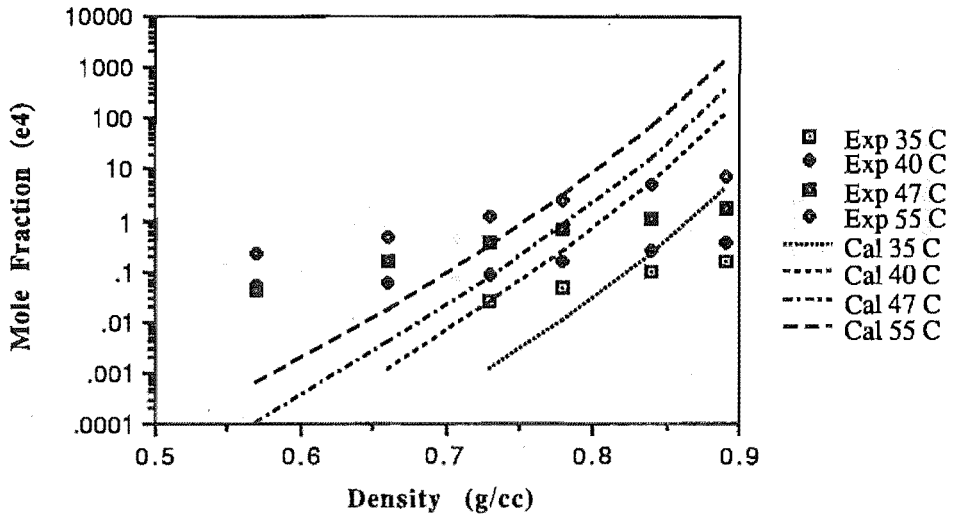

Figure 6.27 Comparison Between Experimental Solubility and Prediction (CSvdW) for Tripalmitin in CO_2

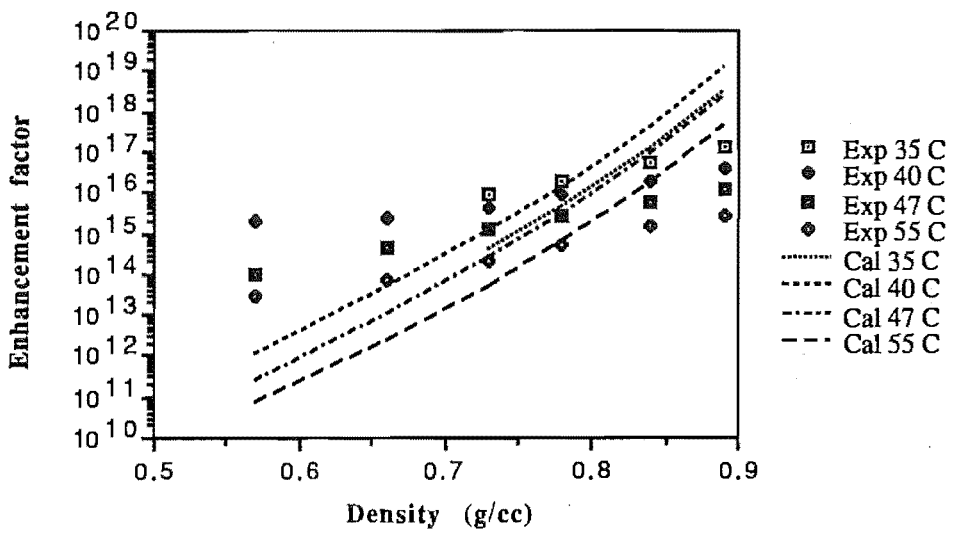

Figure 6.28 Comparison Between Experimental Enhancement Factor and Prediction (CSvdW) for Tripalmitin in CO_2

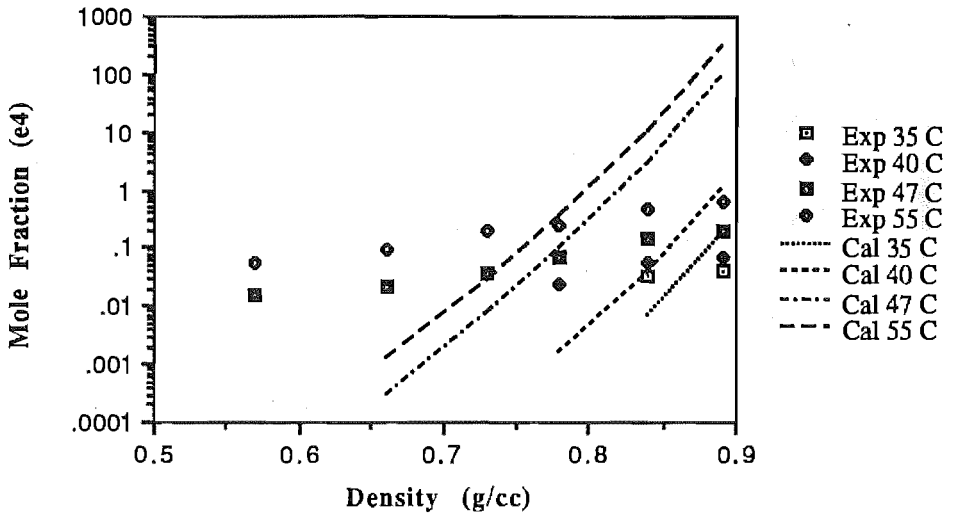

Figure 6.29 Comparison Between Experimental Solubility and Prediction (CSvdW) for Tristearin in CO_2

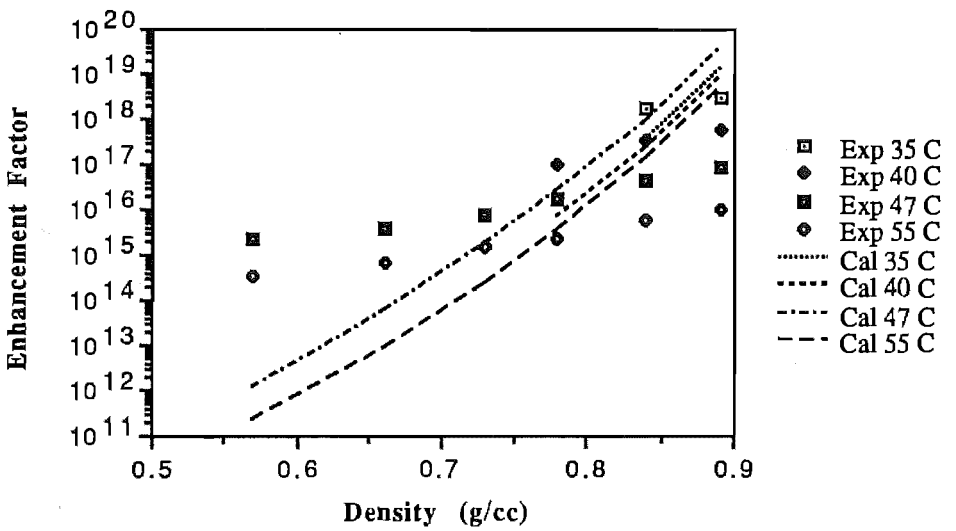

Figure 6.30 Comparison Between Experimental Enhancement Factor and Prediction (CSvdW) for Tristearin in CO_2

It was decided to try to improve the quality of the fit, by describing a_{12} as a linear function of T, ρ and molecular mass. It was found that the deviation between the experimental and calculated solubilities was minimised when the solutes were considered individually and a functional form for a_{12} of;

$$a_{12} = a + bT + c\rho \qquad (6.17)$$

was assumed. The curves from this function (used in equations 6.14 and 6.15) are compared to the experimental solubilities in figures 6.31 to 6.34. The parameters a, b and c for each solute are listed in table 6.4.

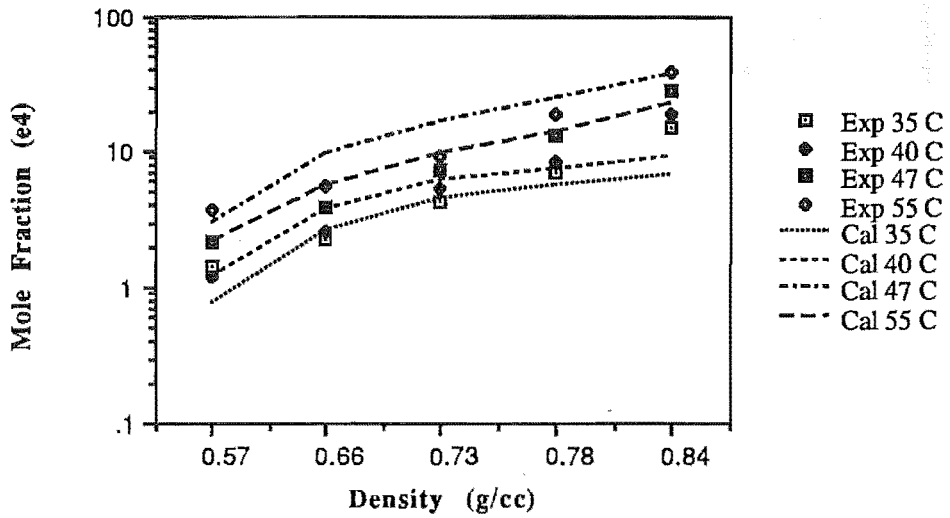

Figure 6.31 Comparison Between Experimental Solubility and Prediction (Equation 6.17) for Trilaurin in CO_2

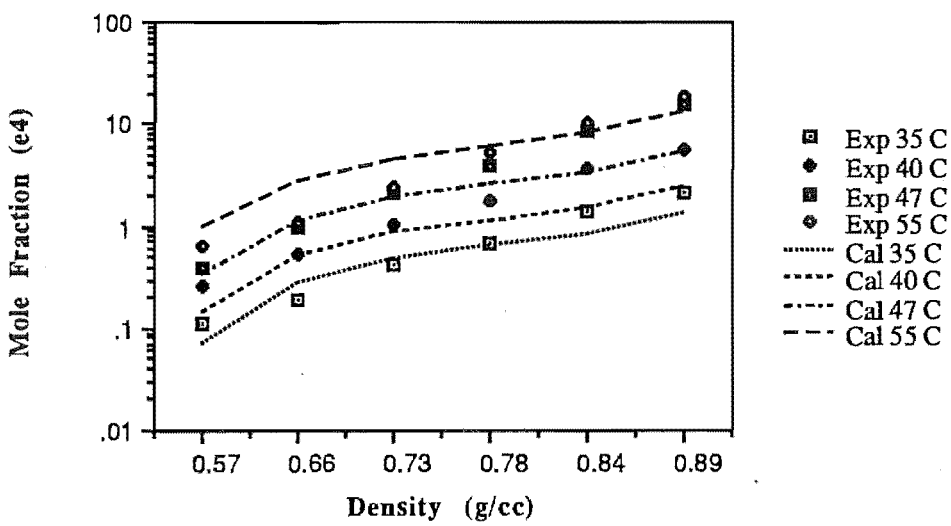

Figure 6.32 Comparison Between Experimental Solubility and Prediction (Equation 6.17) for Trimyristin in CO_2

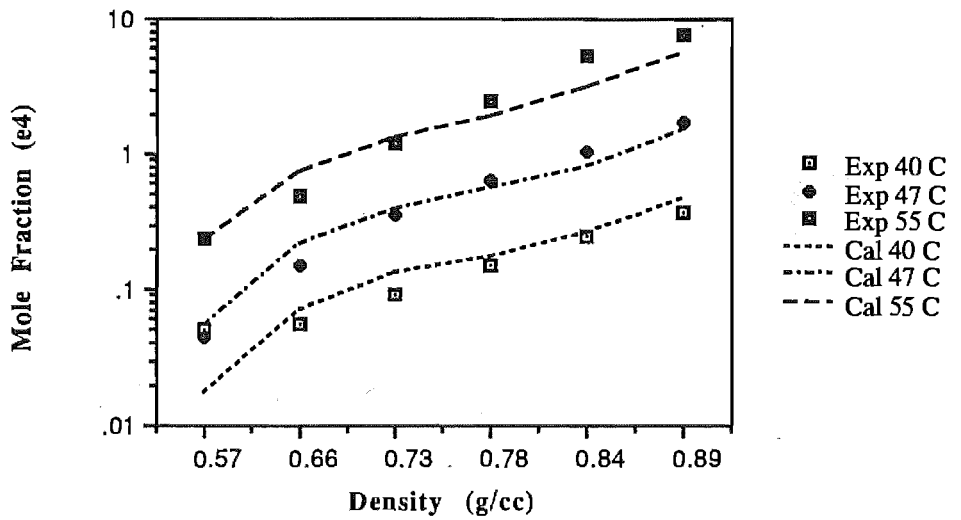

Figure 6.33 Comparison Between Experimental Solubility and Prediction (Equation 6.17) for Tripalmitin in CO_2

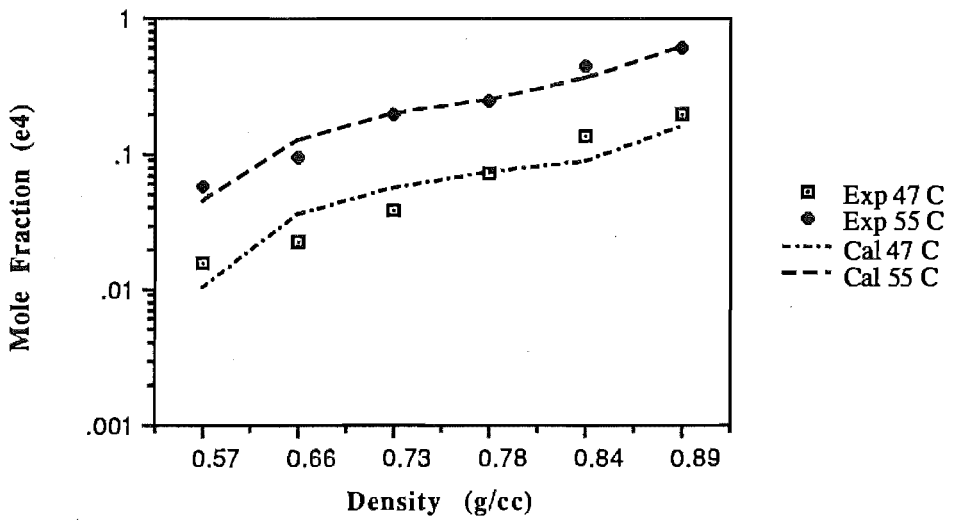

Figure 6.34 Comparison Between Experimental Solubility and Prediction (Equation 6.17) for Tristearin in CO_2

Table 6.4 Parameters for Equation 6.17

Triglyceride	a	b	c
Trilaurin	9.962	-1.79×10^{-2}	-2.314
Trimyristin	10.588	-1.82×10^{-2}	-2.721
Tripalmitin	11.241	-1.85×10^{-2}	-3.125
Tristearin	12.772	-2.17×10^{-2}	-3.627

These figures illustrate that by accounting for the variation of solvent density in the fitting parameter a_{12}, the fit is improved markedly. When equations 6.8 and 6.13 to 6.15 were used, an $\overline{RMS}$ value of 260 was obtained (cf 6.2×10^{-3} for phenanthrene/ethylene). When equation 6.17 was used, an $\overline{RMS}$ value of 3.61 (cf 2.2×10^{-3} for phenanthrene/ethylene) was obtained This illustrates the improvement in the prediction if a_{12} is considered to be dependent on the solvent density.

When a_{12} was fitted to an equation of the form;

$$a_{12} = a + bT + c\rho + dMr \qquad (6.18)$$

an $\overline{RMS}$ value of 5.43 was obtained. The graphs and parameters from this fit are presented in Appendix 6.

By fitting equation 6.17 to the a_{12} values, the number of fitting parameters is reduced from n to three, where n is the number of isotherms to be fitted. With the three parameter fit, the spacing of the isotherms is closely predicted, tending to overestimate the spacing for Trilaurin and Trimyristin. The coefficients obtained with three parameters show a weak variation with the solute molecular mass. This suggests that it would be possible to interpolate (between 600 and 900 Mr units) to predict solubilities and possibly extrapolate solubilities for solutes of molecular masses of 1000 or 500. The predictions could be correct to within half an order of magnitude.

It is interesting to return to the original definitions of a_{12} from the van der Waals EOS. The intermolecular attractive term, a in equation 2.17, can be directly related to the critical properties of a compound. By solving the EOS at the critical point, the variable a can be defined (Reid *et al* (1987));

$$a = \frac{27}{64}\frac{R^2T_c^2}{P_c} \qquad (6.19)$$

Now generally a geometric mean assumption is used to find the binary interaction parameter, a_{12};

$$a_{12} = (a_{11}a_{22})^{\frac{1}{2}} \qquad (6.20)$$

Therefore, it should be possible to to define a_{12} strictly in terms of the critical properties of the two components;

$$a_{12} = \frac{27}{64} R^2 \left[\frac{T_{c1}^2\, T_{c2}^2}{P_{c1}\, P_{c2}}\right]^{\frac{1}{2}} \qquad (6.21)$$

Equation 6.21 is independent of temperature and density. The geometric mean assumption can be relaxed and a form such as that suggested by Astin and Watson (1973) used;

$$a_{12} = \Psi(a_{11}a_{22})^{\frac{1}{2}} \qquad (6.22)$$

Ψ = some arbitrary function

This function equals one for the geometric mean. This assumption can also be relaxed by using a $(1\text{-}l_{12})$ form (equation 6.7). In fitting an equation of the form of 6.17 (or 6.18) to equation 6.22, Ψ has been defined and the effect of the van der Waals interaction parameter (equation 6.21) is included in the three fitted parameters.

In practice, the van der Waals EOS is known to give good qualitative agreement with many systems and predicts many types of binary phase equilibria (van Konyenberg and Scott, 1970). By describing the binary interaction parameter as a linear function of temperature and density, the basic structure of the equation is retained and a better qualitative description of the system is found. It is doubtful whether the replacement of the van der Waals repulsion term (§2b.2) with either a Peng & Robinson or a Redlich & Kwong repulsion term would improve the fit since both of these equations require that the parameters are fitted to the experimental data. None of these EOS models provide a good enough description of the real behaviour to predict the solubility of highly asymmetric, non-ideal systems *a priori*.

6.5 Empirical Methods

6.5.1 Correlation of Experimental Data

The triglyceride experimental solubilities were fitted with a linear function of temperature and density. The fit was an unweighted linear least squares regression. The equation fitted was of the form;

$$\log(y_2) = a' + b'T + c'\rho \qquad (6.23)$$

and the parameters are presented in table 6.5.

Table 6.5 Regression Parameters for Equation 6.23

Triglyceride	a'	b' (K^{-1})	c' ($cm^3.g^{-1}$)
Trilaurin	-7.00	2.09×10^{-2}	4.02
Trimyristin	-8.98	4.03×10^{-2}	4.56
Tripalmitin	-11.23	7.12×10^{-2}	4.34
Tristearin	-11.21	7.14×10^{-2}	3.48

These coefficients were plotted against solute molecular mass (figures 6.35 to 6.37) to determine if there were any solute related trends. It appears as though these coefficients are functions of molecular mass. The constants reflect the observed trends in the data, that the solubility decreased for a given density and temperature when the molecular mass was increased. The relations obtained from fits to figures 6.35 to 6.37 were then used to 'predict' the solubility of the solutes.

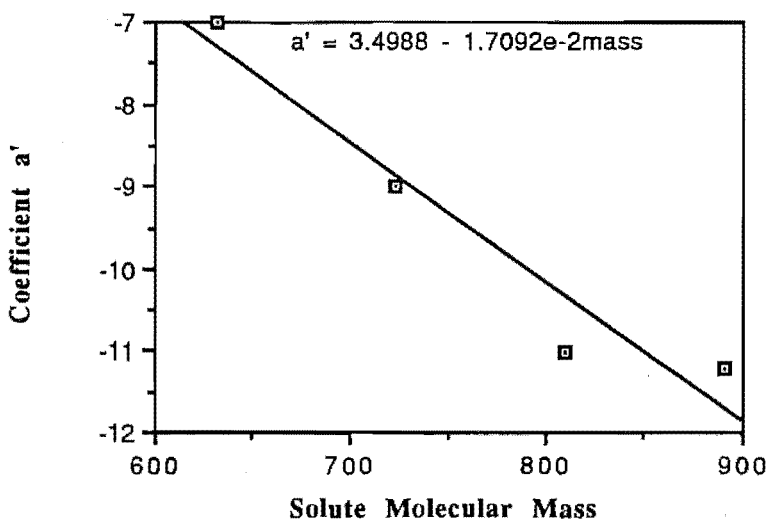

Figure 6.35 Variation of parameter "a' " (Equation 6.23) with Solute Molecular Mass

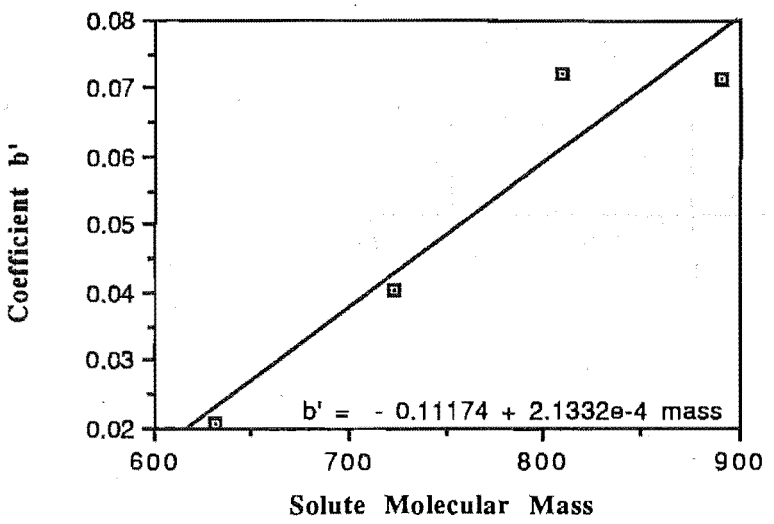

Figure 6.36 Variation of parameter "b' " (Equation 6.23) with Solute Molecular Mass

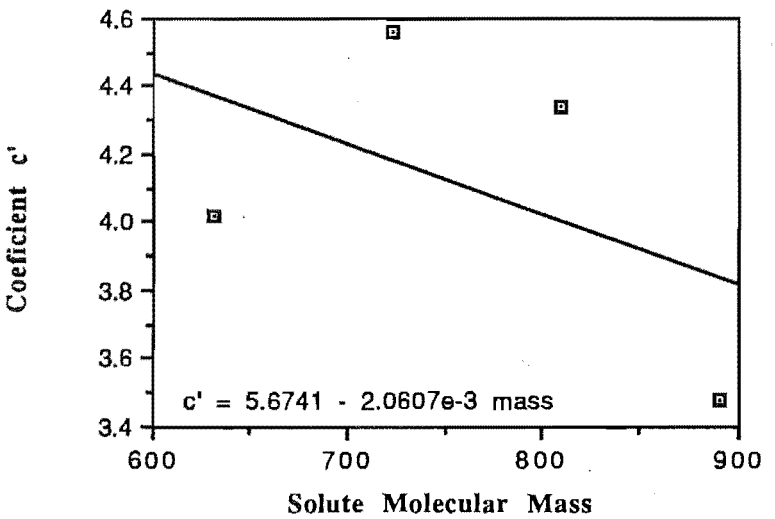

Figure 6.37 Variation of parameter "c' " (Equation 6.23) with Solute Molecular Mass

Figures 6.38 to 6.41 show the results of these predictions. An $\overline{RMS}$ value of 0.13×10^{-3} was obtained.

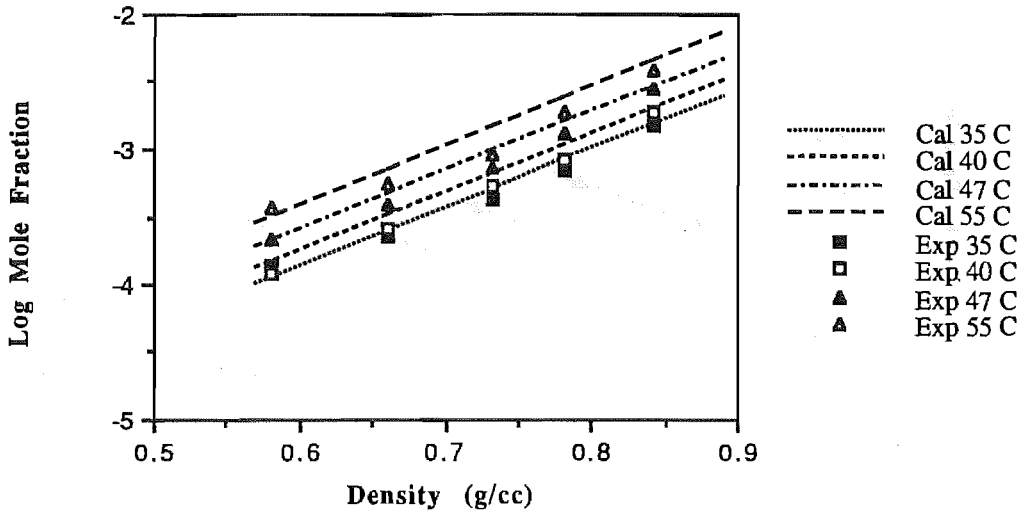

Figure 6.38 Comparison Between Experimental Solubility and Prediction (Equation 6.23) for Trilaurin in CO_2

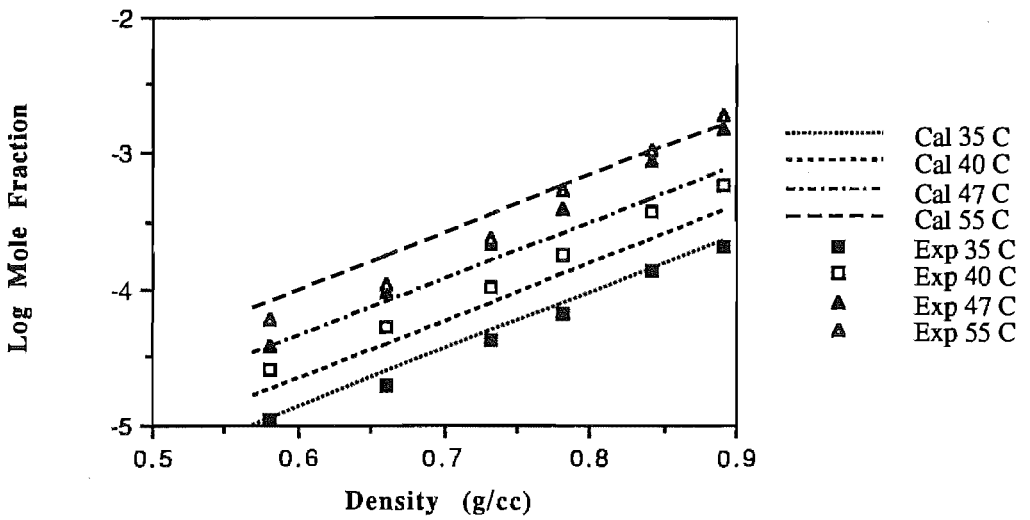

Figure 6.39 Comparison Between Experimental Solubility and Prediction (Equation 6.23) for Trimyristin in CO_2

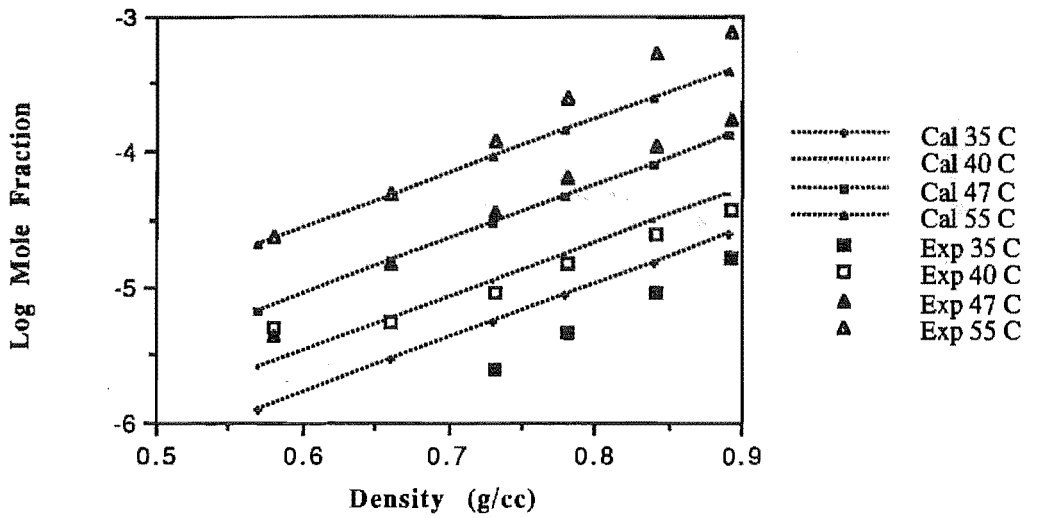

Figure 6.40 Comparison Between Experimental Solubility and Prediction (Equation 6.23) for Tripalmitin in CO_2

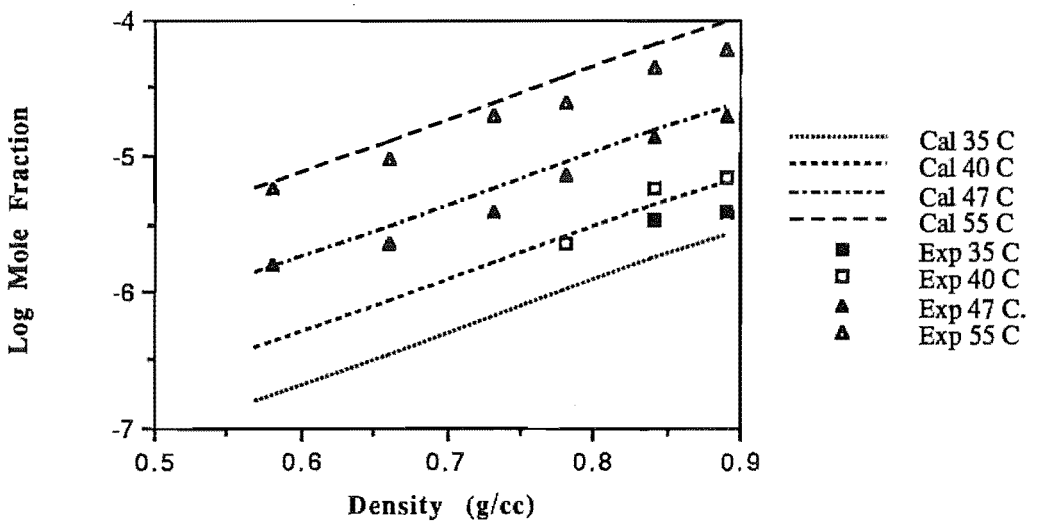

Figure 6.41 Comparison Between Experimental Solubility and Prediction (Equation 6.23) for Tristearin in CO_2

The experimental solubilities were then regressed according to the equation;

$$\log(y_2) = a'' + b''T + c''\rho + d''Mr \qquad (6.24)$$

with constants;

Table 6.6 Coefficients for Equation 6.24

a''	-2.74
b'' (K^{-1})	4.14×10^{-2}
c'' ($cm^{-3}.g^{-1}$)	4.22
d'' ($mol.g^{-1}$)	-8.37×10^{-3}

The solubilities were estimated using equation 6.24 and the results are plotted in figures 6.42 to 6.45. An $\overline{RMS}$ value of 0.17×10^{-3} was obtained from these predictions.

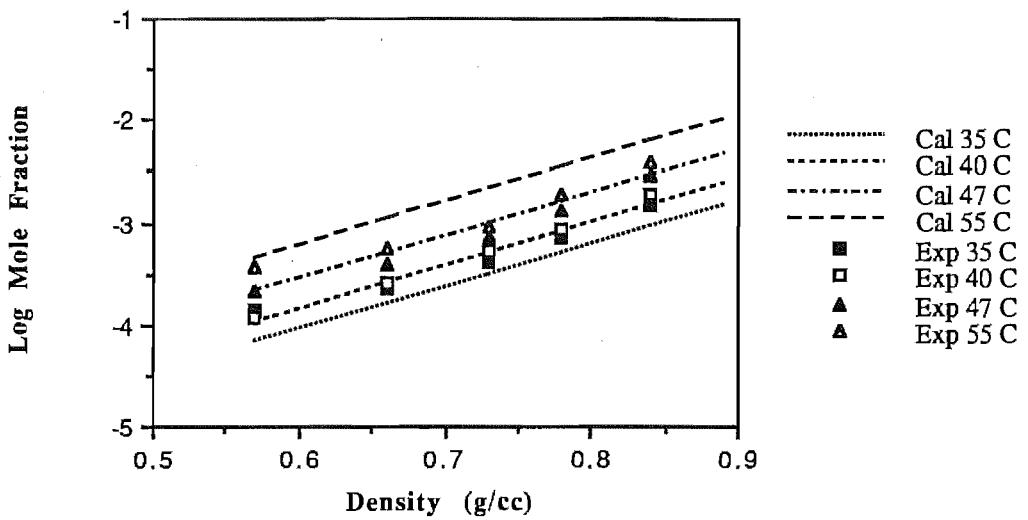

Figure 6.42 Comparison Between Experimental Solubility and Prediction (Equation 6.24) for Trilaurin in CO_2

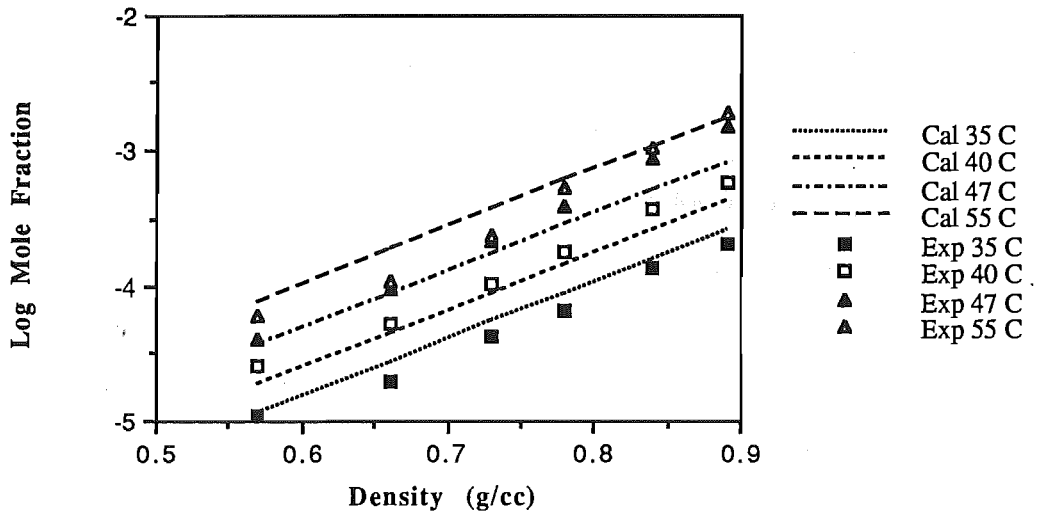

Figure 6.43 Comparison Between Experimental Solubility and Prediction (Equation 6.24) for Trimyristin in CO_2

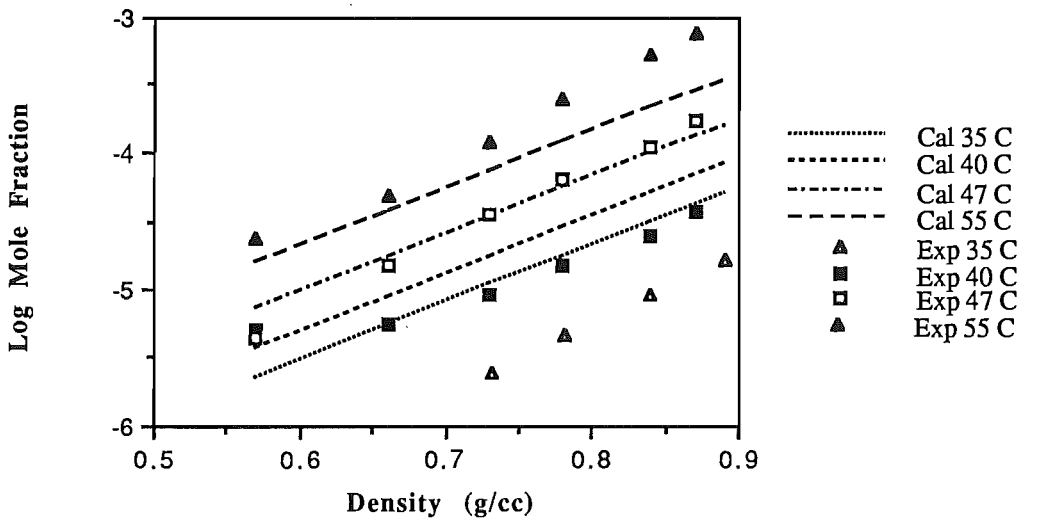

Figure 6.44 Comparison Between Experimental Solubility and Prediction (Equation 6.24) for Tripalmitin in CO_2

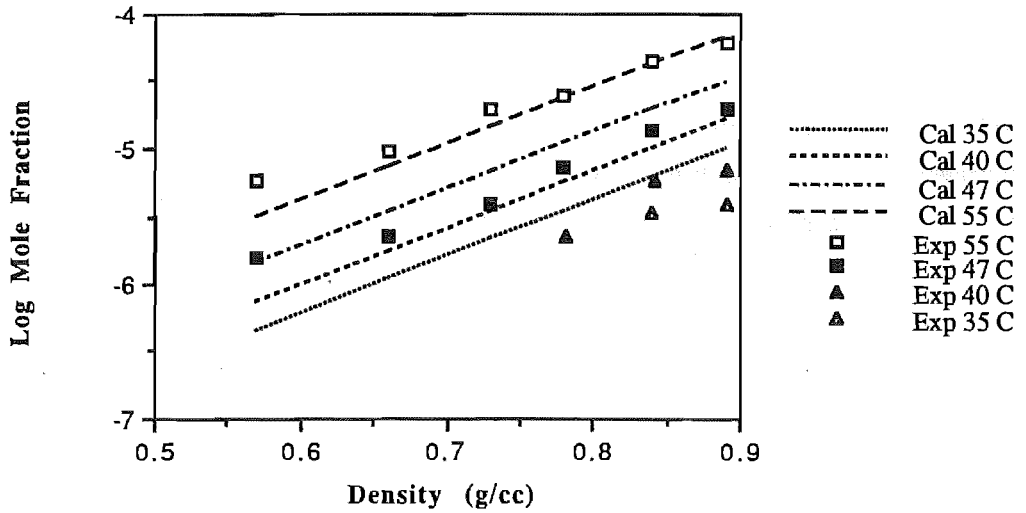

Figure 6.45 Comparison Between Experimental Solubility and Prediction (Equation 6.24) for Tristearin in CO_2

The addition of a term in molecular mass has the effect of overestimating the effect of temperature for Trilaurin and Trimyristin and underestimating the temperature effect on the other two solutes. It should be remembered that for Tripalmitin, experimental solubilities at three temperatures and for Tristearin experimental solubilities at two temperatures were used to determine parameters in equations 6.23 and 6.24. This lack of data may account for poor temperature representation of these two solutes. The maximum deviation between the experimental solubilities and the values calculated from equations 6.23 and 6.24 was less than 30%.

6.5.2 The Method of Chrastil

Chrastil's method (1982) assumes that it is possible to describe the solution process in terms of an equilibrium relation;

$$A + kB \Leftrightarrow AB_k \qquad (6.25)$$

where A & B are molecular species

k = the number of B molecules that associate with each A molecule

Chrastil (1982) then goes on to derive an equation for the solubility of a solute in a solvent;

$$y_2 = \rho^k \exp\left\{\frac{a}{T} + b\right\} \qquad (6.26)$$

where y_2 = the solubility of the solute in $g.l^{-1}$

a, b = constants of the equation 6.26 (fitted to the solubilities) and

ρ = the solvent density in $g.l^{-1}$

The form of the equation suggests that there will be a straight line relationship on a log-log plot between the solute solubility and solvent density. Furthermore, this method assumes that there will be a unique value for k for any given solute and that this value will be a constant over the whole solvent density range.

Table 6.7 Regression Parameters for Equation 6.27

Triglyceride	A	B
Trilaurin		
35°C	-19.37	7.01
40°C	-22.01	7.96
47°C	-20.70	7.57
55°C	-18.72	6.93
Trimyristin		
35°C	-22.57	7.79
40°C	-22.97	8.08
47°C	-25.97	9.23
55°C	-24.90	8.89
Tripalmitin		
35°C	-31.50	10.48
40°C	-22.07	7.40
47°C	-26.86	9.26
55°C	-26.18	9.24
Tristearin		
47°C	-21.05	6.96
55°C	-19.01	6.45

The solubilities presented in Chapter 5 were correlated using this method. Graphs are presented in figures 6.46 to 6.49 and equations of the form;

$$\log y = A + B \log \rho \qquad (6.27)$$

were fitted. The regression parameters from these fits are presented in table 6.7.

The model assumes that the values of the density exponent, k, are the same for all temperatures. That is, that the isotherms will be parallel. If the isotherms are not parallel, then it is necessary to use some mean value of k in equation 6.26. Inspection of figures 6.46 to 6.49 shows that most of the isotherms are parallel. However a mean value of k needs to be determined, introducing errors into the calculations.

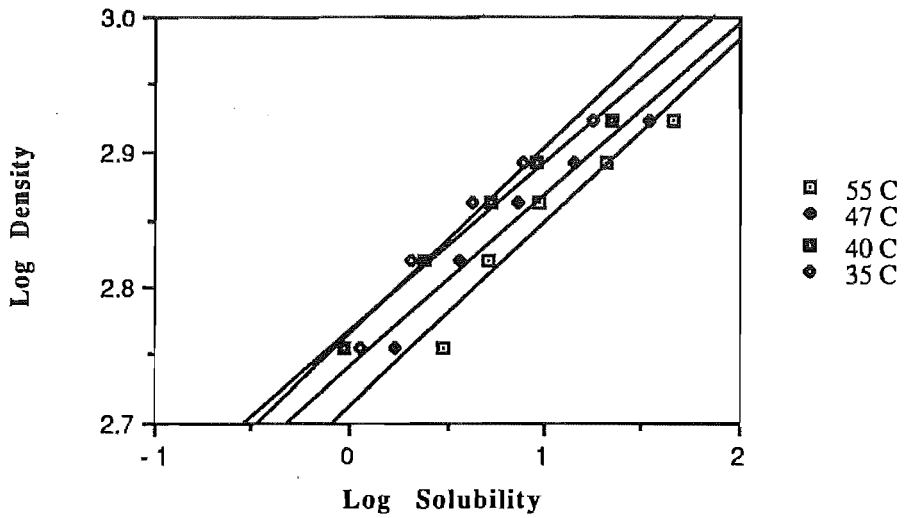

Figure 6.46 Regression Lines used in Chrastil Prediction Method (Equation 6.27) for Trilaurin

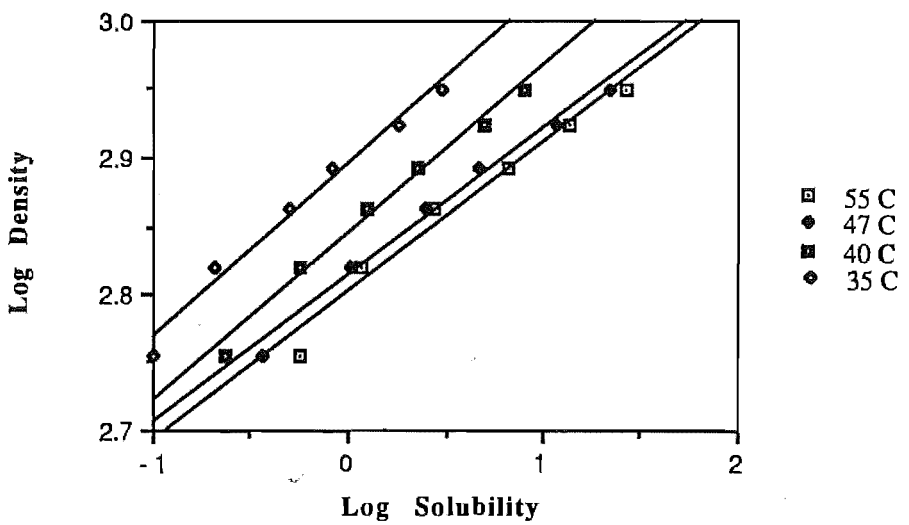

Figure 6.47 Regression Lines used in Chrastil Prediction Method (Equation 6.27) for Trimyristin

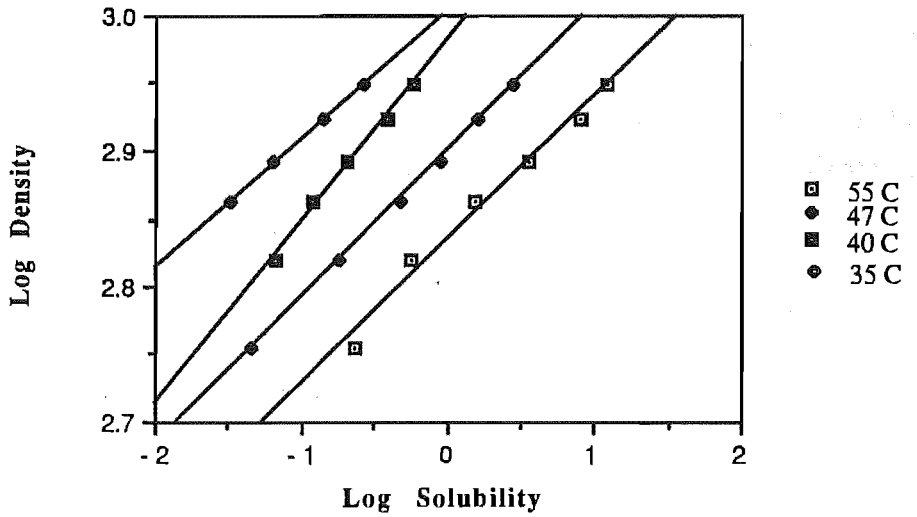

Figure 6.48 Regression Lines used in Chrastil Prediction Method (Equation 6.27) for Tripalmitin

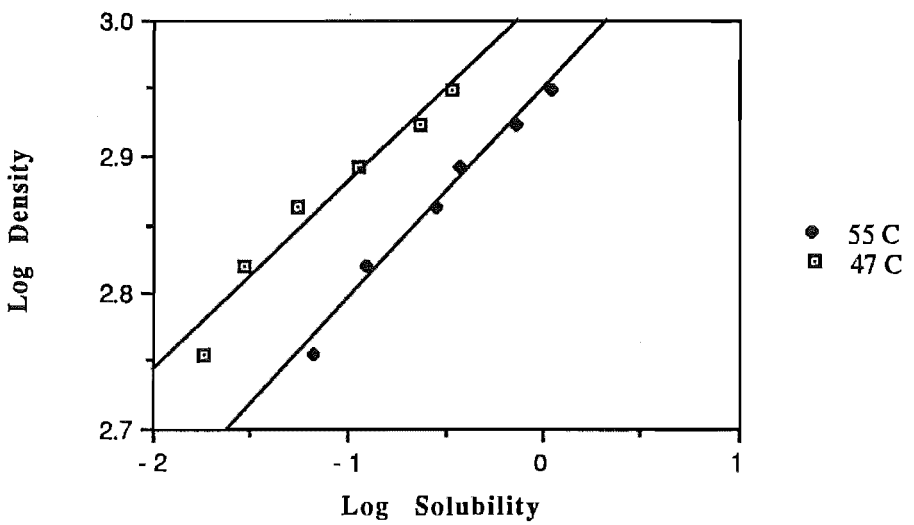

Figure 6.49 Regression Lines used in Chrastil Prediction Method (Equation 6.27) for Tristearin

To determine the constants, a and b, Chrastil suggests plotting log density against log solubility for two isotherms at temperatures T_1 and T_2, and using the following relations;

$$k = \frac{1}{\text{slope of the isotherms}} \qquad (6.28)$$

$$a = \frac{k\, T_1 T_2 \ln\left[\frac{I_1}{I_2}\right]}{T_2 - T_1} \qquad (6.29)$$

where I = the intercept of the isotherm at log solubility = 0

$$b = -k \ln I_1 - \frac{a}{T_1} \quad (= -k \ln I_2 - \frac{a}{T_2}) \qquad (6.30)$$

According to the method, it should make no difference to equation 6.26 which values of the intercepts are used in the determination of a & b. The parameters determined in this manner are listed in table 6.8. In determining these parameters, care was taken to select parallel isotherms. Figures 6.50 to 6.53 show the predictions based upon this model.

Table 6.8. Chrastil Parameters for Triglycerides

Triglyceride	k	a	b
Trilaurin	7.64	-6577.2	-27.68
Trimyristin	8.65	-5780.7	-38.17
Tripalmitin	9.14	-18157.6	-4.32
Tristearin	6.89	-14650.0	-2.17

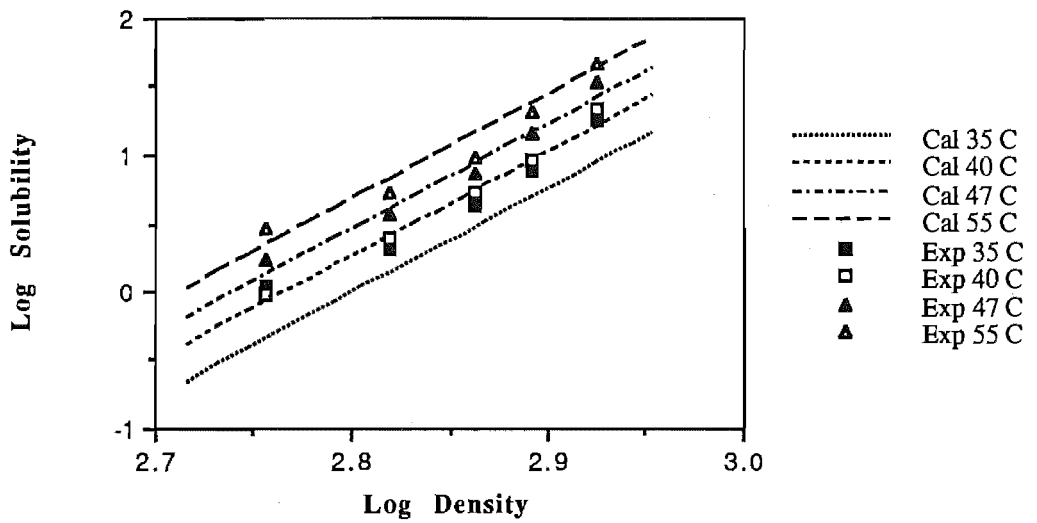

Figure 6.50 Comparison Between Experimental Solubility and Prediction (Equation 6.26) for Trilaurin in CO_2

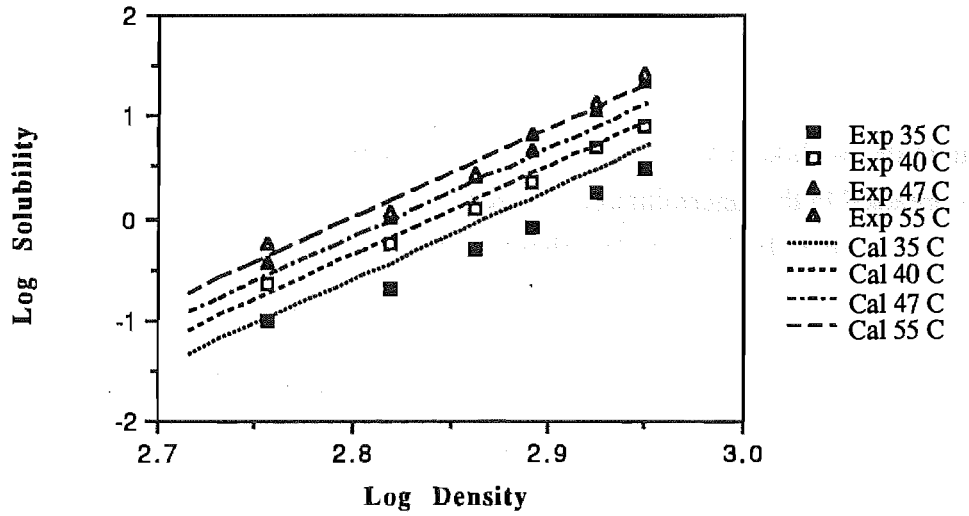

Figure 6.51 Comparison Between Experimental Solubility and Prediction (Equation 6.26) for Trimyristin in CO_2

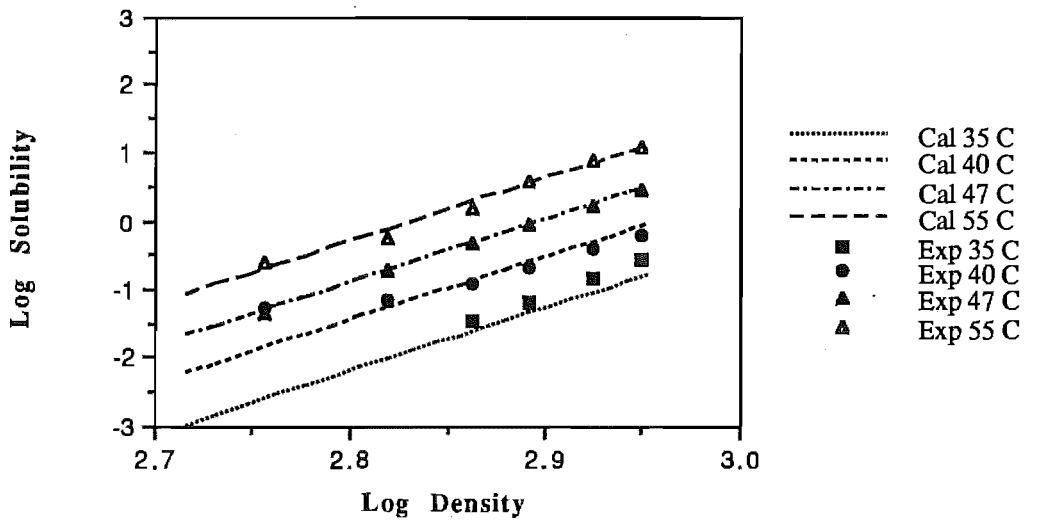

Figure 6.52 Comparison Between Experimental Solubility and Prediction (Equation 6.26) for Tripalmitin in CO_2

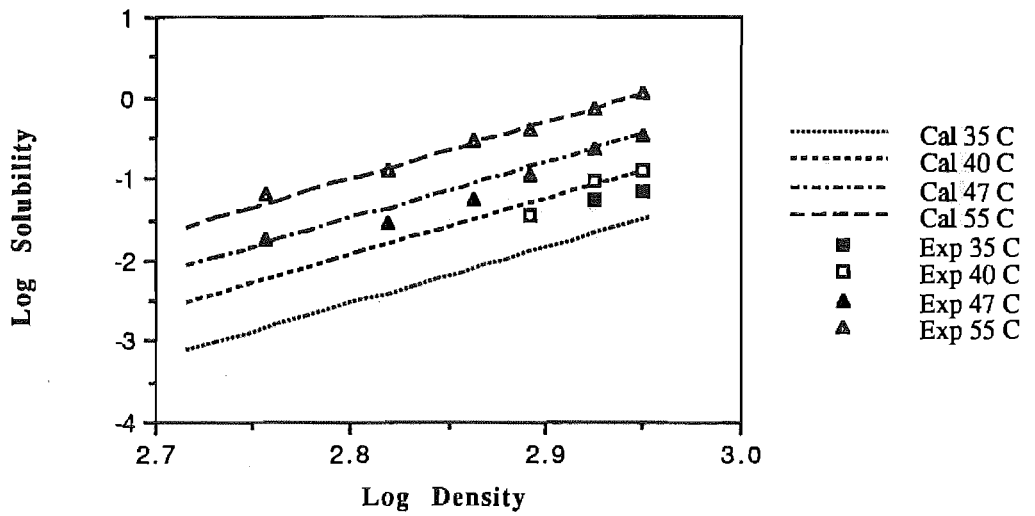

Figure 6.53 Comparison Between Experimental Solubility and Prediction (Equation 6.26) for Tristearin in CO_2

To test the sensitivity of this method to the choice of parameters, the parameters were re-evaluated, but this time isotherms that were not parallel were selected for use in equations 6.29 and 6.30. The results of these fits are presented in figures 6.54 to 6.56. For Trilaurin, the spread of isotherms is underestimated and for Tripalmitin and Trimyristin, the spread is overestimated.

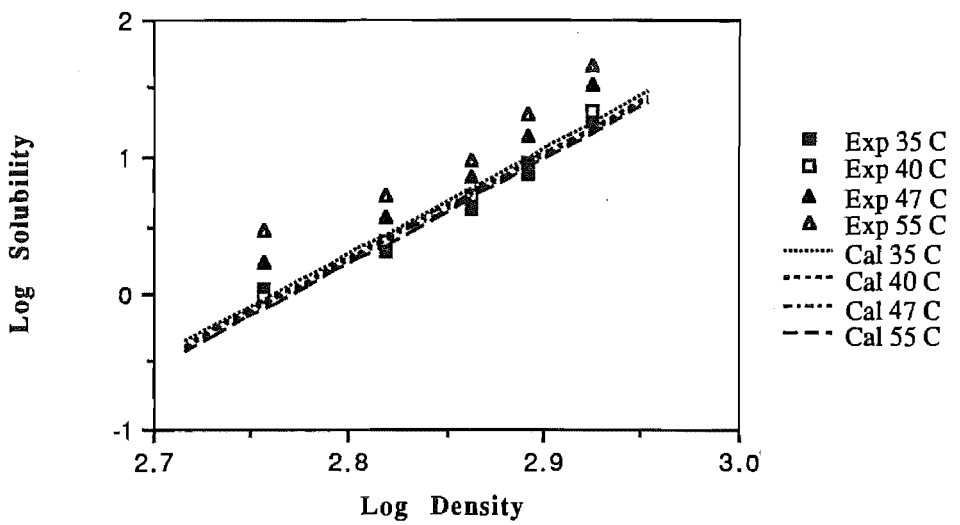

Figure 6.54 Sensitivity of Predictions using Equation 6.26 for Trilaurin from Solubility Results of this Work

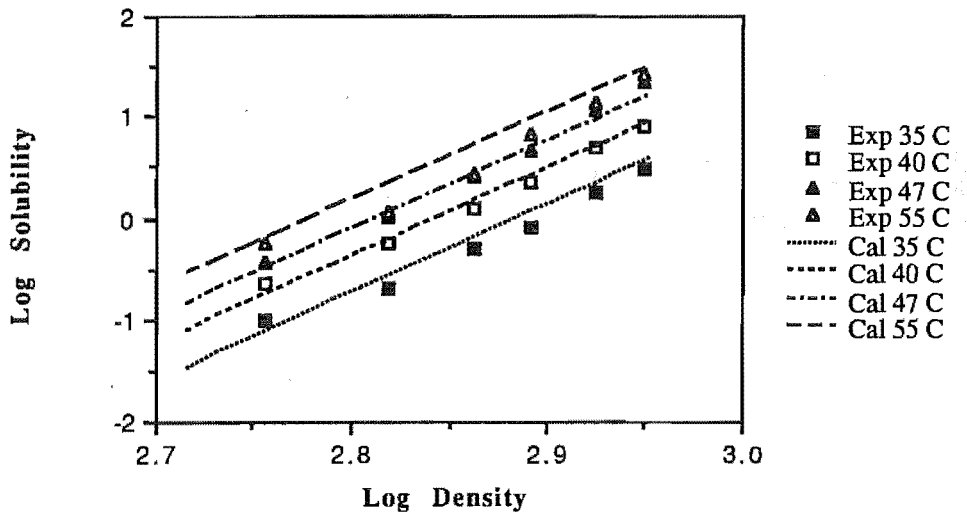

Figure 6.55 Sensitivity of Predictions using Equation 6.26 for Trimyristin from Solubility Results of this Work

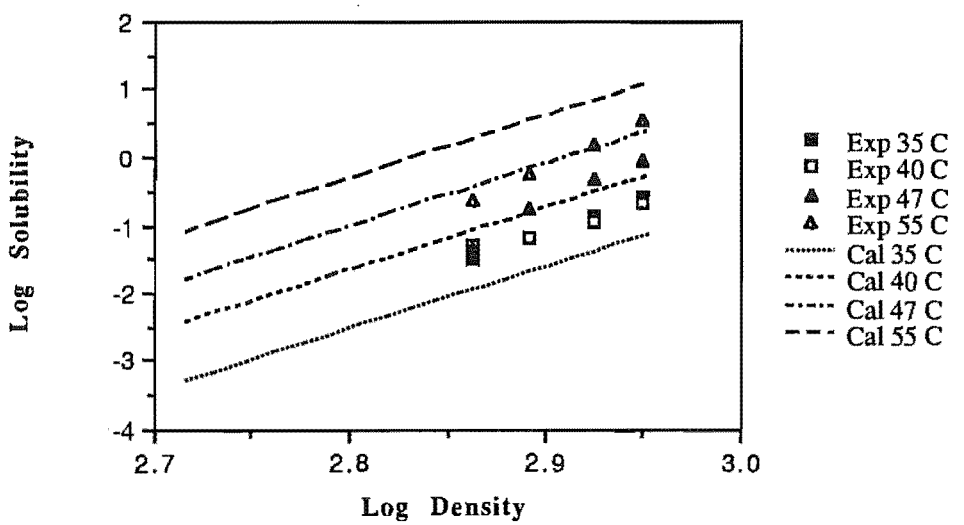

Figure 6.56 Sensitivity of Predictions using Equation 6.26 for Tripalmitin from Solubility Results of this Work

In general, the method closely represents the spread of the isotherms and describes the solubility of the triglycerides to within half an order of magnitude. The $\overline{RMS}$ value for the best fit was found to be 2.30, while for the sensitivity test, an $\overline{RMS}$ value of 5.02 was obtained.

Table 6.8 shows that the a and b parameters do not seem to correlate with solute molecular mass. The values for the k, a and b parameters determined for Tripalmitin and Tristearin

disagree with those determined by Chrastil. A comparison between the parameters determined for this work and those presented by Chrastil is given in table 6.9.

Table 6.9 Comparison of parameters for Tripalmitin and Tristearin

Triglyceride	Parameter	This Work	Chrastil
Tripalmitin	k	9.14	2.98
	a	-18157.6	-2387.8
	b	-4.32	-12.15
Tristearin	k	6.89	9.75
	a	-14650.0	-8771.6
	b	-2.16	-39.44

As can be seen, there is a large discrepancy between the constants determined in the two studies. This could be explained by the inaccuracy of Chrastil's data.

The difference between the two solutes compared in table 6.9 is in the length of the fatty acid chains - Tristearin has two additional -CH_2- groups in each chain. One would expect to see similar values for the three parameters for both triglycerides.

Chrastil has related these constants a & b to physical properties as;

$$a = \frac{\Delta_{sol}H + \Delta_v H}{R} \qquad (6.31)$$

$$b = \ln(Mr_A + kMr_B) + q - k \ln Mr_B \qquad (6.32)$$

where Mr_x = the molecular mass of the species x,
q = a constant of equation 6.32 and
$\Delta_{sol}H$ = the heat of solution for the reaction described by equation 6.25

Equations 6.31 and 6.32 suggest that the coefficients a and b should correlate with molecular mass in some uniform manner. Whether the variation is positive or negative will depend upon the manner in which $\Delta_{sol}H$ varies with solute molecular mass. This variation in the parameters (both between solutes (table 6.8) and between workers (table 6.9)) suggests that this method would be inappropriate for extrapolation to other solutes. Once experimental measurements are made, this method does give a good description of the data and could be used for interpolation.

The method assumes that log solubility will be a linear function of log density. One can see from figure 6.50 (for example) that this is not so.

Del Valle and Aguilera (1988) have suggested using an equation of the form;

$$I = b' + \frac{m'}{T} + \frac{n'}{T^2} \tag{6.33}$$

to replace the $\left[\frac{a}{T} + b\right]$ exponential term in equation 6.26. This method may improve the fit, with the addition of an another parameter, but was not considered in this study.

6.5.3 Ziger's Method

The correlation of Ziger and Eckert (1983) is based upon a regular solution approach to phase equilibria. By writing the solubility as;

$$y_2 = \frac{P_2^{sat}}{P\,\phi_2} \exp\left\{ \int_0^{\infty} \frac{v_2^s\, dP}{RT} \right\} \tag{6.34}$$

they derive an expression for the enhancement factor;

$$\ln E = \ln\left(\frac{P\,y_2}{P_2^{sat}}\right) = -\ln \phi_2 + \int_0^{\infty} \frac{v_2^s\, dP}{RT} \tag{6.35}$$

where E = the enhancement factor (the ratio of real to ideal solubilities)

An approach suggested by Prausnitz (1965) to apply Regular Solution Theory to phase equilibria is used and equation 6.36 is derived;

$$\ln E = \ln \frac{f_2^L}{f_2^{mo}} - \frac{v_2^L}{RT} \Phi_1^2 (\delta_2 - \delta_1)^2 + \ln\left(\frac{P}{P_2^{sat}}\right) \tag{6.36}$$

where f_2^{mo} = the fugacity of component 2 at standard state in the mixed phase and

f_2^L = the fugacity of component 2 in the liquid phase

They then obtain another expression for the enhancement factor, E;

$$\log E = \varepsilon_2^* \Delta (2-\Delta) - \log\left[1 + \frac{\delta_1^2}{P}\right] \tag{6.37}$$

where $\Delta = \frac{\delta_1}{\delta_2}$ and

$$\varepsilon_2^* = \frac{\delta_2^2 \, v_2^L}{2.3RT}$$

It is realised by Ziger and Eckert that equation 6.37 will only give a good qualitative description of the enhancement factor and they introduce two parameters v_1 and η_1 to correlate this equation against a variety of solutes.

$$\log E = \eta_1 \left\{ \varepsilon_2^* \frac{\Delta}{y_1} \left(2 - \frac{\Delta}{y_1}\right) - \log \left[1 + \frac{\delta_1^2}{P} \right] \right\} + v_1 \qquad (6.38)$$

where y_1 = the mole fraction of the solvent (≈ 1 for the triglyceride/CO_2 systems)

From their work, they observed that η_1 should be constant for each solvent and that v_1 should be solute dependent. This implies that for a given solute in a given solvent, the solubility data should lie on a straight line of slope η_1 (equation 6.39). One should be able to use this correlation to estimate the solubility at some different temperature and pressure for this solute/solvent combination.

$$\log E - v_1 = \eta_1 \left\{ \varepsilon_2^* \frac{\Delta}{y_1} \left(2 - \frac{\Delta}{y_1}\right) - \log \left[1 + \frac{\delta_1^2}{P} \right] \right\} \qquad (6.39)$$

To test this correlation, the solubility parameters presented in table 6.2 were used. The individual triglycerides were correlated using equation 6.38 and the parameters are listed in Table 6.10. Using the v_1 parameters, the term 'log E-v_1' (equation 6.39) was determined and figures 6.57 to 6.60 were plotted.

Table 6.10 Parameters from Equation 6.38

Parameter v_1				
Triglyceride	Perry	Barton	Bailey	Data
Trilaurin	-2.04	5.06	5.49	4.00
Trimyristin	-7.08	4.75	5.51	3.98
Tripalmitin	-4.68	6.16	6.98	5.74
Tristearin	-10.46	5.33	6.60	5.39
Parameter η_1				
Trilaurin	0.67	0.17	0.14	0.24
Trimyristin	0.89	0.19	0.15	0.23
Tripalmitin	0.78	0.18	0.14	0.20
Tristearin	1.01	0.20	0.14	0.19

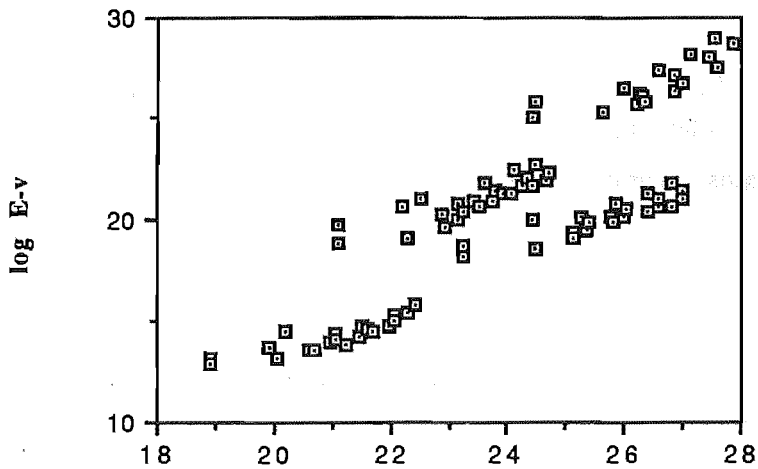

$$\varepsilon_2^* \frac{\Delta}{y_1}\left(2 - \frac{\Delta}{y_1}\right) - \log\left[1 + \frac{\delta_1^2}{P}\right]$$

Figure 6.57 Correlation of Triglycerides using Equation 6.39 and the Solubility Parameters from the Values of Perry

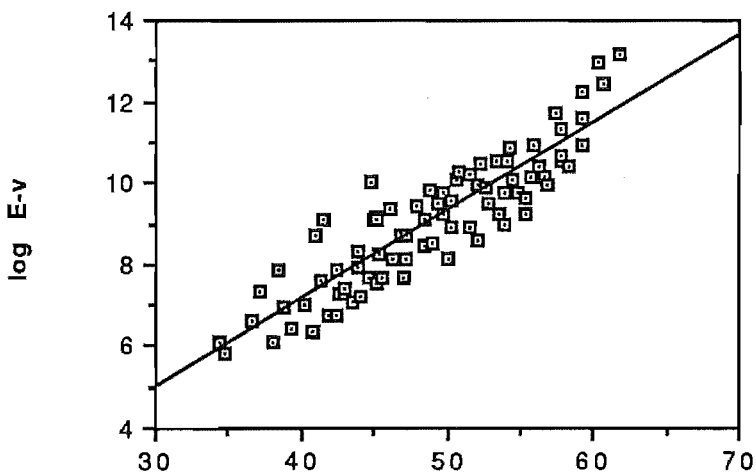

$$\varepsilon_2^* \frac{\Delta}{y_1}\left(2 - \frac{\Delta}{y_1}\right) - \log\left[1 + \frac{\delta_1^2}{P}\right]$$

Figure 6.58 Correlation of Triglycerides using Equation 6.39 and the Solubility Parameters from the Values of Barton

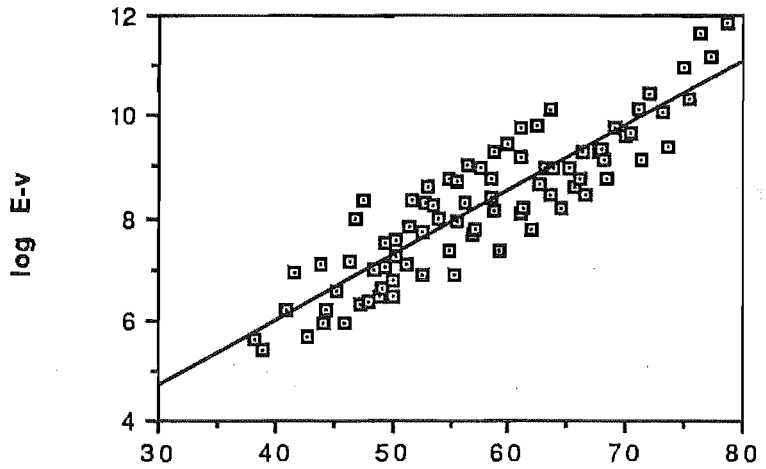

Figure 6.59 Correlation of Triglycerides using Equation 6.39 and Solubility Parameters from the Values of Bailey

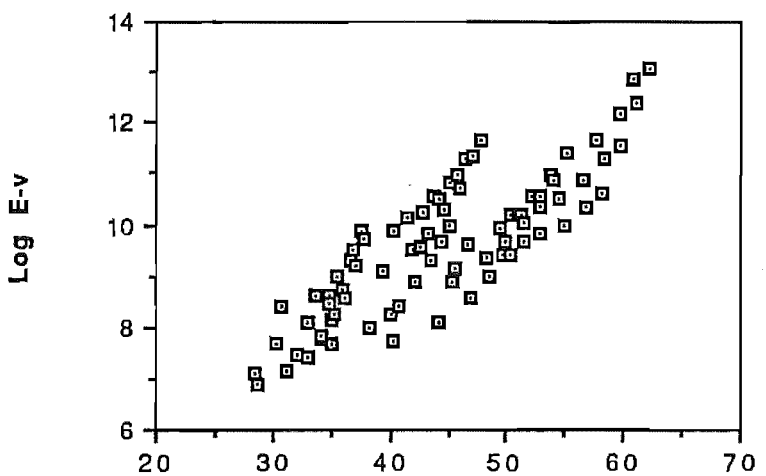

Figure 6.60 Correlation of Triglycerides using Equation 6.39 and Solubility Parameters from Fitting Experimental Solubilities

These figures illustrate that this correlation is very sensitive to the value of the solute solubility parameter used. As solute solubility parameter values decrease, the relative difference between the solute and solvent solubility parameters is decreased and small differences between the solute solubility parameters become more pronounced. The net

effect of this seen in figure 6.57 where the data no longer fall on a single line (for CO_2). Instead, the individual solutes are evident. As the solute solubility parameters are increased, the opposite effect is seen. The scatter in the data for the individual triglycerides in figure 6.57 is approximately ± one order of magnitude. In figure 6.58, the scatter in the data is ± two orders of magnitude. Therefore one can say that as the correlation becomes more general, the accuracy decreases.

From figures 6.58 and 6.59, the constant η_1 was determined to be 0.21 and 0.12 respectively. These values do not agree with the values of 0.497 determined for CO_2 by Ziger and Eckert (1983), and 0.493 determined by Gurdial *et al* (1989) and are clearly dependent on the value of solute solubility parameter used in determining the abscissa.

The uncertainty in solute solubility parameter determination has hindered the assessment of this correlation method.

6.6 Comparison Between the Methods

The use of solubility parameters for activity coefficient estimation was not found to be satisfactory. The implementation of this model was hampered by a lack of reliable heats of vaporisation values for the triglycerides. When the experimental data were fitted by equation 6.6, the values for the solubility parameters obtained were lower than those of similar solutes (e.g. naphthalene $\delta_2 = 9.9$ (Hildebrand and Scott, 1962)). This method did give a good qualitative description of the observed behaviour, but the numerical accuracy of the method was poor. That the method comes to within several orders of magnitude of the experimental solubilities is remarkable, when one considers the comments of Hildebrand and Scott (§6.2).

The use of the Carnahan Starling van der Waals equation of state illustrated that modelling the solubility of systems with a cubic equation of state is not satisfactory if the components are of dissimilar sizes. When the binary interaction parameter, a_{12}, is made a linear function of temperature and density, the experimental data can be more accurately modelled. When, however, molecular mass is added as a further independent variable, the fit is worse. This suggests that making the a_{12} parameter a linear function of temperature, density and molecular mass would not be be suitable for the prediction of the solubilities of other triglycerides. The parameters used in equation 6.17 are given in table 6.4. These parameters appear to be weak functions of solute molecular mass and therefore it would be possible to determine functional forms for the parameters and re-estimate the experimental data. Given the applicability of the model to the CO_2/triglyceride systems, it is doubtful whether this additional information would be useful.

Chrastil's equation (6.26) does provide an adequate representation of experimental solubilities. The wide variation in the model constants (tables 6.8 and 6.9) makes it injudicious to try to use this method for extrapolation.

Given the sensitivity of Ziger's method to the choice of solute solubility parameter, this method cannot be recommended for the prediction of solubilities of triglycerides.

The ability of all these models to predict solubility data has been seriously limited by the lack of essential physical property data. Until more physical property data are determined, model performance will continue to be poor.

For two of the temperatures considered (47 and 55°C), Trilaurin was in a liquid state. The presence of a liquid does not affect the performance of the models studied. In the CSvdW model, the molar volumes and the vapour pressures are used in the model. These properties will change with the change from solid to liquid phase, but no effect of these changes was evident from the figures.

Table 6.11 presents a statistical comparison between the methods discussed in sections 6.3 and 6.4.

Table 6.11 Statistical Comparison of Models

Method	$\overline{RMS}$ value	Mean Percentage Error	log $\overline{RMS}$
Chrastil	2.304	23.89	0.157
Chrastil (variation)	5.022	30.26	0.238
Data Regression (T,ρ)	0.13×10^{-3}	21.86	0.119
Data Regression (T,ρ,Mr)	0.163×10^{-3}	27.23	0.146
CSvdW ($a_{12} = f(T)$)	261.5	2775.6	1.427
CSvdW ($a_{12} = f(T,\rho)$)	3.605	34.0	0.197
CSvdW ($a_{12} = f(T,\rho,Mr)$)	5.429	106.9	0.383
Phenanthrene (CSvdW)	6.2×10^{-3}	34.14	0.276
Phenanthrene (regressed)	2.2×10^{-3}	15.5	0.090

$$\text{where } \log \overline{RMS} = \sqrt{\frac{\sum (\log x_e - \log x_c)^2}{N}} \qquad (6.40)$$

One can see from these data that a simple regression of the experimental data provides the best method of correlating the data. When the experimental data are correlated against solute molecular mass, there is a small decrease in the quality of the fit, but an increase in generality. This method would be the most reliable for extrapolation to other solutes in the triglyceride series.

7

Conclusions and Recommendations for Further Work

7.1 Conclusions

This work has shown that it has not been possible to predict *a priori* the solubility of triglycerides in supercritical carbon dioxide. It was found that when the experimental solubilities were made a linear function of temperature and density, the deviations between experimental values and predicted results were lowest. When molecular mass was added as a further linear parameter, the deviations decreased. The four parameter equation that the regression provided could be used to predict the solubility of a saturated triglyceride of molecular mass between 600 and 900 mass units, to within half an order of magnitude. This equation could be used to predict solubilities for saturated mono-acid triglycerides outside this molecular weight range to within an order of magnitude.

Of the other methods examined in this study, the use of the Hildebrand solubility parameter theory gave a good qualitative description of the experimental data, but the numerical fit was poor. When the binary interaction parameter, a_{12}, was made a linear function of temperature and density, the Carnahan Starling van der Waals EOS gave a good representation of the experimental data. The method of Chrastil was found to be satisfactory for interpolation purposes, but was not considered suitable for extrapolation to other triglycerides.

7.2 Recommendations for Future Work

7.2.1 Continuation of This Work

The experimental programme should be extended to investigate triglyceride mixtures in CO_2. Work should include pure solvents and those with entrainers. This work would lead onto the investigation of natural mixtures (butter and oils) and eventually to the removal of fats from

protein. Each step of this programme should be accompanied by an attempt to account for the observed behaviour with a suitable extension to the theory.

Solubility data should be determined for the triglycerides studied in a variety of solvents. With such data it would be possible to determine the most suitable solvent for commercial plant design. Other triglycerides in addition to those examined during this work should also be investigated. These should include mono-unsaturated, poly-unsaturated, di- and tri-acid triglycerides. From these data it should be possible to determine the effect of degree of unsaturation and molecular mass of triglycerides on the observed solubility.

There is considerable scope to explore the effect of entrainers on the solubility of triglycerides. Such a study could include the effect of amount of addition, and define a method of selecting a suitable entrainer for a given extraction.

With the entrainer addition there should be a parallel investigation into the phase behaviour of the mixtures. Such a study would be most important where there is doubt as to whether there are one of more phases present inside the pressure vessel.

7.2.2 General

Further investigation needs to be made into the solubility of liquid solutes in supercritical solvents. The limited work with Tributyrin (§4.6) demonstrated that it is possible to determine the solubility of a very soluble liquid with the present experimental apparatus. The use of continuous solute addition to the system should be further explored with a variety of solutes, solvents, operating conditions and solute addition rates.

To parallel the solubility, phase equilibria and physical property work, there is scope for the tandem development of equipment and methods for transport property determination. These data are vital to the chemical engineering designer, and must be obtained if SFE has a chance of being given due consideration during evaluating separation processes.

There is plenty of scope for theoretical development in the prediction of pure component solubilities. Research could include investigating the effects of molecular size, functional group and molecular polarity. Such work would lead to predictions of complex mixture solubilities.

8

References

Allada, S.R., 1984, Solubility Parameters of Supercritical Fluids., *Ind. Chem. Eng. Process Des. Dev.* **23**, 344-348.

Angus, S., Armstrong, B., and de Reuck, K.M., (Eds), 1976, "International Thermodynamic Tables of the Fluid State - 3. Carbon Dioxide", Pergamon Press, Oxford.

Arnold, L.K., Choudhury, R.B.R. and Guzman, A., 1963, Solubilities of five triglycerides in aqueous ethanol, *JAOCS*, **40**, 33-34.

Arul, J., Boudreau, A., Makhlouf, J., Tardif, R. and Sahasrabudhe, M.R., 1987, Fractionation of Anhydrous Milk Fat by supercritical carbon dioxide., *J. Food Sci.*, **52** (5), 1231-1236.

Astin, D.K. and Watson, I.D., 1973, Thermodynamic Excess Functions of Regular Solutions According to Some Equations of State based on the Perturbed Hard Sphere Model, *Aust. J. Chem.*, **26** 2071-2076.

Bakalyar, S.R. and Spruce, B., 1983, *Technical Notes 5, Rheodyne Corporation*, 5.

Bailey, A.E., 1950, "Melting and Solidification of Fats", Interscience, New York.

Bamberger, T., Erickson, J.C., Cooney, C.L. and Kumar, S.K., 1988, Measurement and Model Prediction of Solubilities of pure fatty acids, pure triglycerides and mixtures of triglycerides in SC CO_2 *J. Chem. Eng. Data,* **33**(3), 327.

Barker, J.A., 1963, "Lattice Theories of the Liquid State", Pergamon Press, London.

Barton, A.F.M., 1983, "Handbook of Solubility Parameters", CRC Press, Boca Raton, Florida.

Billoni, N., Jose, J and Merlin, J.C., Solubility of Heavy Components in Supercritical CO_2 using directly coupled SFC-HPLC. Paper presented at the Symposium on Supercritical Fluids, Nice France, October 1988, 373-380.

Booth, H.S. and Bidwell, R.M., 1949, Solubility Measurement in the Critical Region, *Chem. Rev.*, **44**, 477-513.

Brennecke, J.F. and Eckert, C.A., 1989, Phase Equilibria for Supercritical Fluid Process Design, *AIChE. J.*, **35**(9), 1409-1427.

Brunetti, L., Daghetta, A., Fedeli, E., Kikic, I. and Zanderghi, L., 1989, Deacidification of Olive Oils by supercritical Carbon Dioxide, *JAOCS*, **66**(12), 209-217.

Calame J.P. and Steiner R., 19 June 1982, CO_2 Extraction in the Flavour and Perfumery Industry.*Chem. & Ind.*, 399-402.

Carnahan, N.F. and Starling, K.E., 1972, Intermolecular Repulsions and the Equation of State for Fluids, *AIChE. J.*, **18**(8), 1184-1189.

Chang, H. and Morrell, D.G., 1985, Solubilities of Methoxy-1-tetralone and methyl nitrobenzoate isomers and their mixtures in supercritical carbon dioxide., *J. Chem. Eng. Data*, **30** (1), 74-78.

Charbonnet, G.H. and Singleton, W.S., 1947, Thermal Properties of Fats and Oils. VI. Heat Capacity, Heats of Fusion and Transition and Entropy of Trilaurin, Trimyristin, Tripalmitin and Tristearin. *J. Am. Oil Chem. Soc.*, **5**, 140.

Chimowitz, E.H. and Pennisi, K.J., 1986, Process Synthesis Concepts for Supercritical Gas Extraction in the Cross-over Region., *AIChE J.*, **32** (10), 1665-1676.

Chrastil, J., 1982, Solubility of Solids and Liquids in Supercritical Gases., *J. Phys. Chem.*, **86** (15), 3016-3021.

Coppella, S.J. and Barton, P., 1985, Supercritical Carbon Dioxide Extraction of Lemon Oil., *Am. Chem. Soc. Div. Fuel Chem.*, **30** (3), 195.

Daubert, T.E., 1985, "Chemical Engineering Thermodynamics", McGraw-Hill, New York.

Debenedetti, P.G., 1984, "Diffusion in Supercritical Fluids", Ph.D. Thesis, Massachusetts Institute of Technology.

Diepen, G.A.M. and Scheffer, F.E.C., 1948, The Solubility of Naphthalene in Supercritical Ethylene. *J. Am. Chem. Soc.*, **70**, 4085-4089.

Dobbs, J.M., Wong, J.M. and Johnston, K.P., 1986, Nonpolar Co-Solvents for Solubility Enhancement in Supercritical Fluid Carbon Dioxide., *J. Chem. Eng. Data*, **31** (3), 303-308.

Dobbs, J.M., Wong, J.M., Lahiere, R.J. and Johnston, K.P., 1987, Modification of Supercritical Fluid Phase Behaviour Using Polar Cosolvents., *Ind. Eng. Chem. Res.*, **26**, 56-65.

Ely, J.F. and Baker, J.K., 1983, A Review of Supercritical Fluid Extraction., *NBS Technical Note 1070*, U.S. Dept. of Commerce/National Bureau of Standards.

Flory, P.J., 1970, Thermodynamics of Polymer Solutions, *Trans. Faraday Soc.*, **49**, 7.

Friedrich, J.P. and Pryde, E.H., 1984, Supercritical CO_2 Extraction of Lipid Bearing Materials and Characterisation of the Products., *JAOCS*, **61** (2), 223-228.

Guggenheim, E.A., 1952, "Mixtures", Clarendon Press, Oxford.

Gurdial, G.S., Wells, P.A., Foster, N.R. and Chaplin, R.P., 1989, *J. Supercrit. Fluids*, **2**(2&3), 85.

Hannay, J.B. and Hogarth, J., 1879, On the Solubility of Solids in Gases., *Proc. Royal Soc.*, **29** 324.

Hansen, P.C., 1985, Binary supercritical fluid enhancement factors for separation processes, Ph.D. Thesis, University of Illinois, Urbana-Campaign.

Haselow, J.S., Han, S.J., Greenkorn, R.A. and Chao, K.C., 1986, Chapter 7. in "Equations of State, Theory and Applications.", Chao and Robinson, Eds. A.C.S. Washington D.C.

Helling, R.K., 1986, "Oxidation Kinetics of Simple Compounds in Supercritical Water: Carbon Monoxide, Ammonia and Ethanol", Ph.D. Thesis, Massachusetts Institute of Technology.

Hicks Jr., P.J. and Prausnitz, J.M., 1981, Solubility of Acetone and Isopropyl Ether in Compressed Nitrogen, Methane and Carbon Dioxide., *J. Chem. Eng. Data*, **26**, 74-80.

Hildebrand, J.H. and Scott, R.L., 1962, "Regular Solutions", Prentice-Hall, New Jersey.

Huang, F-H., Meng-Hui, Lui, Lee, L.L. and Starling, K.E., 1985, An Accurate Equation of State for Carbon Dioxide, *J. Chem. Soc. Japan*, **18**(6), 490-496.

Ikushima, Y., Saito, N., Hatakeda, K., Ito, S., Asano, T. and Goto, T., 1985, Effects of Entrainers on the Extraction of Triglycerides with Supercritical Carbon Dioxide, *Chem. Let.*, 1789-1792.

Ikushima, Y., Goto, T. and Masahiko, A., 1987, Modified solubility parameter as an index to correlate solubility in supercritical fluids, *Bull. Chem. Soc. Jpn.*, **60**(11), 4154-4147.

Illingworth, D., 1990, New Zealand Dairy Research Institute, Personal Communication.

Johnston, K.P. and Eckert, C.A., 1981, An Analytical Carnahan-Starling-van der Waals Model for Solubility of Hydrocarbon Solids in Supercritical Fluids., *AIChE J.*, **27** (5), 773-779.

Johnston, K.P. and Kim, S., 1985., Effects of Supercritical Solvents on the Rates of Homogeneous Chemical Reactions., *Am. Chem. Soc. Div. Fuel. Chem.*, **30**(3), 24-25.

Johnston, K.P., Peck, D.G. and Kim, S., 1989, Modelling Supercritical Fluids: How predictive Is It?, *Ind. Eng. Chem. Res.*, **28**(8), 1115.

Johnston, K.P., Ziger, D.H. and Eckert, C.A., 1982, Solubilities of Hydrocarbon Solids in Supercritical Fluids. The Augmented van der Waals Treatment., *Ind. Eng. Chem. Fundam.*, **21**(3), 191.

Katz, D.L. and Kurata, F., 1940, *Ind. Engng. Chem.*, **32**, 817.

Kennedy, G.C., 1950, A Portion of the System Silica-Water., *Econ. Geol.*, **45**, 629.

King, M.B., Bott, T.R., Barr, M.J. and Mahmud, R.S., 1987, Equilibrium and Rate Data for the Extraction of Lipids using Compressed Carbon Dioxide., *Sep. Sci. & Tech.*, **22** (2&3), 1103-1120.

Konynenberg van, P.H. and Scott, R.L., 1980, Critical lines and phase equilibria in binary van der Waals mixtures, *Phil. Trans. Roy. Soc. (London)*, **298**, 495-540.

Kreyszig, E., 1983, "Advanced Engineering Mathematics", Wiley, New York

Krukonis, V.J., 1988, Supercritical Fluid Processing: Current Research and Operations. *Proc. Int. Symp. Supercrit. Fluids*, Nice, France, 541-560.

Krukonis, V.J. and Kurnik. R.T., 1985, Solubility of solid aromatic isomers in carbon dioxide., *J. Chem. Eng. Data*, **30**, 247-249.

Kumar, S.K., 1986, Precipitation polymerisation and partitions in supercritical fluids, Ph.D. Thesis, Massachusetts Institute of Technology.

Kumar, S.K. and Johnston, K.P., 1988, Modelling the Solubility of Solids in supercritical Fluids with Density as the Independent Variable, *J. Supercrit. Fluids*, **1**(1) 15-22.

Kumar, S.K., Suter, U.W. and Reid, R.C., 1987, A Statistical Mechanics Based Lattice Model Equation of State, *Ind. Eng. Chem. Res.*, **26**(12), 2532-2542.

Kurnik, R.T., Holla, S.J. and Reid, R.C., 1981, Solubility of Solids in Supercritical CO_2 and Ethylene., *J. Chem. Eng. Data*, **26** (1), 47-51.

Kurnik, R.T. and Reid, R.C.,1982, Solubility of Solid Mixtures in Supercritical Fluids., *Fluid Phase Equilibria*, **8**, 93-105.

Larsen, K.A. and King, M.L., 1986, Evaluation of SFE in the pharmaceutical industry, *Biotech. Prog.*, **2**(2), June, 73.

Laws, D.R.J., Bath, N.A., Ennis, C.S. and Wheldon, A.G., 1980, Hop Extraction with Carbon Dioxide, *U.S. Patent 4218,* 491.

Lee, B.I. and Kessler, M.G., 1975, A generalised thermodynamic correlation based on three parameter corresponding states, *AIChE. J.*, **21**(3), 510-528.

Lie Ken Jie, M.S.F., 1980, XIX. A quantitative treatment of saturated triglycerides by reversed phase high pressure liquid chromatography, *J. Chrom.*, **192**, 457.

Litchfield, C., 1972, "Analysis of Triglycerides", Academic Press, New York.

McHugh, M.A. and Krukonis, V.J., 1986, Supercritical Fluid Extraction: Principles and Practice., Butterworths, Boston., 69-78.

McHugh, M.A. and Paulaitis, M.E., 1980, Solid solubilities of naphthalene and biphenyl in supercritical Carbon dioxide., *J. Chem. Eng. Data*, **25** (4), 326-329.

MacGibbon, A., 1990, New Zealand Dairy Research Institute, Personal Communication.

Mathias, P.M., Copeman, T.W. and Prausnitz, J.M., 1986, Phase equilibrium for supercritical extraction of lemon flavours and palm oils with CO_2, *Fluid Phase Equilibria*, **29**, 545-554.

Matson, D.W., Norton, K.A and Smith, R.D., 1989, Making powders and films from supercritical fluid solutions, *Chemtech*, August, 480-486.

Messmore, H.E., 1943, *U.S. Patent 2420185*,

Modell, M., Gandet, G.G., Simson, M., Hong, G.T. and Biemann, K., 1982, Supercritical water: Testing reveals new process holds promise, *Solids Waste Management*, August.

Newport Scientific Inc., 1985, Operating Instructions 1600-B for 46-13411-2 Compressor, 7-9.

Niggli, P., 1912, *Z. Anorg, Allgem, Chem.*, **75**, 161.

Norris, R., 1977, "The physical properties of triacylglycerols in relation to milkfat", Ph.D. thesis, Massey University, New Zealand.

Paulaitis, M.E., Krukonis, V.J., Kurnik, R.T. and Reid, R.C., 1983, Supercritical Fluid Extraction.,*Rev. Chem. Eng.*, 1(2), 179-250.

Pearce, D.L. and Jordan, P.J., 1988, Supercritical fluid extraction: Prospects for application in New Zealand, Proceedings of the 1988 IPENZ Conference, New Plymouth, New Zealand, February. 183-193.

Pearce, D.L. and Jordan, P.J., 1989, A Sampling Technique for Supercritical Fluid Extract Solubility using HPLC, Paper presented to the Second International Conference on Fats, Oils and Waxes, Auckland, New Zealand, February. 1989.

Pennisi, K.J. and Chimowitz, E.H., 1986, Solubilities of Solid 1,10-Decanediol and a Solid Mixture of 1,10-Decanediol and Benzoic Acid in Supercritical Carbon Dioxide., *J. Chem. Eng. Data*, **31** (3), 285-288.

Peng, D-Y and Robinson, D.B., 1976, A New Two-Constant Equation of State.,*Ind. Eng. Chem. Fundam.*, **15**, 59.

Perry, E.S., Weber, W.H. and Daubert, B.F., 1949, *J. Am. Chem. Soc.*, **71**(11), 3720.

Prausnitz, J.M., 1965, National Bureau of Standards Technical Note 316.

Prausnitz, J.M., Lichtenthalter, R.N. and Gomes de Azevedo, E., 1986 "Molecular Thermodynamics of Fluid Phase Equilibria", Prentice-Hall, New Jersey.

Randall, L.G., 1982, The present status of dense (supercritical) gas extraction and dense gas chromatography: Impetus for DGC/MS development, *Sep. Sci. Tech.*, **17**(1), 1-118.

Redlich, O. and Kwong, J.N.S., 1949, On the Thermodynamics of Solutions V.,*Chem. Rev.*, **44**, 223.

Reid, R.C., Prausnitz, J.M. and Poling, B.E., 1987, "Properties of Gases and Liquids", McGraw-Hill, New York.

Schmid, P., 1973, Extraction and purification of lipids: II Why is Chloroform-Methanol such a good lipid solvent, *Physiol. Chem. & Physics*, **5**, 141-150.

Schmitt, W.J. and Reid, R.C., 1986, The Use of Entrainers in Modifying the Solubility of Phenanthrene and Benzoic Acid in Supercritical Carbon Dioxide and Ethane., *Fluid Phase Equilibria*, **32**, 77-99.

Shigley, J.E., 1986, "Mechanical Engineering Design", McGraw Hill, New York.

Stahl, E., Schilz., W., Schütz, E. and Willing, E., 1980, A Quick Method for the Microanalytical Evaluation of the Dissolving Power of Supercritical Gases. In "Extraction with Supercritical Gases" Schneider, G.M., Stahl, E. and Wilke, G., (eds), Verlag Chemie, Weinheim.

Swaan Arons de J., 1989, Fascinating Phenomena in the Critical Region, *Paper presented at 5th Int. Conf. on Fluid Props. and Phase Equil. for Chem. Proc. Des.*, Banff, Canada.

Swern, D.,1964, Chapter 3 in "Bailey's Industrial Oil and Fat Products", D. Swern (Ed) Interscience, New York.

Tan, Chung-Sung. and Weng, Jin-Yih., 1987, Solubility measurements of Naphthol isomers in supercritical CO_2 by a recycle technique., *Fluid Phase Equilibria*, **34** (1), 37-47.

Unger, K.K. and Roumeliotis, P., 1983, On-line high pressure extraction-HPLC: 1. Equipment design and operation variables, *J. Chromatogr.*, **282**, 519.

Valle del, J.M. and Aguilera, J.M., 1988, An improved equation for predicting the solubility of vegetable oils in supercritical CO_2. *Ind. & Eng. Chem. Res.*, **27**(8), 1551-1553.

Waals van der, J.D., 1873, Ph.D. Dissertation, Leiden, The Netherlands.

Weast, R.C., 1987, CRC Handbook of Chemistry and Physics, First Student Edition, CRC Press, Boca Raton, Florida, C-666 - C-682.

Williamson, A.G., 1967, "An Introduction to Non-Electrolyte Solutions", Oliver & Boyd, London.

Williams, D.F., 1981, Review Article No. 5. Extraction with Supercritical Gases.,*Chem. Eng. Sci.*, **36**(11), 1769-2788.

Willson, R.C., 1987, "Fermentation Product Recovery by Supercritical Fluid Extraction: Microbiological and Phase Equilibrium Aspects" Ph.D. Thesis, Massachusetts Institute of Technology.

Wong, J.M. and Johnston, K.P.,1986, Solubilization of Biomolecules in Carbon Dioxide Based Supercritical Fluids. *Biotech. Prog.*, **2** (1).

Wu, A.H., Stammer, A. and Prausnitz, J.M., 1988, Extraction of Fatty-Acid Methyl Esters with Supercritical Carbon Dioxide., *Proceedings of the International Symposium on Supercritical Fluids, Nice France*, 107-114.

Zhuze, T.P., 1959, *Vesnik Akad. Nauk. S.S.S.R.*, **29**, 47.

Ziger, D.H. and Eckert, C.A., 1983, Correlation and Prediction of Solid-Supercritical Fluid Phase Equilibria., *Ind. Eng. Chem. Process Des. Dev.*, **22**(4), 582.

Zosel, K., 1978, Separation with Supercritical Gases: Practical Applications, *Angew. Chem. Int. Ed.*, **17**(10), 702-709.

Appendices

A 1

Equipment Drawings

The following Autoclave Engineers' valves and fittings were used in the construction of the equipment.

Valves:	10V2071, 10V2072, 10V2082 Regulating and Shut-off valves, 10VRMM Micrometering valve,	
Fittings:	SL2200	Elbows,
	ST2220	Tees,
	SX2222	Cross,
	SS2600	Bursting Disc Unit,
	SLF2200-5/10 and -10/35 Filters (on the CO_2 inlet and the system recycle lines respectively)	
	SWB2200	Ball Check Valve,
Tubing:	15-051	316 SS Cold Drawn Seamless Tube 3.18 mm OD x 1.57 mm ID.

In addition, the following valves and hardware were used,

Rheodyne Corp. (Cotati, California, U.S.A.) 7000 6-port sample valves with Rheodyne 10, 20 and 100µl sample loops,

2 Swagelok (Solon, Ohio, U.S.A.) 4R3A1 Relief valves. One was placed between the supply cylinder and the check valve (this valve was fitted with a 750-1500 psi spring) and one was placed on the inlet side of the pressure cell (this one was fitted with a 4000-5000 psi spring).

A Tescom (Elk River, Minnesota, U.S.A.) 26-1722-24 Back Pressure Regulator.

The CO_2 purge line was fitted with a Swagelok SS-4F-7 7µm pore filter.

A Gapmeter (Croydon, England) flow measuring device with a C6 tube and a hollow Duralumin float (100-2 000 $cm^3.min^{-1}$ air at NTP)

3D Instruments Inc. (Huntington Beach, California, U.S.A.) type 25504-39B11-ISOD pressure gauges (range 0 - 100 MPa)

A -10 to 110°C mercury-in-glass thermometer graduated in 0.1°C.

The following drawings were used by the workshop during the construction of the equipment.

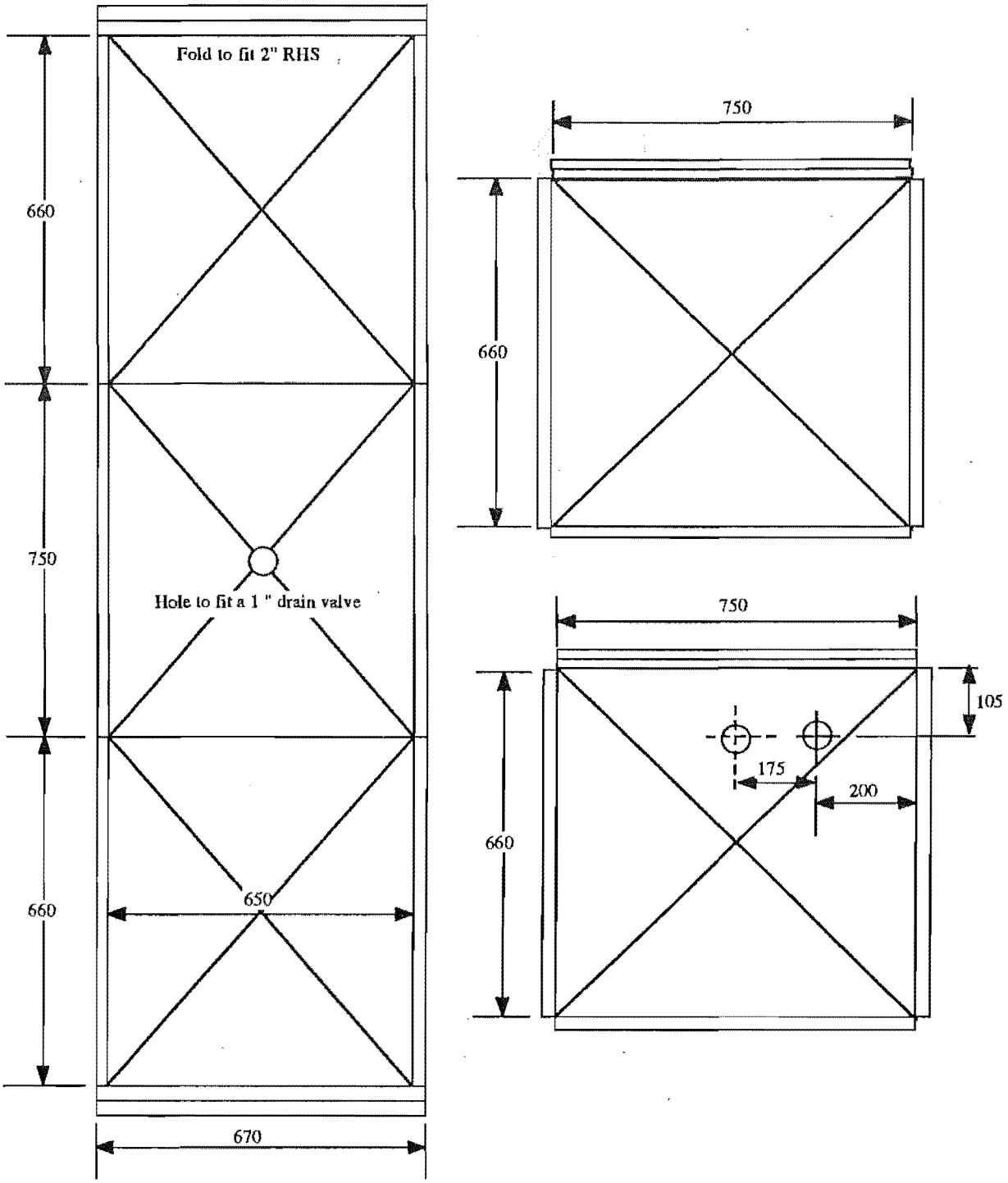

Figure A1.1 Main Water Bath

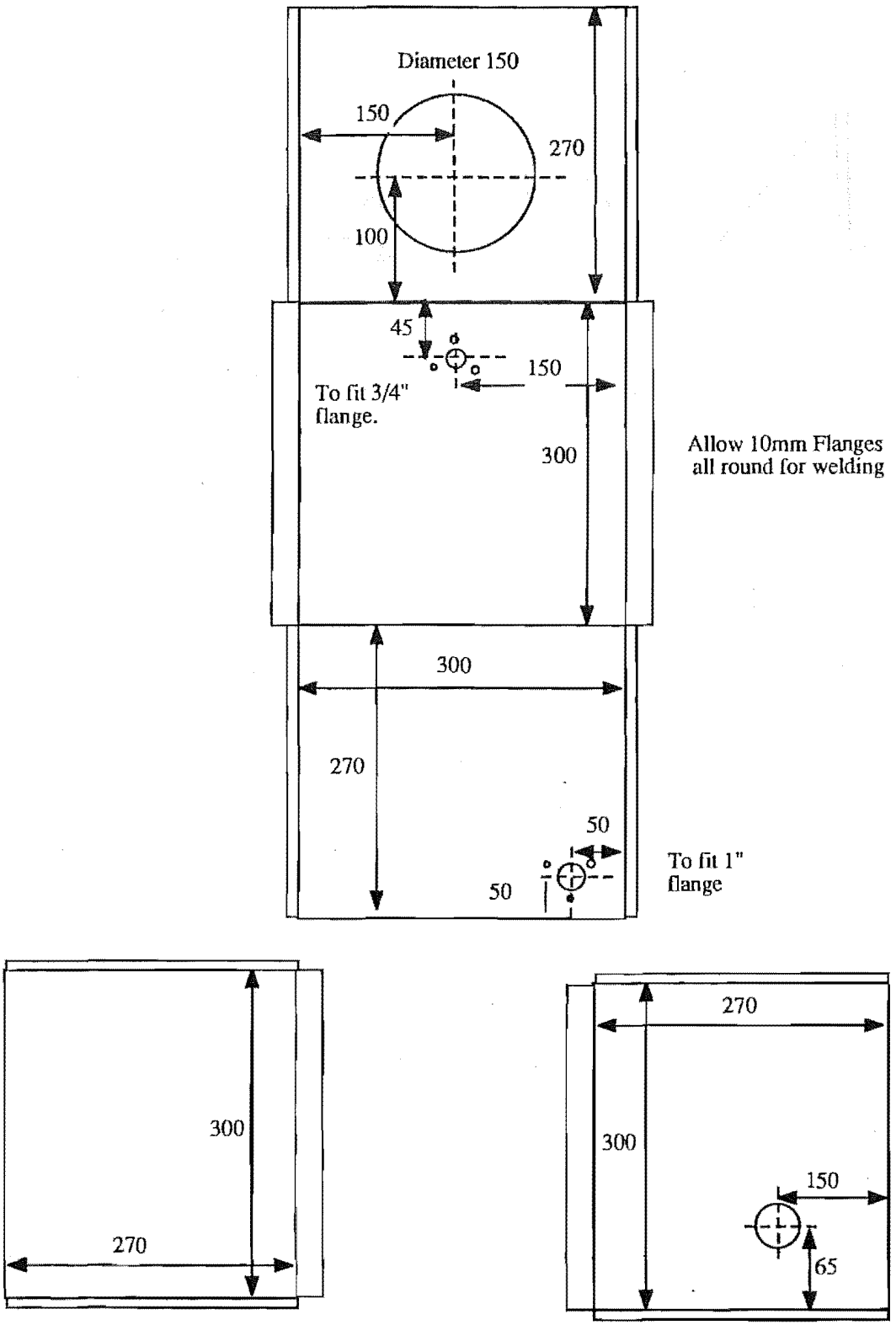

Figure A1.2 Workshop Drawing of Compressor Water Bath

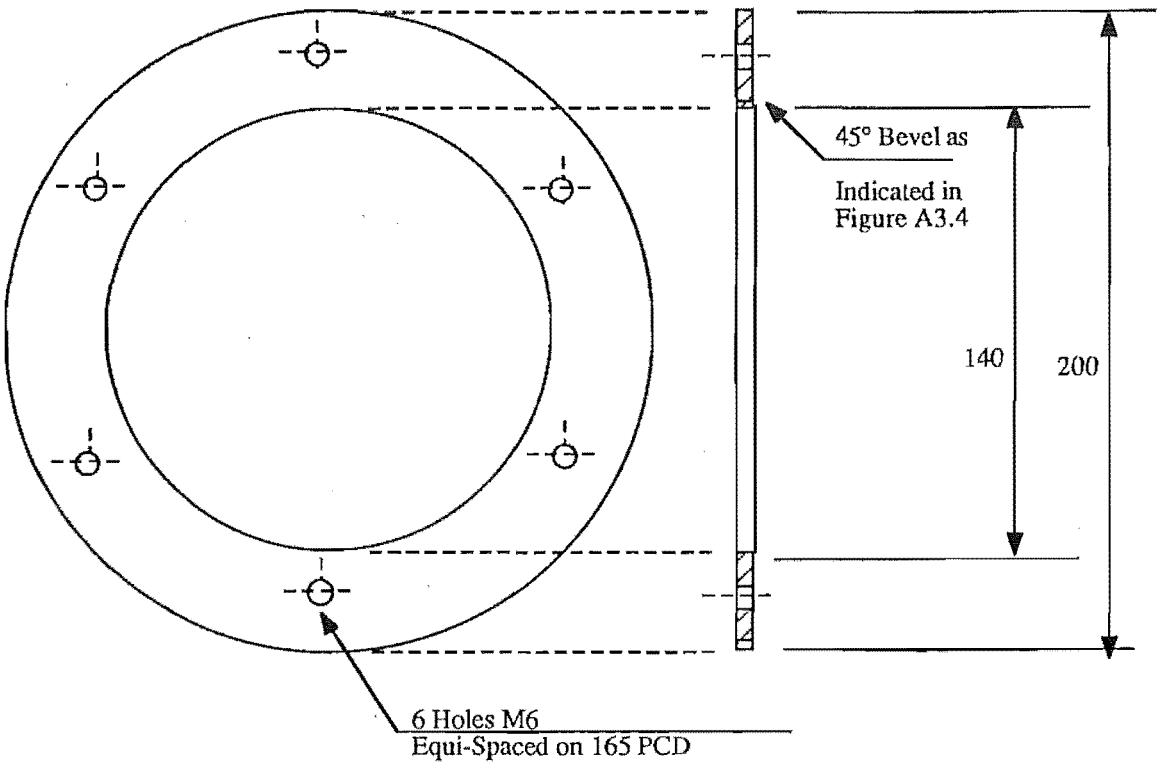

MATERIAL; Brass

SCALE: 1 : 2

Figure A1.3 Ring for Head Compressor Seal

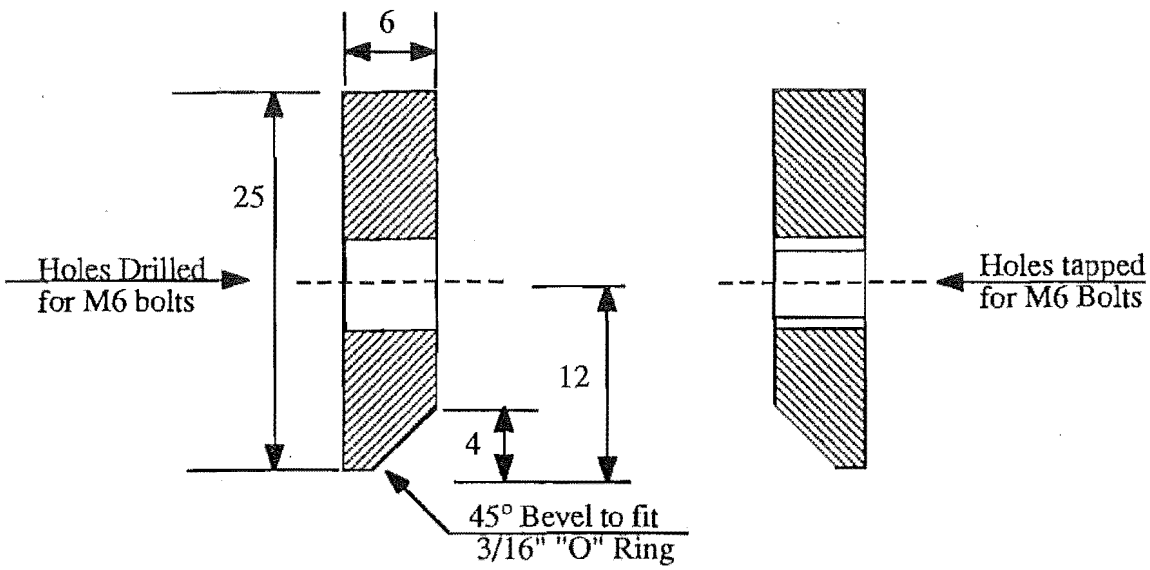

MATERIAL: Brass

SCALE: 2:1

Figure A1.4 Compressor Head Seal Details

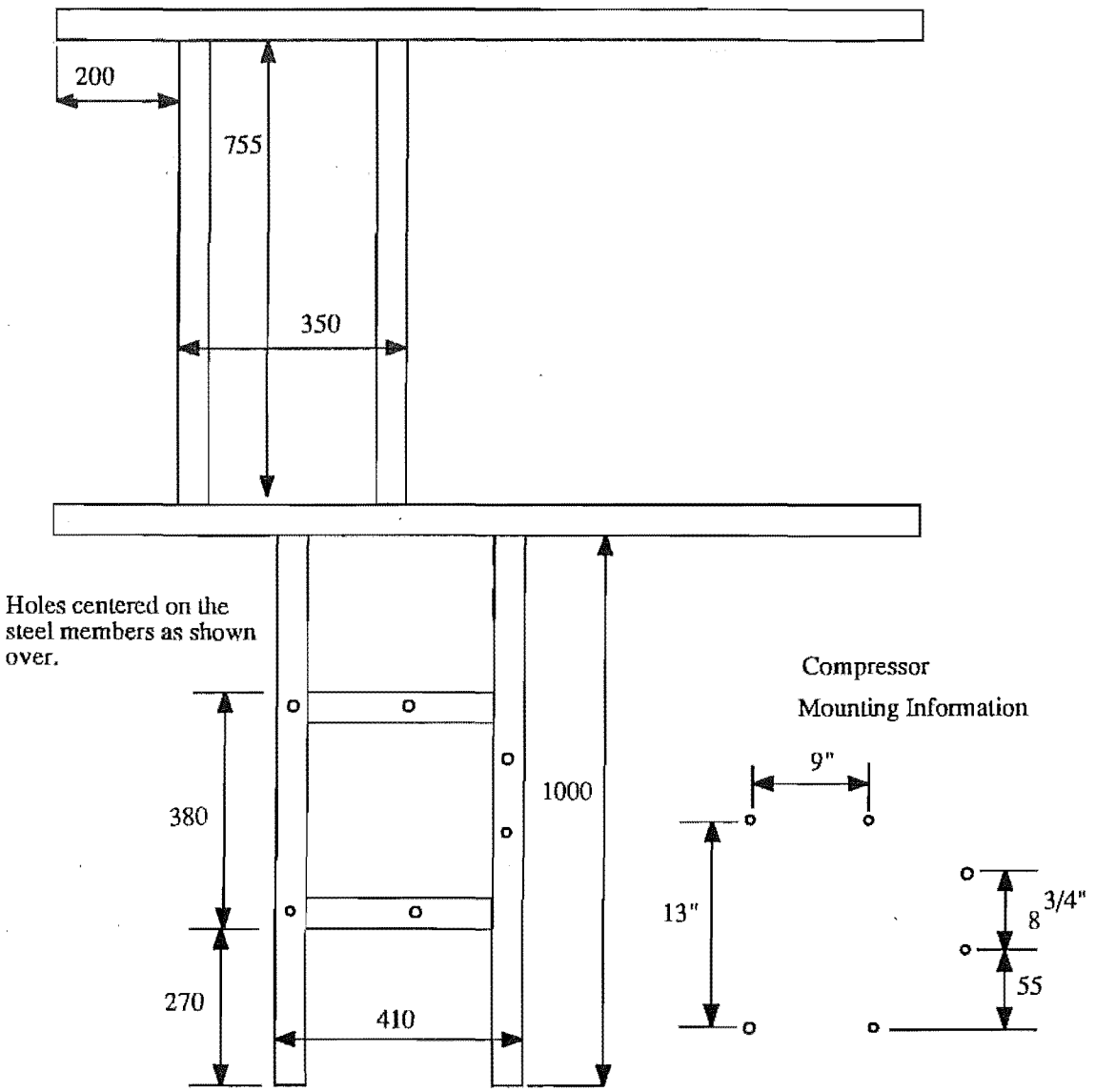

Figure A1.5 Workshop Drawing of Support Frame (Plan)

Main Frame and Tank Support: Side 1.

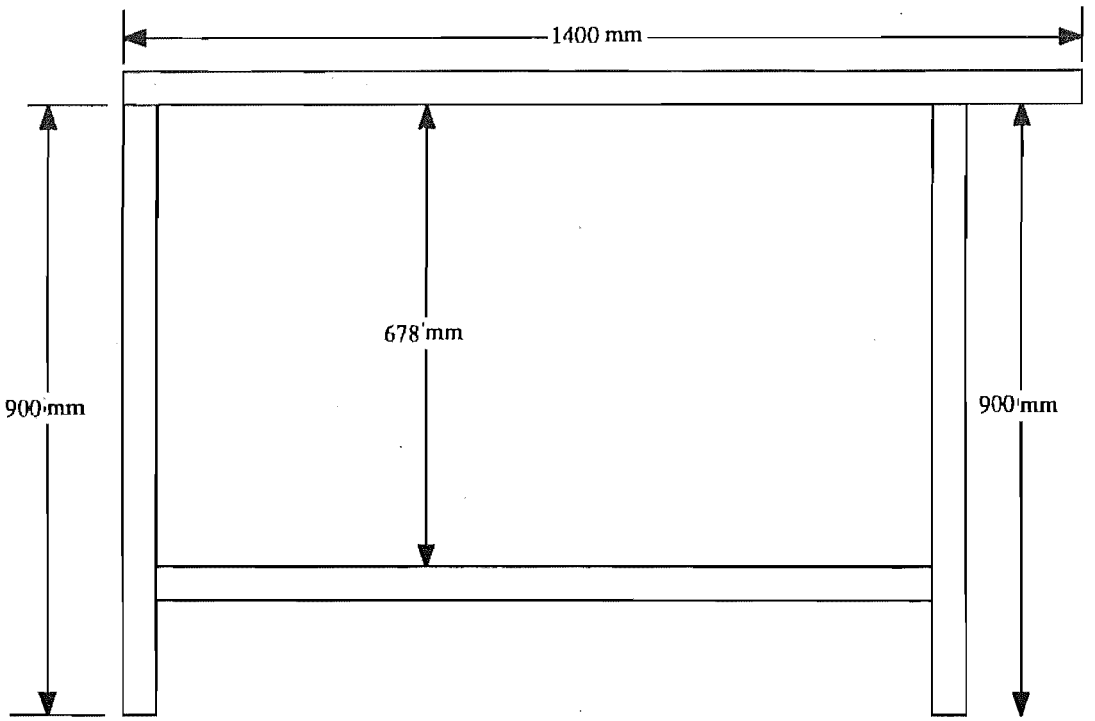

Material: 2" x 2" Mild Steel RHS

Scale 1:10

Figure A1.6 Workshop Drawing of Support Frame (Elevation 1)

Main Frame and Tank Support; Side 2.

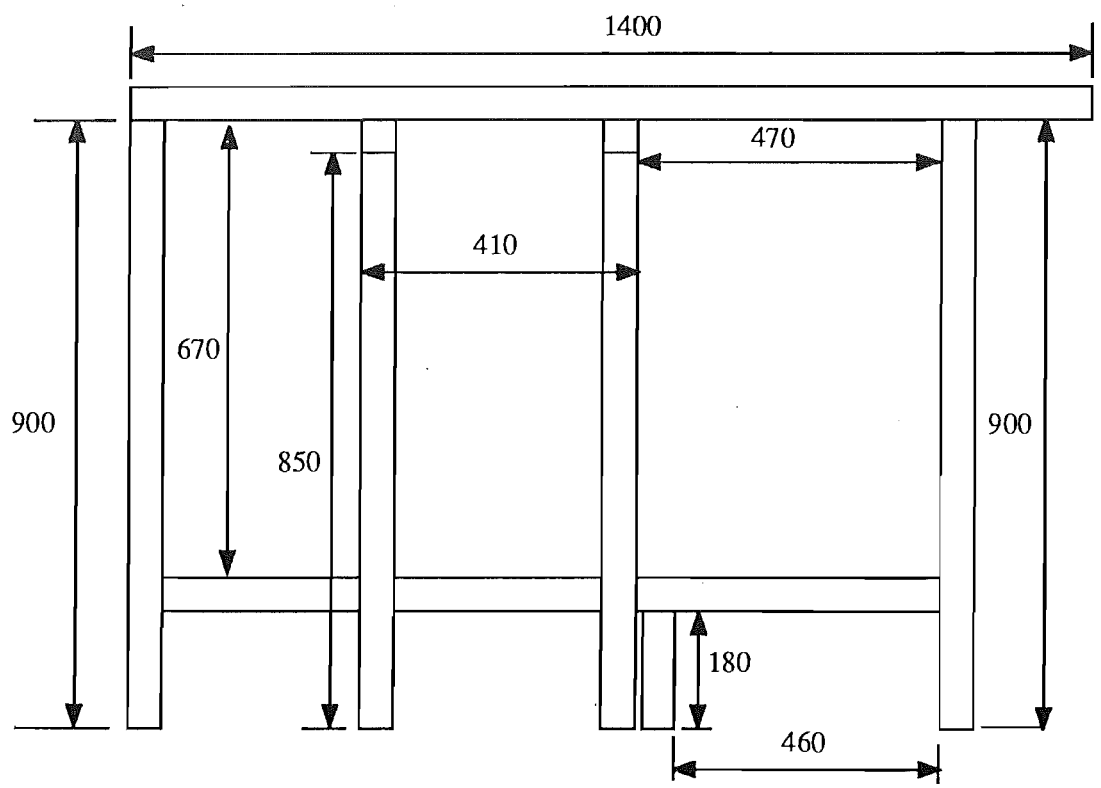

Figure A1.7 Workshop Drawing of Support Frame (Elevation 2)

Arrow indicates direction of elevation.
A - F, indicates continuation of line between elevations
1-11, valve number (see figure 3.7)

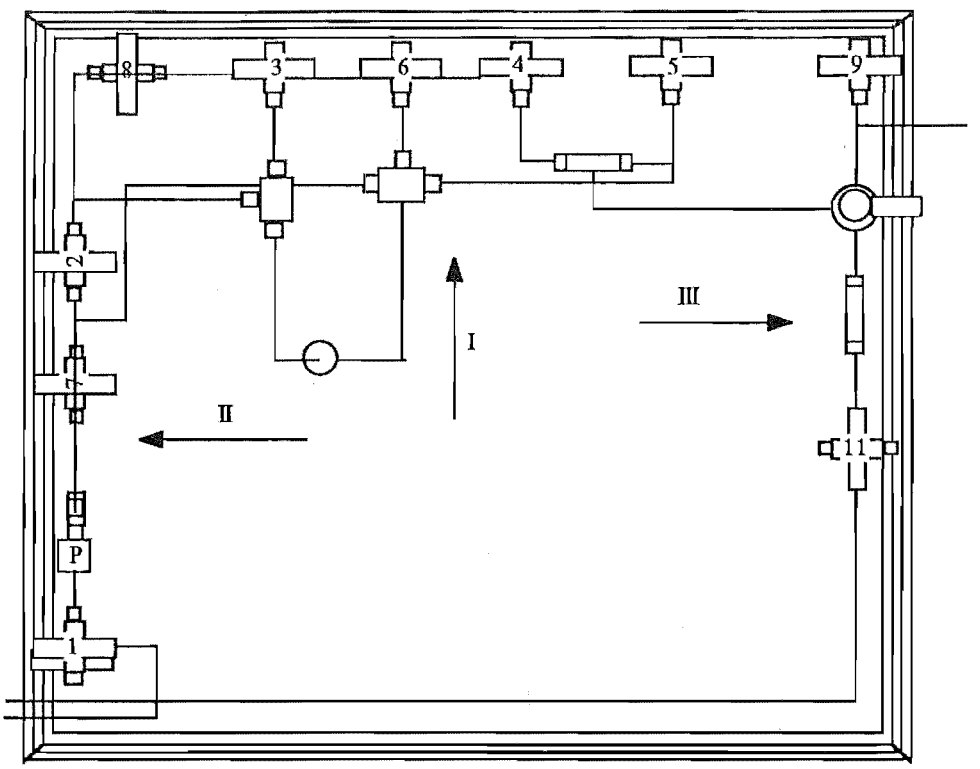

Figure A1.8a. Plan of Valve Layout

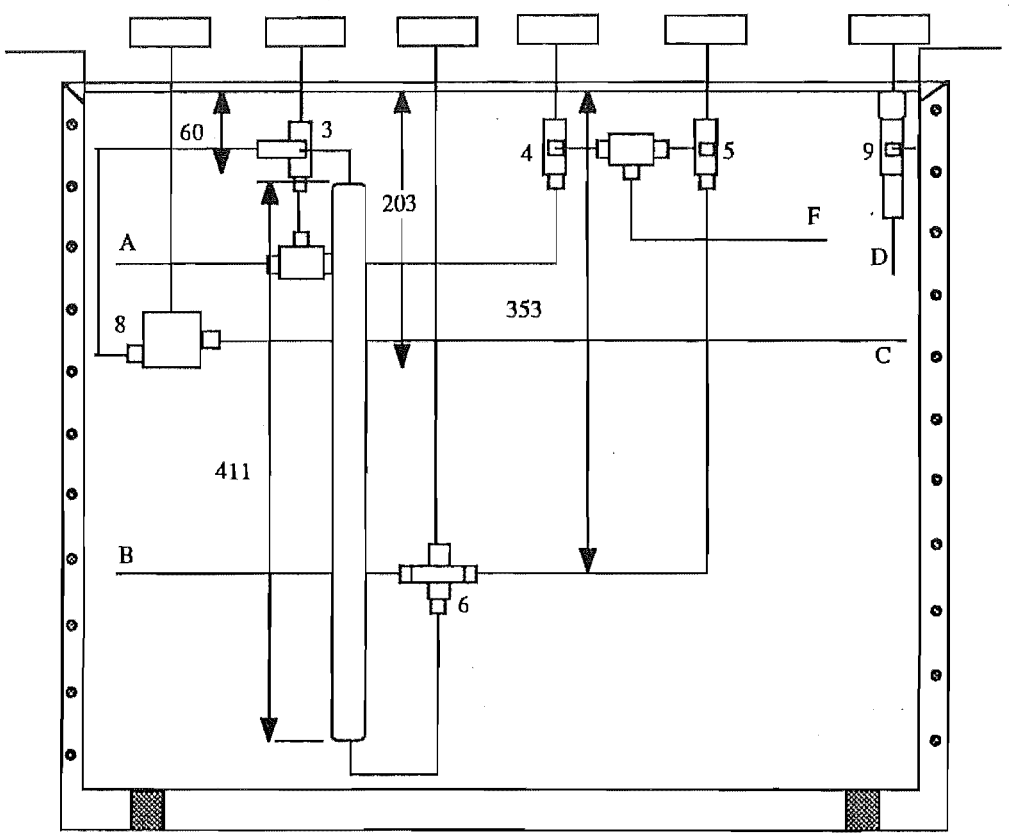

Figure A1.8b Elevation I

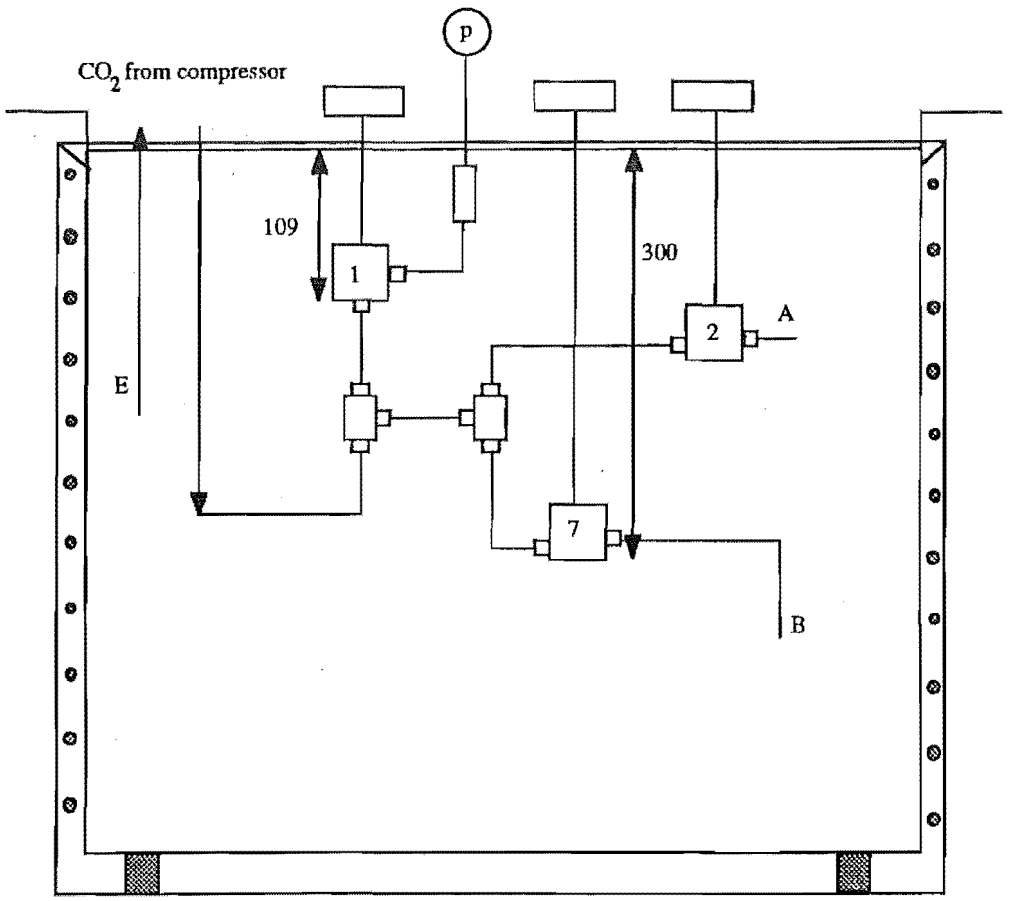

Figure A1.8c Elevation II

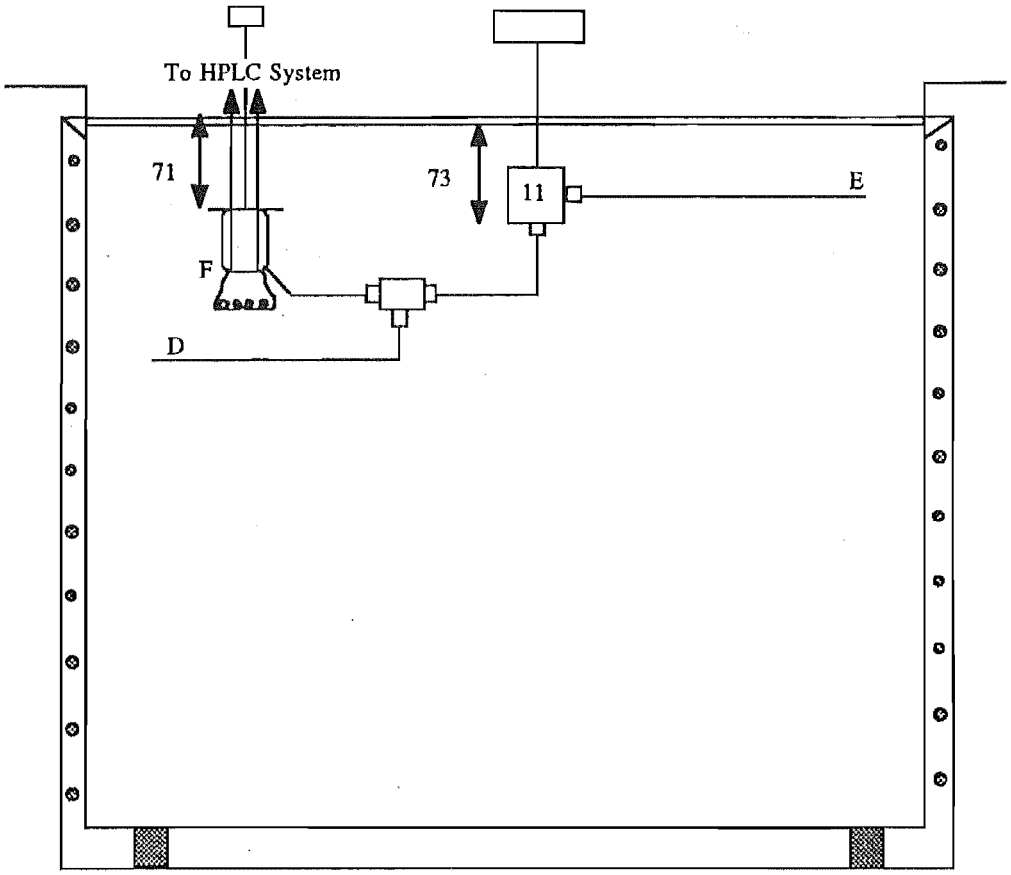

Figure A1.8d Elevation III

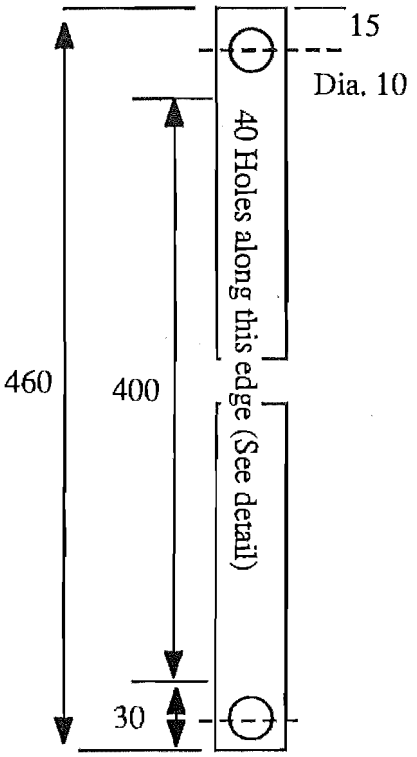

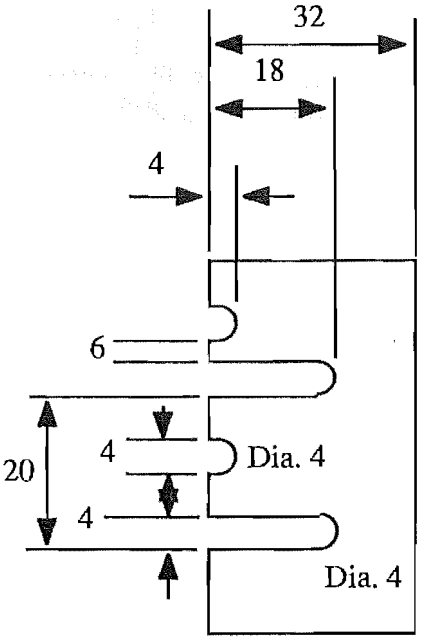

20 of each type of
hole. Spaced as indicated.

Material: 1.25" * 0.325 " Brass Flat
4 Off.
These pieces are the corners of a
650*550 rectangle. This cage fits outside
the valve cage (fig A3.8)

Figure A1.9 Support Frame for Heating Coils

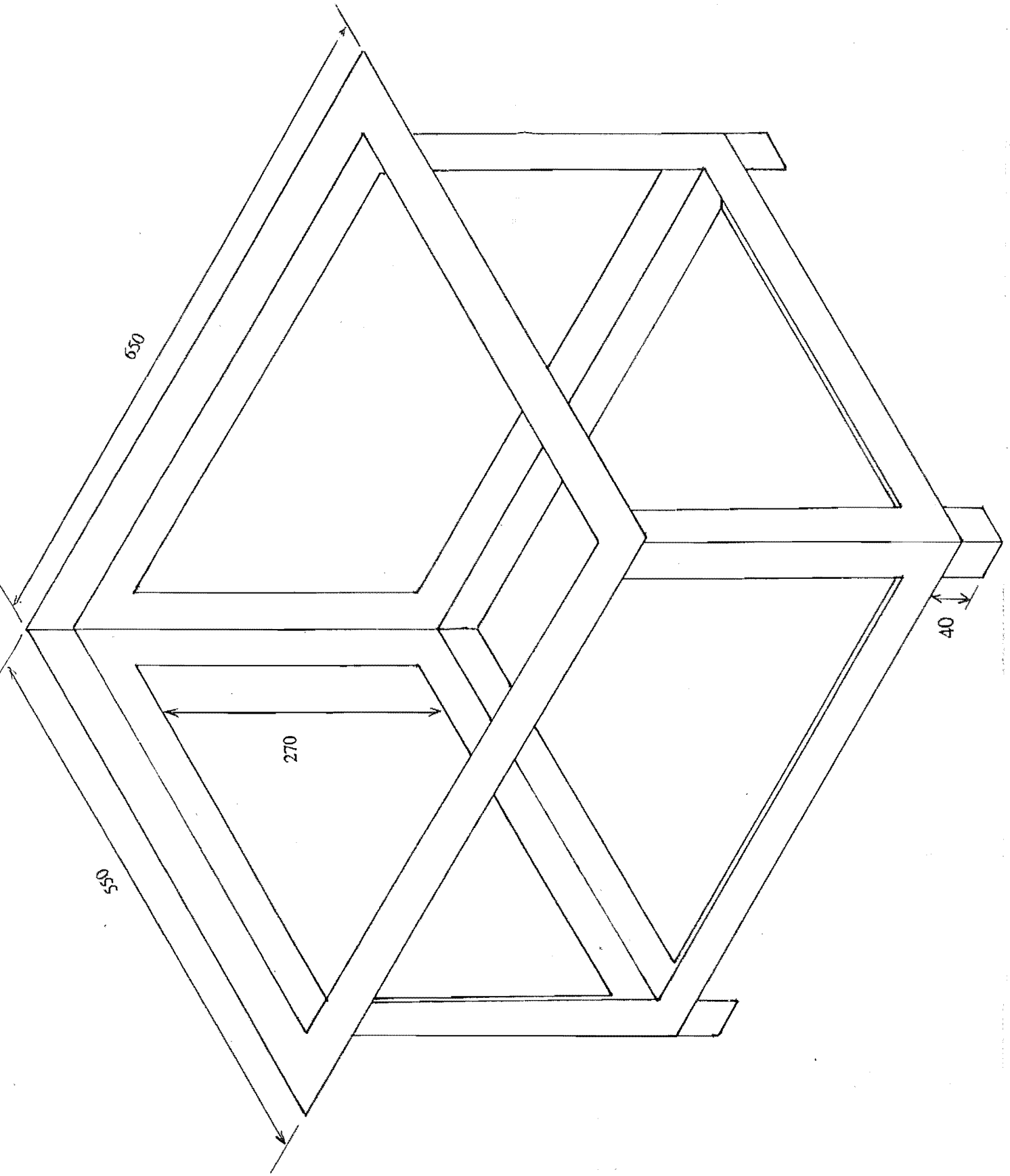

Figure A1.10 Isometric Drawing of Valve Cage

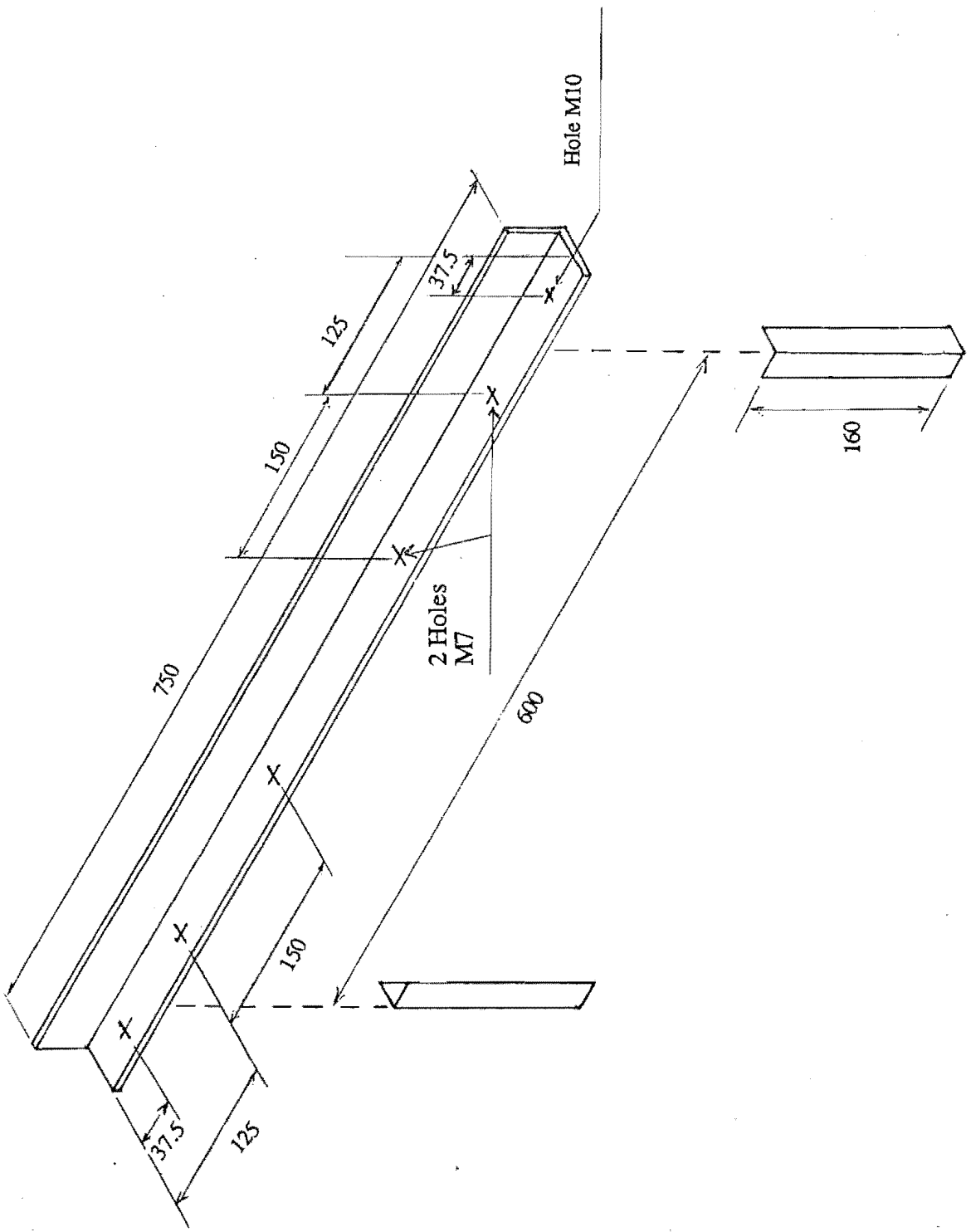

Figure A1.11 Isometric Drawing of Valve Cage Support

A 2

Vessel Designs

A2.1 700 Bar Pressure Vessel

A2.1.1 Material Selection

Stainless steel was chosen as the construction material because of strength and hygiene. Dr J. Smaill of the Mechanical Engineering Department was consulted and suggested that in the construction of a pressure vessel, a duplex, ferritic, austenitic stainless steel was required. The local supplier, Mico Wakefield, was approached on the availability of such a stainless steel. They recommended the brand, Avesta, and the steel Avesta 2205. This steel has the following Physical and Mechanical properties.

Table A2.1 Characteristic Temperatures of Avesta 2205

	Temp °C
Solidification Range	1445-1385
Scaling Temperature in Air	1000
Sigma Phase Formation	700-900
Carbide Precipitation	450-800
"475-embrittlement"	350-525
Hot Forming	1150-950
Quench Annealing	1050 air/water
Stress Relief Annealing	1020-1070
Pressure Vessel Application	(-10)-300

Table A2.2 Physical Properties of Avesta 2205 at 20°C.

Density	g/cm^3	7.8
Modulus of Elasticity	kN/mm^2	200
Linear Expansion 20-100°C	$x\ 10^{-6}$ /°C	13
Thermal Conductivity	W/m°C	20
Heat Capacity	J/kg°C	450
Electrical Resistivity	nΩm	850

Table A2.3 Mechanical Properties of Avesta 2205 at 20°C

Plate, max 30 mm. Transverse specimens.

Yield strength	$R_{p0.2}$	N/mm^2	min	480
Tensile strength	R_m	N/mm^2	min	680
Elongation	A_5	%	min	25
Hardness	HB		max	290
Impact Value	KCV	J/cm^2	min	100

Table A2.4 Tensile Properties of Avesta 2205 at elevated temperatures

Plate max 30 mm. Transverse specimens.

	50°C	100°C	200°C	300°C
$R_{p0.2}$ min	400	360	310	280
R_m min	660	620	570	560

The 0.2% proof stress ($R_{p0.2}$) value of 360 N/mm^2 at 100°C was chosen to be the design limit of the pressure vessel.

A2.1.2 Wall Thickness

The chosen volume for the cell was 300 cm^3. The pressure vessel internal diameter was chosen to be 46 mm, and the depth of the cavity was then set at 168 mm. The maximum

design pressure was taken to be 10 000 psi, or 68.9 MPa. To determine the wall thickness, the Maximum Shear Stress Failure theory was used (Shigley, 1986).

$$q_{max} = \frac{\text{Yield Stress}}{2} \qquad \text{(A2.1)}$$

Yield Stress $= 360\ N/mm^2$

$\therefore q_{max} = 180\ N/mm^2.$

Now for a thick walled cylinder,

$$q_{max} = P\left[\frac{a^2}{a^2 - b^2}\right] \qquad \text{(A2.2)}$$

where a = the vessel O.D.,
b = the vessel I.D and
P = the design pressure ($70\ N/mm^2$).

$$\text{therefore } 180 = 70\left[\frac{1}{1-d^2}\right] \qquad \text{(A2.3)}$$

where $d = \frac{b}{a}$

$\therefore d^2 = 0.611 \Rightarrow d = 0.7817$

Hence, $a = 1.28\ b \Rightarrow a = 58.84$ mm, a 6 mm wall thickness.

It would be prudent to allow for a safety factor of at least 2 in the calculations, and so the minimum wall thickness can be taken to be at least 12 mm. This gives an O.D. of at least 70 mm. However, this O.D. does not allow for any means of mounting the pressure vessel. The next largest size billet that was available has an O.D. of 101.6 mm (4 inches). It was decided to use this O.D., thus allowing bolting holes to be drilled into the outside of the cell wall, without weakening the pressure vessel. It is now possible to estimate the maximum pressure that the pressure vessel will hold;

$d = \frac{b}{a} = 0.4528.$

So $180\ (1-d^2) = P$

$P = 0.795 \times 180$

$P = 143.1\ N/mm^2$, over twice the design pressure.

The general shape of the closure is for a cylindrical vessel body and a threaded plug closure. Figure A2.2 shows a dimensioned drawing of the pressure vessel.

A2.1.3. Thread Design.

A2.1.3.1 Pressure Load.

The plug diameter was set to be 72 mm, with an exposed face of 65 mm diameter. The worst possible case for the thread is if the gasket fails and the threaded closure has to hold the pressure in the cell. The pressure of the system is 70 MPa, and the exposed cross-sectional area of the plug is 3318.3 mm^2. This gives a pressure loading of 228.4kN.

A2.1.3.2 Bolting Load.

The bolting load upon the thread depends on the load required to seat the gasket. The gasket chosen was from Advanced Products Co.(North Haven, Connecticut, U.S.A.) and had a part number EVI-002076-07-07-2-NPA. This is a V-ring gasket of free height 0.094", the circumference is 6.54". The manufacturer seating load is stated to be 400 lb/in circumference. This gives a seating load of 2613.81 lb force or 11.6kN.

The torque required to produce this seating load is found from (Shigley, 1986)

$$T=KF_id \qquad \text{(A2.4)}$$

where T = the required torque
K = a material specific constant (0.2 for Stainless Steels)
F_i = the applied force (11.6kN)
d = the face diameter in mm (65)

From this relation the torque required was estimated to be 150 Nm (113 ft.lb force)

The bolting load combined with the pressure load gives a maximum thread loading of 238741 N.

A2.1.3.3 Thread Choice

The thread chosen was an ISO thread with a 60° angle and a 6 mm pitch (BS3643(I) recommended the pitch and angle for this diameter 'bolt').

For a perfectly triangular thread, the thread depth will be 5.2 mm. To allow for rounding during the thread manufacture, a depth of 4 mm was assumed. Shigley suggests that the thread will shear along the minor diameter of 65.5 mm. The root circumference through one turn of the thread is therefore (Kreyszig, 1983) 209.2 mm giving an effective area of shear on a single thread of 966.5 mm^2. The shear stress is then defined as the force per unit area.

In this case it is 247 $N.mm^{-2}$. The design stress of the material is 360 $N.mm^{-2}$, therefore the thread will hold the applied pressure. The threaded length was chosen to be 72 mm (12 threads). A dimensioned drawing of the threaded closure is found in figure A2.3

A2.1.4 Pressure Relief

To allow for fluid to escape (in the event of a gasket failure), an 8 mm hole is drilled in the side of the vessel, between the gasket and the end of the thread (see figure A2.4). An exploded view of the pressure vessel, threaded closure, sealing plate and slip ring is presented in figure A2.1.

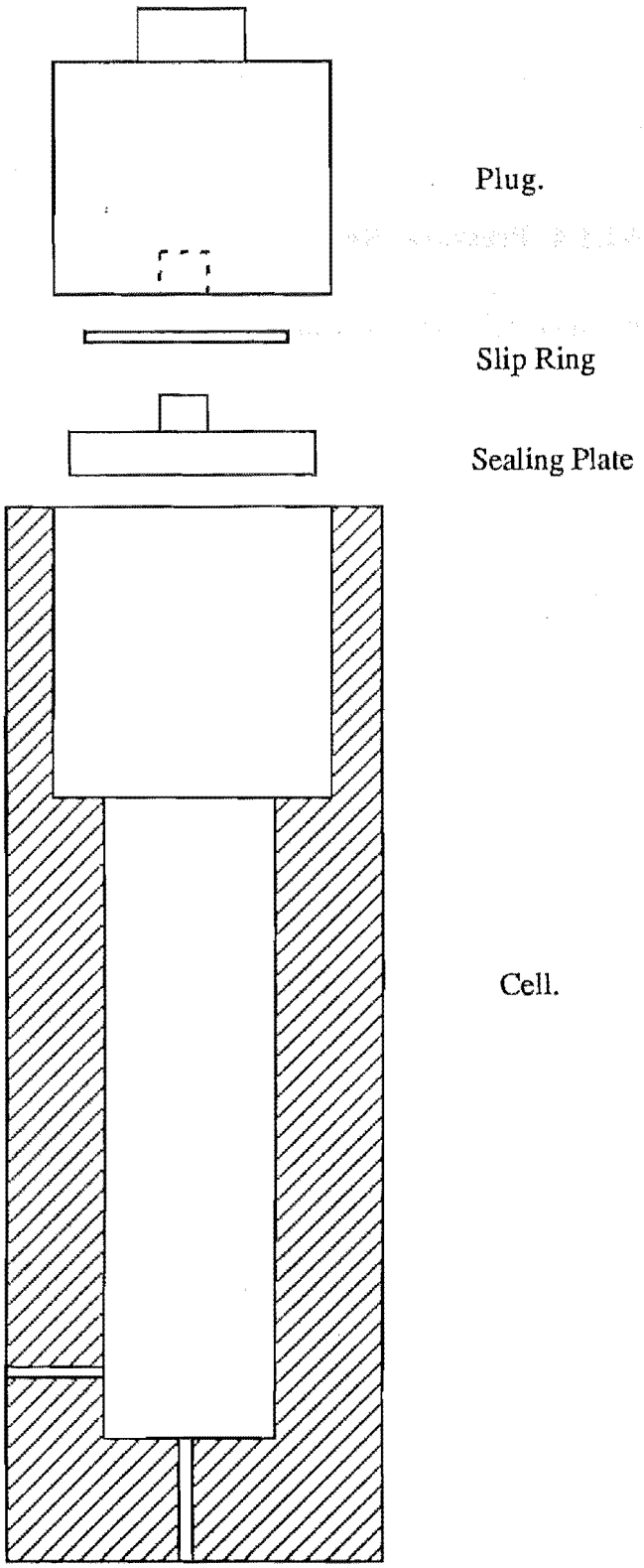

Figure A2.1 Exploded View of the 700 Bar Cell

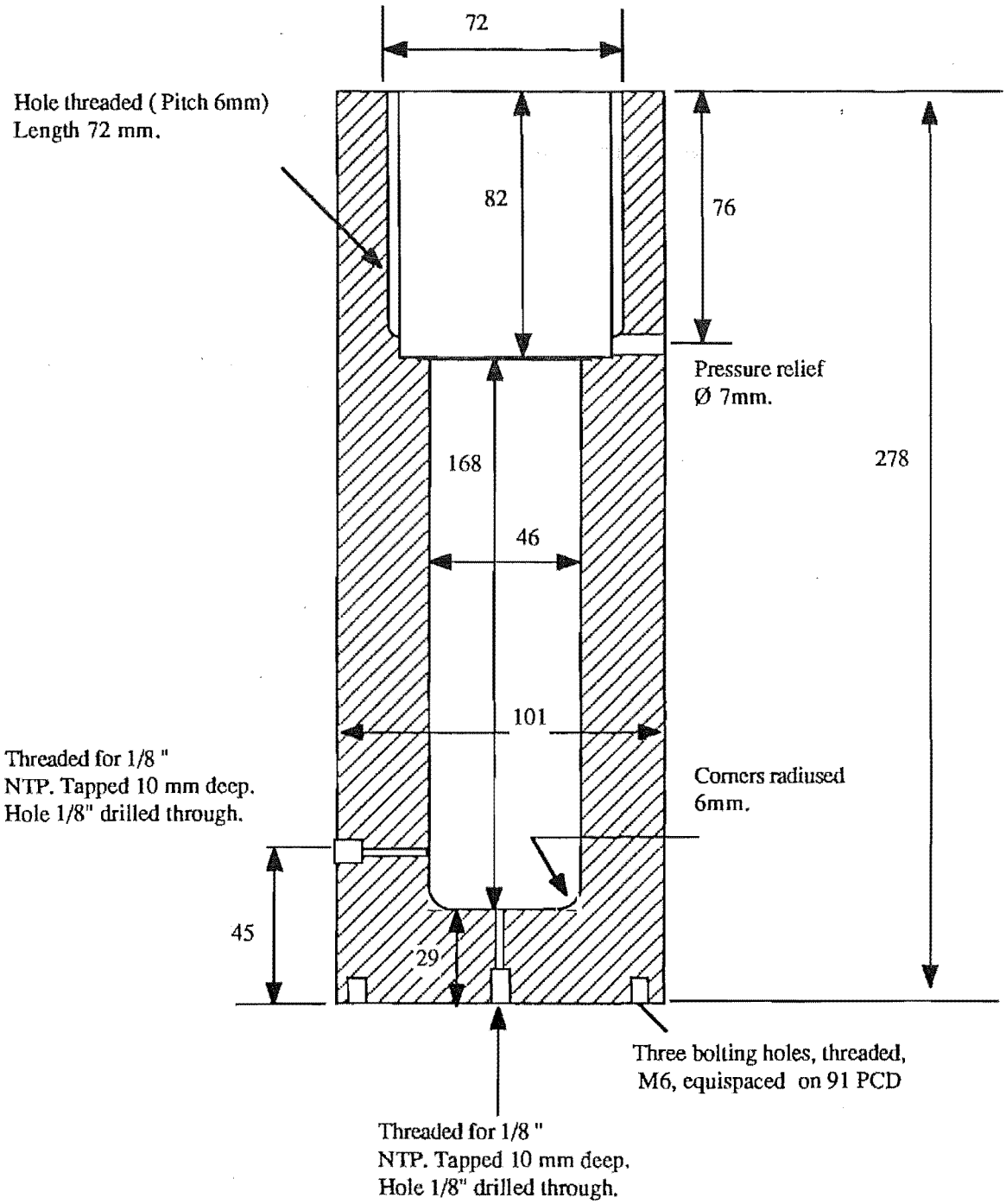

Figure A2.2 Workshop Drawing of the 700 Bar Cell

Gasket and Thread Details Scale 4:1.

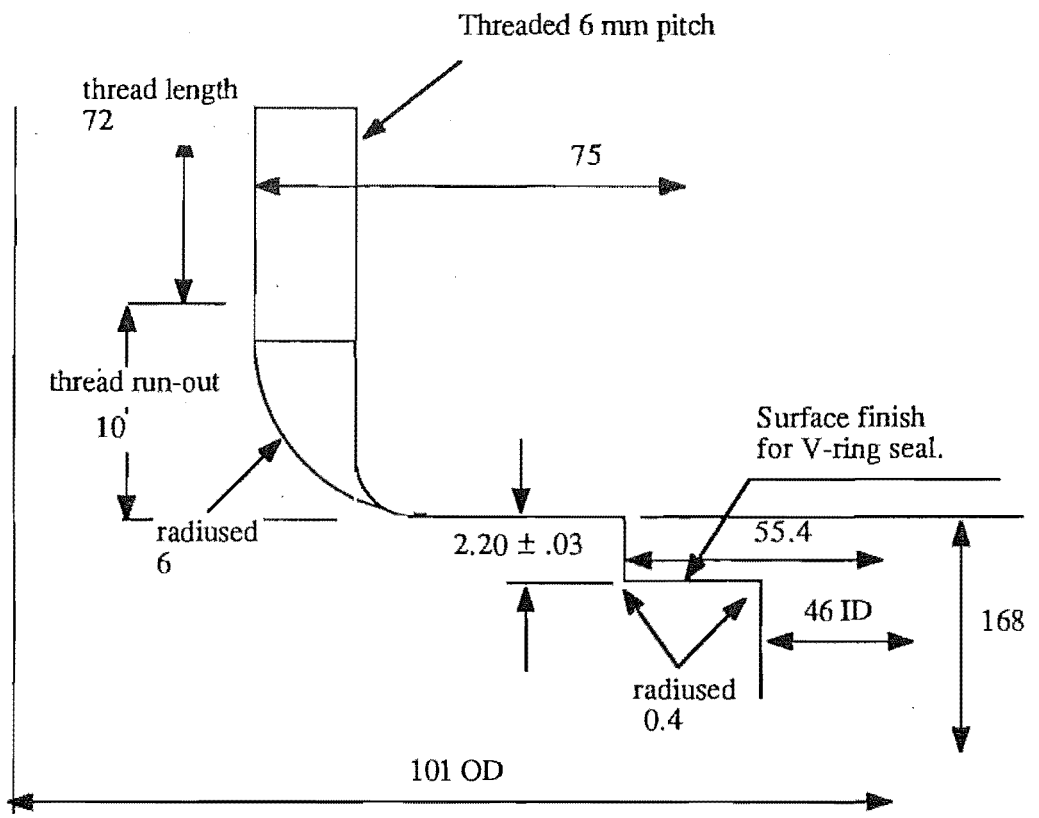

Figure A2.3 Workshop Drawing of the 700 Bar Cell. Thread and Gasket Details

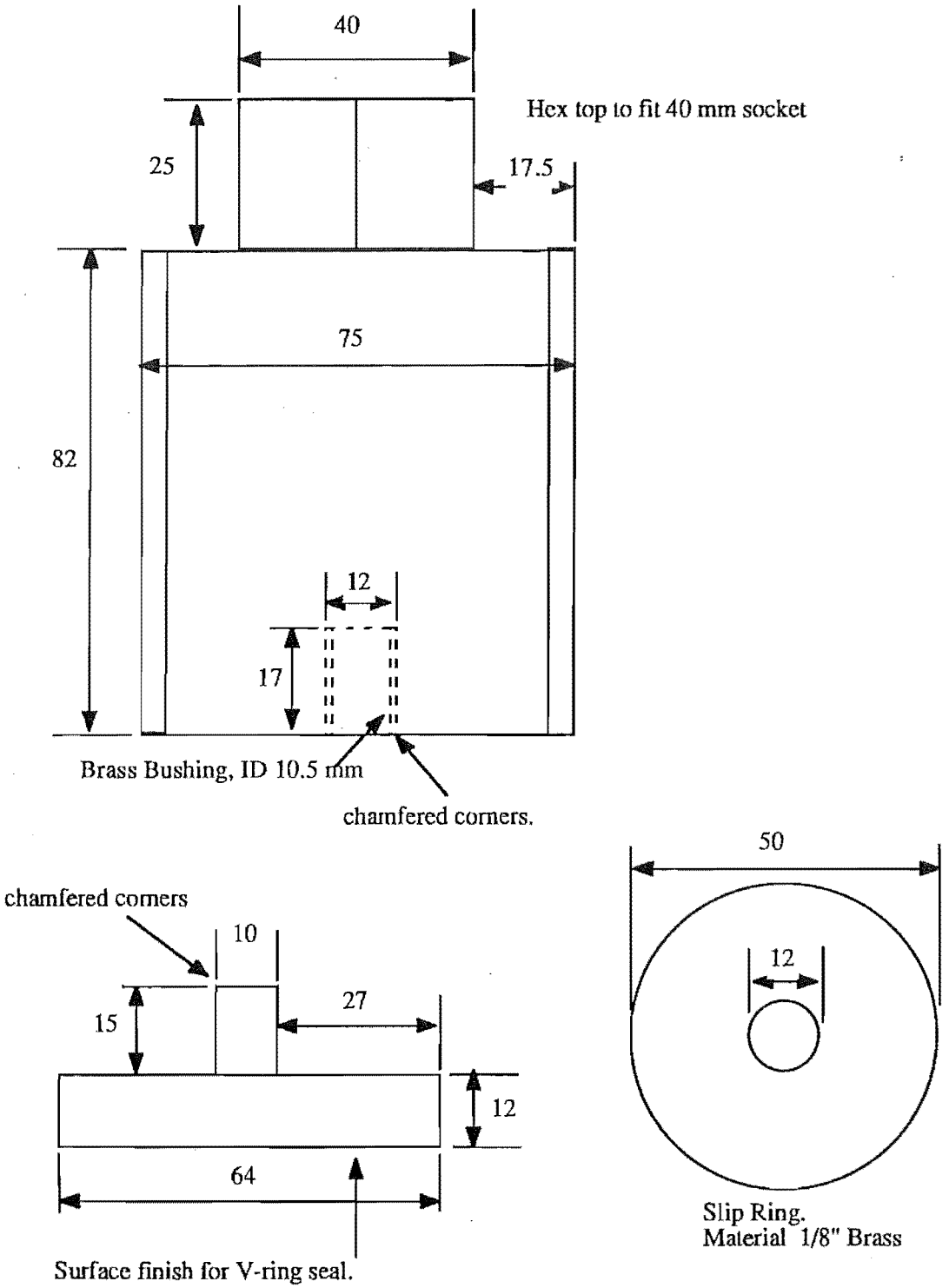

Figure A2.4 Workshop Drawing of the 700 Bar Cell. Plug and Seal Details

A2.2 Liquid Sample Holder

Workshop drawings for the liquid sample holder are presented in figures A2.5 to A2.8.

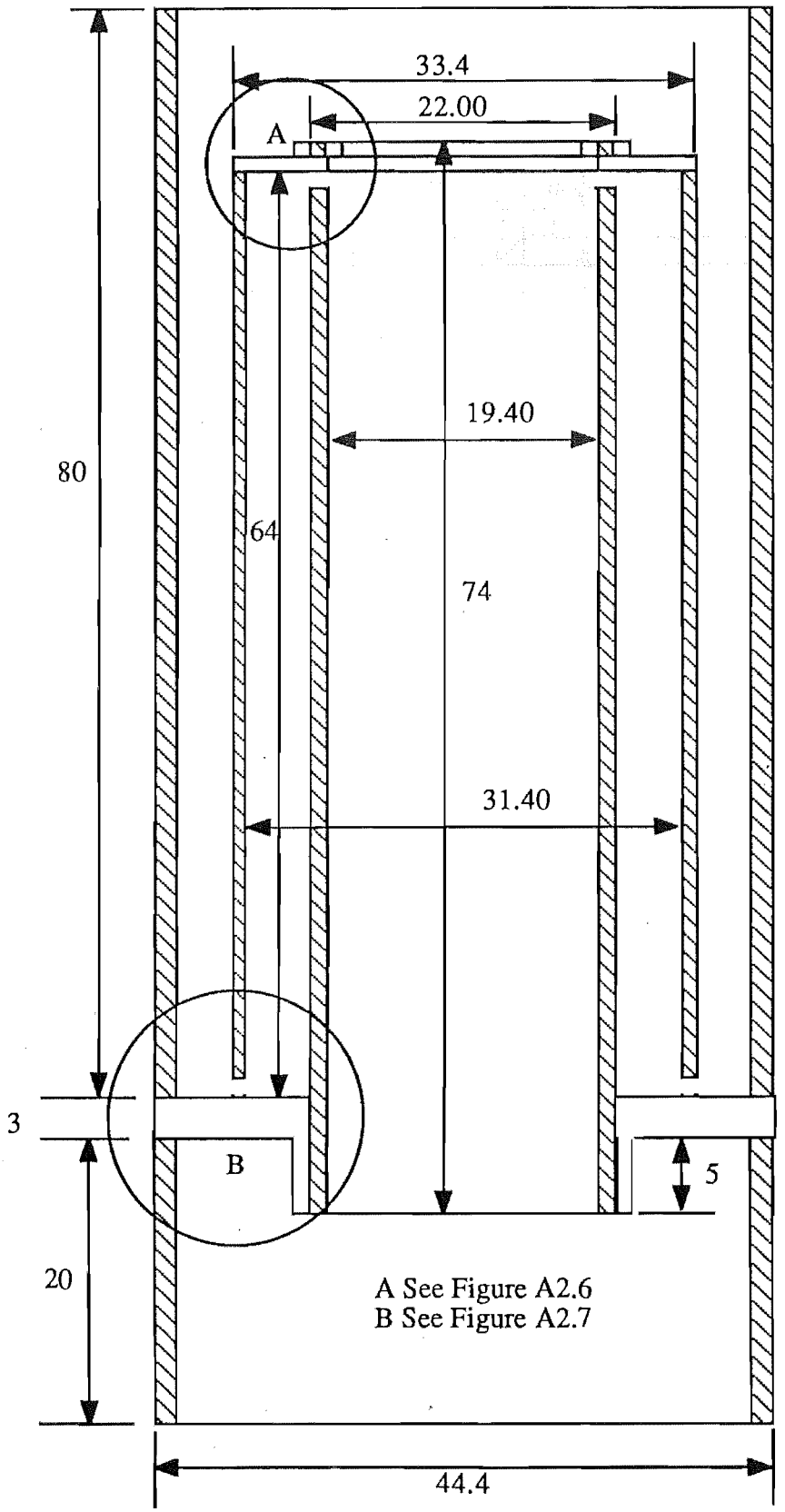

Figure A2.5 Workshop Drawing of the Liquid Sample Holder

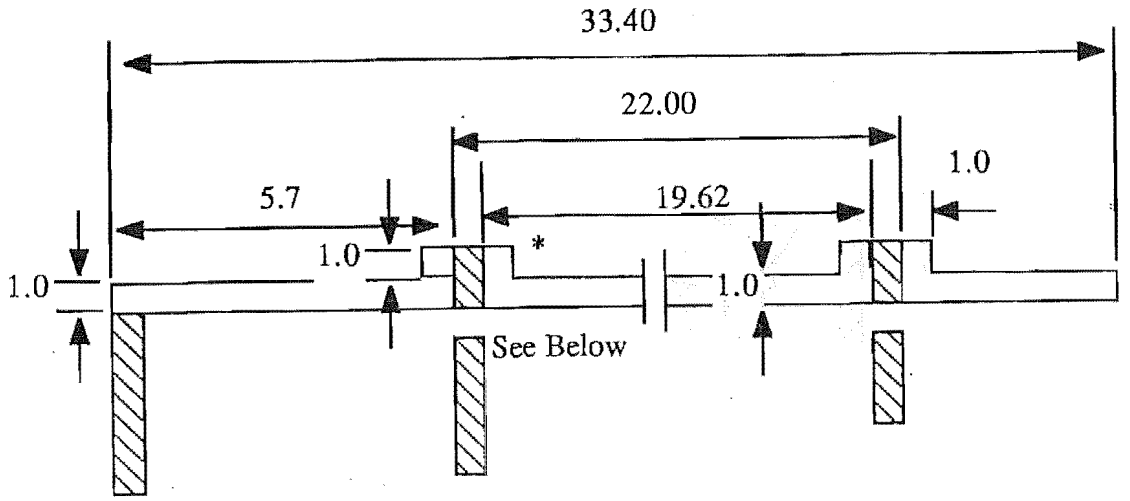

* Pieces machined for argon welding

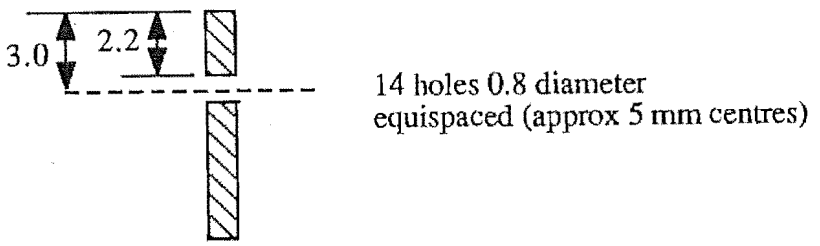

Figure A2.6 Workshop Drawing of the Liquid Sample Holder. Detail 'A'

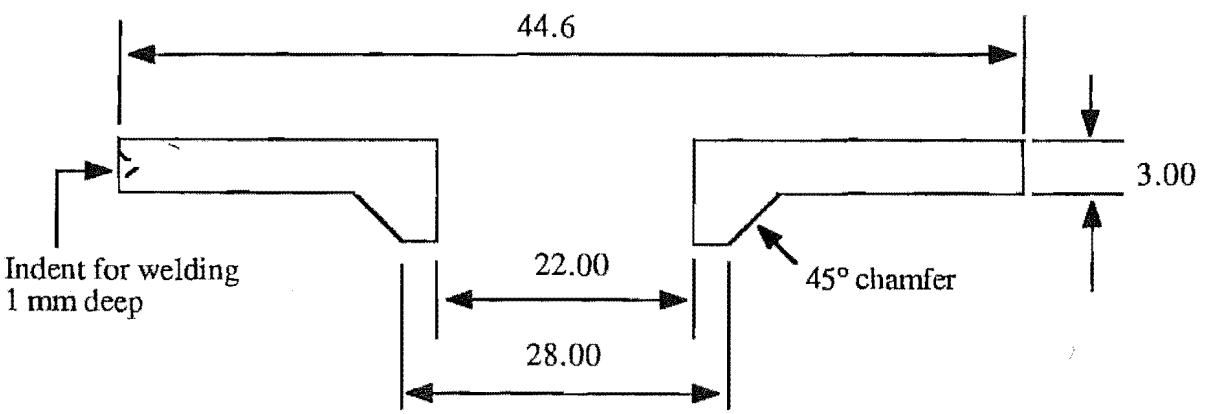

Holes at detail B, 0.8 mm diameter
20 off equispaced.

Figure A2.7 Workshop Drawing of the Liquid Sample Holder. Detail 'B'

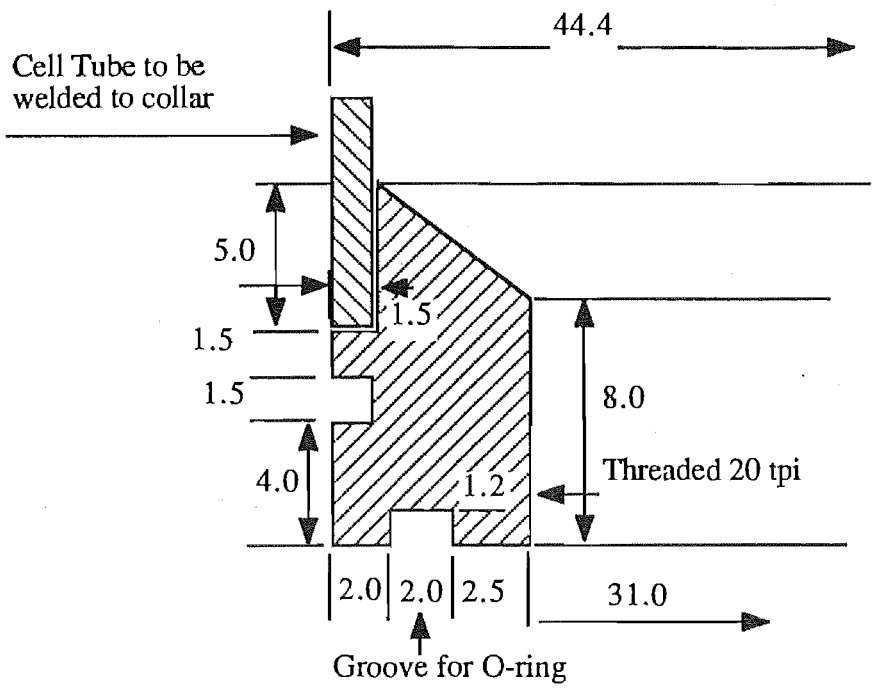

Boss. To be welded to the bottom of the tube. Scale 4:1

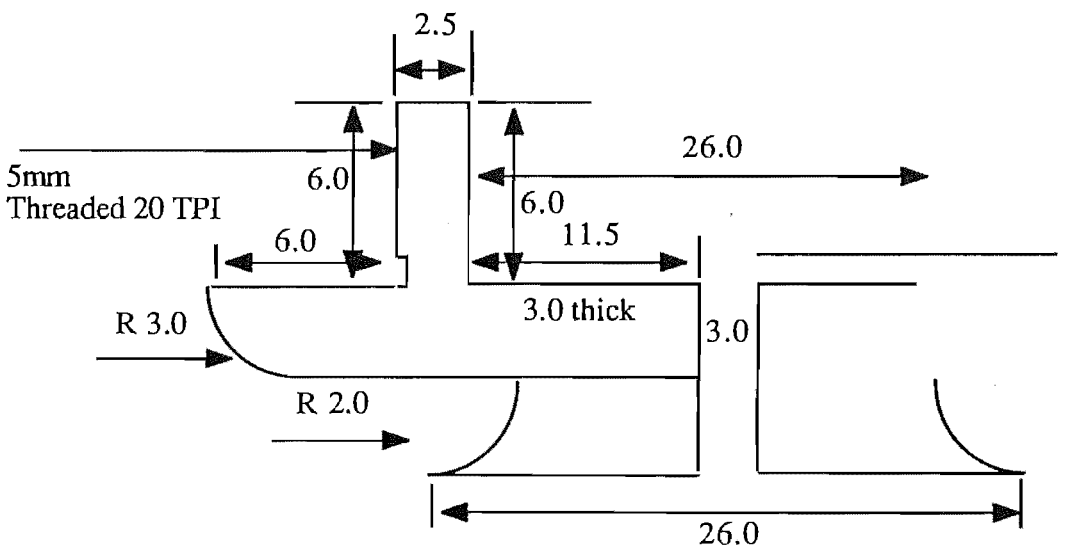

This base piece, radiused 3mm as for the example, to take a 25x6mm O-ring.

Cap for liquid cell, Scale 4:1

Figure A2.8 Workshop Drawing of the Liquid Sample Holder. End Cap Details

A 3

HPLC Calibrations

The Refractive Index detector was calibrated with standard solutions of triglycerides in chloroform. The triglycerides were weighed into sample bottles and a known mass of chloroform was added. The HPLC was operated with identical mobile phase composition and detector settings to those used during the solubility experiments.

The masses were determined with a Mettler AE200 electronic balance. The estimated error in each mass reading is ±0.05mg. This error is insignificant in the context of the experiments.

The calibration data are presented in tables A3.1 and figures A3.1 to A3.4. Regression equations are presented below the table. These equations were determined by the plotting package Cricket Graph (Cricket Software, Inc. Malvern, Pennsylvania, U.S.A.). These lines were used in the data determination. The equation determined for Tripalmitin gave negative solubilities for the lowest data values. The mass and area data were regressed using a linear least squares equation that was forced through the origin (see below)

Table A3.1 Calibration data for Triglycerides

Trilaurin		**Trimyristin**		**Tripalmitin**		**Tristearin**	
Mass (10^5) g	Area	Mass (10^5) g	Area	Mass (10^5) g	Area	Mass (10^5) g	Area
0.809	816	0.850	1695	0.654	2860	0.374	1450
2.510	2244	1.951	4296	1.166	5856	1.36	6197
4.720	4408	2.872	6649	2.857	13842	2.85	11796
12.05	11066	5.489	12355	6.583	30548	8.88	36740
19.55	18458	8.844	19937	11.24	49298	10.77	43094
41.00	41646	9.963	22523	19.36	91797		
66.44	65596	24.095	53891	32.02	131625		

Regression Equations. (Y = mass in the sample loop (x 10^5 g), X = measured HPLC Area)

Trilaurin:	$Y = 0.309 + 1.003 \times 10^{-3} X$	$R^2 = 0.999$
Trimyristin:	$Y = -1.52 \times 10^{-2} + 4.46 \times 10^{-4} X$	$R^2 = 1.000$
Tripalmitin:	$Y = 0 + 2.32 \times 10^{-4} X$	$R^2 = ***$
Tristearin:	$Y = -5.97 \times 10^{-2} + 2.477 \times 10^{-4} X$	$R^2 = 0.999$

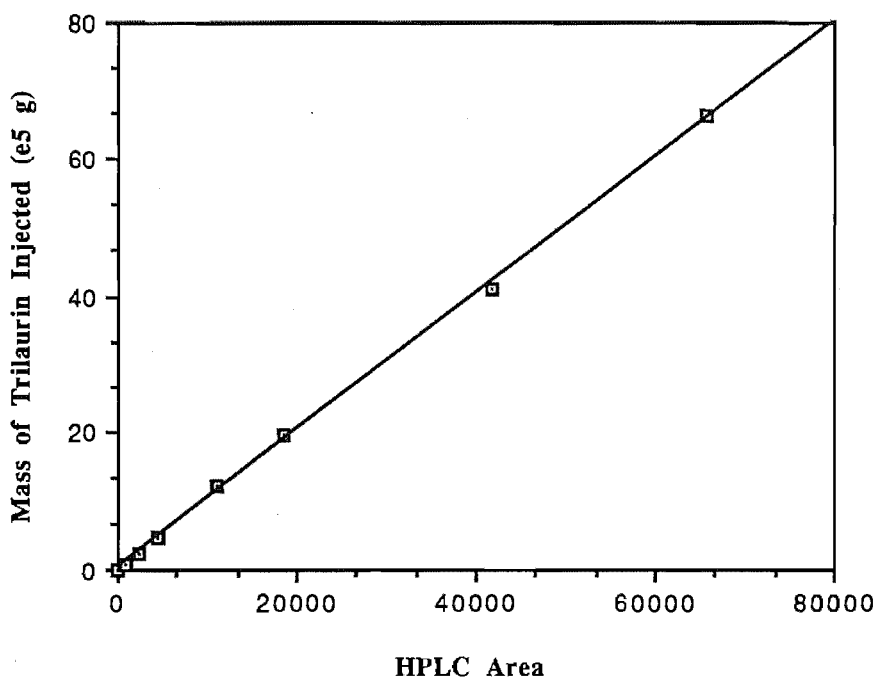

Figure A3.1 HPLC Calibration Curve for Trilaurin in a 64/36 v/v Acetone/Acetonitrile Mixture

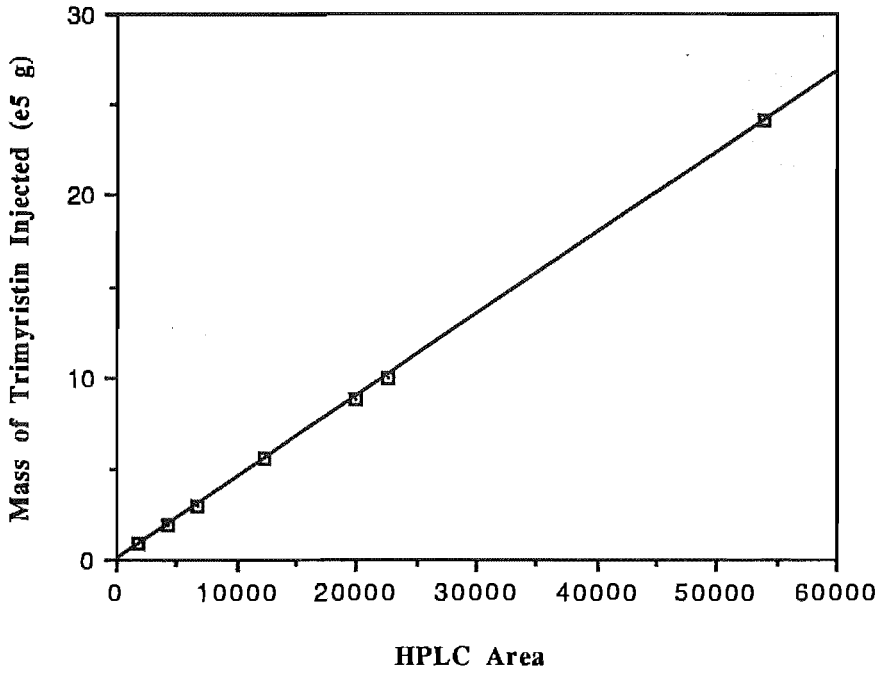

Figure A3.2 HPLC Calibration Curve for Trimyristin in a 75/25 v/v Acetone/Acetonitrile Mixture

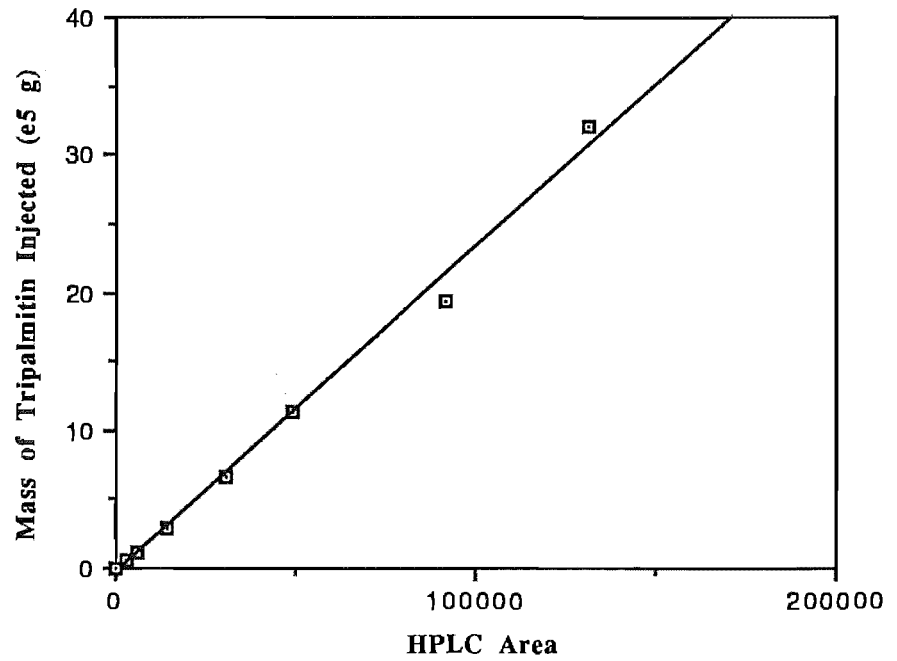

Figure A3.3 HPLC Calibration Curve for Tripalmitin in an 83/17 v/v Acetone/Acetonitrile Mixture

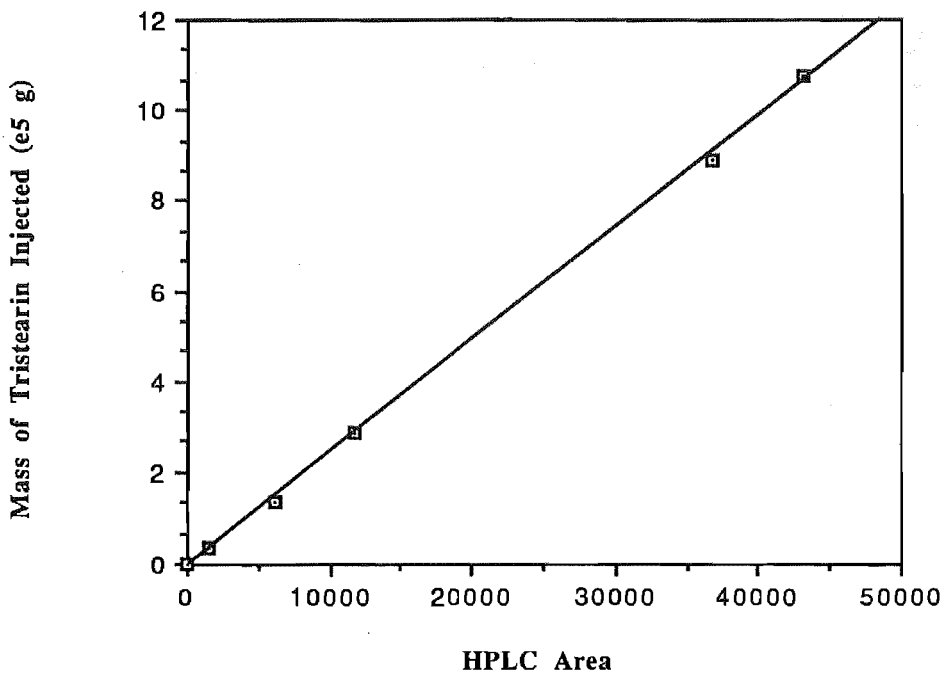

Figure A3.4 HPLC Calibration Curve for Tristearin in an 85/15 v/v Acetone/Acetonitrile Mixture

A4

Raw Solubility Measurements

The measurements presented below were collected during the course of this experimental programme. Values marked with a '#' symbol were not used in the determination of mean areas. These values are generally further than three standard deviations away from the mean value. An area value was not used when it was clear that the system was not at steady state, or for some unexplained reason a rogue measurement was taken. A '***' symbol in the tables indicates that an area was unobtainable.

For Trilaurin, the experiments at 35°C were repeated to see if the observed crossing of the 35 and 40°C isotherms was correct. All the recorded solubility data for Trimyristin (including the duplicated experiments used to determine whether the system was operating correctly) are included. HPLC areas for Tristearin at 0.84 and 0.89 g.cm^{-3} at 55°C were obtained with a 20µl sample loop. The remainder of the Tristearin measurements were taken using the 100µl sample loop.

Table A4.1. Raw Solubility Data for Trilaurin

T (°C)	P (MPa)	Run Number	HPLC Area	Mean Area	Std. Dev.
35.0	8.3	DEC15.1	11233#		
		DEC15.2	4887#		
		DEC15.3	2194		
		DEC15.4	3749#		
		DEC15.5	1774		
		DEC15.6	1880		
		DEC15.7	1941		
		DEC15.8	1791		
				1846.5	78.3
	9.0	DEC15.9	1989#		
		DEC15.10	2691#		
		DEC15.11	2934		
		DEC15.12	3486		
		DEC15.13	3238		
		DEC15.14	6751#		
		DEC15.15	7071#		
		DEC15.16	5441#		

		DEC15.17	5193#		
		DEC15.18	5030#		
		DEC15.19	3177		
		DEC15.20	3332		
		DEC15.21	3033		
				3200	199.9
	10.5	DEC15.22	5139#		
		DEC15.23	6074#		
		DEC15.24	6075#		
		DEC15.25	6609		
		DEC15.26	6540		
		DEC15.27	6694		
		DEC15.28	6749		
				6648.0	92.2
	12.7	DEC15.29	6674#		
		DEC15.30	10010#		
		DEC15.31	10632#		
		DEC15.32	12671		
		DEC15.33	11963		
		DEC15.34	12121		
		DEC15.35	12530		
				12321.3	333.8
	17.1	DEC15.36	20158#		
		DEC15.37	26867		
		DEC15.38	26841		
		DEC15.39	28175		
		DEC15.40	17019#		
		DEC15.41	28631		
		DEC15.42	30657		
		DEC15.43	32124		
		DEC15.44	40532#		
		DEC15.45	39189#		
		DEC15.46	33424		
				27628.5	2586
	8.3	FEB1.1	21636#		
		FEB1.2	2710#		
		FEB1.3	1296		
		FEB1.4	1571		
		FEB1.5	1809		
		FEB1.6	1297		
		FEB1.7	1288		
		FEB1.8	1669		
				1316.2	120.2
	9.0	FEB1.9	1761#		
		FEB1.10	1874#		
		FEB1.11	2491		
		FEB1.12	2702		
		FEB1.13	3053		
		FEB1.14	2771		
		FEB1.15	2828		
				2769.0	203.6
	10.5	FEB1.16	3227#		
		FEB1.17	3450#		
		FEB1.18	4747#		

		FEB1.19	5527		
		FEB1.20	5941		
		FEB1.21	6314		
		FEB1.22	6110		
		FEB1.23	6234		
				6040	319.4
	12.7	FEB1.24	6456#		
		FEB1.25	8561#		
		FEB1.26	10888		
		FEB1.27	10851		
		FEB1.28	11755		
		FEB1.29	11291		
				11196.3	422.5
	17.1	FEB1.30	13298#		
		FEB1.31	14233#		
		FEB1.32	20518		
		FEB1.33	24973		
		FEB1.34	25993		
		FEB1.35	26468		
				25811.3	763.8
40.0	9.5	DEC10.1	1143		
		DEC10.2	1256		
		DEC10.3	1099		
		DEC10.4	1261		
		DEC10.5	801		
				1112.0	188.0
	10.5	DEC10.6	1542#		
		DEC10.7	2326#		
		DEC10.8	3209		
		DEC10.9	3308		
		DEC10.10	3289		
		DEC10.11	3374		
				3295.0	67.9
	12.5	DEC10.12	3675#		
		DEC10.13	3913#		
		DEC10.14	5377#		
		DEC10.15	***#		
		DEC10.16	8258		
		DEC10.17	7521		
		DEC10.18	7137		
				7639.0	569.0
	15.0	DEC10.19	7546#		
		DEC10.20	7984#		
		DEC10.21	8403#		
		DEC10.22	8814#		
		DEC10.23	11849		
		DEC10.24	12589		
		DEC10.25	13802		
		DEC10.26	13549		
		DEC10.27	15090		
				13313.3	639.9
	20.0	DEC10.28	15330#		
		DEC10.29	15659#		
		DEC10.30	16829#		

		DEC10.31	22791#		
		DEC10.32	26563#		
		DEC10.33	30860		
		DEC10.34	32843		
		DEC10.35	33467		
		DEC10.36	37029		
				32390	1361.0
47.0	10.8	DEC11.1	14631#		
		DEC11.2	9037#		
		DEC11.3	21185#		
		DEC11.4	22897#		
		DEC11.5	19219#		
		DEC11.6	23741#		
		DEC11.7	19752#		
				***	***
	10.8	DEC13.1	7700#		
		DEC13.2	4982#		
		DEC13.3	4500#		
		DEC13.4	3548#		
		DEC13.5	2545		
		DEC13.6	1951		
		DEC13.7	2823		
		DEC13.8	1967		
				2115.8	433.74
	12.7	DEC10.8	34143#		
		DEC10.9	18968#		
		DEC10.10	6695#		
		DEC10.11	3286#		
		DEC10.12	4979		
		DEC10.13	5383		
		DEC11.14	5602		
		DEC11.15	4870		
		DEC11.16	4729		
				5112.4	366.5
	15.3	DEC11.17	9735		
		DEC11.18	10296		
		DEC11.19	10687		
		DEC11.20	10884		
		DEC11.21	11119		
				10721.5	357
	18.5	DEC11.22	13148#		
		DEC11.23	16900#		
		DEC11.24	19848		
		DEC11.25	20078		
		DEC11.26	21613		
		DEC11.27	21655		
				20797	970.9
	24.0	DEC13.9	14143#		
		DEC13.10	19218#		
		DEC13.11	35158#		
		DEC13.12	45439		
		DEC13.13	49435		
		DEC13.14	49759		
		DEC13.15	48002		

		DEC13.16	53449		
				50161.3	2321
55.0	13.1	DEC12.1	151848#		
		DEC12.2	13018#		
		DEC12.3	6867#		
		DEC12.4	4045		
		DEC12.5	5611		
		DEC12.6	3635		
		DEC12.7	4047		
		DEC12.8	3542		
				4176	834
	15.2	DEC12.9	6783		
		DEC12.10	11346#		
		DEC12.11	7325		
		DEC12.12	6769		
		DEC12.13	8859		
		DEC12.14	***#		
		DEC12.15	5880		
				7434	984
	18.5	DEC12.16	11872		
		DEC12.17	11892		
		DEC12.18	12501		
		DEC12.19	13121		
		DEC12.20	13696		
		DEC12.21	14333		
		DEC12.22	14186		
		DEC12.23	13952		
		DEC12.24	15894		
				13631.5	699
	22.5	DEC12.25	106263#		
		DEC12.26	44637#		
		DEC12.27	35481#		
		DEC12.28	29818		
		DEC12.29	29819		
		DEC12.30	30833		
		DEC12.31	30281		
		DEC12.32	29812		
				30112.6	450.2
	28.9	DEC12.33	32069#		
		DEC12.34	33186#		
		DEC12.35	39370#		
		DEC12.36	67672		
		DEC12.37	67631		
		DEC12.38	68456		
		DEC12.39	65399		
		DEC12.40	73198		
				67289.5	1316

TABLE A4.2. Raw Solubility Data for Trimyristin

T (°C)	P (MPa)	Run Number	HPLC Area	Mean Area	Std. Dev.
35.0	8.3	SEP3.1	1444#		
		SEP3.2	604#		
		SEP3.3	991#		
		SEP3.4	388		
		SEP3.5	470		
		SEP3.6	437		
		SEP3.7	497		
				448.0	46.9
	9.0	SEP3.8	817		
		SEP3.9	747		
		SEP3.10	903		
		SEP3.11	818		
		SEP3.12	744		
				805.8	65.1
	10.5	SEP3.13	2247		
		SEP3.14	1809		
		SEP3.15	1794		
		SEP3.16	1762		
		SEP3.17	1803		
				1792.0	20.9
	12.7	SEP3.18	2913		
		SEP3.19	3005		
		SEP3.20	2999		
		SEP3.21	2718		
		SEP3.22	2751		
				2877.2	135.7
	17.1	SEP4.1	3807		
		SEP4.2	3713		
		SEP4.3	3506		
		SEP4.4	3697		
		SEP4.5	3336		
				3680.7	126.2
		SEP5.6	4966#		
		SEP5.7	5276		
		SEP5.8	6121		
		SEP5.9	17736#		
		SEP5.10	6399		
		SEP5.11	6154		
				6224	151
	24.0	SEP4.6	4582		
		SEP4.7	5671		
		SEP4.8	5578		
		SEP4.9	5523		
		SEP4.31	2585#		
		SEP4.32	1900#		
		SEP4.33	2926#		
				5583.2	62.8
		SEP5.12	***#		

		SEP5.13	9989		
		SEP5.14	10112		
		SEP5.15	10734		
		SEP5.16	10352		
		SEP5.16	10699		
				10377.2	336.3
40.0	9.5	JUL1.1	1103		
		JUL1.2	2045#		
		JUL1.3	875		
		JUL1.4	989		
		JUL1.5	986		
		JUL3.1	1470		
		JUL3.2	965		
		JUL3.3	620		
		JUL3.4	690		
		JUL3.5	836		
		JUL6.1	975		
		JUL6.2	845		
		JUL6.3	770		
		JUL6.4	833		
		JUL6.5	725		
				905.8	209.9
	10.5	AUG9.1	2335		
		AUG9.2	2679		
		AUG9.3	3572#		
		AUG9.4	2174		
		AUG9.5	1833		
		AUG9.6	1901		
		AUG10.1	3489#		
		AUG10.2	2637		
		AUG10.3	1999		
		AUG10.4	2100		
		AUG10.5	2065		
		AUG10.6	2105		
				2025.3	286.8
	12.5	JUL1.6	3576		
		JUL1.7	4215		
		JUL1.8	4352		
		JUL1.9	4451		
		JUL1.10	4448		
		JUL1.11	4386		
		JUL3.6	4300		
		JUL3.7	4418		
		JUL3.8	4223		
		JUL3.9	4257		
		JUL6.6	2934#		
		JUL6.7	4118		
		JUL6.8	4070		
		JUL6.9	4511		
		JUL6.10	4383		
		JUL6.11	3915		
				4289.1	168.2
	15.0	JUL1.12	6611		
		JUL1.13	7614		

		JUL1.14	7671		
		JUL1.15	7365		
		JUL1.16	7442		
		JUL1.17	9486#		
		JUL1.18	14384#		
		JUL4.1	7985		
		JUL4.2	8313		
		JUL4.3	9000		
		JUL7.1	8414		
		JUL7.2	7869		
		JUL7.3	7294		
		JUL7.4	7521		
		JUL7.5	6883		
				7670.1	451.3
	20.0	JUL2.1	7657#		
		JUL2.2	16812		
		JUL2.3	17002		
		JUL2.4	17338		
		JUL2.5	16517		
		JUL7.6	11810#		
		JUL7.7	15699		
		JUL7.8	16547		
		JUL7.9	16339		
		JUL7.10	16910		
				16645.5	495.7
	26.8	JUL5.6	22813#		
		JUL5.7	25619		
		JUL5.8	27710		
		JUL5.9	29207		
		JUL5.10	28259		
		JUL7.11	26906		
		JUL7.12	28634		
		JUL7.13	30646		
		JUL7.14	27384		
				28045.6	1523.2
47.0	10.8	AUG12.1	13671#		
		AUG12.2	3782#		
		AUG12.3	2289#		
		AUG12.4	1564		
		AUG12.5	2130#		
		AUG12.6	10350#		
		SEP1.1	5607#		
		SEP1.2	2215#		
		SEP1.3	1555		
		SEP1.4	1332		
		SEP1.5	1167		
		SEP1.6	1048		
				1275.5	54.7
	12.7	SEP2.1	17914#		
		SEP2.2	7292#		
		SEP2.3	5481		
		SEP2.4	4720		
		SEP2.5	5217		
		SEP2.6	4581		

		SEP2.7	***#		
				5224.7	358.7
	15.3	SEP1.7	5967#		
		SEP1.8	7275#		
		SEP1.9	8547		
		SEP1.10	8262		
		SEP1.11	8671		
		SEP1.12	8456		
				8484.0	421.6
	18.5	SEP1.13	11703#		
		SEP1.14	15478		
		SEP1.15	16249		
		SEP1.16	16596		
		SEP1.17	18395		
				16170	467.3
	24.0	SEP1.18	23904#		
		SEP1.19	39367		
		SEP1.20	34589		
		SEP1.21	29059#		
		SEP1.22	39199		
		SEP2.8	17247#		
		SEP2.9	29875#		
		SEP2.10	39373		
		SEP2.11	37552		
		SEP2.12	39061		
				33035.1	18707
	31.5	SEP2.13	51848#		
		SEP2.14	56844#		
		SEP2.15	72627		
		SEP2.16	76076		
		SEP2.17	68347		
		SEP2.18	59555#		
				74634.0	364.4
55.0	13.1	AUG2.1	5472#		
		AUG2.2	2181		
		AUG2.3	2711		
		AUG2.4	1884		
		AUG2.5	1780		
		AUG2.6	1721		
		AUG5.1	6268#		
		AUG5.2	2167		
		AUG5.3	2164		
		AUG5.4	2122		
		AUG5.5	1914		
				2030.2	165.9
	15.2	AUG10.7	6163#		
		AUG10.8	4236		
		AUG10.9	3923		
		AUG10.10	8885#		
		AUG10.11	3930		
		AUG10.12	3945		
				4010	150.0
	18.5	AUG2.7	3643#		
		AUG2.8	7215#		

		AUG2.9	9169		
		AUG2.10	9221		
		AUG2.11	9164		
		AUG2.12	9661		
		AUG5.6	5496#		
		AUG5.7	9112		
		AUG5.8	9523		
		AUG5.9	9688		
		AUG5.10	10157		
				9362.5	251.8
	22.3	AUG6.1	13342#		
		AUG6.2	20733		
		AUG6.3	21405		
		AUG6.4	22215		
		AUG6.5	22140		
		AUG7.1	31601#		
		AUG7.2	25330		
		AUG7.3	22431		
		AUG7.4	21241		
		AUG7.5	22311		
				22225.7	1392.1
	28.9	AUG6.6	25005#		
		AUG6.7	38328#		
		AUG6.8	47704		
		AUG6.9	49239		
		AUG6.10	50680		
		AUG7.6	27256#		
		AUG7.7	30365#		
		AUG7.8	41953		
		AUG7.9	44481		
		AUG7.10	46274		
		AUG7.11	44341		
		AUG7.12	46083		
		AUG7.13	46087		
				46861.1	2220
	36.9	AUG8.1	27995#		
		AUG8.2	45630#		
		AUG8.3	83274		
		AUG8.4	86926		
		AUG8.5	89805		
		AUG8.6	92232		
		AUG8.7	90289		
		AUG8.8	66029#		
				90775.3	1284.5

TABLE A4.3. Raw Solubility Data for Tripalmitin

T (°C)	P (MPa)	Run Number	HPLC Area	Mean Area	Std. Dev.
35.0	8.3	NOV4.1	***#		
		NOV4.2	***#		
		NOV4.3	***#		
				***	***
	9.0	NOV4.4	***#		
		NOV4.5	***#		
		NOV4.6	***#		
		NOV4.7	***#		
		NOV4.8	***#		
				***	***
	10.5	NOV4.9	***#		
		NOV4.10	***#		
		NOV4.11	571#		
		NOV4.12	197		
		NOV4.13	208		
		NOV4.14	371		
				258.6	97
	12.7	NOV4.15	594		
		NOV4.16	549		
		NOV4.17	***		
		NOV4.18	717		
		NOV4.19	832		
		NOV4.20	586		
				655.6	117
	17.1	NOV4.21	1700		
		NOV4.22	1750		
		NOV4.23	2160#		
		NOV4.24	1750		
		NOV4.25	1500		
		NOV4.26	1500		
				1640	129.4
	23.4	NOV4.27	2161		
		NOV4.28	3984		
		NOV4.29	2600		
		NOV4.30	3930		
		NOV4.31	2585		
		NOV4.32	1900		
		NOV4.33	2926		
				3205	700
40.0	9.5	NOV2.14	28930#		
		NOV2.15	541		
		NOV2.16	755		
		NOV2.17	***#		
		NOV2.18	561		
		NOV2.19	468		

		NOV2.20	***#		
				523.3	48.95
	10.5	NOV2.21	7710#		
		NOV2.22	561		
		NOV2.23	880		
		NOV2.24	890		
		NOV2.25	507		
		NOV2.26	691		
				659.8	165.9
	12.5	NOV2.27	1373		
		NOV2.28	1267		
		NOV2.29	1341		
		NOV2.30	844#		
		NOV2.31	1405		
		NOV2.32	992#		
				1346.5	59.09
	15.0	NOV1.4	896#		
		NOV1.5	2274		
		NOV1.6	2061		
		NOV1.7	3545#		
		NOV1.8	2574		
		NOV1.9	3414#		
		NOV1.10	5255#		
				2303	257.7
	20.0	NOV2.1	***		
		NOV2.2	4216		
		NOV2.3	4830		
		NOV2.4	4397		
		NOV2.5	4844		
		NOV2.6	4826		
				4724.3	218
	26.8	NOV2.7	6517#		
		NOV2.8	7395		
		NOV2.9	13031#		
		NOV2.10	6939		
		NOV2.11	7333		
		NOV2.12	7336		
		NOV2.13	8949#		
				7354.6	34.9
47.0	10.8	DEC1.1	1188#		
		DEC1.2	456		
		DEC1.3	***		
		DEC1.4	323		
		DEC1.5	376		
		DEC1.6	386		
				385	54.7
	12.7	DEC1.7	2045		
		DEC1.8	1995		
		DEC1.9	2448		
		DEC1.10	2131		
		DEC1.11	2448		
				2154.7	***
	15.3	DEC1.12	5635		
		DEC1.13	6801		

		DEC1.14	8221#		
		DEC1.15	5683		
		DEC1.16	6388		
				5903.0	421.6
	18.5	DEC1.17	11276		
		DEC1.18	11181		
		DEC1.19	13950		
		DEC1.20	11855		
		DEC1.21	11346		
				11276.3	467.3
	24.0	DEC1.22	16404#		
		DEC1.23	19621		
		DEC1.24	21078		
		DEC1.25	21163		
		DEC1.26	20517		
		DEC1.36	26871#		
		DEC1.37	24463#		
		DEC1.38	23028#		
				20594.5	709.6
	31.5	DEC1.27	17055#		
		DEC1.28	18708#		
		DEC1.29	20654#		
		DEC1.30	8023#		
		DEC1.31	12442#		
		DEC1.32	35924		
		DEC1.33	35421		
		DEC1.34	35689		
		DEC1.35	35076		
				35527.5	364.4
55.0	13.1	DEC2.1	4019#		
		DEC2.2	3731#		
		DEC2.3	3472#		
		DEC2.4	2869		
		DEC2.5	2896		
		DEC2.6	2995		
		DEC2.7	6529#		
				2920	66.3
	15.2	DEC2.8	6758		
		DEC2.9	7863		
		DEC2.10	6777		
		DEC2.11	7330		
		DEC2.12	8292		
		DEC2.13	7260		
		DEC2.14	7387		
				7229.1	415.7
	18.5	DEC2.15	15857#		
		DEC2.16	19305		
		DEC2.17	19824		
		DEC2.18	18986		
		DEC2.19	20366		
		DEC2.20	20138		
				19723.5	573.1
	22.3	DEC2.21	26318#		
		DEC2.22	33874#		

		DEC2.23	42004#		
		DEC2.24	43586		
		DEC2.25	46049		
		DEC2.26	45986		
		DEC2.27	46092		
				45428.3	1229
	28.9	DEC3.1	***		
		DEC3.2	92815#		
		DEC3.3	99856		
		DEC3.4	102749		
		DEC3.5	102189		
		DEC3.6	92566#		
		DEC3.7	90865#		
				101598	1534
	36.9	DEC3.8	108062#		
		DEC3.9	112788#		
		DEC3.10	177439#		
		DEC3.11	151990		
		DEC3.12	155325		
		DEC3.13	153883		
		DEC3.14	159755		
				155238	3306

TABLE A4.4. Raw Solubility Data for Tristearin

T (°C)	P (MPa)	Run Number	HPLC Area	Mean Area	Std. Dev.
35.0	9.0	DEC4.1	***#		
		DEC4.2	***#		
		DEC4.3	***#		
		DEC4.4	***#		
				***	***
	10.5	DEC4.5	***#		
		DEC4.6	***#		
		DEC4.7	***#		
		DEC4.8	***#		
		DEC4.9	***#		
				***	***
	12.7	DEC4.10	***#		
		DEC4.11	***#		
		DEC4.12	***#		
		DEC4.13	***#		
		DEC4.14	***#		
				***	***
	17.1	DEC4.15	2737		
		DEC4.16	2877		
		DEC4.17	2467		
		DEC4.18	3284		
		DEC4.19	3366		
				2693.6	208.4
	23.4	DEC4.20	3529		
		DEC4.21	3391		
		DEC4.22	2598		
		DEC4.23	2385		
		DEC4.24	***		
				2975.8	568.7
40.0	9.5	DEC5.1	***#		
		DEC5.2	***#		
		DEC5.3	***#		
		DEC5.4	***#		
		DEC5.5	***#		
				***	***
	10.5	DEC5.6	***#		
		DEC5.7	***#		
		DEC5.8	***#		
		DEC5.9	***#		
				***	***
	12.5	DEC5.10	***#		
		DEC5.11	***#		
		DEC5.12	***#		
		DEC5.13	***#		
		DEC5.14	***#		
				***	***
	15.0	DEC6.1	***#		
		DEC6.2	2411		

		DEC6.3	1441		
		DEC6.4	1315		
		DEC6.5	1670		
				1787.3	563
	20.0	DEC6.6	4733		
		DEC6.7	5467#		
		DEC6.8	4100		
		DEC6.9	4113		
		DEC6.10	4632		
				4351.2	378.9
	26.8	DEC6.11	6036		
		DEC6.12	5729		
		DEC6.13	5710		
		DEC6.14	5203		
		DEC6.15	5006		
				5536.8	345.8
47.0	10.8	DEC6.16	1764#		
		DEC6.17	1207		
		DEC6.18	***#		
		DEC6.19	989		
		DEC6.20	718		
				984.3	204.2
	12.7	DEC6.21	1552		
		DEC6.22	1554		
		DEC6.23	1470		
		DEC6.24	***#		
				1500	***
	15.3	DEC6.25	2561		
		DEC6.26	2737		
		DEC6.27	2561		
		DEC6.28	2708		
		DEC6.29	2123#		
				2651.6	114.3
	18.5	DEC7.1	5569		
		DEC7.2	4745		
		DEC7.3	5240		
		DEC7.4	4946		
		DEC7.5	4844		
				5068.8	335.3
	24.0	DEC7.6	10292		
		DEC7.7	10838		
		DEC7.8	10763		
		DEC7.9	9868		
		DEC7.10	9593		
				10311.6	499.4
	31.5	DEC7.11	14233		
		DEC7.12	15171		
		DEC7.13	15041		
		DEC7.14	16478		
				15230.7	929.3
55.0	13.1	DEC8.1	5742#		
		DEC8.2	4494		
		DEC8.3	3106		
		DEC8.4	2832		

		DEC8.5	2292		
				3101.3	400
	15.2	DEC8.6	5609		
		DEC8.7	5570		
		DEC8.8	6042		
		DEC8.9	5133		
		DEC8.10	4774		
				5576.0	511
	18.5	DEC8.11	13895		
		DEC8.12	12500		
		DEC8.13	11133		
		DEC8.14	13078		
		DEC8.15	11362		
				12500.0	1092.7
	22.3	DEC8.16	15590		
		DEC8.17	17140		
		DEC8.18	16067		
		DEC8.19	16955		
		DEC8.20	17444		
				16639.2	778.8
	28.9	FEB2.5	8299		
		FEB2.6	***#		
		FEB2.7	7577		
		FEB2.8	7434		
		FEB2.9	9114#		
				8106	***
	36.9	FEB2.10	11512		
		FEB2.11	11926		
		FEB2.12	11958		
				11767.6	223.5

A5

Graphical Results

This appendix presents the experimental solubilities at constant temperature and constant density.

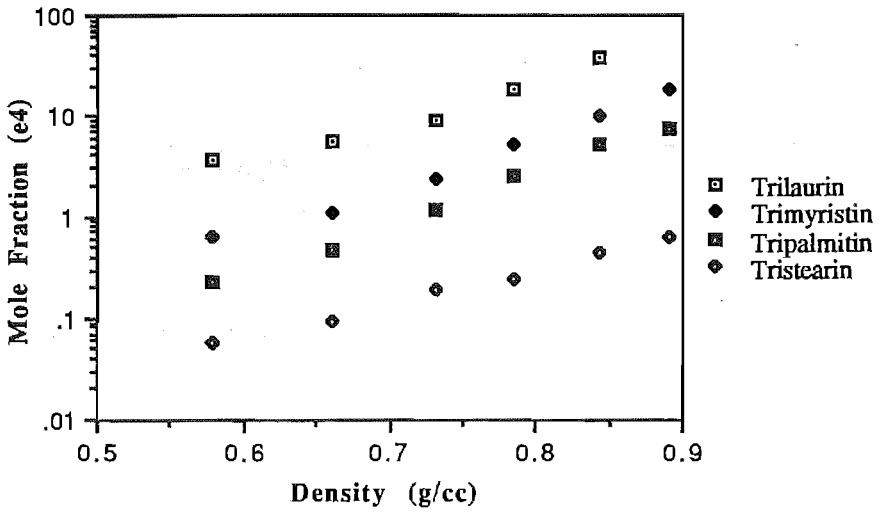

Figure A5.1 Variation of Triglyceride Solubility with Density at 55°C

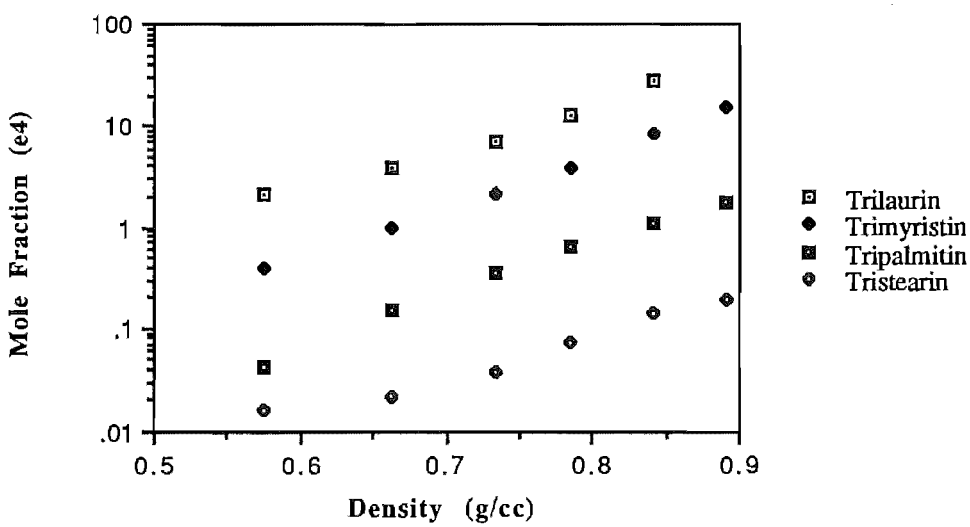

Figure A5.2 Variation of Triglyceride Solubility with Density at 47°C

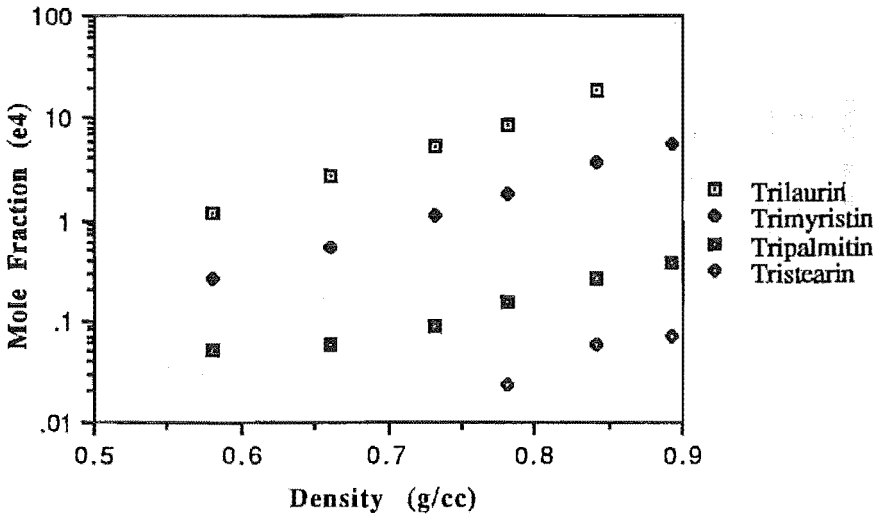

Figure A5.3 Variation of Triglyceride Solubility with Density at 40°C

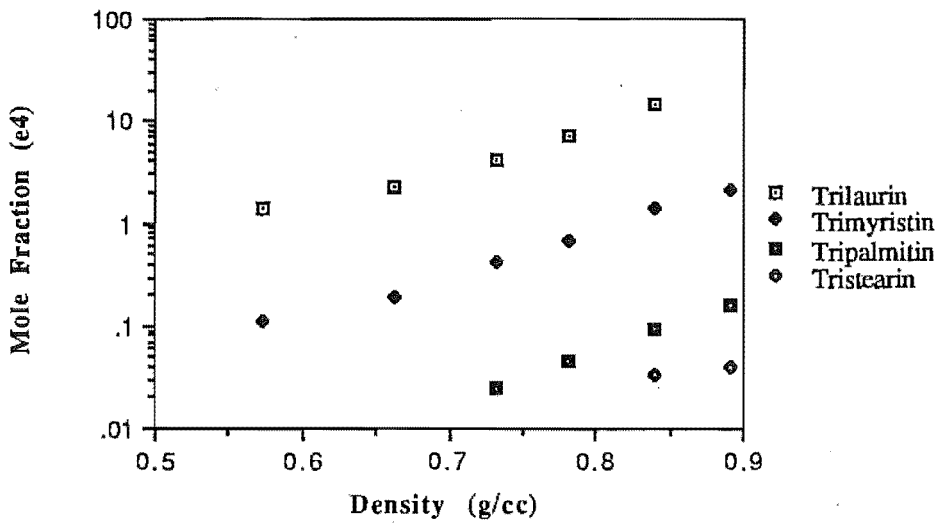

Figure A5.4 Variation of Triglyceride Solubility with Density at 35°C

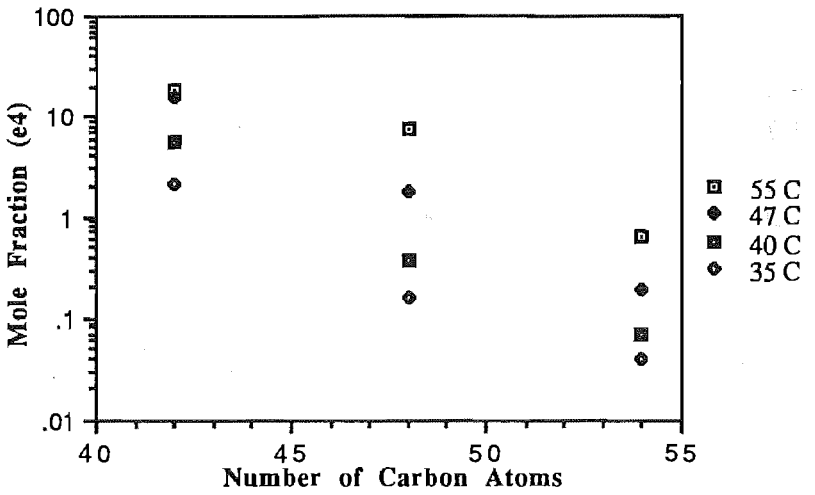

Figure A5.5 Variation of Triglyceride Solubility with Number of Carbon Atoms at a CO_2 Density of 0.89 $g.cm^{-3}$

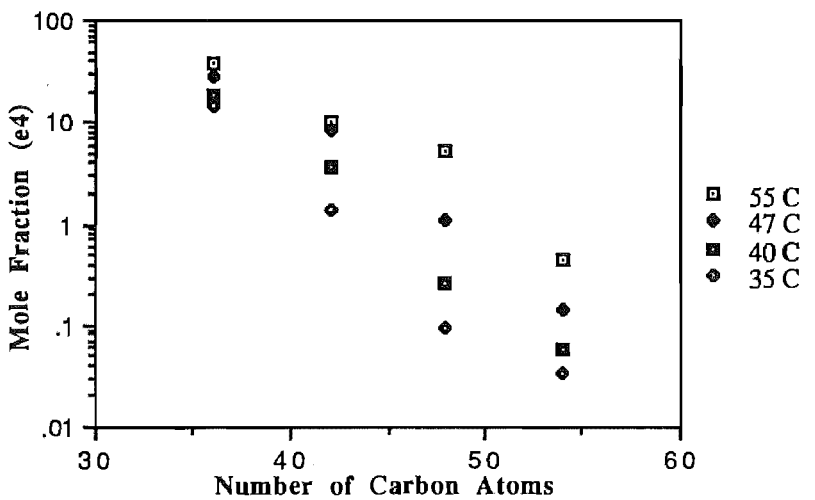

Figure A5.6 Variation of Triglyceride Solubility with Number of Carbon Atoms at a CO_2 Density of 0.84 $g.cm^{-3}$

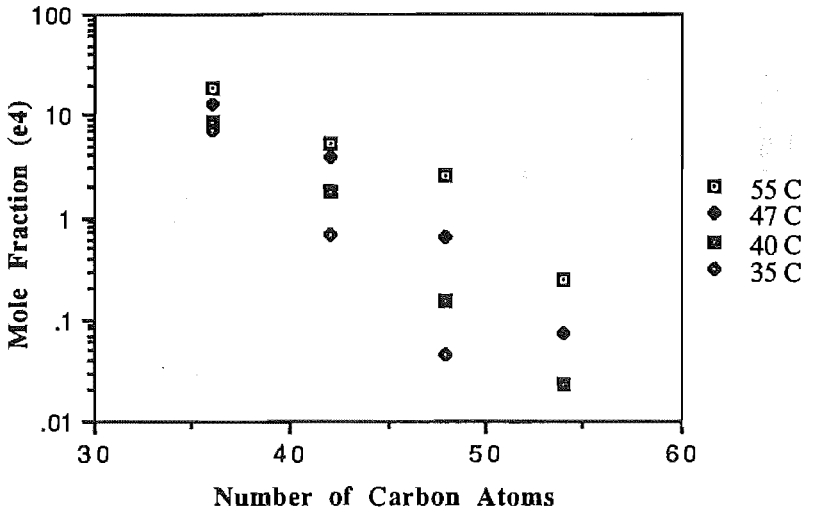

Figure A5.7 Variation of Triglyceride Solubility with Number of Carbon Atoms at a CO_2 Density of 0.78 $g.cm^{-3}$

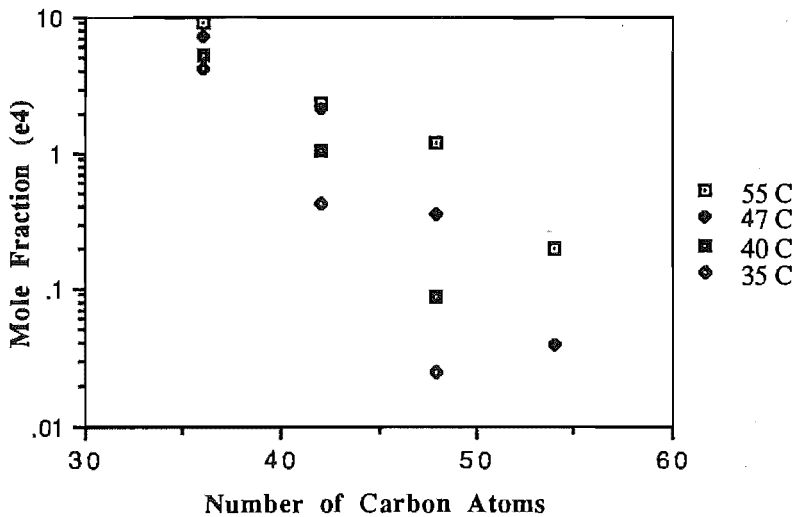

Figure A5.8 Variation of Triglyceride Solubility with Number of Carbon Atoms at a CO_2 Density of 0.73 $g.cm^{-3}$

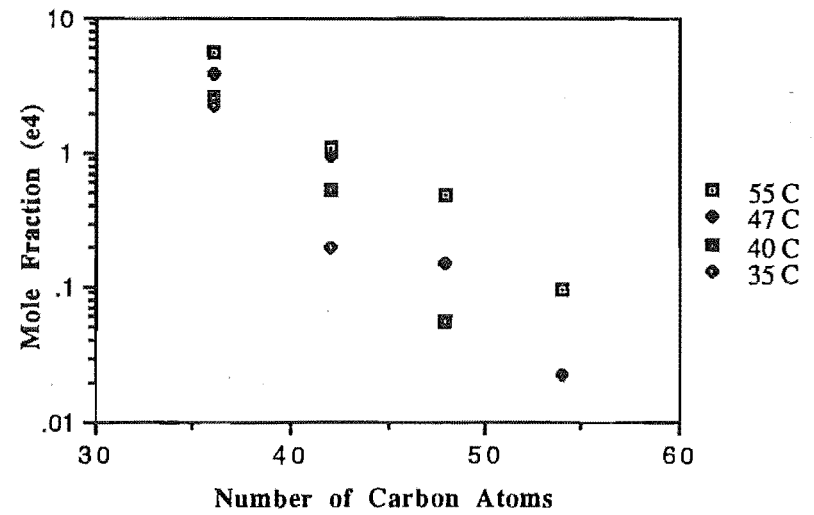

Figure A5.9 Variation of Triglyceride Solubility with Number of Carbon Atoms at a CO_2 Density of 0.66 g.cm^{-3}

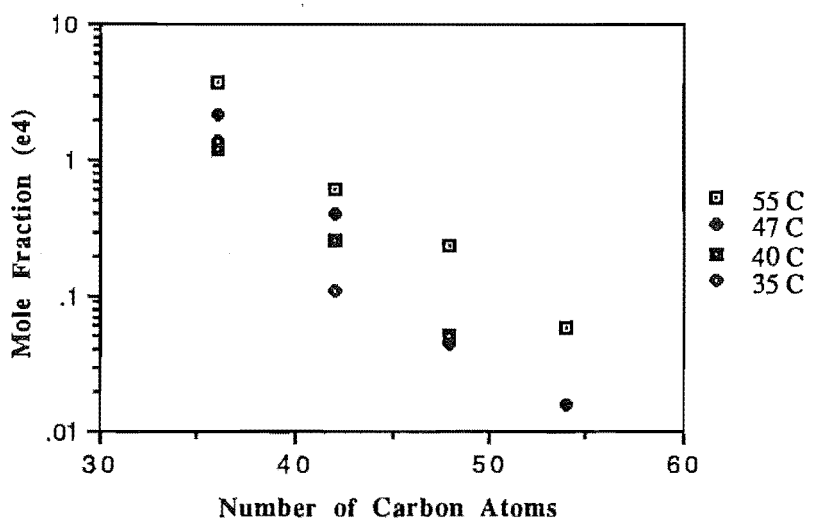

Figure A5.10 Variation of Triglyceride Solubility with Number of Carbon Atoms at a CO_2 Density of 0.57 g.cm^{-3}

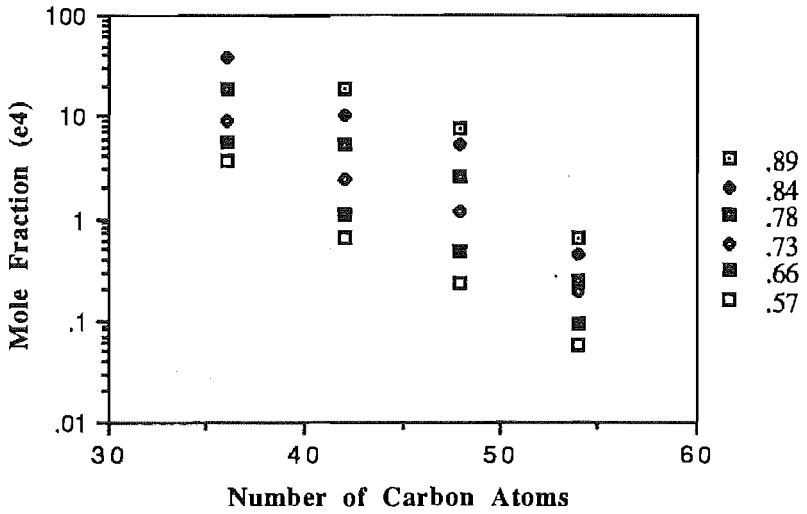

Figure A5.11 Variation of Triglyceride Solubility with Number of Carbon Atoms at 55°C

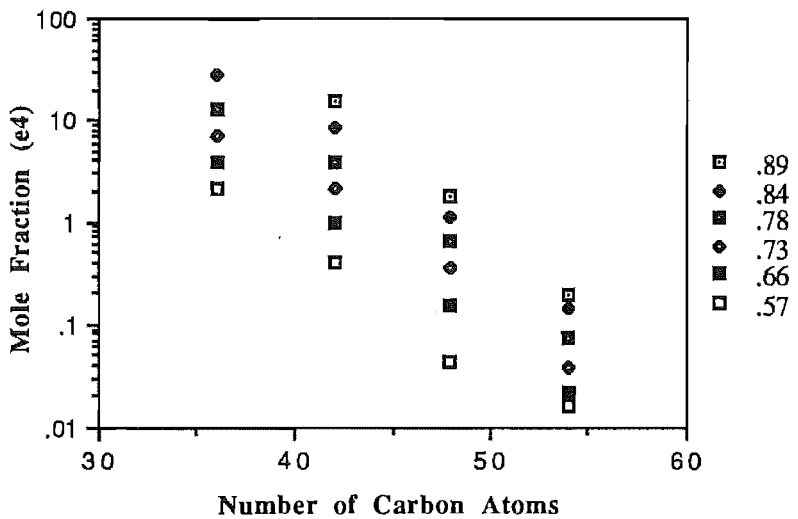

Figure A5.12 Variation of Triglyceride Solubility with Number of Carbon Atoms at 47°C

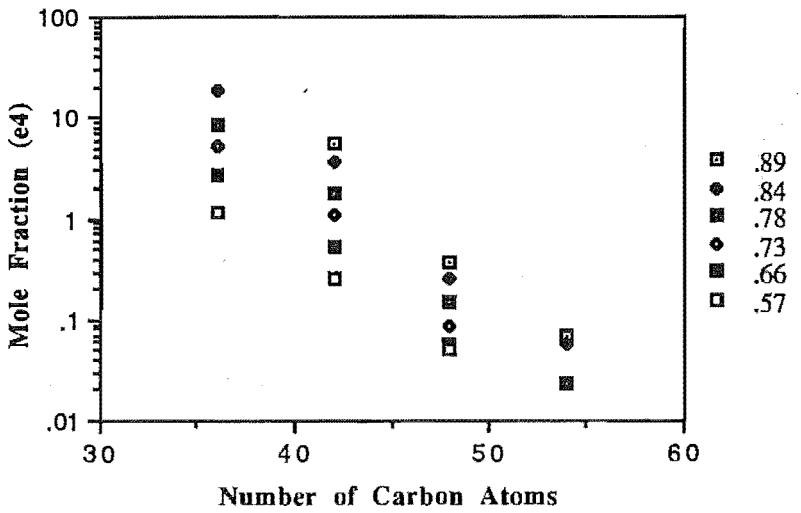

Figure A5.13 Variation of Triglyceride Solubility with Number of Carbon Atoms at 40°C

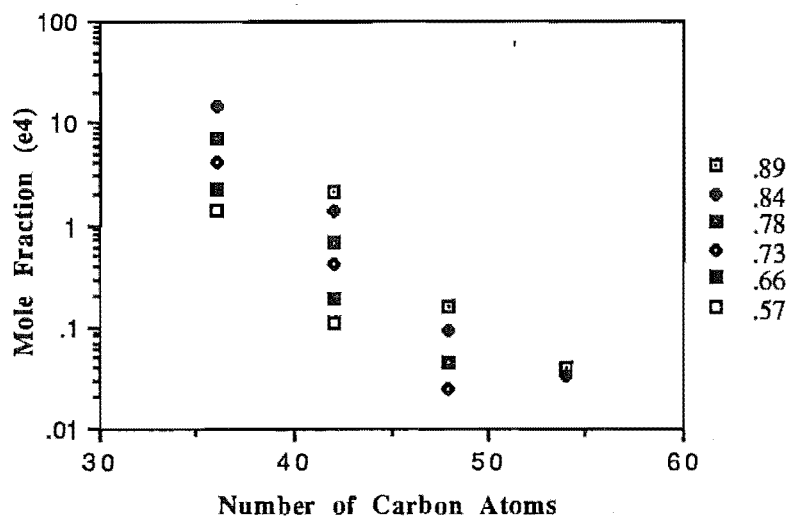

Figure A5.14 Variation of Triglyceride Solubility with Number of Carbon Atoms at 35°C

A6

Regression Parameters and Graphs

Table A6.1 Parameters for Equation 6.18

This equation is of the form $a_{12} = a + bT + c\rho + dMr$.

a	8.996
b	2.64e-2
c	-1.88e-2
d	-2.88

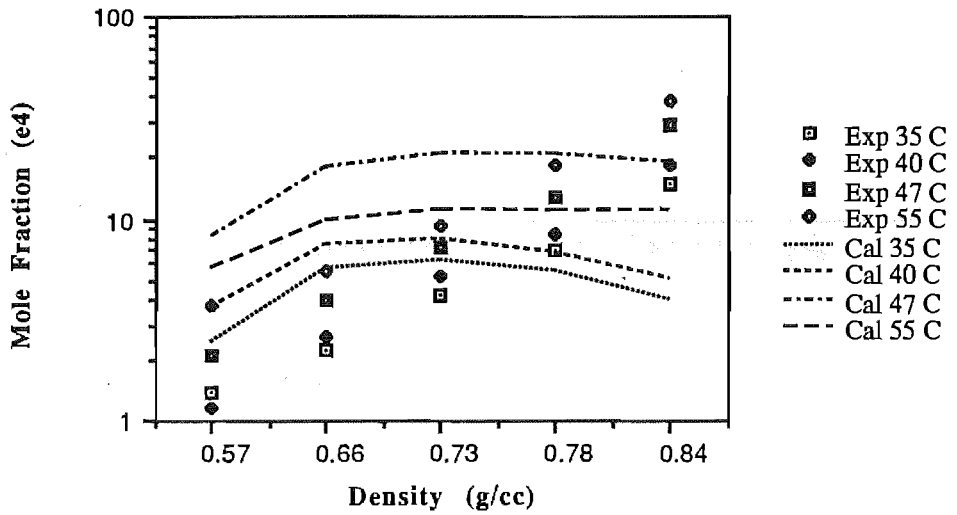

Figure A6.1 Comparison Between Experimental Solubility and Prediction (Equation 6.17) for Trilaurin in CO_2

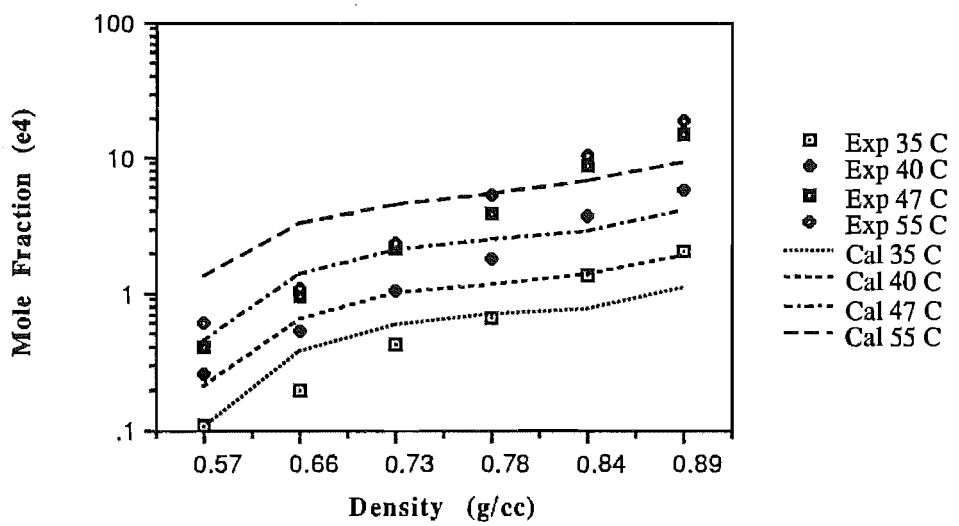

Figure A6.2 Comparison Between Experimental Solubility and Prediction (Equation 6.17) for Trimyristin in CO_2

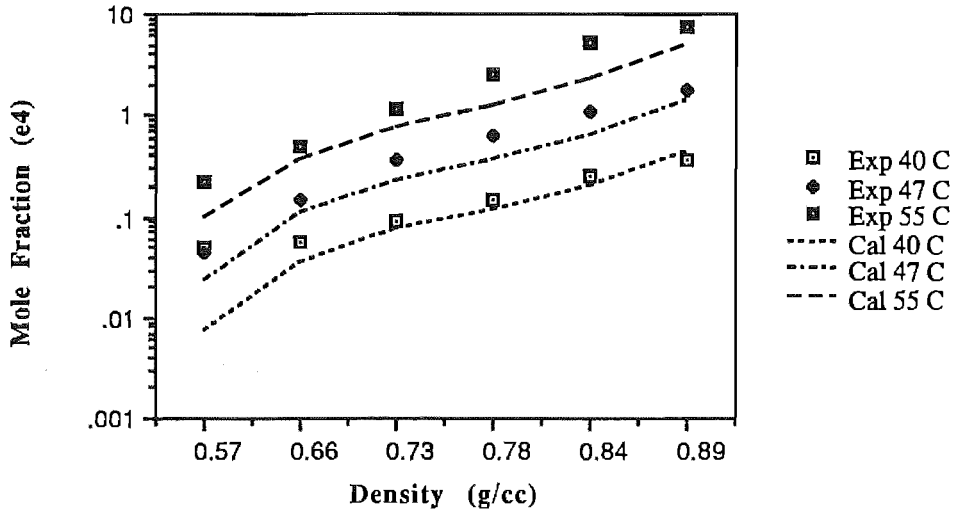

Figure A6.3 Comparison Between Experimental Solubility and Prediction (Equation 6.17) for Tripalmitin in CO_2

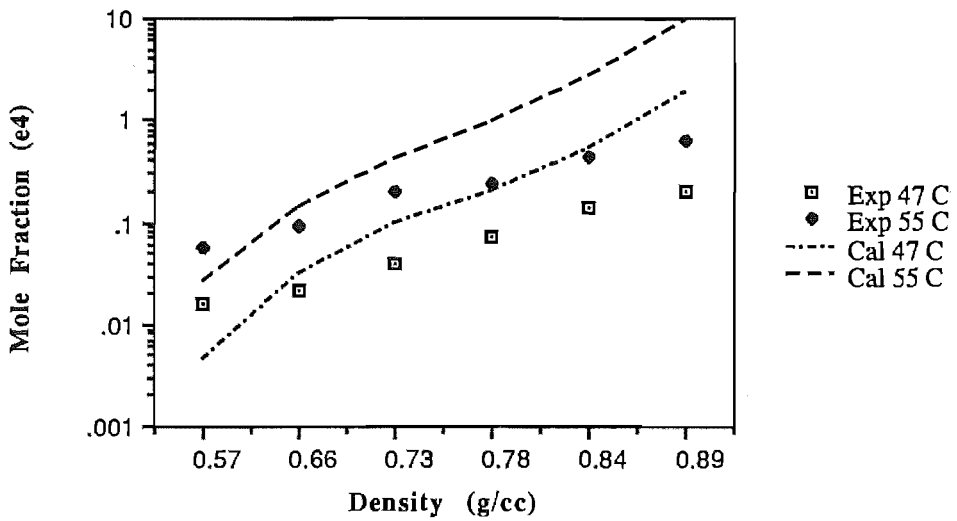

Figure A6.4 Comparison Between Experimental Solubility and Prediction (Equation 6.17) for Tristearin in CO_2

A7

Density Calculations

The CO_2 densities used during the course of this work were determined from the equation of Huang *et al* (1985).

To evaluate this equation, a FORTRAN routine was written. This programme requires the temperature and the pressure to be supplied. The density is then returned. A step-halving routine is utilised to converge on density.

This programme was tested and the output densities were compared to those of Angus *et al* (1976) (IUPAC). Table A7.1 lists the density returned for given conditions, and the IUPAC densities for the same conditions. The maximum absolute percentage deviation between the densities from this code and those of Angus *et al* was $\pm$ 1%.

Table A7.2 lists densities for selected conditions as calculated by the method of Huang *et al* (1985). This shows the variation in the density resulting from a small variation in the recorded pressure. If an error in the pressure readings of $\pm$ 0.2 MPa is used, the maximum deviation in density is $\pm$ 5%.

Table A7.1 Density Comparison Huang *et al* (1985) and IUPAC

Temperature (K) deviation	Pressure (MPa)	Huang (g/cc)	IUPAC (g/cc)	%
310	9.0	0.6104	0.6156	0.8
	15.0	0.8029	0.8033	
	25.0	0.8933	0.8939	
	35.0	0.9456	0.9464	0.09
330	9.0	0.2469	0.2474	0.2
	15.0	0.6356	0.6369	
	25.0	0.8016	0.8025	
	35.0	0.8741	0.8752	0.12

Table A7.2 Density Variation from Huang *et al* (1985)

Temperature (K)	Pressure (MPa)	Density (g/cc)	Variation (%)
310	8.8	0.5810	5.0
	9.2	0.6317	3.5
	34.8	0.9447	0.09
	35.2	0.9464	0.09
330	8.8	0.2361	4.37
	9.2	0.2582	4.6
	34.8	0.8729	0.14
	35.2	0.8752	0.12

Programme CO2_DEN.FOR.

```
C
C     A test programme to evaluate the density of Carbon
C     Dioxide for pressures (up to 310.3 MPa) and over a temperature
C     range of 216-423K.
C
C     The equation is of the form Z=P/ro*R*T, where Z is a complex function
C     of the reduced density and reduced temperature.
C
```

```
      character*2 A
      CALL LIB$ERASE_PAGE(1,1)
      WRITE(6,23)
23    FORMAT(//,18x,'*** Programme to estimate CO2 Densities. ***',//,
     1 ' Using Z=f(T,RO), Z is estimated for the given T and RO.',/,
     1 ' The equation P=Z*R*T*RO is used to give the pressure',/,
     1 ' explicitly for the input conditions. RO is then changed',/,
     1 ' (by step halving) until the calculated pressure equals the',/,
     1 ' given pressure.',/,' N.B. The pressure and temperature',/,
     1 ' are REAL variables.',///)
C
      CALL LIB$SET_SCROLL(14,24)
888   WRITE (6,3814)
      READ (5,3815) T
3814  FORMAT(/,1X,'Enter Temperature (deg C) ? ',$)
3815  FORMAT (F6.2)
      T=T+273.15
889   WRITE (6,4814)
      READ (5,4815) PIN
4814  FORMAT(/,1X,'Enter Pressure (MPa) (1MPa = 145psi)? ',$)
4815  FORMAT (F8.4)
C
      TDASH=T/304.19
      DELT=1.-1./TDASH
      CC=DELT*DELT
      DA=TDASH*TDASH
      DB=TDASH*DA
      DC=TDASH*DB
      DD=TDASH*DC
      ROMIN=80.
      ROMAX=1252800.
      ROEST=10634.
C
C     LOOP FROM HERE
C
      TEST=1.0
      DO WHILE (TEST.GE.1E-03)
       RODASH=ROEST/10634.
       DELRO=1.-1./RODASH
```

```
      AA=RODASH*RODASH
      AB=RODASH*AA
      AC=RODASH*AB
      AD=RODASH*AC
      BB=DELRO*DELRO
      B2=(0.376194+0.118836/TDASH+(-3.04379/DA)+2.27453/DB+
     #  (-1.23863/DC)+(0.250442/DD))
      B3=(-0.11535+(0.675104/TDASH)+(0.198861/DA))
      B4=(0.216124+(-0.583148/TDASH))
      B5=(0.119747E-1+(0.537278E-1/TDASH))
      B6=(0.265216E-1/TDASH)
      B7=((-2.79498/DB)+(5.62393/DC)+(-2.93831/DD))
      B8=((0.988759/DB)+(-3.04711/DC)+(2.32316/DD))
      A1=B2*RODASH
      A2=B3*AA
      A3=B4*AB
      A4=B5*AC
      A5=B6*AD
      ARG1=-1.07379*AA
      A6=B7*AA*EXP(ARG1)
      A7=B8*AC*EXP(ARG1)
      ARG2=80000.*CC
      ARG3=-10.*BB-ARG2
      ARG4=-50.*BB-ARG2
      A8=-0.599724E-4*RODASH*EXP(-ARG2)
      A9=0.885339E-4*(DELRO/RODASH)*EXP(ARG3)
      A10=0.316418E-2*DELRO/RODASH*EXP(ARG4)
      Z=1.+A1+A2+A3+A4+A5+A6+A7+A8+A9+A10
      P1=Z*T*ROEST*8.314
      p1=p1/1e6
      TEST=ABS(PIN-P1)
      IF(P1.GT.PIN) THEN
       ROMAX=ROEST
      ELSE
       ROMIN=ROEST
      END IF
      ROEST=(ROMIN+ROMAX)/2
     ENDDO
     CETRO=RODASH*0.468
```

```
      WRITE(6,256)T,PIN,ROEST,cetro
256   FORMAT(//, ' The density at ',F6.2,' K, and ',F8.4,' MPa is
     # ',F11.4,' kg mol/m^3',/,' Or',f11.4,'g/cc by Starling.')
C
      WRITE(6,257)Z
257   FORMAT(/,' The Z-factor is ',F8.4,//)
      WRITE(6,24)
24    FORMAT(/,' Do you want to have another run? ',$)
      CALL READCHR(K)
      IF(K.NE.89.AND.K.NE.121) GOTO 1888
      WRITE(6,124)
124   FORMAT(/,' Do you want to use the same temperature? ',$)
      CALL READCHR(K)
      IF(K.EQ.89.OR.K.EQ.121) GOTO 889
      GOTO 888
1888  CALL LIB$ERASE_PAGE(1,1)
      END
```